

UC Berkeley

UC Berkeley Electronic Theses and Dissertations

Title

Entanglement and Geometry

Permalink

<https://escholarship.org/uc/item/6b247491>

Author

Akers, Christopher Nelson

Publication Date

2019

Peer reviewed|Thesis/dissertation

Entanglement and Geometry

by

Chris Akers

A dissertation submitted in partial satisfaction of the

requirements for the degree of

Doctor of Philosophy

in

Physics

in the

Graduate Division

of the

University of California, Berkeley

Committee in charge:

Professor Raphael Bousso, Chair

Professor Yasunori Nomura

Professor Birgitta Whaley

Summer 2019

Entanglement and Geometry

Copyright 2019
by
Chris Akers

Abstract

Entanglement and Geometry

by

Chris Akers

Doctor of Philosophy in Physics

University of California, Berkeley

Professor Raphael Bousso, Chair

There is now strong evidence of a deep connection between entanglement in quantum gravity and the geometry of spacetime. In this dissertation, we study multiple facets of this connection. We start by quantifying the entanglement of a scalar quantum field theory as a function of the curvature of its background. We then shift our focus to the AdS/CFT duality, and we prove multiple logical relationships between geometric statements in AdS and entropic statements in the CFT. Many of these proofs work in the presence of quantum corrections, and we prove under which geometric conditions entanglement wedge nesting continues to imply the quantum null energy condition (QNEC) when the CFT is on an arbitrary curved background. We also demonstrate that the non-gravitational limit of the quantum focusing conjecture implies the QNEC, given the same geometric conditions. Next, we prove the connection between the boundary of the future of a surface and the null geodesics originating orthogonally from that surface. This theorem is important for proving that the area of holographic screens increases monotonically. Finally, we derive the holographic prescription for computing Renyi entropies of a CFT with the formalism of quantum error-correction. In the process, we provide evidence that the quantum gravity degrees of freedom related to the AdS geometry are maximally-mixed.

To my parents,
Denise Akers & Jim Akers,
for their constant support
and encouragement.

Contents

Contents	ii
List of Figures	iv
1 Introduction	1
2 Entanglement and RG in the $O(N)$ vector model	3
2.1 Introduction	3
2.2 Review of Entanglement Flow Equations	4
2.3 $O(N)$ on a sphere	6
2.4 Entanglement entropy	14
2.5 Boundary perturbations	21
3 Geometric Constraints from Subregion Duality Beyond the Classical Regime	27
3.1 Introduction	27
3.2 Glossary	30
3.3 Relationships Between Entropy and Energy Inequalities	37
3.4 Relationships Between Entropy and Energy Inequalities and Geometric Constraints	38
3.5 Discussion	51
4 The Quantum Null Energy Condition, Entanglement Wedge Nesting, and Quantum Focusing	54
4.1 Introduction and Summary	54
4.2 Entanglement Wedge Nesting	56
4.3 Connection to Quantum Focusing	65
4.4 Discussion	72
5 The Boundary of the Future	75
5.1 Theorem	75
5.2 Conjugate Points to a Surface	79
5.3 Proof of the Theorem	86

6	Holographic Renyi Entropy from Quantum Error Correction	89
6.1	Introduction	89
6.2	Operator-algebra Quantum Error Correction	92
6.3	Interpretation of OQEC	95
6.4	Cosmic Brane Prescription in OQEC	100
6.5	Tensor Networks	104
6.6	Discussion	106
A	Appendix	109
A.1	F_Λ counterterm	109
A.2	Notation and Definitions	110
A.3	Surface Variations	114
A.4	z -Expansions	116
A.5	Details of the EWN Calculations	119
A.6	The $d = 4$ Case	121
A.7	Proof of Lemma 14	123
A.8	Flat Renyi Spectrum	125
	Bibliography	126

List of Figures

2.1	The equator of S^d is split into two equal cap-like regions A and B (shown in blue and red respectively). The entanglement entropy is the von Neumann entropy of the density matrix living on the blue region.	4
2.2	(a) At large N the Schwinger-Dyson equation for the 2-pt function simplifies to become the gap equation (2.16). (b) Iterating (a) gives a sum of cactus diagrams, such as the one shown above.	8
3.1	The logical relationships between the constraints discussed in this paper. The left column contains semi-classical quantum gravity statements in the bulk. The middle column is composed of constraints on bulk geometry. In the right column is quantum field theory constraints on the boundary CFT. All implications are true to all orders in $G\hbar \sim 1/N$. We have used dashed implication signs for those that were proven to all orders before this paper.	29
3.2	The causal relationship between $e(A)$ and $D(A)$ is pictured in an example space-time that violates $\mathcal{C} \subseteq \mathcal{E}$. The boundary of A 's entanglement wedge is shaded. Notably, in $\mathcal{C} \subseteq \mathcal{E}$ violating spacetimes, there is necessarily a portion of $D(A)$ that is timelike related to $e(A)$. Extremal surfaces of boundary regions from this portion of $D(A)$ are necessarily timelike related to $e(A)$, which violates EWN. . .	39
3.3	The boundary of a BCC-violating spacetime is depicted, which gives rise to a violation of $\mathcal{C} \subseteq \mathcal{E}$. The points p and q are connected by a null geodesic through the bulk. The boundary of p 's lightcone with respect to the AdS boundary causal structure is depicted with solid black lines. Part of the boundary of q 's lightcone is shown with dashed lines. The disconnected region A is defined to have part of its boundary in the timelike future of q while also satisfying $p \in D(A)$. It follows that $e(A)$ will be timelike related to $D(A)$ through the bulk, violating $\mathcal{C} \subseteq \mathcal{E}$. . .	40
3.4	The surface M and N are shown touching at a point p . In this case, $\theta_M < \theta_N$. The arrows illustrate the projection of the null orthogonal vectors onto the Cauchy surface.	43
3.5	This picture shows the various vectors defined in the proof. It depicts a cross-section of the extremal surface at constant z . $e(A)_{vac}$ denotes the extremal surface in the vacuum. For flat cuts of a null plane on the boundary, they agree. For wiggly cuts, they will differ by some multiple of k^i	49

- 4.1 Here we show the holographic setup which illustrates Entanglement Wedge Nesting. A spatial region A_1 on the boundary is deformed into the spatial region A_2 by the null vector δX^i . The extremal surfaces of A_1 and A_2 are connected by a codimension-one bulk surface \mathcal{M} (shaded blue) that is nowhere timelike by EWN. Then the vectors $\delta \bar{X}^\mu$ and s^μ , which lie in \mathcal{M} , have nonnegative norm. 57
- 5.1 Possibilities for how a null geodesic orthogonal to a surface can exit the boundary of its future. In this example, a parabolic surface K (blue line) lies in a particular spatial slice. A future-directed null geodesic (red line) is launched orthogonally from p . At q , it encounters a caustic, entering the interior of the future of K (red dashed line). The point q is conjugate to K . Other null geodesics orthogonal to K (black lines) encounter nonlocal intersections with other such geodesics along the green line, where they exit the boundary of the future of K 76
- 5.2 In this generic Penrose diagram, the codimension-two surface K (black dot) splits a Cauchy surface Σ (dashed line) into two parts $\Sigma_{in}, \Sigma_{out}$. This induces a splitting of the spacetime M into four parts: the past and future of K (red, yellow) and the domains of dependence of Σ_{in} and Σ_{out} (green, blue) [25]. Theorem 1 guarantees that this splitting is fully characterized by the four orthogonal null congruences originating on K (black diagonal lines). 77
- 5.3 An illustration of the exponential map \exp , which takes a vector in TM to a point in M , and the Jacobian of the exponential map, which takes a vector in the tangent space TTM of TM to a vector in TM 80
- 5.4 An illustration of the surface-orthogonal exponential map \exp_K evaluated at $p \in K$, which takes a vector in $T_p K^\perp$ to a point $c_{p,v}(1)$ in M . Here, as in text, the tangent space at p , $T_p M$, is broken up as a product $T_p K^\perp \times T_p K$. Also shown is the Jacobian \exp_{K*} at $v \in T_p K^\perp$, which takes a vector $w = (w_1, w_2) \in T_{p,v} NK = T_p K \times T_v T_p K^\perp$ to a vector in $T_{c_{p,v}(1)} M$ 82
- 5.5 The two types of conjugate points defined in Defs. 17 and 19. The point q_1 is conjugate to the *point* p_1 , with the Jacobi field illustrated by the red arrows. The point q_2 is conjugate to the *surface* K (blue line), at the point p_2 , with the Jacobi field illustrated by the green arrows. Geodesics orthogonal to K are shown in black. If a general conjugate point lies along an orthogonal null geodesic, then by Lemma 16 there exists a Jacobi field such that the conjugate point is of the *surface* type. Hence, this type of conjugacy appears in Theorem 1. 85
- 5.6 Possibilities in the proof. The sequence of timelike geodesics γ_n (black) connects K with a sequence of points $q_n \in I^+(K)$ on the orthogonal null geodesic γ (red) that joins $p \in K$ with q , after which γ leaves $\dot{I}^+(K)$ (red dashed). In the case on the left, γ' (green) is distinct from γ , so condition (iii) fails. In the case on the right, $\gamma' = \gamma$, which we prove corresponds to a failure of condition (ii). 88

- 6.1 Decomposing a lattice gauge theory into subregions a and \bar{a} requires the introduction of extra degrees of freedom (denoted as white dots) at the entangling surface (denoted by a dashed red line). 95
- A.1 Two diagrams of order N which contribute to the Green's function $\langle \vec{\phi}^2(x) \vec{\phi}^2(y) \rangle$. Solid and dashed lines represent propagators of the scalar, $\vec{\phi}$, and auxiliary field, s , respectively. The dots represent insertions of $\vec{\phi}^2$ 110

Acknowledgments

I have been fortunate to have many great role models during my time at Berkeley. I would like to thank my advisor Raphael Bousso for his guidance and sharing his excitement for his work. I am also thankful to have worked with Stefan Leichenauer and Michael Smolkin, who were both happy to discuss my ideas and were exceedingly patient in answering my questions. I appreciate that Yasunori Nomura and Birgitta Whaley agreed to be on my thesis committee, and that Holger Muller agreed to be on my qualifying exam committee.

I am grateful for my other collaborators as well— Omer Ben-Ami, Vlad Rosenhaus, Shimon Yankielowicz, Adam Levine, Jason Koeller, Arvin Shahbazi-Moghaddam, Ven Chandrasekaran, Illan Halpern, Grant Remmen, and Pratik Rath.

I would also like to thank others who made this time in the Berkeley Center for Theoretical Physics very enjoyable and intellectually rewarding: Katelin Schutz, Zach Fisher, Mudassir Moosa, Fabio Sanchez, Chris Mogni, Ning Bao, Vincent Su, Misha Usatyuk, Sean Jason Weinberg, and Christian Schmid.

Chapter 1

Introduction

To answer our universe's deepest questions, we need a theory of quantum gravity. Straightforward attempts to unify quantum mechanics and general relativity have led to inconsistencies, and cleverer connections need to be drawn.

Arguably our best window into the properties of quantum gravity is the Anti-de Sitter / Conformal Field Theory duality (AdS/CFT) [140]. This duality conjectures that a theory of quantum gravity in a $d + 1$ dimensional asymptotically-anti de Sitter (AdS) spacetime is dynamically equivalent to a conformal field theory (CFT) living on the d dimensional boundary of the AdS spacetime.

AdS/CFT has pointed to a fundamental connection between entanglement and geometry in quantum gravity. Two notable examples of this are the following.

1. The entanglement entropy of a subregion of the CFT equals the geometric area of an extremal surface embedded in AdS [171]. It seems that the entanglement of certain CFT degrees of freedom are somehow related to the AdS metric.
2. The AdS dual of a CFT in a thermal state is a black hole. But the AdS dual of two CFTs, each in a thermal state but entangled together into a joint pure state, is that of two black holes connected together by a wormhole [141]! Somehow the entanglement between the two CFTs gives rise to a geometric connection in quantum gravity.

These facts motivate an improved understanding of the detailed connection between entanglement and geometry in gravity. In this dissertation, we explore multiple facets of this connection.

Summary We start in Chapter 2 by quantifying the entanglement in a quantum field theory as a function of the curvature scale of its background. We compute the entanglement entropy of the $\mathcal{O}(N)$ vector model on a spherical time-slice as a function of the radius of the sphere. This chapter is based on reference [3].

In Chapter 3 we consider nine known geometric and entropic statements in AdS/CFT, and we present proofs of the logical relationships between each of them. Five of the ten proofs are new. This chapter is based on reference [4].

In Chapter 4, we study the near-boundary implications of entanglement wedge nesting in holographic CFTs on arbitrary curved backgrounds. We find necessary and sufficient conditions for it to imply the so-called quantum null energy condition (QNEC) in less than six spacetime dimensions. We also study the non-gravitational limit of the Quantum Focusing Conjecture (QFC), and we find that it implies the QNEC under the same geometric conditions. This chapter is based on reference [5].

Causal structure plays a key role in relating geometry and entanglement, as seen in e.g. the covariant entropy bound [20] and the GSL for holographic screens [24, 21]. In Chapter 5, we rigorously prove the connection between the boundary of the future of a surface and the null geodesics originating orthogonally from that surface. This theorem is important for proving that the area of holographic screens monotonically increase. This chapter is based on reference [2].

What are naively paradoxes in the emergence of geometry from entanglement in holographic CFTs have been understood as simply properties of quantum error-correction. Indeed, understanding the CFT as a quantum error-correcting code (QECC) has gone beyond its original purpose and explained the intimate connection between Ryu-Takayangi [171] and subregion duality. In Chapter 6, we further illustrate the power of understanding AdS/CFT as a QECC by deriving the holographic prescription for computing Renyi entropies. In the process, we learn the particular entanglement structure of the AdS degrees of freedom that might be naturally interpreted as the quantum gravity degrees of freedom that build up the geometry. This chapter is based on reference [1].

Chapter 2

Entanglement and RG in the $O(N)$ vector model

2.1 Introduction

An important aspect of quantum field theory is the renormalization group (RG) flow between conformal field theories [192, 35, 129, 128]. Recent results, such as the proof of the F-theorem by Casini and Heurta [38, 37], strongly suggest entanglement entropy plays an important role in characterizing such flows. For some recent studies of entanglement and RG, see [149, 84, 15, 157, 74, 162, 42, 85]. To date, most explicit field theoretic computations of entanglement entropy have focused on the vicinity of fixed points. It is the purpose of this paper to compute entanglement entropy along an entire RG trajectory. We do this for the interacting vector $O(N)$ model at large N in 4 and $4 - \epsilon$ dimensions.

In Sec. 2.2 we review the entanglement flow equations and recent results in perturbative calculations of entanglement entropy. We establish the setup of our problem: the Euclidean spacetime is taken to be a sphere, and the entangling surface is the bifurcation surface of the equator (see Fig. 2.1). The radius ℓ of the sphere sets the RG scale. The flow equations for the variation of entanglement entropy with respect to ℓ reduce to a one-point function of the trace of the stress-tensor.

In Sec. 2.3 we introduce the vector $O(N)$ model. Within the ϵ expansion, the RG flow is from the Gaussian fixed point in the UV to the Wilson-Fisher fixed point in the IR. We work to leading order in $1/N$, so that the dynamics is encoded in the mass gap equation. We take the theory to have arbitrary non-minimal coupling in the UV. We renormalize the theory, solve for the beta functions, and compute the expectation value of the trace of the stress-tensor.

In Sec. 2.4 we find the entanglement entropy as a function of ℓ . This follows immediately from the results of the previous sections; the general expression is presented in Sec. 2.4. It is instructive to first directly find the entanglement entropy in various limits, and in Sections 2.4, 2.4, we study the UV and IR limits, respectively. In Sec. 2.4 we warm up with the case

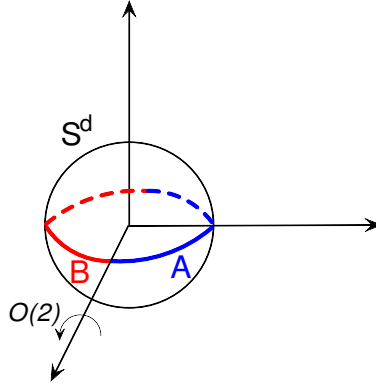


Figure 2.1: The equator of S^d is split into two equal cap-like regions A and B (shown in blue and red respectively). The entanglement entropy is the von Neumann entropy of the density matrix living on the blue region.

of strictly four dimensions; this does not have a UV fixed point, but one may still study the entanglement entropy between two points along the RG trajectory.

In Sec. 2.5 we discuss the implications of our results for computations on backgrounds with conical deficits. The entanglement flow equations imply entanglement entropy is sensitive to the amount of non-minimal coupling to gravity, even in the flat space limit and with interactions. We show this is consistent with replica-trick calculations, but only if one accounts for the contribution of the conical singularity. In fact, this conclusion is unavoidable: even if one chooses to discard such boundary terms, quantum corrections will generate them [143].

2.2 Review of Entanglement Flow Equations

In this Section we review the entanglement flow equations. The main equation, Eq. 2.8, expresses the entanglement entropy in terms of the expectation value of the trace of the stress-tensor.

Entanglement entropy is the von Neumann entropy of a reduced density matrix, ρ . The entanglement (or modular) Hamiltonian is defined through the reduced density matrix as

$$\rho = e^{-K}, \quad \text{Tr } \rho = 1. \quad (2.1)$$

It trivially follows that entanglement entropy is given by the expectation value of the entanglement Hamiltonian,

$$S_{EE} \equiv -\text{tr}(\rho \log \rho) = \langle K \rangle. \quad (2.2)$$

Viewing the expectation value in (2.2) through the Euclidean path integral representation, the entanglement flow equations [166, 165] follow:

$$\frac{\partial \mathcal{S}_{\text{EE}}}{\partial \lambda} = - \int \langle \mathcal{O}(x) K \rangle \quad (2.3)$$

$$2 \frac{\delta \mathcal{S}_{\text{EE}}}{\delta g^{\mu\nu}(x)} = - \sqrt{g(x)} \langle T_{\mu\nu}(x) K \rangle, \quad (2.4)$$

where the integral runs over the entire Euclidean manifold parametrized by x . These equations describe the change in entanglement entropy under a deformation of the coupling λ of some operator \mathcal{O} , or under a change in the background metric $g_{\mu\nu}$.¹

A planar entangling surface in Minkowski space, or a spherical entangling surface in de Sitter space, are especially useful contexts in which to study the flow equations. In these two cases the symmetry in the transverse directions to the entangling surface implies that the entanglement Hamiltonian is proportional to the boost generator (or rotation generator, in the Euclidean continuation) [121]

$$K = \int_A T_{\mu\nu} \xi^\mu n^\nu + c, \quad (2.5)$$

where n^ν is normal to the entangling surface, ξ^μ is the Killing vector associated with the symmetry, and c is a normalization constant such that $\text{Tr } \rho = 1$. It should be noted that Eq. 2.5 is valid for any Lorentz invariant quantum field theory.

Let us review a few properties of the flow equation (2.3). Since the correlator $\langle T_{ab} \mathcal{O} \rangle$ vanishes for a CFT, the change in entanglement entropy under a deformation away from a fixed point vanishes to first order in λ [165, 168]. This demonstrates the stationarity of entanglement entropy at the fixed points on a sphere, providing an affirmative answer to the question raised in [124].² The distinction between the conformally and nonconformally coupled scalar is something we will return to. The second order in λ part of entanglement entropy is fixed by the correlators $\langle T_{ab} \mathcal{O} \mathcal{O} \rangle$ and $\langle \mathcal{O} \mathcal{O} \rangle$, and is thereby completely universal: the result agrees with both free field and holographic computations [167]. And while these calculations are done for a planar entangling surface, the result for this universal entanglement entropy (log term) is independent of the shape of the entangling surface [167], as was verified holographically [119].

For a planar entangling surface, one can give an independent derivation of (2.3) [168]. In addition, through use of spectral functions, one can give a compact expression for the

¹Eq. 2.4 can also be used to study shape dependence of entanglement entropy [165], although there are unresolved issues at second order [167]. Shape dependence will not be the focus of our study, see however [176, 7, 144, 136, 36, 69, 16].

²In order to see stationarity of entanglement entropy at the conformal fixed points on a sphere, it should be the case that the stress-tensor in the correlator $\langle T_{ab} \mathcal{O} \rangle$ represents CFT degrees of freedom only. In later sections, we will find that when the IR fixed point is reached by an RG flow from the UV, this is not necessarily the case. In our case the stress-tensor for the gapped system does not vanish in the deep IR and gives rise to nonzero entanglement entropy which can be regarded as a remnant of the UV.

entanglement entropy for a general QFT [168], allowing a demonstration of the equivalence of entanglement entropy and the renormalization of Newton's constant [41, 42].

While a planar entangling surface is a useful and simple case to consider, it is a bit too simple for the study of RG flow of entanglement entropy, as it lacks any scale. A spherical entangling surface is the best suited in this regard, as the size of the sphere sets the RG scale. For an entangling surface that is a sphere in flat space, the entanglement Hamiltonian is only known for a CFT [39], which is sufficient for computing entanglement entropy perturbatively near the fixed point [68], but insufficient for finding it along an entire RG trajectory.

In this paper, we study entanglement entropy for a spherical entangling surface in de Sitter space. In this case, one knows the entanglement Hamiltonian along the entire RG trajectory, and the flow equation can be directly applied. The analytic continuation of de Sitter is a sphere S^d , and the Killing vector ξ^μ is the rotation generator. We will study the change of entanglement entropy as we vary the radius l of S^d .

Noting that variation of the radius l of the space S^d can be expressed as,

$$l \frac{\partial}{\partial l} = -2 \int g^{\mu\nu}(x) \frac{\delta}{\delta g_{\mu\nu}(x)}, \quad (2.6)$$

the flow equation (2.4) gives,

$$l \frac{dS_{\text{EE}}}{d\ell} = \int \langle T_\mu^\mu(x) K \rangle. \quad (2.7)$$

As a result of (2.5), the flow of entanglement entropy can be computed from (2.7) provided one knows the 2-pt function of the stress-tensor. In fact, a further simplification can be made. As a result of the maximal symmetry of de Sitter space, as well as the Ward identities, the 2-pt function can be reduced to a 1-pt function, turning (2.7) into [14]

$$l \frac{dS_{\text{EE}}}{d\ell} = -\frac{V_{S^d}}{d} \ell \frac{d}{d\ell} \langle T_\mu^\mu \rangle, \quad (2.8)$$

where V_{S^d} is the volume of a d -dimensional sphere of radius l . Eq. 2.8 can also be found directly from the interpretation of entanglement entropy as the thermal entropy in the static patch [14]. The flow equation in the form (2.8) will be used in Sec. 2.4 to compute entanglement entropy throughout the RG flow, from $l \rightarrow 0$ in the UV to $l \rightarrow \infty$ in the IR.

2.3 $O(N)$ on a sphere

In this Section we introduce the field theory background for the $O(N)$ model on a sphere. We work within the ϵ expansion, so as to have both the free UV and the Wilson-Fisher IR fixed points. We also work at large N , allowing us to sum the infinite class of cactus diagrams, as is concisely encoded in the mass gap equation. For the purposes of computing the β functions near the fixed points, this is equivalent to working at finite N to one-loop.

After introducing the action and the gap equation in Sec. 2.3, we renormalize the theory and compute the β functions in Sec. 2.3, and find the expectation value of the trace of the stress-tensor in Sec. 2.3.

Gap Equation

The Euclidean action of the $O(N)$ vector model living on a d -dimensional sphere of radius ℓ is given by,³

$$I = \int_{S^d} \left[\frac{1}{2} (\partial \vec{\phi})^2 + \frac{t_0}{2} \vec{\phi}^2 + \frac{1}{2} (\xi \eta_c + \eta_0) R \vec{\phi}^2 + \frac{u_0}{4N} (\vec{\phi}^2)^2 \right] + I_g, \quad (2.9)$$

where $R = \frac{d(d-1)}{\ell^2}$ is the scalar curvature and $\eta_c = \frac{d-2}{4(d-1)}$ is the conformal coupling.⁴ We take the theory to have arbitrary non-minimal coupling, parameterized by ξ ; we will be interested in letting ξ have the range $\xi \geq 0$, with $\xi = 0$ corresponding to a minimally coupled scalar and $\xi = 1$ corresponding to a conformally coupled scalar. The lower bound on ξ follows from the requirement that the theory is stable in the UV.

Since we are on a curved space, we have included I_g which describes the purely gravitational counter-terms which must be introduced to cancel the vacuum fluctuations of $\vec{\phi}$,

$$I_g = N \int_{S^d} [\Lambda_0 + \kappa_0 R + a_0 E_4 + c_0 R^2], \quad (2.10)$$

where R is the Riemann scalar and $E_4 = R_{\alpha\beta\gamma\delta} R^{\alpha\beta\gamma\delta} - 4R_{\alpha\beta} R^{\alpha\beta} + R^2$.⁵

Following the standard large N treatment, we introduce a Lagrange multiplier field s and an auxiliary field ρ , so as to write the generating function as

$$Z[\vec{J}] = \int \mathcal{D}s \mathcal{D}\rho \mathcal{D}\vec{\phi} \exp \left(-I - \vec{J} \cdot \vec{\phi} \right), \quad (2.11)$$

where the action is

$$I = \int \left[\frac{1}{2} (\partial \vec{\phi})^2 + \frac{t_0}{2} \vec{\phi}^2 + \frac{1}{2} \xi \eta_c R \vec{\phi}^2 + \frac{1}{2} s (\vec{\phi}^2 - N\rho) + \frac{N}{2} \eta_0 R \rho + N \frac{u_0}{4} \rho^2 \right] + I_g. \quad (2.12)$$

We can integrate out $\vec{\phi}$ to obtain,⁶

$$Z[\vec{J}] = \int \mathcal{D}s \mathcal{D}\rho \exp \left(-\frac{N}{2} \int \left(\frac{u_0}{2} \rho^2 - s\rho + \eta_0 R \rho \right) - \frac{N}{2} \text{Tr} \ln \hat{O}_s + \frac{1}{2} \langle \vec{J}, \hat{O}_s^{-1} \vec{J} \rangle - I_g \right), \quad (2.13)$$

where $\hat{O}_s \equiv -\square + t_0 + \xi \eta_c R + s$ and \langle, \rangle is the L^2 norm. The contours of integration for the auxiliary fields s and ρ are chosen so as to ensure that the path integral converges.

³We do not distinguish between the bare and renormalized ϕ since to leading order in $1/N$ they are identical.

⁴The bare coupling η_0 is introduced to account for the possible counter-terms associated with renormalization of the non-minimal coupling to gravity.

⁵In 4-dimensions E_4 represents the Euler density. Also, since the sphere is conformally flat, there is no Weyl tensor counterterm.

⁶There is no spontaneous symmetry breaking on a sphere, so we are always in the $O(N)$ symmetric phase.

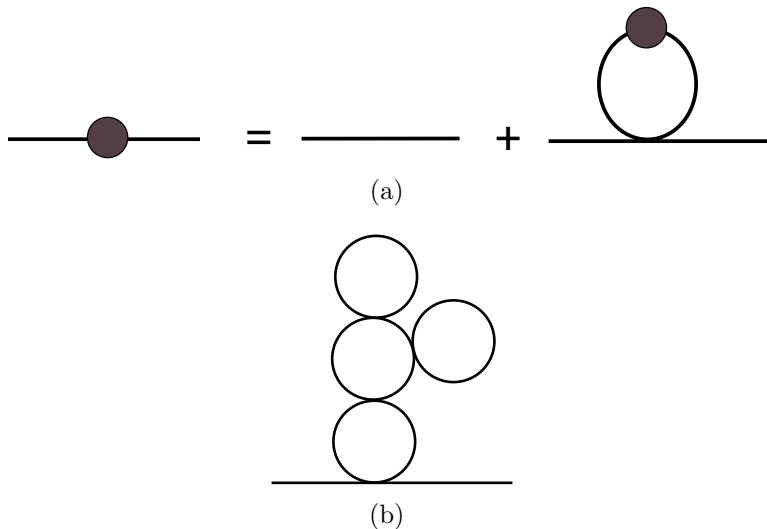


Figure 2.2: (a) At large N the Schwinger-Dyson equation for the 2-pt function simplifies to become the gap equation (2.16). (b) Iterating (a) gives a sum of cactus diagrams, such as the one shown above.

The auxiliary field ρ has trivial dynamics since it appears algebraically in the action. It can easily be integrated out,

$$Z[\vec{J}] = \int \mathcal{D}s \exp \left(-\frac{N}{2} \left(\text{Tr} \ln \hat{O}_s - \int_{S^d} \frac{(s - \eta_0 R)^2}{2u_0} \right) + \frac{1}{2} \langle \vec{J}, \hat{O}_s^{-1} \vec{J} \rangle - I_g \right), \quad (2.14)$$

The remaining auxiliary field s encodes the full dynamics of the original N physical degrees of freedom; it is an $O(N)$ singlet, which significantly simplifies the $1/N$ expansion. At large N the theory is dominated by the saddle point, $s(x) = \bar{s}$, which satisfies

$$\bar{s} = u_0 \langle \phi^2 \rangle + \eta_0 R, \quad \langle \phi^2 \rangle \equiv \langle x | \hat{O}_{\bar{s}}^{-1} | x \rangle. \quad (2.15)$$

It is convenient to re-express (2.15) in terms of the physical mass,⁷ $m^2 \equiv t_0 + \bar{s}$,

$$m^2 = t_0 + u_0 \langle \phi^2 \rangle + \eta_0 R. \quad (2.16)$$

Eq. (2.16) is the gap equation; it has a simple interpretation. At large N , fluctuations of $\vec{\phi}^2$ are suppressed, $\langle \vec{\phi}^2(x) \vec{\phi}^2(y) \rangle \approx \langle \vec{\phi}^2(x) \rangle \langle \vec{\phi}^2(y) \rangle$. The quartic interaction in the action (4.41) is thus effectively the square of a quadratic, and at leading order in $1/N$ the theory can in some sense be regarded as a free theory with the mass fixed self-consistently through (2.16). Equivalently, at large N the propagator is found by summing over all cactus diagrams (see Fig. 2.2); this sum is encoded in (2.16), as can be seen by iterating (2.16) starting with the bare mass t_0 .

⁷If the space-time is flat, then m^2 corresponds to a pole in the 2-point function.

To solve the gap equation (2.16) we need the two-point function on a sphere for a free field of mass squared $m^2 + \xi\eta_c R$,

$$\langle \phi_a(x)\phi_c(y) \rangle = \delta_{ac} \frac{l^{2-d}}{(4\pi)^{d/2}} \frac{\Gamma(\lambda)\Gamma(-\lambda + d - 1)}{\Gamma(d/2)} {}_2F_1\left(\lambda, d - 1 - \lambda, \frac{d}{2}; \cos^2 \frac{\chi}{2}\right), \quad (2.17)$$

where χ is the angle of separation between x, y and

$$\lambda = \frac{d-1}{2} + i\sqrt{(m\ell)^2 - \frac{1}{4} + \frac{d(d-2)(\xi-1)}{4}}. \quad (2.18)$$

In the limit of coincident points (2.17) becomes

$$\langle \phi^2 \rangle = \frac{\Gamma(1-d/2)\Gamma(\lambda)\Gamma(d-1-\lambda)}{\pi(4\pi)^{d/2}\ell^{d-2}} \sin\left(\frac{\pi}{2}(d-2\lambda)\right), \quad (2.19)$$

Eq. (2.19) exhibits a logarithmic divergence in the vicinity of $d = 4$, and so we must renormalize the theory.

Beta functions to leading order in $1/N$

We first consider the counter terms needed to renormalize the couplings t, u, η in the action for ϕ . This is done through use of the gap equation and the requirement of a finite mass m .

The divergent piece in the gap equation (2.16) can be obtained by expanding (2.19) in $\epsilon \equiv 4 - d \ll 1$,

$$\langle \phi^2 \rangle = \left(\frac{(1-\xi)}{4\pi^2\ell^2} - \frac{m^2}{8\pi^2} \right) \frac{m^{-\epsilon}}{\epsilon} + \mathcal{O}(\epsilon^0). \quad (2.20)$$

To ensure a finite mass gap, m^2 , the bare parameters u_0, t_0 and η_0 in Eq. (2.16) should be renormalized. To find the relation between the bare and renormalized couplings we rewrite Eq. (2.16) as,

$$\frac{m^2}{u_0} = \frac{t_0}{u_0} + \frac{\eta_0}{u_0} R - \frac{m^2\ell^\epsilon}{8\pi^2\epsilon} + \frac{(1-\xi)\ell^\epsilon}{4\pi^2\ell^2\epsilon} + \dots, \quad (2.21)$$

where ellipsis encode finite terms independent of the bare couplings. The absence of poles in the gap equation therefore gives the following relation between the bare and renormalized parameters:

$$\frac{1}{u_0} = \frac{1}{u\mu^\epsilon} - \frac{1}{8\pi^2\epsilon\mu^\epsilon}, \quad \frac{t_0}{u_0} = \frac{t}{u\mu^\epsilon}, \quad \frac{\eta_0}{u_0} = \frac{\eta}{u\mu^\epsilon} - \frac{1-\xi}{48\pi^2\epsilon\mu^\epsilon}, \quad (2.22)$$

where t, u, η are the renormalized variables and depend on the RG scale μ .⁸

⁸The couplings u and η are dimensionless, and we use the minimal subtraction scheme throughout the paper.

Applying $\mu \frac{d}{d\mu}$ to both sides of (2.22), and recalling that the bare couplings are independent of μ , leads to the following set of RG equations:

$$\begin{aligned} \beta_u &\equiv \mu \frac{du}{d\mu} = -\epsilon u + \frac{u^2}{8\pi^2} = \frac{u}{8\pi^2}(u - u^*) , \\ \beta_t &\equiv \mu \frac{dt}{d\mu} = \frac{ut}{8\pi^2} , \\ \beta_\eta &\equiv \mu \frac{d\eta}{d\mu} = \frac{u}{8\pi^2} \left(\eta - \frac{1-\xi}{6} \right) . \end{aligned} \tag{2.23}$$

Here $u^* = 8\pi^2\epsilon$ is the well-known Wilson-Fisher IR fixed point⁹, while the Gaussian UV fixed point is at $u = 0$.

Our discussion has been general, in that we have allowed the theory to have an arbitrary non-minimal coupling in the UV. Given our conventions for the coefficient of non-minimal coupling to gravity, $(\xi\eta_c + \eta_0)R\bar{\phi}^2$ in the action (4.41), we impose that $\eta = 0$ at the UV fixed point. Since the constant η_c was picked to be $\eta_c = 1/6$ in 4 dimensions, this ensures that for $\xi = 1$ the scalar is conformally coupled in the UV, while for $\xi = 0$ it is minimally coupled. In fact, (2.23) tells us that independent of our choice of ξ , the IR endpoint of the flow is the same: $\eta^* = \frac{1-\xi}{6}$ at the Wilson-Fisher fixed point, and therefore $\xi\eta_c + \eta^* = 1/6$. Thus to leading order in ϵ , a family of weakly interacting, non-conformally coupled massive scalar fields, parametrized by $\xi \geq 0$ in the vicinity of the Gaussian fixed point, all flow to the conformally coupled theory at the Wilson-Fisher fixed point.

Gravitational counter-terms and energy-momentum tensor

The β functions for u and t found in (2.23) are obviously the same as those in flat space. In addition to η , the sphere background requires the introduction of gravitational counterterms (2.10). In this section we compute their β functions; the expectation value of the trace of the energy-momentum tensor will then follow. We note that knowing the contribution of the gravitational counterterms is essentially irrelevant for our purposes. We are interested in the area law piece of entanglement entropy, which by necessity involves the mass. The contribution of the gravitational counterterms aE_4 and cR^2 only involves the sphere radius ℓ and correspondingly will give some constant contribution to the entanglement entropy. The computation of these counterterms is for completeness; the reader uninterested in the details may skip to the result, Eq. (2.41).

Our analysis and notation will closely follow the discussion in Ref. [29]. We work on an arbitrary conformally flat curved background,¹⁰ specializing to a sphere at the end. The

⁹At finite N the Wilson-Fisher fixed point is at $u^* = N \frac{8\pi^2\epsilon}{N+8} = 8\pi^2\epsilon + O(1/N)$. Note that as a result of the normalization of the quartic term in the lagrangian by a factor of N , u^* has an additional factor of N as compared to the usual ϵ expansion conventions.

¹⁰Conformally flat because we do not bother to include the Weyl tensor counter term.

relation between the bare and renormalized parameters is [29]

$$\begin{aligned}
\eta_0 &= (\eta + F_\eta)Z_2^{-1}, & Z_2^{-1} &\equiv \frac{t_0}{t}, \\
\Lambda_0 &= \mu^{d-4}(\Lambda + t_0^2 F_\Lambda), \\
\kappa_0 &= \mu^{d-4}(\kappa + 2t_0\eta_0 F_\Lambda + t_0 F_\kappa), \\
a_0 &= \mu^{d-4}(a + F_a), \\
c_0 &= \mu^{d-4}(c + \eta_0^2 F_\Lambda + \eta_0 F_\kappa + F_c),
\end{aligned} \tag{2.24}$$

where all counter terms, Z_2^{-1} , F_η , F_Λ , F_κ , F_a and F_c , are dimensionless functions of the renormalized coupling u , and we choose a scheme where they contain only an ascending series of poles in $\epsilon = 4 - d$. As argued in [29], these functions are independent of the renormalized coupling η . Furthermore, from (2.22) we immediately find,

$$\begin{aligned}
Z_2^{-1} &= \left(1 - \frac{u}{8\pi^2\epsilon}\right)^{-1}, \\
F_\eta &= \frac{(\xi - 1)u}{48\pi^2\epsilon}.
\end{aligned} \tag{2.25}$$

To calculate F_Λ and F_κ , one can use the definition of the renormalized operator $[\vec{\phi}^2]$ [29]:¹¹

$$t[\vec{\phi}^2] = t_0\vec{\phi}^2 + N\mu^{-\epsilon}t_0\left(4(t_0 + \eta_0 R)F_\Lambda + 2RF_\kappa\right), \tag{2.26}$$

and require that its vev is finite. The result is,

$$\begin{aligned}
F_\Lambda &= \frac{1}{2(4\pi)^2\epsilon} \left(1 - \frac{u}{8\pi^2\epsilon}\right), \\
F_\kappa &= \frac{\xi - 1}{96\pi^2\epsilon} \left(1 - \frac{u}{8\pi^2\epsilon}\right).
\end{aligned} \tag{2.27}$$

In Appendix A.1 we carry out an independent calculation of F_Λ , finding agreement with [74] and the above result. Using these counter terms together with (2.24), one can evaluate the RG flow equations for Λ and κ ,

$$\begin{aligned}
\mu \frac{d\Lambda}{d\mu} &= \epsilon\Lambda + \frac{t^2}{2(4\pi)^2}, \\
\mu \frac{d\kappa}{d\mu} &= \epsilon\kappa + \frac{t}{(4\pi)^2} \left(\eta - \frac{1 - \xi}{6}\right).
\end{aligned} \tag{2.28}$$

The RG equation for κ can then be solved,

$$\kappa = \frac{\eta}{2u} t + \bar{\kappa}\mu^\epsilon, \tag{2.29}$$

¹¹In our case the relative sign of the counter terms is flipped since we are using Euclidean signature.

where $\eta^* = (1 - \xi)/6$ and $\bar{\kappa}$ is some constant that will still need to be fixed.

Turning to the a and c coefficients,

$$\begin{aligned}\beta_a &\equiv \mu \frac{da}{d\mu} = \epsilon a + f_a^{(1)} , \\ \beta_c &\equiv \mu \frac{dc}{d\mu} = \epsilon c + \frac{\eta^2}{2(4\pi)^2} + \eta \frac{\xi - 1}{96\pi^2} + f_c^{(1)} ,\end{aligned}\tag{2.30}$$

where $f_a^{(1)}$ and $f_c^{(1)}$ are the residues of the simple poles in the definitions of F_a and F_c ,

$$\begin{aligned}F_a &= \frac{f_a^{(1)}}{\epsilon} + \frac{f_a^{(2)}}{\epsilon^2} + \dots , \\ F_c &= \frac{f_c^{(1)}}{\epsilon} + \frac{f_c^{(2)}}{\epsilon^2} + \dots .\end{aligned}\tag{2.31}$$

To calculate F_a and F_c we will require that the energy-momentum tensor has a finite vev.

Energy-momentum tensor

The energy-momentum tensor of the $O(N)$ model is given by $T_{\mu\nu} = T_{\mu\nu}^\phi + T_{\mu\nu}^g$ where $T_{\mu\nu}^\phi$ is the contribution from ϕ ,

$$\begin{aligned}T_{\mu\nu}^\phi &\equiv \frac{2}{\sqrt{g}} \frac{\delta I_g}{\delta g^{\mu\nu}} = \nabla_\mu \vec{\phi} \nabla_\nu \vec{\phi} - g_{\mu\nu} \left(\frac{1}{2} (\partial \vec{\phi})^2 + \frac{1}{2} t_0 \vec{\phi}^2 + \frac{1}{2} \xi \eta_c R \vec{\phi}^2 + \frac{u_0}{4N} (\vec{\phi}^2)^2 \right) \\ &\quad + \xi \eta_c R_{\mu\nu} \vec{\phi}^2 + \xi \eta_c (g_{\mu\nu} \nabla^2 - \nabla_\mu \nabla_\nu) \vec{\phi}^2 ,\end{aligned}\tag{2.32}$$

and $T_{\mu\nu}^g$ is the gravitational contribution, defined through the variation of the action,

$$T_{\mu\nu} = \frac{2}{\sqrt{g}} \frac{\delta I_g}{\delta g^{\mu\nu}}.\tag{2.33}$$

Taking the trace gives

$$T \equiv g^{\mu\nu} T_{\mu\nu} = -t_0 \vec{\phi}^2 - \frac{d-2}{2} E_0 + (d-4) \frac{u_0}{4N} (\vec{\phi}^2)^2 + (d-1)(\xi-1) \eta_c \nabla^2 \vec{\phi}^2 + T^g ,\tag{2.34}$$

where E_0 is the equation of motion operator

$$E_0 = \vec{\phi} \left(-\nabla^2 + \xi \eta_c R + t_0 + \frac{u_0}{N} (\vec{\phi}^2) \right) \vec{\phi} ,\tag{2.35}$$

and T^g is the trace of the gravitational part,

$$\frac{1}{N} T^g \equiv \frac{1}{N} g^{\mu\nu} T_{\mu\nu}^g = -d\Lambda_0 - (d-2)\kappa_0 R - (d-4)(a_0 E_4 + c_0 R^2) ,\tag{2.36}$$

where we dropped a term proportional to $\nabla^2 R$, since it vanishes on a sphere.

Taking the vev of the energy-momentum trace and using the gap equation (2.16): $\langle \vec{\phi}^2 \rangle = N(m^2 - t_0 - \eta_0 R)/u_0$, yields¹²

$$\frac{1}{N} \langle T \rangle = -\frac{t_0}{u_0} (m^2 - t_0 - \eta_0 R) + (d-4) \frac{1}{4u_0} (m^2 - t_0 - \eta_0 R)^2 + \frac{1}{N} T^g. \quad (2.37)$$

By definition, this expression is finite after the bare parameters are expressed in terms of the renormalized parameters. Substituting (2.22), (2.24), (2.25) and (2.27) into (2.37), we get after some algebra,

$$\begin{aligned} \frac{\mu^\epsilon}{N} \langle T \rangle &= \frac{m^4}{2(4\pi)^2} \left(1 - \frac{u^*}{u}\right) + \frac{t}{u} \left(t - m^2 + \frac{\epsilon}{2} \left(m^2 - \frac{t}{2}\right)\right) - (4 - \epsilon)\Lambda \\ &+ \left((\epsilon - 2)\kappa + \left(1 - \frac{\epsilon}{2}\right) \frac{\eta}{u} t + \left(\epsilon \frac{\eta}{2u} + \frac{\xi - 1}{96\pi^2}\right) m^2 \right) R \\ &+ \epsilon(a + F_a)E_4 + \epsilon \left(c - \frac{\eta^2}{4u} + F_c + \left(\frac{\xi - 1}{96\pi^2\epsilon}\right)^2 u \right) R^2 + \mathcal{O}(\epsilon^2). \end{aligned} \quad (2.38)$$

Imposing that $\langle T \rangle$ be finite leads to the following large- N results:

$$\begin{aligned} F_a &= \frac{f_a^{(1)}}{\epsilon}, \\ F_c &= \frac{f_c^{(1)}}{\epsilon} - \left(\frac{\xi - 1}{96\pi^2}\right)^2 \frac{u}{\epsilon^2}. \end{aligned} \quad (2.39)$$

Both $f_a^{(1)}$ and $f_c^{(1)}$ are not fixed. However, to leading order in $1/N$ they are identical to their free field values, and we get

$$\begin{aligned} F_a &= \frac{-1}{360(4\pi)^2\epsilon}, \\ F_c &= -\left(\frac{\xi - 1}{96\pi^2}\right)^2 \frac{u}{\epsilon^2}. \end{aligned} \quad (2.40)$$

Combining with (2.29), the final expression for the trace of energy-momentum tensor takes the form

$$\begin{aligned} \frac{\mu^\epsilon}{N} \langle T \rangle &= \frac{m^4}{2(4\pi)^2} \left(1 - \frac{u^*}{u}\right) + \frac{t}{u} \left(t - m^2 + \frac{\epsilon}{2} \left(m^2 - \frac{t}{2}\right)\right) - (4 - \epsilon)\Lambda \\ &+ \left((\epsilon - 2)\bar{\kappa}\mu^\epsilon + \left(\epsilon \frac{\eta}{2u} + \frac{\xi - 1}{96\pi^2}\right) m^2 \right) R \\ &+ \epsilon \left(a - \frac{1}{360(4\pi)^2\epsilon} \right) E_4 + \epsilon \left(c - \frac{\eta^2}{4u} \right) R^2 + \mathcal{O}(\epsilon^2), \end{aligned} \quad (2.41)$$

¹²Note that the vev of the equation of motion operator vanishes identically. The same holds for vevs of total derivatives on a sphere.

where recall that R is the curvature of the sphere, the renormalized couplings are evaluated at RG scale μ , the constant ξ parameterizes the non-minimal coupling ($\xi = 1$ for conformally coupled), and m is the physical mass found through the gap equation. In the next section, we use (2.41) to calculate entanglement entropy.

2.4 Entanglement entropy

Having assembled the necessary field theory ingredients in the previous section, we now compute the entanglement entropy. In what follows we account for the leading order in $1/N$ contributions.

The entanglement entropy is found by solving the flow equation (2.8), which involves the derivative of $\langle T \rangle$ (2.41) with respect to the sphere radius ℓ . Since the renormalized couplings t, u, η, κ are independent of ℓ ,¹³ we get

$$\ell \frac{dS_{\text{EE}}}{d\ell} = -\frac{2\pi N A_{\Sigma} \mu^{-\epsilon}}{(4-\epsilon)(3-\epsilon)} \ell^2 \left(\frac{m^2}{(4\pi)^2} \left(1 - \frac{u^*}{u} \right) \ell \frac{dm^2}{d\ell} + \frac{t}{u} \left(\frac{\epsilon}{2} - 1 \right) \ell \frac{dm^2}{d\ell} - 2(\epsilon - 2)\bar{\kappa}\mu^{\epsilon} R \right) + s_0, \quad (2.42)$$

where A_{Σ} is the area of the entangling surface $\Sigma = S^{d-2}$, s_0 collectively denotes the contribution of curvature square terms in (2.41), and we used solutions of RG equations for κ and η/u to simplify the linear curvature term in (2.41), see (2.29) and (2.66). We ignore the s_0 terms as they are m -independent, and therefore just give some constant contribution to the entanglement entropy. The solution for entanglement entropy along the RG trajectory follows upon substituting the solutions of the gap equation (2.16) and the beta functions (2.23) into (2.42) and integrating.

There are, however, a few caveats associated with the standard ambiguities of renormalization. Indeed, the couplings in the above expression depend on an arbitrary RG scale, μ , as well as on the choice of renormalization scheme. This ambiguity is unsurprising, and reflects the well-known fact that entanglement entropy in field theory depends on the details of the regularization procedure, and is therefore scheme dependent. However, certain contributions to the entanglement entropy, ‘universal entanglement entropy’, are unaffected by a change in the regularization scheme. It is these terms that we will be interested in calculating.

There are three competing scales: μ , ℓ , and the asymptotic mass m_{∞} given through the solution of the gap equation (2.16) in the limit of flat space.¹⁴ Since the curvature of the sphere sets the characteristic energy scale, we must have $\mu \sim \ell^{-1}$. The constant of proportionality between μ and ℓ^{-1} is arbitrary, though this is no different than the usual freedom to rescale μ . In our context, this constant of proportionality is exchanged for the entanglement entropy at some radius ℓ . Or, put differently, we can express the entanglement entropy at radius ℓ_1 in terms of the entanglement entropy at some other radius ℓ_0 .

¹³The couplings of local interactions should not know about the global geometry.

¹⁴It is apparent that m should depend on ℓ : the mass was found by summing cactus diagrams, which probe the entire sphere.

Furthermore, there is a substantial difference between the two cases characterized by $\epsilon = 0$ and $\epsilon \neq 0$. In the former case the theory is not UV complete; as $m\ell$ runs from small to large values, it flows from a nonconformal interacting field theory in the UV to a Gaussian IR fixed point. In contrast, for finite $\epsilon \ll 1$, the system flows from the Gaussian UV fixed point at $m_\infty \ell \ll \epsilon \ll 1$, into the interacting Wilson-Fisher IR fixed point at $m_\infty \ell \gg \epsilon^{-1} \gg 1$. In particular, there is no smooth limit which interpolates between the two cases, and we analyze them separately. We consider $\epsilon = 0$ in Sec. 2.4, and finite ϵ in Sec. 2.4, 2.4, and 2.4. Note that in 4-dimensions, the coefficient of the log term is universal. In $4 - \epsilon$ dimensions there is no log term, however a $1/\epsilon$ term turns into a log in the limit of $\epsilon \rightarrow 0$.

Four dimensions

In this section we compute the entanglement entropy in 4 dimensions. Taking the limit $\epsilon \rightarrow 0$ results in the following RG flow equations,

$$\begin{aligned} \mu \frac{du}{d\mu} &= \frac{u^2}{8\pi^2}, \\ \mu \frac{d}{d\mu} \left(\frac{\eta}{u} \right) &= \frac{\xi - 1}{48\pi^2}. \end{aligned} \quad (2.43)$$

Integrating gives,

$$\begin{aligned} u(\mu) &= \frac{u_0}{1 - \frac{u_0}{8\pi^2} \log(\mu\delta)}, \\ \frac{\eta}{u} &= \frac{\xi - 1}{48\pi^2} \log(\mu\delta), \end{aligned} \quad (2.44)$$

where we imposed the initial conditions $(u, \eta) = (u_0, 0)$ at the UV scale δ . In the deep IR (2.44) gives $(0, (1 - \xi)/6)$.

The 4D counterparts of (2.41) and (2.42) are

$$\frac{\langle T \rangle}{N} = \frac{m^4}{2(4\pi)^2} + \frac{t}{u} (t - m^2) - 4\Lambda - \left(2\bar{\kappa} + \frac{1 - \xi}{96\pi^2} m^2 \right) R - \frac{E_4}{360(4\pi)^2}, \quad (2.45)$$

and

$$\ell \frac{dS_{\text{EE}}}{d\ell} = \frac{\pi N A_\Sigma}{6} \ell^2 \left(\frac{t}{u} \ell \frac{dm^2}{d\ell} - 4\bar{\kappa} R \right) + s_0, \quad (2.46)$$

while the gap equation (2.16) can be succinctly written as

$$\frac{t}{u} = \frac{m^2}{u(m)} - \frac{\xi - 1}{4\pi^2 \ell^2} \log(m\delta) - \langle \phi^2 \rangle_{\text{reg}}, \quad (2.47)$$

where we used (2.44), and the last term denotes the regular part of the 4D two-point function in the limit of coincident points, see (2.20),

$$\langle \phi^2 \rangle_{\text{reg}} \equiv \lim_{\epsilon \rightarrow 0} \left[\langle x | (-\square + m^2 + \xi \eta_c R)^{-1} | x \rangle - \left(\frac{(1-\xi)}{4\pi^2 \ell^2} - \frac{m^2}{8\pi^2} \right) \frac{m^{-\epsilon}}{\epsilon} \right]. \quad (2.48)$$

Applying a derivative with respect to ℓ to both sides of (2.47), yields

$$\ell \frac{dm^2}{d\ell} \left(1 + \frac{u(m)}{8\pi^2} \left(\frac{1-\xi}{(m\ell)^2} - \frac{1}{2} \right) \right) = u(m) \frac{1-\xi}{2\pi^2 \ell^2} \log(m\delta) + u(m) \ell \frac{d}{d\ell} \langle \phi^2 \rangle_{\text{reg}} \quad (2.49)$$

This expression together with (2.46) and (2.47) provides a full solution for entanglement entropy flow on a sphere. Note that the RG scale μ is completely eliminated from the final answer. Effectively its role is played by the radius of the sphere, ℓ , as the curvature of the background sets the characteristic energy scale for excitations. In particular, the deep IR and UV are defined by $m\ell \gg 1$ and $m\ell \ll 1$, respectively. Of course, we have assumed that the physical scales m and ℓ are far away from the microscopic UV cut off δ ,

$$m\delta \ll 1 \quad \text{and} \quad \ell \gg \delta. \quad (2.50)$$

Now we explicitly evaluate EE in the UV and IR regimes. We start from the former. Using (2.19) to evaluate $\langle \phi^2 \rangle_{\text{reg}}$ and substituting the result into (2.49), yields¹⁵

$$\ell \frac{dm^2}{d\ell} \Big|_{m\ell \ll 1} = u(m) \frac{\xi - 1}{2\pi^2 \ell^2} (\log(m\ell) - \log(m\delta) + \dots) + \mathcal{O}(u(m)^2), \quad (2.51)$$

where ellipsis denote subleading terms in $m\ell \ll 1$. Similarly, from the gap equation (2.47), we get

$$u(m) \frac{t(\mu)}{u(\mu)} \Big|_{m\ell \ll 1} = m^2 + 2 \frac{\xi - 1}{\ell^2} + \dots. \quad (2.52)$$

Only the first term on the right hand side contributes to the ‘area law’, while other terms are either subleading corrections or contribute to a constant term in the entanglement entropy. Hence,

$$\ell \frac{dS_{\text{EE}}}{d\ell} \Big|_{m\ell \ll 1} = N(\xi - 1) \frac{A_\Sigma m^2}{12\pi} \log \frac{\ell}{\delta} - 8\pi N A_\Sigma \bar{\kappa} + \dots, \quad (2.53)$$

Similarly, in the IR regime we have

$$\ell \frac{dS_{\text{EE}}}{d\ell} \Big|_{m\ell \gg 1} = N(1 - \xi) \frac{A_\Sigma m^2}{12\pi} \log(m\delta) - 8\pi N A_\Sigma \bar{\kappa} + \dots. \quad (2.54)$$

The above behavior of entanglement entropy has a simple physical interpretation. In the UV regime we have $1 \ll \frac{\ell}{\delta} \ll \frac{1}{m\delta}$, and the universal ‘area law’ of entanglement scales as

¹⁵Note that based on (2.50) $u(m) \simeq -\frac{8\pi^2}{\log(m\delta)} \ll 1$

$\ell^2 \log(\ell/\delta)$, i.e., there is a logarithmic enhancement relative to the standard growth $\sim \ell^2$. This enhancement persists as we increase ℓ until $\ell m \sim 1$ is reached. Effectively, the universal ‘area law’ at $m\ell \sim 1$ is built from all the massive degrees of freedom which have almost decoupled at this point. As we continue increasing ℓ , the universal ‘area law’ continues growing like ℓ^2 until the hierarchy of scales is reversed, $1 \ll \frac{1}{m\delta} \ll \frac{\ell}{\delta}$, and the flow terminates at the IR fixed point.

In particular, the logarithmic ‘area law’ in the deep IR represents entanglement of UV degrees of freedom. It has nothing to do with the IR field theory, which is empty in our case. As was noted in [165, 168] (see Sec. 2.2), the universal entanglement entropy vanishes for a conformally coupled scalar. Setting $\xi = 1$ in (2.54) and (2.53) recovers this result.

Wilson-Fisher fixed point

In this section we calculate the entanglement entropy at the Wilson-Fisher fixed point in $4 - \epsilon$ dimensions. This requires evaluating the right hand side of (2.42), which involves the derivative of m^2 with respect to ℓ .

We start by expanding (2.19) in $m\ell \gg \epsilon^{-1} \gg 1$,¹⁶

$$\langle \phi^2 \rangle = \frac{(4\pi)^{\frac{\epsilon}{2}}}{(2\pi)^2 \epsilon (\epsilon - 2)} \Gamma\left(1 + \frac{\epsilon}{2}\right) m^{2-\epsilon} \left(1 - \frac{(\epsilon - 4)(\epsilon - 2)(6(1 - \xi) + \epsilon(3\xi - 2))}{24(m\ell)^2} + \mathcal{O}((m\ell)^{-4})\right) \quad (2.55)$$

Now using (2.16), (2.22) and (2.55) results in

$$t^* = \frac{2(4\pi)^{\frac{\epsilon}{2}}}{(2 - \epsilon)} \Gamma\left(1 + \frac{\epsilon}{2}\right) m^2 \left(\frac{m}{\mu}\right)^{-\epsilon} \left(1 - \frac{(\epsilon - 4)(\epsilon - 2)(6(1 - \xi) + \epsilon(3\xi - 2))}{24(m\ell)^2} + \mathcal{O}((m\ell)^{-4})\right), \quad (2.56)$$

where the asterisk in t^* denotes that the system sits at the Wilson-Fisher fixed point. Differentiating (2.56) with respect to ℓ yields,

$$\ell \frac{dm^2}{d\ell} \Big|_{m\ell \gg 1} = m^2 \left(-\frac{(\epsilon + 2)(\epsilon - 4)(\epsilon - 2)(6(1 - \xi) + \epsilon(3\xi - 2))}{24(m\ell)^2} + \mathcal{O}((m\ell)^{-4}) \right), \quad (2.57)$$

Substituting this expression and (2.56) into (2.42) gives

$$\begin{aligned} \ell \frac{dS_{\text{EE}}}{d\ell} \Big|_{m\ell \gg 1} &= \frac{(4\pi)^{\frac{\epsilon}{2}-1} (\epsilon - 2)(6(1 - \xi) + \epsilon(3\xi - 2))}{12 \epsilon (3 - \epsilon)} \Gamma\left(2 + \frac{\epsilon}{2}\right) N A_{\Sigma} m^{2-\epsilon} \left(1 + \mathcal{O}((m\ell)^{-2})\right) \\ &+ 4\pi(\epsilon - 2) N A_{\Sigma} \bar{\kappa} + s_0, \end{aligned} \quad (2.58)$$

The first thing to note about (2.58) is that the ‘area law’ term does not have any μ -dependence, and therefore it is not sensitive to the constant of proportionality in the relation

¹⁶We do not expand in ϵ . Note also that $\mathcal{O}((m\ell)^{-4})$ and higher order terms in (2.55) are proportional to ϵ , and therefore they do not contribute to the divergence of $\langle \phi^2 \rangle$ when $\epsilon \rightarrow 0$.

$\mu \sim \ell^{-1}$, i.e., as expected, the value of entanglement entropy at the fixed point is invariant under reparametrizations of the RG trajectory.

It is instructive to compare (2.58) with its counterpart in [143]. The results in [143] are intrinsic to the Wilson-Fisher fixed point since their setup, unlike ours, confines the RG flow to the IR end. The geometry in [143] is flat, and therefore the gravitational coupling, $\bar{\kappa}$, which appears in (2.58) is absent. In addition, as we argue in section 2.5, the computation of [143] corresponds to $\xi = 1$ at the Wilson-Fisher fixed point. Thus, to leading order in $\epsilon \ll 1$, Eq. (2.58) reduces to

$$\ell \frac{dS_{\text{EE}}}{d\ell} \Big|_{m\ell \gg 1} \simeq -N \frac{A_{\Sigma} m_{\infty}^{2-\epsilon}}{72\pi} \Leftrightarrow S_{\text{EE}} \simeq -N \frac{A_{\Sigma} m_{\infty}^{2-\epsilon}}{144\pi}, \quad (2.59)$$

where m_{∞} is the mass gap in the limit of flat space. Eq. (2.59) is in agreement with [143]. A simple derivation of (2.59) was later given by Casini, Mazzitelli and Testé [41]. The authors noticed that to leading order in ϵ , the anomalous dimension vanishes at the Wilson-Fisher fixed point, and thus (2.59) may be found from the entanglement entropy for a free field. One distinction between our work and that of [41], is that [41] advocates that the entanglement Hamiltonian has a discontinuous jump at the UV fixed point. Namely, that the entanglement entropy takes the value for the minimally coupled scalar at the free field endpoint of the RG trajectory, whereas it takes the conformally coupled value at all other locations. In our setup, the entanglement entropy behaves smoothly along the entire RG trajectory. As found from the beta functions (2.23), starting with either a minimally or nonminimally coupled field in the UV leads to the conformally coupled field in the IR.

Let us now expand the numerical coefficient of the ‘area law’ term in (2.58) in $\epsilon \ll 1$

$$\begin{aligned} \ell \frac{dS_{\text{EE}}}{d\ell} \Big|_{m\ell \gg 1} &= \frac{N A_{\Sigma} m^{2-\epsilon}}{12} \left(\frac{-1}{6\pi} + (\xi - 1) \left(\frac{1}{\pi\epsilon} - \frac{2\gamma + 2/3 - 2 \log(4\pi)}{4\pi} \right) + \mathcal{O}(\epsilon, (m\ell)^{-2}) \right) \\ &+ 4\pi(\epsilon - 2) N A_{\Sigma} \bar{\kappa} + s_0. \end{aligned} \quad (2.60)$$

In the next section, we will see that the $1/\epsilon$ term in (2.60) is associated with UV degrees of freedom.¹⁷ The presence of this UV remnant is a result of using the full energy-momentum tensor (2.41) to calculate entanglement entropy at any scale $\mu \sim \ell^{-1}$.

To isolate entanglement entropy intrinsic to the scale ℓ , one needs to use some kind of subtraction scheme. There is no unique or preferred choice of such a scheme. Renormalized entanglement entropy [138] is one possibility. This prescription proved to be particularly powerful in three dimensions, and was used in the proof [38] of the F-theorem [118], see also [44]. Unfortunately, it is not clear that renormalized entanglement entropy has analogous properties, such as monotonicity, in integer dimensions higher than the 3; nor is it clear how to apply it in non-integer dimensions.

For the particular choice of $\xi = 1$, the theory is conformally coupled along the entire RG trajectory, and the contribution of UV degrees of freedom to the ‘area law’ in the vicinity of

¹⁷The IR theory is empty, as we have only massive degrees of freedom which decouple in the deep IR.

$d = 4$ ($\epsilon = 0$) vanishes. Since in this case (2.58) is not contaminated by UV physics, it can be used to find an approximation for entanglement entropy at the interacting IR fixed point in three dimensional flat space. Substituting $\xi = \epsilon = 1$ and $\bar{\kappa} = 0$ into (2.58), gives

$$S_{\text{EE}}^{\text{IR}} \Big|_{d=3} \simeq -\frac{N}{64} m A_{\Sigma} . \quad (2.61)$$

We note that the constant $\bar{\kappa}$ is arbitrary; it can be exchanged for the entanglement entropy at some scale l_1 . A choice that would seem natural is to demand that entanglement entropy vanishes in the deep IR (as a result of the mass gap, all degrees of freedom decouple in the IR, and the Wilson-Fisher fixed point is thus empty). This results in

$$S_{\text{EE}} \Big|_{m\ell \gg 1} = 0 \quad \Rightarrow \quad \bar{\kappa} = m^{2-\epsilon} \frac{(4\pi)^{\frac{\epsilon}{2}-2} (6(\xi-1) - \epsilon(3\xi-2))}{12\epsilon(3-\epsilon)} \Gamma\left(2 + \frac{\epsilon}{2}\right) . \quad (2.62)$$

The above subtraction scheme is special to a curved manifold with nondynamical gravity, where there is an extra parameter $\bar{\kappa}$. However in flat space $\bar{\kappa} = 0$, and one is forced to adopt a different subtraction scheme. Another drawback of the choice (2.62) is that it modifies entanglement entropy at all points along the RG trajectory, and not only in the deep IR limit. The latter makes it difficult to extrapolate the results for an ‘area law’ on a sphere to flat space which has no analog of $\bar{\kappa}$. In what follows we simply leave $\bar{\kappa}$ unspecified.

Gaussian fixed point

This time we expand (2.19) in $m\ell \ll \epsilon \ll 1$. In this regime the theory flows to the Gaussian UV fixed point where u asymptotically vanishes, $u \ll \epsilon$. From the gap equation,

$$\langle \phi^2 \rangle \Big|_{m\ell \ll 1} = \alpha_1 m^2 \ell^\epsilon \left(\frac{1}{(m\ell)^2} + \alpha_2 + \mathcal{O}((m\ell)^2) \right) , \quad (2.63)$$

where $\lambda_0 = \lambda|_{m\ell=0}$ and for brevity we introduced the following constants

$$\begin{aligned} \alpha_1 &\equiv \frac{\Gamma\left(\frac{\epsilon-2}{2}\right) \Gamma(\lambda_0) \Gamma(\bar{\lambda}_0) \cosh\left(\frac{\pi(\lambda_0 - \bar{\lambda}_0)}{4i}\right)}{\pi(4\pi)^{\frac{4-\epsilon}{2}}} , \\ \alpha_2 &\equiv 2 \frac{\psi(\bar{\lambda}_0) - \psi(\lambda_0) + i\pi \tanh\left(\frac{\pi(\lambda_0 - \bar{\lambda}_0)}{4i}\right)}{\lambda_0 - \bar{\lambda}_0} , \end{aligned} \quad (2.64)$$

where $\psi(\lambda)$ is the digamma function. The two terms that we kept in (2.63) are the only ones that diverge as $\epsilon \rightarrow 0$. We now substitute this expansion into (2.16) and use (2.22)

$$m^2 \left(\frac{1}{u} - \frac{1}{8\pi^2\epsilon} \right) = \frac{t}{u} + \alpha_1 m^2 (\mu\ell)^\epsilon \left(\frac{1}{(m\ell)^2} + \alpha_2 + \mathcal{O}((m\ell)^2) \right) + \left(\frac{\eta}{u} - \frac{1-\xi}{48\pi^2\epsilon} \right) R . \quad (2.65)$$

Solving the RG equation for η and u gives

$$\frac{\eta}{u} = \frac{1-\xi}{48\pi^2\epsilon} . \quad (2.66)$$

Hence, we can drop the last term in (2.65),

$$\ell \frac{dm^2}{d\ell} \Big|_{m\ell \ll 1} = u \alpha_1 m^2 (\mu\ell)^\epsilon \left(\frac{\epsilon - 2}{(m\ell)^2} + \epsilon \alpha_2 + \mathcal{O}((m\ell)^2) \right) + \mathcal{O}(u^2). \quad (2.67)$$

Substituting (2.65) and (2.67) into (2.42), we finally deduce,

$$\ell \frac{dS_{\text{EE}}}{d\ell} \Big|_{m\ell \ll 1} = -\frac{2\pi\alpha_1(2-\epsilon)}{(4-\epsilon)(3-\epsilon)} N A_\Sigma m^2 \ell^\epsilon \left(1 + \mathcal{O}(u) \right) + 4\pi(\epsilon - 2) N A_\Sigma \bar{\kappa} + \mathcal{O}((m\ell)^4) + s_0. \quad (2.68)$$

Expanding the coefficient of $A_\Sigma m^2 \ell^\epsilon$ in $\epsilon \ll 1$, we get

$$\ell \frac{dS_{\text{EE}}}{d\ell} \Big|_{m\ell \ll 1} = N A_\Sigma m^2 \ell^\epsilon \left(\frac{\xi - 1}{12\pi\epsilon} + \mathcal{O}(\epsilon, u) \right) + 4\pi(\epsilon - 2) N A_\Sigma \bar{\kappa} + \mathcal{O}((m\ell)^4) + s_0. \quad (2.69)$$

As in the previous case, the μ dependence drops out of the final answer. While we implicitly assumed that $\mu \sim \ell^{-1}$, the final answer for entanglement entropy at the fixed point should not be sensitive to the $\mathcal{O}(1)$ coefficient of proportionality between μ and ℓ . Furthermore, the $1/\epsilon$ term is the same term that appears in (2.58), which, as mentioned in the previous section and now seen explicitly in (2.69), represents entanglement entropy of the UV degrees of freedom.

For a minimally coupled scalar field, $\xi = 0$, and we recover the well-known universal ‘area law’, in agreement with [143] and [105, 112, 135] (this is just N times the answer for a free scalar). If, however, the field is non-minimally coupled, we get a different answer which vanishes at the conformal point $\xi = 1$. In Sec. 2.5, we show how to generalize the calculation at the Gaussian fixed point presented in [143], so as to take into account the contribution from non-minimal coupling.

Along the RG trajectory

In this section we write down the entanglement entropy for the $O(N)$ model for a conformally coupled scalar, at leading order in $1/N$ in dimension $4 - \epsilon$, for any sphere of radius ℓ . The ingredients have been worked out in the previous sections; here we just collect them.

Solving the RG equation (2.23) gives

$$u(\mu) = \frac{u^*}{1 + \left(\frac{\mu}{\mu_0}\right)^\epsilon}, \quad (2.70)$$

where μ_0 is an arbitrary constant scale and u^* is u at the Wilson-Fisher fixed point. We want to take $\mu = 1/\ell$, and we let $\mu_0 = \ell_0^{-1}$.¹⁸ We will write this as

$$u(\ell) = \frac{u^*}{1 + \left(\frac{\ell_0}{\ell}\right)^\epsilon}. \quad (2.71)$$

¹⁸Since the only scale is ℓ , it must be that μ is proportional to ℓ^{-1} . The constant of proportionality can be absorbed into μ_0 .

Note that the entanglement entropy will contain the constant ℓ_0 . This is analogous to how correlation functions contain an arbitrary scale which is calibrated through some measurement. In our context, it means entanglement entropy needs to be measured at one value of ℓ , and can then be predicted at all other values.

The gap equation is given by

$$m^2 \left(\frac{1}{u} - \frac{1}{u^*} \right) = \frac{t}{u} + \ell^{-\epsilon} \langle \phi^2 \rangle, \tag{2.72}$$

where for simplicity we chose $\xi = 1$ (hence, $\eta = 0$ along the entire RG flow) and $\langle \phi^2 \rangle$ is given by (2.19). Also,

$$\ell \frac{d}{d\ell} (\ell^{-\epsilon} \langle \phi^2 \rangle) = \left(\ell \frac{d\lambda}{d\ell} \frac{\partial}{\partial \lambda} - 2 \right) (\ell^{-\epsilon} \langle \phi^2 \rangle), \tag{2.73}$$

where λ is a function of $m\ell$ and is given by (2.18). Differentiating (2.72) and using (2.73), we can solve for $\ell \frac{dm^2}{d\ell}$.

The entanglement entropy is given by (2.42), where we substitute $u(\ell)$ given by (2.71) and t/u given by (2.72). We thus have a complete expression for entanglement entropy in terms of the mass m and radius ℓ .

2.5 Boundary perturbations

In the previous Section we computed entanglement entropy along the entire RG flow, and in particular in the proximity of the fixed points. The entanglement entropy was found to be sensitive to the non-minimal coupling parameter ξ . This sensitivity is robust: it persists in the flat space limit, and away from the UV fixed point.

In light of these results, in this Section we revisit the replica-trick calculations of entanglement entropy near fixed points. The fact that entanglement entropy depends on ξ , even in flat space, is manifest in the context of the replica-trick, and is a consequence of the curvature associated with the conical singularity. What is unclear is if this boundary term which gives ξ dependence is real, or an artifact of the replica-trick which should be discarded. The results of Sec. 2.4 suggest the former.

In Sec. 2.5 we review the replica-trick calculation of entanglement entropy for a free scalar field using heat kernel techniques. In Sec. 2.5 we review a calculation of Metlitski, Fuertes, and Sachdev [143] which finds that loop corrections generate a boundary term, and we argue that this has a simple interpretation as the classical boundary term of Sec. 2.5 due to the curvature of the conical singularity. In Sec. 2.5 we generalize the calculation of [143] of entanglement entropy at the Gaussian fixed point, so as to incorporate non-minimal coupling, and find agreement with the results of Sec. 2.4.

Replica trick: Free energy

Here we perform the standard replica trick calculation for a free massive scalar [120, 31, 181]. Recall that entanglement entropy is computed from the variation of the free energy,

$$S = \left(\beta \frac{\partial}{\partial \beta} - 1 \right) \Big|_{\beta=2\pi} (\beta F) , \tag{2.74}$$

where the effective action (βF) is evaluated on a space which is a cone with a deficit angle $2\pi - \beta$. Eq. (2.74) is just the standard thermodynamic equation for entropy; the need to vary the temperature away from $1/2\pi$ introduces a conical singularity at the origin. The effective action, after integrating out the matter, is expanded in derivatives of the metric,

$$\beta F = -\frac{1}{2} \int_{\mathcal{M}} \int_{\delta^2}^{\infty} \frac{ds}{(4\pi s)^{d/2}} e^{-sm^2} \left(\frac{c_0}{s} + c_1 R + \mathcal{O}(s) \right) \tag{2.75}$$

The relevant term is the one proportional to the scalar curvature, whose integral on a cone is $\int_{\mathcal{M}} R = 2\mathcal{A}_{\Sigma} (2\pi - \beta)$. Thus the entropy is,

$$S = 2\pi c_1 \mathcal{A}_{\Sigma} \int_{\delta^2}^{\infty} \frac{ds}{(4\pi s)^{d/2}} e^{-sm^2} . \tag{2.76}$$

Specializing to $d = 4$ and expanding the exponential in (2.76) to extract the log divergent piece, we get,

$$S = \frac{c_1}{4\pi} m^2 \mathcal{A}_{\Sigma} \log(\delta) . \tag{2.77}$$

For the minimally coupled scalar $c_1 = 1/6$, while for the conformally coupled scalar $c_1 = 0$ [183].

This computation is, of course, not new. However, it conflicts with the belief that (in the flat space limit) entanglement entropy should, like correlation functions, be unable to distinguish a minimally from nonminimally coupled scalar field. The agreement of (2.77) with the independent results of Sec. 2.4 suggests Eq. (2.77) should be taken seriously.

Loops generate a boundary term

In [143] entanglement entropy is computed using the replica-trick approach. Introducing the standard replica symmetry around a given codimension-two entangling surface, the entanglement entropy is given by

$$S_{\text{EE}} = \lim_{n \rightarrow 1} \frac{1}{1-n} \log \frac{Z_n}{Z_1^n} , \tag{2.78}$$

where Z_n is the partition function of the theory on an n -sheeted Riemannian manifold, \mathcal{M}_n . The entangling surface is where the n sheets are glued together, and is the location of the conical singularity. In computing correlation functions on \mathcal{M}_n , it is important to note that

\mathcal{M}_n has separate translation symmetries in the directions parallel to the entangling surface, and in the directions orthogonal to it. Clearly, the entangling surface is a special location.

In [143] the authors consider the loop corrections that a correlation function on \mathcal{M}_n , such as a two-point function, will receive from interactions. They find that as a result of loops in the vicinity of the entangling surface, new divergences are generated, forcing the introduction of a boundary counter-term in the action,

$$\delta I = \frac{c}{2} \int_{\Sigma} \vec{\phi}^2, \tag{2.79}$$

where the integral is restricted to the entangling surface, Σ . Performing an RG analysis gives (to leading order in the large- N expansion) the renormalized coupling, c , at the Wilson-Fisher fixed point [143]

$$c^* = -\frac{2\pi}{3}(n-1). \tag{2.80}$$

In fact, as we now show, this result has a simple interpretation in terms of the conformal coupling to the background metric. Recall that the action (4.41) contains the term $\int \frac{1}{2}(\xi\eta_c + \eta_0)R\phi^2$. Solving the RG equations, we found in Sec. 2.3 that at the Wilson-Fisher fixed point $\eta^* + \xi\eta_c = 1/6$ to leading order in ϵ . At the Wilson-Fisher fixed point this part of the action is therefore,

$$\delta I = \frac{1}{12} \int R \phi^2. \tag{2.81}$$

As we have mentioned before, and is reflected in (2.81), the RG flow leads to conformal coupling in the IR, regardless of the non-minimal coupling ξ in the UV. Now we need to evaluate (2.81) on the background \mathcal{M}_n . Recall that to linear order in $(n-1)$, the expansion of the curvature scalar, $R^{(n)}$, on a replicated manifold is given by [80]

$$R^{(n)} = R^{\text{reg}} + 4\pi(1-n)\delta_{\Sigma} + \dots, \tag{2.82}$$

where R^{reg} is the regular curvature in the absence of the conical defect. The term δ_{Σ} is a two-dimensional delta function with support on the entangling surface Σ , and reduces the d -dimensional integral over the entire manifold to an integral over the entangling surface.¹⁹ Inserting (2.82) into (2.81) gives

$$\delta I = -\frac{\pi}{3}(n-1) \int_{\Sigma} \phi^2, \tag{2.83}$$

in agreement with (2.79) i.e., the induced boundary perturbation (2.79) is just the conformally coupled action evaluated on the conical defect.

¹⁹The higher order terms in (2.82) are ambiguous [80], and therefore in general only linear order terms in $(n-1)$ are reliable.

Including non-minimal coupling

In Sec. 2.5 we showed that entanglement entropy for a free scalar is different depending on if the scalar is minimally or conformally coupled. The calculation was done using the replica trick, combined with heat kernel techniques. In [143], entanglement entropy was calculated at the Gaussian fixed point using the replica trick, and by evaluating a 2-pt function on the conical background. The computation in [143] was implicitly for a minimally coupled scalar. For completeness, here we generalize the calculation to incorporate non-minimal coupling,

At the Gaussian fixed point the action for the $O(N)$ model simplifies to

$$I = \int \left(\frac{1}{2} (\partial \vec{\phi})^2 + \frac{t}{2} \vec{\phi}^2 + \frac{1}{2} \xi \eta_c R \vec{\phi}^2 \right). \quad (2.84)$$

It follows from (2.78) that,

$$\frac{d}{dt} S_{\text{EE}} = \lim_{n \rightarrow 1} \frac{1}{1-n} \frac{d}{dt} \log \frac{Z_n}{Z_1}. \quad (2.85)$$

Using (2.82) to expand Z_n , and keeping only terms of order $n-1$,

$$Z_n = \int \mathcal{D}\phi \left(1 + 2\pi\eta_c(n-1) \int_{\Sigma} \phi^2 + \dots \right) \exp \left(- \int_{\mathcal{M}_n} \frac{1}{2} (\partial \vec{\phi})^2 + \frac{t}{2} \vec{\phi}^2 + \frac{1}{2} \xi \eta_c R^{\text{reg}} \vec{\phi}^2 \right). \quad (2.86)$$

Now taking a derivative with respect to t gives

$$\frac{d}{dt} \log Z_n = -\frac{1}{2} \int_{\mathcal{M}_n} \langle \vec{\phi}^2 \rangle_n - \pi \xi \eta_c (n-1) \int_{\mathcal{M}_1} \int_{\Sigma} \langle \vec{\phi}^2 \vec{\phi}^2 \rangle_1 + \dots \quad (2.87)$$

Note that to leading order in $(n-1)$, we can take both the integral and the two-point function in Eq. (2.87) to be over a single sheet. Thus, we obtain

$$\frac{dS_{\text{EE}}}{dt} = \lim_{n \rightarrow 1} \frac{1}{n-1} \left[\frac{1}{2} \left(\int_{\mathcal{M}_n} \langle \vec{\phi}^2 \rangle_n - n \int_{\mathcal{M}_1} \langle \vec{\phi}^2 \rangle_1 \right) + \pi \xi \eta_c (n-1) \int_{\mathcal{M}_1} \int_{\Sigma} \langle \vec{\phi}^2 \vec{\phi}^2 \rangle_1 \right]. \quad (2.88)$$

It is convenient to specialize to the case of a planar entangling surface embedded in flat space; the ‘area law’ terms are insensitive to this choice. For $\xi = 0$, only the first two terms in (2.88) survive and evaluate to [143]

$$\lim_{n \rightarrow 1} \frac{1}{n-1} \left[\frac{1}{2} \left(\int_{\mathbb{R}_n^d} \langle \vec{\phi}^2 \rangle_n - n \int_{\mathbb{R}^d} \langle \vec{\phi}^2 \rangle_1 \right) \right] = \frac{-N}{24\pi\epsilon}, \quad (2.89)$$

where the $1/\epsilon$ pole signals that there is a logarithmic divergence as $\epsilon \rightarrow 0$.

For $\xi \neq 0$, the last term in (2.88) must be included. To evaluate it, we first note that

$$\begin{aligned} \langle \phi_a(x) \phi_c(0) \rangle_1 &= \frac{\delta_{ac}}{(2\pi)^{\frac{d}{2}}} \left(\frac{\sqrt{t}}{|x|} \right)^{\frac{d-2}{2}} K_{\frac{d-2}{2}}(\sqrt{t}x^2), \\ \langle \vec{\phi}^2(x) \vec{\phi}^2(0) \rangle_1 &= \frac{2N}{(2\pi)^d} \left(\frac{t}{x^2} \right)^{\frac{d-2}{2}} K_{\frac{d-2}{2}}^2(\sqrt{t}x^2). \end{aligned} \quad (2.90)$$

where $K_{\frac{d-2}{2}}$ is the modified Bessel function. Hence,

$$\pi\xi\eta_c \int_{\mathcal{M}_1} \int_{\Sigma} \langle \vec{\phi}^2 \vec{\phi}^2 \rangle_1 = \frac{N\xi\eta_c}{(4\pi)^{\frac{d-2}{2}} \Gamma(\frac{d}{2})} t^{\frac{d-4}{2}} A_{\Sigma} \int_0^{\infty} dr r K_{\frac{d-2}{2}}^2(r) = \frac{N\xi\eta_c \Gamma(\frac{4-d}{2})}{2(4\pi)^{\frac{d-2}{2}}} t^{\frac{d-4}{2}} A_{\Sigma} . \tag{2.91}$$

where we introduced a dimensionless variable $r = \sqrt{t}x^2$. Substituting $d = 4 - \epsilon$ and expanding in $\epsilon \ll 1$ gives

$$\pi\xi\eta_c \int_{\mathcal{M}_1} \int_{\Sigma} \langle \vec{\phi}^2 \vec{\phi}^2 \rangle_1 = \frac{N\xi}{24\pi\epsilon} A_{\Sigma} + \mathcal{O}(\epsilon^0) . \tag{2.92}$$

Combining the above results, we recover the $1/\epsilon$ term in (2.69). Note also that the integrand on the right hand side of (2.91) decays exponentially fast in the IR. In particular, the $1/\epsilon$ enhancement comes entirely from the UV regime ($r \sim 0$).

Comments

We close with a few comments. The question of if a minimally and non-minimally coupled scalar have the same entanglement entropy in flat space is an old one, see e.g., [131], in which interest has recently revived [124, 150, 132, 106, 62, 168, 41, 14]. A practical question concerns the computation of entanglement entropy on a lattice [179, 112, 139] and whether certain boundary terms should be included even for a scalar theory. Such boundary terms were advocated in [55, 40, 56, 59] for gauge theories. The lattice calculation is carried out in flat space and naively the non-minimal coupling plays no role. To what extent this claim is true requires further investigation. In particular, it is essential to understand how one splits the Hilbert space in a conformally invariant way. We note that for a CFT the lattice computation of the universal entanglement entropy whose coefficient is fixed by the trace anomaly is not affected by this issue. In particular, for a massless free scalar field it seems not to depend on whether one uses the canonical or the improved energy-momentum tensor.

In Sec. 2.5 we found a term localized on the tip of the cone, originating from the non-minimal coupling to the background geometry. In e.g., [175, 109, 177], the authors also found such a contribution,²⁰ but they regarded it as an artifact of the replica-trick and discarded it. However, our result (2.69) relies on neither the replica trick nor free field calculations, and is consistent with the presence, but not the absence, of the term on the tip of the cone. Finally, the analysis of [143] in the interacting case did not include the contribution of the non-minimal coupling at the tip of the cone (or alternatively, their scalar field is implicitly minimally coupled). Yet, their results imply that quantum fluctuations on the conical background force the introduction of the boundary counter terms which, as we have argued, have a simple interpretation in terms of induced non-minimal coupling to the background geometry. And, as the RG equations show, this occurs even if the theory is

²⁰ Such a contribution was discussed in these works in the context of the leading non universal (A/δ^2) area law piece of entanglement entropy. However, the term in question contributes to the universal part of entanglement entropy as well.

minimally coupled in the UV. We conclude that QFT on the cone background is incomplete without the inclusion of boundary terms.

Chapter 3

Geometric Constraints from Subregion Duality Beyond the Classical Regime

3.1 Introduction

AdS/CFT implies constraints on quantum gravity from properties of quantum field theory. For example, field theory causality requires that null geodesics through the bulk are delayed relative to those on the boundary. Such constraints on the bulk geometry can often be understood as coming from energy conditions on the bulk fields. In this case, bulk null geodesics will always be delayed as long as there is no negative null energy flux [82].

In this paper, we examine two constraints on the bulk geometry that are required by the consistency of the AdS/CFT duality. The starting point is the idea of subregion duality, which is the idea that the state of the boundary field theory reduced to a subregion A is itself dual to a subregion of the bulk. The relevant bulk region is called the entanglement wedge, $\mathcal{E}(A)$, and consists of all points spacelike related to the extremal surface anchored on ∂A , on the side towards A [46, 104]. The validity of subregion duality was argued [50, 90] to follow from the Ryu-Takayanagi-FLM formula [170, 171, 111, 71, 134, 53], and the consistency of subregion duality immediately implies two constraints on the bulk geometry.

The first constraint, which we call Entanglement Wedge Nesting (EWN), is that if a region A is contained in a region B on the boundary (or more generally, if the domain of dependence of A is contained in the domain of dependence of B), then $\mathcal{E}(A)$ must be contained in $\mathcal{E}(B)$. This condition was previously discussed in [46, 189].

The second constraint is that the set of bulk points $I^-(D(A)) \cap I^+(D(A))$, called the causal wedge $\mathcal{C}(A)$, is completely contained in the entanglement wedge $\mathcal{E}(A)$. We call this $\mathcal{C} \subseteq \mathcal{E}$. See [46, 189, 67, 110, 104] for previous discussion of .

We refer to the delay of null geodesics passing through the bulk relative to their boundary counterparts [82] as the Boundary Causality Condition (BCC), as in [63]. These three

conditions, and their connections to various bulk and boundary inequalities relating entropy and energy, are the primary focus of this paper.

In section 3.2 we will spell out the definitions of EWN and $\mathcal{C} \subseteq \mathcal{E}$ in more detail, as well as describe their relations with subregion duality. Roughly speaking, EWN encodes the fact that subregion duality should respect inclusion of boundary regions. $\mathcal{C} \subseteq \mathcal{E}$ is the statement that the bulk region dual to a given boundary region should at least contain all those bulk points from which messages can be both received from and sent to the boundary region.

Even though EWN, $\mathcal{C} \subseteq \mathcal{E}$, and the BCC are all required for consistency of AdS/CFT, part of our goal is to investigate their relationships to each other as bulk statements independent of a boundary dual. As such, we will demonstrate that EWN implies $\mathcal{C} \subseteq \mathcal{E}$, and $\mathcal{C} \subseteq \mathcal{E}$ implies the BCC. Thus EWN is in a sense the strongest statement of the three.

Though this marks the first time that the logical relationships between EWN, $\mathcal{C} \subseteq \mathcal{E}$, and the BCC have been independently investigated, all three of these conditions are known in the literature and have been proven from more fundamental assumptions in the bulk [189, 110]. In the classical limit, a common assumption about the bulk physics is the Null Energy Condition (NEC).¹ However, the NEC is known to be violated in quantum field theory. Recently, the Quantum Focussing Conjecture (QFC), which ties together geometry and entropy, was put forward as the ultimate quasi-local “energy condition” for the bulk, replacing the NEC away from the classical limit [26].

The QFC is currently the strongest reasonable quasi-local assumption that one can make about the bulk dynamics, and indeed we will show below that it can be used to prove EWN. Additionally, there are other, weaker, restrictions on the bulk dynamics which follow from the QFC. The Generalized Second Law (GSL) of horizon thermodynamics is a consequence of the QFC. In [67], it was shown that the GSL implies what we have called $\mathcal{C} \subseteq \mathcal{E}$. Thus the QFC, the GSL, EWN, and $\mathcal{C} \subseteq \mathcal{E}$ form a square of implications. The QFC is the strongest of the four, implying the three others, while the $\mathcal{C} \subseteq \mathcal{E}$ is the weakest. This pattern continues in a way summarized by Figure 3.1, which we will now explain.

The QFC, the GSL, and the Achronal Averaged Null Energy Condition (AANEC) reside in the first column of Fig. 3.1. As we have explained, the QFC is the strongest of these three, while the AANEC is the weakest [190]. In the second column we have EWN, $\mathcal{C} \subseteq \mathcal{E}$, and the BCC. In addition to the relationships mentioned above, it was shown in [82] that the ANEC implies the BCC, which we extend to prove the BCC from the AANEC.

The third column of Figure 3.1 contains “boundary” versions of the first column: the Quantum Null Energy Condition (QNEC) [26, 27, 126], the Quantum Half Averaged Null Energy Condition (QHANEC), and the boundary AANEC.² These are field theory statements which can be viewed as nongravitational limits of the corresponding inequalities in the first column. The QNEC is the strongest, implying the QHANEC, which in turn implies the AANEC. All three of these statements can be formulated in non-holographic theories, and

¹See [104] for a related classical analysis of bulk constraints from causality, including .

²For simplicity we are assuming throughout that the boundary theory is formulated in Minkowski space. There would be additional subtleties with all three of these statements if the boundary were curved.

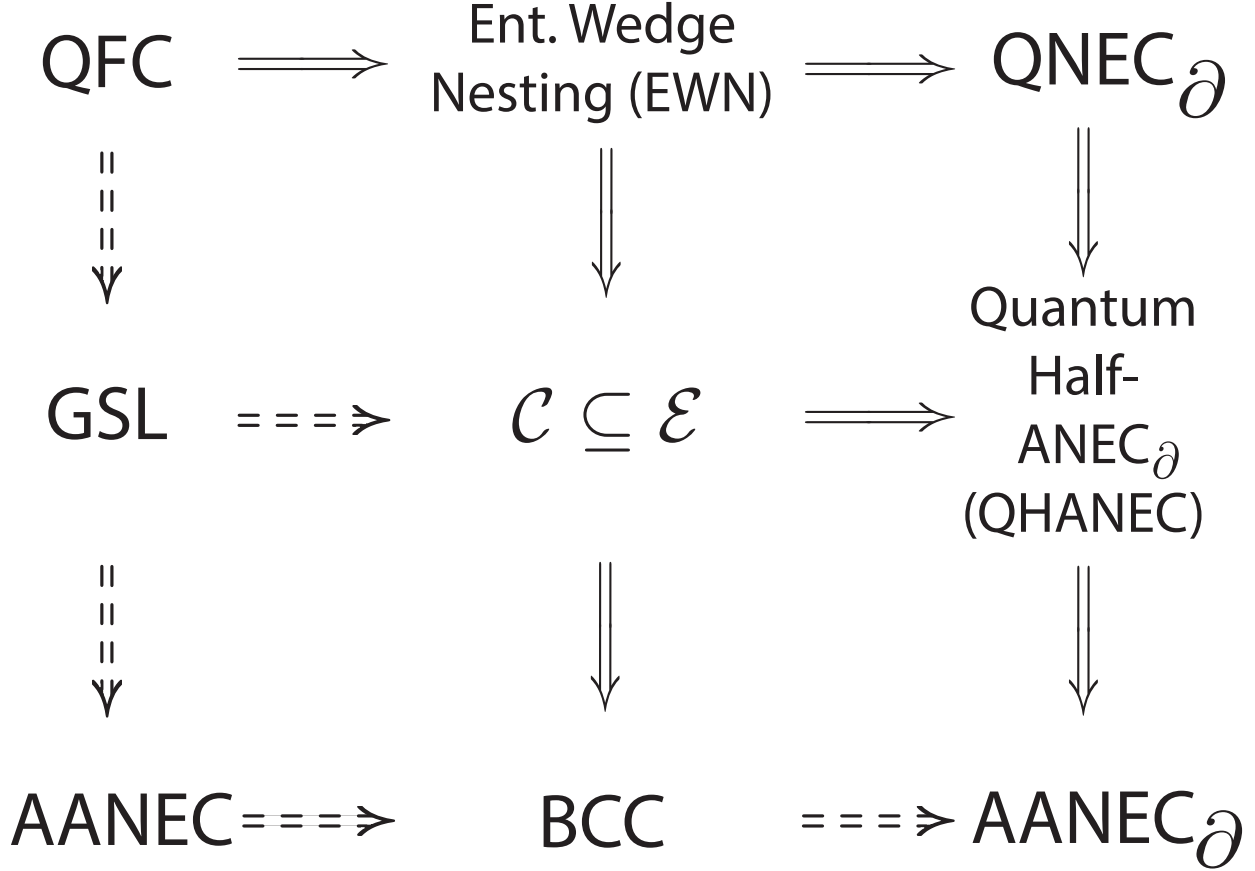


Figure 3.1: The logical relationships between the constraints discussed in this paper. The left column contains semi-classical quantum gravity statements in the bulk. The middle column is composed of constraints on bulk geometry. In the right column is quantum field theory constraints on the boundary CFT. All implications are true to all orders in $G\hbar \sim 1/N$. We have used dashed implication signs for those that were proven to all orders before this paper.

all three are conjectured to be true generally. (The AANEC was recently proven in [73] as a consequence of monotonicity of relative entropy and in [95] as a consequence of causality.)

In the case of a holographic theory, it was shown in [126] that EWN in the bulk implies the QNEC for the boundary theory to leading order in $G\hbar \sim 1/N$. We demonstrate that this relationship continues to hold with bulk quantum corrections. Moreover, in [122] the BCC in the bulk was shown to imply the boundary AANEC. Here we will complete the pattern of implications by showing that $\mathcal{C} \subseteq \mathcal{E}$ implies the boundary QHANEC.

In the classical regime, the entanglement wedge is defined in terms of a codimension-2 surface with extremal area [111, 71, 104, 53]. It has been suggested that the correct quantum generalization should be defined in terms of the “quantum extremal surface”: a Cauchy-splitting surface which extremizes the generalized entropy to one side [67]. Indeed,

we find that the logical structure of Fig. 3.1 persists to all orders in perturbation theory in $G\hbar \sim 1/N$ if and only if the entanglement wedge is defined in terms of the quantum extremal surface. This observation provides considerable evidence for prescription of [67].

The remainder of this paper is organized as follows. In Section 3.2 we will define all of the statements we set out to prove, as well as establish notation. Then in Sections 3.3 and 3.4 we will prove the logical structure encapsulated in Figure 3.1. Several of these implications are already established in the literature, but for completeness we will briefly review the relevant arguments. We conclude with a discussion in Section 6.6.

3.2 Glossary

Regime of Validity Quantum gravity is a tricky subject. We work in a semiclassical (large- N) regime, where the dynamical fields can be expanded perturbatively in $G\hbar \sim 1/N$ about a classical background [188].³ For example, the metric has the form

$$g_{ab} = g_{ab}^0 + g_{ab}^{1/2} + g_{ab}^1 + O((G\hbar)^{3/2}) , \quad (3.1)$$

where the superscripts denote powers of $G\hbar$. In the semi-classical limit — defined as $G\hbar \rightarrow 0$ — the validity of the various inequalities we consider will be dominated by their leading non-vanishing terms. We assume that the classical $O((G\hbar)^0)$ part of the metric satisfies the null energy condition (NEC), without assuming anything about the quantum corrections. For more details on this type of expansion, see Wall [190].

We primarily consider the case where the bulk theory can be approximated as Einstein gravity with minimally coupled matter fields. In the semiclassical regime, bulk loops will generate Planck-suppressed higher derivative corrections to the gravitational theory and the gravitational entropy.⁴ We will comment on the effects of these corrections throughout.

We consider a boundary theory on flat space, possibly deformed by relevant operators. When appropriate, we will assume the null generic condition, which guarantees that every null geodesic encounters matter or gravitational radiation.

Geometrical Constraints

There are a number of known properties of the AdS bulk causal structure and extremal surfaces. At the classical level (i.e. at leading order in $G\hbar \sim 1/N$), the NEC is the standard assumption made about the bulk which ensures that these properties are true [189]. However, some of these are so fundamental to subregion duality that it is sensible to demand them

³The dimensionless expansion parameter would be $G\hbar/\ell^{D-2}$, where ℓ is a typical length scale in whatever state we are considering. We will leave factors of ℓ implicit.

⁴Such corrections are also necessary for the generalized entropy to be finite. See Appendix A of [26] for details and references. Other terms can be generated from, for example, stringy effects, but these will be suppressed by the string length ℓ_s . For simplicity, we will not separately track the ℓ_s expansion. This should be valid as long as the string scale is not much different from the Planck scale.

and to ask what constraints in the bulk might ensure that these properties hold, even under quantum corrections. Answering this question is one key focus of this paper.

In this section, we review three necessary geometrical constraints. In addition to defining each of them and stating their logical relationships (see Figure 3.1), we explain how each is critical for subregion duality.

Boundary Causality Condition (BCC)

A standard notion of causality in asymptotically-AdS spacetimes is the condition that *the bulk cannot be used for superluminal communication relative to the causal structure of the boundary*. More precisely, any causal bulk curve emanating from a boundary point p and arriving back on the boundary must do so to the future of p as determined by the boundary causal structure.

This condition, termed “BCC” in [63], is known to follow from the averaged null curvature condition (ANCC) [82]. Engelhardt and Fischetti have derived an equivalent formulation in terms of an integral inequality for the metric perturbation in the context of linearized perturbations to the vacuum [63].

Microcausality in the boundary theory requires that the BCC hold. If the BCC were violated, a bulk excitation could propagate between two spacelike-separated points on the boundary leading to nonvanishing commutators of local fields at those points. In Sec. 3.4 we will show that BCC is implied by $\mathcal{C} \subseteq \mathcal{E}$. Thus BCC is the weakest notion of causality in holography that we consider.

$\mathcal{C} \subseteq \mathcal{E}$

Consider the domain of dependence $D(A)$ of a boundary region A . Let us define the causal wedge of a boundary region A to be $\mathcal{C}(A) \equiv I^-(D(A)) \cap I^+(D(A))$.⁵

By the Ryu-Takayanagi-FLM formula, the entropy of the quantum state restricted to A is given by the area of the extremal area bulk surface homologous to A plus the bulk entropy in the region between that surface and the boundary [170, 171, 111, 71, 134, 53]. This formula was shown to hold at $O((1/N)^0)$ in the large- N expansion. In [67], Engelhardt and Wall proposed that the all-orders modification of this formula is to replace the extremal area surface with the Quantum Extremal Surface (QES), which is defined as the surface which extremizes the generalized entropy: the surface area plus the entropy in the region between the surface and A . Though the Engelhardt-Wall prescription remains unproven, we will assume that it is the correct all-orders prescription for computing the boundary entropy of A . We denote the QES of A as $e(A)$.

The entanglement wedge $\mathcal{E}(A)$ is the bulk region spacelike-related to $e(A)$ on the A side of the surface. This is the bulk region believed to be dual to A in subregion duality [46].

⁵ $I^\pm(S)$ represent respectively the chronological future and past of the set S . The causal wedge was originally defined in [104] in terms of the causal future and past, $J^\pm(S)$, but for our purposes the chronological future and past are more convenient.

Dong, Harlow and Wall have argued that this is the case using the formalism of quantum error correction [50, 90].

$\mathcal{C} \subseteq \mathcal{E}$ is the property that *the entanglement wedge $\mathcal{E}(A)$ associated to a boundary region A completely contains the causal wedge $\mathcal{C}(A)$ associated to A* . can equivalently be formulated as stating that $e(A)$ is out of causal contact with $D(A)$, i.e. $e(A) \cap (I^+(D(A)) \cup I^-(D(A))) = \emptyset$. In our proofs below we will use this latter characterization.

Subregion duality requires $\mathcal{C} \subseteq \mathcal{E}$ because the bulk region dual to a boundary region A should at least include all of the points that can both send and receive causal signals to and from $D(A)$. Moreover, if $\mathcal{C} \subseteq \mathcal{E}$ were false then it would be possible to use local unitary operators in $D(A)$ to send a bulk signal to $e(A)$ and thus change the entropy associated to the region [46, 189, 67, 104]. That is, of course, not acceptable, as the von Neumann entropy is invariant under unitary transformations.

This condition has been discussed at the classical level in [104, 189]. In the semiclassical regime, Engelhardt and Wall [67] have shown that it follows from the generalized second law (GSL) of causal horizons. We will show in Sec. 3.4 that $\mathcal{C} \subseteq \mathcal{E}$ is also implied by Entanglement Wedge Nesting.

Entanglement Wedge Nesting (EWN)

The strongest of the geometrical constraints we consider is EWN. In the framework of subregion duality, EWN is the property that a strictly larger boundary region should be dual to a strictly larger bulk region. More precisely, *for any two boundary regions A and B with domain of dependence $D(A)$ and $D(B)$ such that $D(A) \subset D(B)$, we have $\mathcal{E}(A) \subset \mathcal{E}(B)$* .

This property was identified as important for subregion duality and entanglement wedge reconstruction in [46, 189], and was proven by Wall at leading order in $G\hbar$ assuming the null curvature condition [189]. We will show in Sec. 3.4 that the Quantum Focussing Conjecture (QFC) [26] implies EWN in the semiclassical regime assuming the generalization of HRT advocated in [67].

Constraints on Semiclassical Quantum Gravity

Reasonable theories of matter are often assumed to satisfy various energy conditions. The least restrictive of the classical energy conditions is the null energy condition (NEC), which states that

$$T_{kk} \equiv T_{ab} k^a k^b \geq 0, \quad (3.2)$$

for all null vectors k^a . This condition is sufficient to prove many results in classical gravity. In particular, many proofs hinge on the classical focussing theorem [186], which follows from the NEC and ensures that light-rays are focussed whenever they encounter matter or gravitational radiation:

$$\theta' \equiv \frac{d}{d\lambda} \theta \leq 0, \quad (3.3)$$

where θ is the expansion of a null hypersurface and λ is an affine parameter.

Quantum fields are known to violate the NEC, and therefore are not guaranteed to focus light-rays. It is desirable to understand what (if any) restrictions on sensible theories exist in quantum gravity, and which of the theorems which rule out pathological phenomenon in the classical regime have quantum generalizations. In the context of AdS/CFT, the NEC guarantees that the bulk dual is consistent with boundary microcausality [82] and holographic entanglement entropy [189, 32, 102, 104], among many other things.

In this subsection, we outline three statements in semiclassical quantum gravity which have been used to prove interesting results when the NEC fails. They are presented in order of increasing strength. We will find in sections 3.3 and 3.4 that each of them has a unique role to play in the proper functioning of the bulk-boundary duality.

Achronal Averaged Null Energy Condition

The achronal averaged null energy condition (AANEC) [187] states that

$$\int T_{kk} d\lambda \geq 0 , \tag{3.4}$$

where the integral is along a complete achronal null curve (often called a “null line”). Local negative energy density is tolerated as long as it is accompanied by enough positive energy density elsewhere. The *achronal* qualifier is essential for the AANEC to hold in curved spacetimes. For example, the Casimir effect as well as quantum fields on a Schwarzschild background can both violate the ANEC [125, 185] for chronal null geodesics. An interesting recent example of violation of the ANEC for chronal geodesics in the context of AdS/CFT was studied in [81].

The AANEC is fundamentally a statement about quantum field theory formulated in curved backgrounds containing complete achronal null geodesics. It has been proven for QFTs in flat space from monotonicity of relative entropy [73], as well as causality [95]. Roughly speaking, the AANEC ensures that when the backreaction of the quantum fields is included it will focus null geodesics and lead to time delay. This will be made more precise in Sec. 3.4 when we discuss a proof of the boundary causality condition (BCC) from the AANEC.

Generalized Second Law

The generalized second law (GSL) of horizon thermodynamics states that the generalized entropy (defined below) of a causal horizon cannot decrease in time.

Let Σ denote a Cauchy surface and let σ denote some (possibly non-compact) codimension-2 surface dividing Σ into two distinct regions. We can compute the von Neumann entropy of

the quantum fields on the region outside of σ , which we will denote S_{out} ⁶. The generalized entropy of this region is defined to be

$$S_{gen} = S_{grav} + S_{out} \quad (3.5)$$

where S_{grav} is the geometrical/gravitational entropy which depends on the theory of gravity. For Einstein gravity, it is the familiar Bekenstein-Hawking entropy. There will also be Planck-scale suppressed corrections⁷, denoted Q , such that it has the general form

$$S_{grav} = \frac{A}{4G\hbar} + Q \quad (3.6)$$

There is mounting evidence that the generalized entropy is finite and well-defined in perturbative quantum gravity, even though the split between matter and gravitational entropy depends on renormalization scale. See the appendix of [26] for details and references.

The *quantum expansion* Θ can be defined (as a generalization of the classical expansion θ) as the functional derivative per unit area of the generalized entropy along a null congruence [26]:

$$\Theta[\sigma(y); y] \equiv \frac{4G\hbar}{\sqrt{h}} \frac{\delta S_{gen}}{\delta \sigma(y)} \quad (3.7)$$

$$= \theta + \frac{4G\hbar}{\sqrt{h}} \frac{\delta Q}{\delta \sigma(y)} + \frac{4G\hbar}{\sqrt{h}} \frac{\delta S_{out}}{\delta \sigma(y)} \quad (3.8)$$

where \sqrt{h} denotes the determinant of the induced metric on σ , which is parametrized by y . These functional derivatives denote the infinitesimal change in a quantity under deformations of the surface at coordinate location y along the chosen null congruence. To lighten the notation, we will often omit the argument of Θ .

A future (past) causal horizon is the boundary of the past (future) of any future-infinite (past-infinite) causal curve [114]. For example, in an asymptotically AdS spacetime any collection of points on the conformal boundary defines a future and past causal horizon in the bulk. The generalized second law (GSL) is the statement that the quantum expansion is always nonnegative towards the future on any future causal horizon

$$\Theta \geq 0, \quad (3.9)$$

with an analogous statement for a past causal horizon.

⁶The choice of “outside” is arbitrary. In a globally pure state both sides will have the same entropy, so it will not matter which is the “outside.” In a mixed state the entropies on the two sides will not be the same, and thus there will be two generalized entropies associated to the same surface. The GSL, and all other properties of generalized entropy, should apply equally well to both.

⁷There will also be stringy corrections suppressed by α' . As long as we are away from the stringy regime, these corrections will be suppressed in a way that is similar to the Planck-suppressed ones, and so we will not separately track them.

In the semiclassical $G\hbar \rightarrow 0$ limit, Eq. (3.7) reduces to the classical expansion θ if it is nonzero, and the GSL becomes the Hawking area theorem [96]. The area theorem follows from the NEC.

Assuming the validity of the GSL allows one to prove a number of important results in semiclassical quantum gravity [191, 67]. In particular, Wall has shown that it implies the AANEC [190], as we will review in Section 3.3, and $\mathcal{C} \subseteq \mathcal{E}$ [67], reviewed in Section 3.4 (see Fig. 3.1).

Quantum Focussing Conjecture

The Quantum Focussing Conjecture (QFC) was conjectured in [26] as a quantum generalization of the classical focussing theorem, which unifies the Bousso Bound and the GSL. The QFC states that the functional derivative of the quantum expansion along a null congruence is nowhere increasing:

$$\frac{\delta\Theta[\sigma(y_1); y_1]}{\delta\sigma(y_2)} \leq 0. \quad (3.10)$$

In this equation, y_1 and y_2 are arbitrary. When $y_1 \neq y_2$, only the S_{out} part contributes, and the QFC follows from strong subadditivity of entropy [26]. For notational convenience, we will often denote the “local” part of the QFC, where $y_1 = y_2$, as⁸

$$\Theta'[\sigma(y); y] \leq 0. \quad (3.11)$$

Note that while the GSL is a statement only about causal horizons, the QFC is conjectured to hold on any cut of any null hypersurface.

If true, the QFC has several non-trivial consequences which can be teased apart by applying it to different null surfaces [26, 21, 67]. In Sec. 3.4 we will see that EWN can be added to this list.

Quantum Null Energy Condition

When applied to a locally stationary null congruence, the QFC leads to the Quantum Null Energy Condition (QNEC) [26, 126]. Applying the Raychaudhuri equation and Eqs. (3.5), (3.7) to the statement of the QFC (4.40), we find

$$0 \geq \Theta' = -\frac{\theta^2}{D-2} - \sigma^2 - 8\pi G T_{kk} + \frac{4G\hbar}{\sqrt{h}} (S''_{out} - S'_{out}\theta) \quad (3.12)$$

where S''_{out} is the local functional derivative of the matter entropy to one side of the cut. If we consider a locally stationary null hypersurface satisfying $\theta^2 = \sigma^2 = 0$ in a small neighborhood,

⁸Strictly speaking, we should factor out a delta function $\delta(y_1 - y_2)$ when discussing the local part of the QFC [27, 126]. Since the details of this definition are not important for us, we will omit this in our notation.

this inequality reduces to the statement of the *Quantum Null Energy Condition* (QNEC) [26]:

$$T_{kk} \geq \frac{\hbar}{2\pi\sqrt{\hbar}} S''_{out} \quad (3.13)$$

It is important to notice that the gravitational coupling G has dropped out of this equation. The QNEC is a statement purely in quantum field theory which can be proven or disproven using QFT techniques. It has been proven for both free fields [27] and holographic field theories at leading order in $G\hbar$ [126].⁹ In Section 3.4 of this paper, we generalize the holographic proof to all orders in $G\hbar$. These proofs strongly suggest that the QNEC is a true property of general quantum field theories.¹⁰ In the classical $\hbar \rightarrow 0$ limit, the QNEC becomes the NEC.

Quantum Half-Averaged Null Energy Condition

The quantum half-averaged energy condition (QHANEC) is an inequality involving the integrated stress tensor and the first null derivative of the entropy on one side of any locally-stationary Cauchy-splitting surface subject to a causality condition (described below):

$$\int_{\lambda}^{\infty} T_{kk} d\tilde{\lambda} \geq -\frac{\hbar}{2\pi\sqrt{\hbar}} S'(\lambda), \quad (3.14)$$

Here k^a generates a null congruence with vanishing expansion and shear in a neighborhood of the geodesic and λ is the affine parameter along the geodesic. The geodesic thus must be of infinite extent and have $R_{ab}k^ak^b = C_{abcd}k^ak^c = 0$ everywhere along it. The aforementioned causality condition is that the Cauchy-splitting surfaces used to define $S(\lambda)$ should not be timelike-related to the half of the null geodesic T_{kk} is integrated over. Equivalently, $S(\lambda)$ should be well-defined for all λ from the starting point of integration all the way to $\lambda = \infty$.

The causality condition and the stipulation that the null geodesic in (3.14) be contained in a locally stationary congruence ensures that the QHANEC follows immediately from integrating the QNEC (Eq. (3.13)) from infinity (as long as the entropy isn't evolving at infinite affine parameter, i.e., $S'(\infty) = 0$). Because the causality condition is a restriction on the global shape of the surface, there will be situations where the QNEC holds locally but we cannot integrate to arrive at a QHANEC.

The QHANEC appears to have a very close relationship to monotonicity of relative entropy. Suppose that the modular Hamiltonian of the portion of a null plane above an arbitrary cut $u = \sigma(y)$ (where u is a null coordinate) is given by

$$K[\sigma(y)] = \int d^{d-2}y \int_{\sigma(y)}^{\infty} d\lambda (\lambda - \sigma(y)) T_{kk} \quad (3.15)$$

⁹There is also evidence [79] that the QNEC holds in holographic theories where the entropy is taken to be the casual holographic information [110], instead of the von Neumann entropy.

¹⁰The free-field proof of [27] was for arbitrary cuts of Killing horizons. The holographic proof of [126] (generalized in this paper) showed the QNEC for a locally stationary ($\theta = \sigma = 0$) portion of *any* Cauchy-splitting null hypersurface in flat space.

Then (3.45) becomes monotonicity of relative entropy. As of yet, there is no known general proof in the literature of (3.15), though for free theories it follows from the enhanced symmetries of null surface quantization [188]. Eq. (3.15) can be also be derived for holographic field theories [127]. It has also been shown that linearized backreaction from quantum fields obeying the QHANEK will lead to a spacetime satisfying the GSL [188].¹¹

In Sec. 3.4, we will find that $C \subseteq E$ implies the QHANEK on the boundary.

3.3 Relationships Between Entropy and Energy Inequalities

The inequalities discussed in the previous section are not all independent. In this section we discuss the logical relationships between them.

GSL implies AANEC

Wall has shown [190] that the GSL implies the AANEC in spacetimes which are linearized perturbations of classical backgrounds, where the classical background obeys the null energy condition (NEC). Here, we point out that this proof is sufficient to prove the AANEC from the GSL in the semi-classical regime, to all orders in $G\hbar$ (see Sec. 3.2).

Because the AANEC is an inequality, in the semi-classical $G\hbar \rightarrow 0$ limit its validity is determined by the leading non-zero term in the $G\hbar$ expansion. Suppose that this term is order $(G\hbar)^m$. Suppose also that at order $(G\hbar)^{m-1}$ the metric contains a complete achronal null geodesic γ , i.e. a null geodesic without a pair of conjugate points. (If at this order no such geodesics exist, the AANEC holds trivially at this order as well as all higher orders, as higher-order contributions to the metric cannot make a chronal geodesic achronal.) Achronality guarantees that γ lies in both a future and past causal horizon, \mathcal{H}^\pm .

Wall's proof required that, in the background spacetime, the expansion and shear vanish along γ in both \mathcal{H}^+ and \mathcal{H}^- . Wall used the NEC in the background spacetime to derive this, but here we note that the NEC is not necessary given our other assumptions. The "background" for us is the $O((G\hbar)^{m-1})$ part of the metric. Consider first the past causal horizon, \mathcal{H}^- , which must satisfy the boundary condition $\theta(-\infty) \rightarrow 0$. Since γ is achronal, the expansion θ of \mathcal{H}^- cannot blow up to $-\infty$ anywhere along γ . As $\lambda \rightarrow \infty$, θ can either remain finite or blow up in the limit. Suppose first that θ asymptotes to a finite constant as $\lambda \rightarrow \infty$. Then $\lim_{\lambda \rightarrow \infty} \theta' = 0$. Assuming the matter stress tensor dies off at infinity (as it must for the AANEC to be well-defined), Raychaudhuri's equation gives $\lim_{\lambda \rightarrow \infty} \theta' = -\theta^2/(D-2) - \sigma^2$,

¹¹It has been shown [30] that holographic theories also obey the QHANEK when the causal holographic information [110] is used, instead of the von Neumann entropy. This implies a second law for the causal holographic information in holographic theories.

the only solution to which is¹²

$$\lim_{\lambda \rightarrow \infty} \theta = \lim_{\lambda \rightarrow \infty} \sigma = 0 . \quad (3.16)$$

Similar arguments apply to \mathcal{H}^+ . This also implies that $\mathcal{H}^+ = \mathcal{H}^-$. The rest of the proof follows [190]. This proves the AANEC at order $(G\hbar)^m$.

The alternative case is that $|\theta| \rightarrow \infty$ as $\lambda \rightarrow \infty$. But if T_{kk} dies off at infinity, then for large enough λ we have $\theta' < -\theta^2/(D-2) + \epsilon$ for some ϵ . Then a simple modification of the standard focussing argument shows that θ goes to $-\infty$ at finite affine parameter, which is a contradiction.

QFC implies GSL

In a manner exactly analogous to the proof of the area theorem from classical focusing, the QFC can be applied to a causal horizon to derive the GSL. Consider integrating Eq. 4.40 from future infinity along a generator of a past causal horizon:

$$\int d^{d-2}y \sqrt{h} \int_{\lambda}^{\infty} d\tilde{\lambda} \Theta'[\sigma(y, \tilde{\lambda}); y] \leq 0 \quad (3.17)$$

Along a future causal horizon, $\theta \rightarrow 0$ as $\lambda \rightarrow \infty$, and it is reasonable to expect the matter entropy S_{out} to stop evolving as well. Thus $\Theta \rightarrow 0$ as $\lambda \rightarrow \infty$, and the integrated QFC then trivially becomes

$$\Theta[\sigma(y); y] \geq 0 \quad (3.18)$$

which is the GSL.

QHANEK implies AANEK

In flat space, all achronal null geodesics lie on a null plane. Applying the QHANEK to cuts of this null plane taking $\lambda \rightarrow -\infty$ produces the AANEK, Eq. (3.4).

3.4 Relationships Between Entropy and Energy Inequalities and Geometric Constraints

In this section, we discuss how the bulk generalized entropy conditions reviewed in Sec. 3.2 imply the geometric conditions EWN, $\mathcal{C} \subseteq \mathcal{E}$ and BCC (described in Sec. 3.2). We also explain how these geometric conditions imply the boundary QNEC, QHANEK and AANEK.

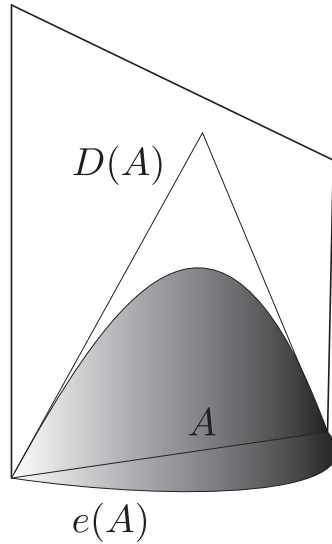


Figure 3.2: The causal relationship between $e(A)$ and $D(A)$ is pictured in an example spacetime that violates $\mathcal{C} \subseteq \mathcal{E}$. The boundary of A 's entanglement wedge is shaded. Notably, in $\mathcal{C} \subseteq \mathcal{E}$ violating spacetimes, there is necessarily a portion of $D(A)$ that is timelike related to $e(A)$. Extremal surfaces of boundary regions from this portion of $D(A)$ are necessarily timelike related to $e(A)$, which violates EWN.

EWN implies $\mathcal{C} \subseteq \mathcal{E}$ implies the BCC

EWN implies $\mathcal{C} \subseteq \mathcal{E}$

The $\mathcal{C} \subseteq \mathcal{E}$ and EWN conditions were defined in Sec. 3.2. There, we noted that $\mathcal{C} \subseteq \mathcal{E}$ can be phrased as the condition that the extremal surface $e(A)$ for some boundary region A lies outside of timelike contact with $D(A)$. We will now prove that EWN implies $\mathcal{C} \subseteq \mathcal{E}$ by proving the contrapositive: we will show that if $\mathcal{C} \subseteq \mathcal{E}$ is violated, there exist two boundary regions A, B with nested domains of dependence, but whose entanglement wedges are not nested.

Consider an arbitrary region A on the boundary. $\mathcal{C} \subseteq \mathcal{E}$ is violated if and only if there exists at least one point $p \in e(A)$ such that $p \in I^+(D(A)) \cup I^-(D(A))$, where I^+ (I^-) denotes the chronological future (past). Then violation of $\mathcal{C} \subseteq \mathcal{E}$ is equivalent to the existence of a timelike curve connecting $e(A)$ to $D(A)$. Because I^+ and I^- are open sets, there exists an open neighborhood $\mathcal{O} \subset D(A)$ such that every point of \mathcal{O} is timelike related to $e(A)$ (see Figure 3.2). Consider a new boundary region $B \subset \mathcal{O}$. Again by the openness of I^+ and I^- , the corresponding entanglement wedge $\mathcal{E}(B)$ also necessarily contains points that are timelike related to $e(A)$. Since $\mathcal{E}(A)$ is defined to be all points *spacelike-related* to $e(A)$ on the side towards A , $\mathcal{E}(B) \not\subseteq \mathcal{E}(A)$. But by construction $D(B) \subseteq D(A)$, and thus EWN is violated.

In light of this argument, we have an additional characterization of the condition $\mathcal{C} \subseteq \mathcal{E}$: is

¹²We absorb the graviton contribution to the shear into the stress tensor.

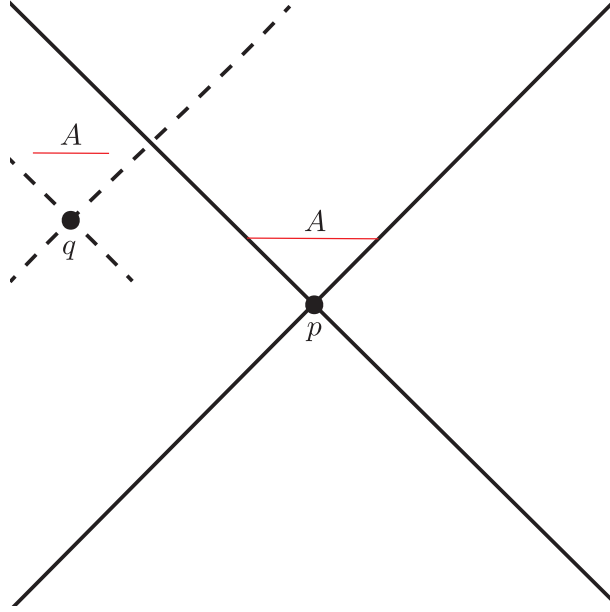


Figure 3.3: The boundary of a BCC-violating spacetime is depicted, which gives rise to a violation of $\mathcal{C} \subseteq \mathcal{E}$. The points p and q are connected by a null geodesic through the bulk. The boundary of p 's lightcone with respect to the AdS boundary causal structure is depicted with solid black lines. Part of the boundary of q 's lightcone is shown with dashed lines. The disconnected region A is defined to have part of its boundary in the timelike future of q while also satisfying $p \in D(A)$. It follows that $e(A)$ will be timelike related to $D(A)$ through the bulk, violating $\mathcal{C} \subseteq \mathcal{E}$.

what guarantees that $\mathcal{E}(A)$ contains $D(A)$, which is certainly required for consistency of bulk reconstruction.

$\mathcal{C} \subseteq \mathcal{E}$ implies the BCC

We prove the contrapositive. If the BCC is violated, then there exists a bulk null geodesic from some boundary point p that returns to the boundary at a point q not to the future of p with respect to the boundary causal structure. Therefore there exist points in the timelike future of q that are also not to the future of p .

If q is not causally related to p with respect to the boundary causal structure, we derive a contradiction as follows. Define a boundary subregion A with two disconnected parts: one that lies entirely within the timelike future of q but outside the future of p , and one composed of all the points in the future lightcone of p on a boundary timeslice sufficiently close to p such that A is completely achronal. By construction, $p \in D(A)$. Moreover, because ∂A includes points timelike related to q , $e(A)$ includes points timelike related to q and by extension p . Therefore A is an achronal boundary subregion whose extremal surface contains points that are timelike related to $D(A)$. See Figure 3.3.

If q is in the past of p , then a contradiction is reached more easily. Define a boundary subregion A as the intersection of p 's future lightcone with any constant time slice sufficiently close to p , chosen so that $e(A)$ is not empty. Then p is in $D(A)$ and q is in $I^-(A)$ according to the boundary causal structure (though according to the bulk causal structure it is in $J^+(p)$). Hence $e(A)$ is timelike related to $D(A)$ in the bulk causal structure, which is the sought-after contradiction.

Semiclassical Quantum Gravity Constraints Imply Geometric Constraints

Quantum Focussing implies Entanglement Wedge Nesting

Consider a boundary region A associated with boundary domain of dependence $D(A)$. As above, we denote the quantum extremal surface anchored to ∂A as $e(A)$. For any other boundary region, B , such that $D(B) \subset D(A)$, we will show that $\mathcal{E}(B) \subset \mathcal{E}(A)$, assuming the QFC.

Since we are treating quantum corrections perturbatively, every quantum extremal surface is located near a classical extremal area surface.¹³ Wall proved in [189] that $\mathcal{E}(B) \subset \mathcal{E}(A)$ is true at the classical level if we assume classical focussing. Thus to prove the quantum statement within perturbation theory we only need to consider those (nongeneric) cases where $e(B)$ happens to intersect the boundary of $\mathcal{E}(A)$ classically.¹⁴ In such a case, one might worry that a perturbative quantum correction could cause $e(B)$ to exit $\mathcal{E}(A)$. We will now argue that this does not happen.¹⁵

First, deform the region B slightly to a new region $B' \subset A$ such that $e(B')$ lies within $\mathcal{E}(A)$ classically. Then, since perturbative corrections cannot change this fact, we will have $\mathcal{E}(B') \subset \mathcal{E}(A)$ even at the quantum level. Now, following [67], we show that in deforming B' back to B we maintain EWN.

The QFC implies that the null congruence generating the boundary of $I^\pm(e(A))$ satisfies $\dot{\Theta} \leq 0$. Combined with $\Theta = 0$ at $e(A)$ (from the definition of quantum extremal surface), this implies that every point on the boundary of $\mathcal{E}(A)$ satisfies $\Theta \leq 0$. Therefore the boundary of $\mathcal{E}(A)$ is a quantum extremal barrier as defined in [67], and so no continuous family of quantum extremal surfaces can cross the boundary of $\mathcal{E}(A)$. Thus, as we deform B' back into B , the quantum extremal surface is forbidden from exiting $\mathcal{E}(A)$. Therefore $e(B) \subset \mathcal{E}(A)$, and by extension $\mathcal{E}(B) \subset \mathcal{E}(A)$.

Finally we will take care of the possibility of a phase transition. A phase transition occurs when there are multiple quantum extremal surfaces for each region, and the identity

¹³Another possibility is that quantum extremal surfaces which exist at finite $G\hbar$ move off to infinity as $G\hbar \rightarrow 0$. In that case there would be no associated classical extremal surface. If we believe that the classical limit is well-behaved, then these surfaces must always be subdominant in the small $G\hbar$ limit, and so we can safely ignore them.

¹⁴The only example of this that we are aware of is in vacuum AdS where A is the interior of a sphere on the boundary and B is obtained by deforming a portion of the sphere in an orthogonal null direction.

¹⁵For now we ignore the possibility of phase transitions. They will be treated separately below.

of the one with minimal generalized entropy switches as we move within the space of regions. This causes the entanglement wedge to jump discontinuously, and if it jumps the “wrong way” then EWN could be violated. Already this would be a concern at the classical level, but it was shown in [189] that classically EWN is always obeyed even accounting for the possibility of phase transitions. So we only need to convince ourselves that perturbative quantum corrections cannot change this fact.

Consider the infinite-dimensional parameter space of boundary regions. A family of quantum (classical) extremal surfaces determines a function on this parameter space given by the generalized entropy (area) of the extremal surfaces. A phase transition occurs when two families of extremal surfaces have equal generalized entropy (or area), and is associated with a codimension-one manifold in parameter space. In going from the purely classical situation to the perturbative quantum situation, two things will happen. First, the location of the codimension-one phase transition manifold in parameter space will be shifted. Second, within each family of extremal surfaces, the bulk locations of the surfaces will be perturbatively shifted. We can treat these two effects separately.

In the vicinity of the phase transition (in parameter space), the two families of surfaces will be classically separated in the bulk and classically obey EWN, as proved in [189]. A perturbative shift in the parameter space location of the phase transition will not change whether EWN is satisfied classically. That is, the *classical* surfaces in each extremal family associated with the neighborhood of *quantum* phase transition will still be separated classically in the bulk. Then we can shift the bulk locations of the classical extremal surfaces to the quantum extremal surfaces, and since the shift is only perturbative there is no danger of introducing a violation of EWN.

It would be desirable to have a more unified approach to this proof in the quantum case that does not rely so heavily on perturbative arguments. We believe that such an approach is possible, and in future work we hope to lift all of the results of [189] to the quantum case by the replacement of “area” with “generalized entropy” without having to rely on a perturbative treatment.

Generalized Second Law implies $\mathcal{C} \subseteq \mathcal{E}$

This proof can be found in [67], but we elaborate on it here to illustrate similarities between this proof and the proof that QFC implies EWN.

Wall’s Lemma We remind the reader of a fact proved as Theorem 4 in [189].¹⁶ Let two boundary anchored co-dimension two, spacelike surfaces M and N , which contain the point $p \in M \cap N$ such that they are also tangent at p . Both surfaces are Cauchy-splitting in the bulk. Suppose that M lies completely to one side of N . In the classical regime, Wall shows that either there exists some point x in a neighborhood of p where

$$\theta_N(x) > \theta_M(x) \tag{3.19}$$

¹⁶Wall’s Lemma is a significant part of the extremal surface barriers argument in [67].

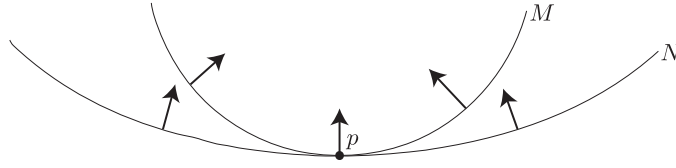


Figure 3.4: The surface M and N are shown touching at a point p . In this case, $\theta_M < \theta_N$. The arrows illustrate the projection of the null orthogonal vectors onto the Cauchy surface.

or the two surfaces agree everywhere in the neighborhood. These expansions are associated to the exterior facing, future null normal direction.

In the semi-classical regime, this result can be improved to bound the quantum expansions

$$\Theta_1(x) > \Theta_2(x) \tag{3.20}$$

where x is some point in a neighborhood of p . The proof of this quantum result requires the use of strong sub-additivity, and works even when bulk loops generate higher derivative corrections to the generalized entropy [191].

We now proceed to prove from the GSL by contradiction. Suppose that the causal wedge lies at least partly outside the entanglement wedge. In this discussion, by the “boundary of the causal wedge,” we mean the intersection of the past of $I^-(\partial D(A))$ with the Cauchy surface on which $e(A)$ lies. Consider continuously shrinking the boundary region associated to the causal wedge. The causal wedge will shrink continuously under this deformation. At some point, $\mathcal{C}(A)$ must shrink inside $\mathcal{E}(A)$. There exists some Cauchy surface such that its intersection with the boundary of the causal wedge touches the original extremal surface as depicted in Figure 3.4. There, M is the intersection of the boundary of the causal wedge of the shrunken region with the Cauchy surface and N is $e(A)$.

Assuming genericity of the state, the two surfaces cannot agree in this neighborhood. At this point, by the above lemma, the quantum expansions should obey

$$\Theta_e(x) > \Theta_c(x) \tag{3.21}$$

for x in some neighborhood of p . The Wall-Engelhardt prescription tells us that the entanglement wedge boundary should be given by the quantum extremal surface [67] and so

$$\Theta_e(x) = 0 > \Theta_c(x) \tag{3.22}$$

Thus, the GSL is violated at some point along this causal surface, which draws the contradiction.

AANEC implies Boundary Causality Condition

The Gao-Wald proof of the BCC [82] uses the fact — which follows from their assumptions of the NEC and null generic condition (discussed below) — that all complete null geodesics

through the bulk contain a pair of conjugate points.¹⁷ Here, we sketch a slight modification of the proof which instead assumes the achronal averaged null energy condition (AANEC).

We prove that the AANEC implies BCC by contradiction. Let the spacetime satisfy the null generic condition [186], so that each null geodesic encounters at least some matter or gravitational radiation.¹⁸ Violation of the BCC implies that the "fastest" null geodesic γ between two boundary points p and q lies in the bulk. Such a null geodesic is necessarily complete and achronal, as p and q are not timelike related. As explained in Sec. 3.3, an achronal null geodesic in an AANEC satisfying spacetime is contained in a congruence that is both a past and future causal horizon. Integrating Raychaudhuri's equation along the entire geodesic then gives $0 \leq -\int(\theta^2 + \sigma^2)$, which implies $\theta = \sigma = 0$ everywhere along the geodesic, and hence $\theta' = 0$. Raychaudhuri's equation then says $\theta' = -T_{kk} = 0$ everywhere, which contradicts the generic condition.

Geometric Constraints Imply Field Theory Constraints

The geometrical constraints EWN, , and BCC have non-trivial implications for the boundary theory. We derive them in this section, which proves the three implications connecting columns two and three of Fig. 3.1. The key idea behind all three proofs is the same: express the geometrical constraints in terms of bulk quantities near the asymptotic boundary, and then use near-boundary expansions of the metric and extremal surfaces to convert them into field theory statements.

Entanglement Wedge Nesting implies the Boundary QNEC

At leading order in $G\hbar \sim 1/N$, this proof is the central result of [126]. There the boundary entropy was assumed to be given by the RT formula without the bulk entropy corrections. We give a proof here of how the $1/N$ corrections can be incorporated naturally. We will now show, in a manner exactly analogous to that laid out in [126], that EWN implies the boundary QNEC. In what follows, we will notice that in order to recover the boundary QNEC, we must use the *quantum extremal surface*, not just the RT surface with FLM corrections [67].

The quantum extremal surface (QES) prescription, as first introduced in [67], is the following. To find the entropy of a region A in the boundary theory, first find the minimal codimension-2 bulk surface homologous to A , $e(A)$, that extremizes the bulk generalized entropy on the side of A . The entropy of A is then given by

$$S_A = S_{gen}(e(A)) = \frac{A_{QES}}{4G\hbar} + S_{bulk} \quad (3.23)$$

¹⁷Intuitively speaking, points p and q along a geodesic γ are conjugate if an infinitesimally nearby geodesic intersects γ at both p and q . This can be shown to be equivalent to the statement that the expansion of a congruence through p approaches $-\infty$ at q . See e.g. [186] for details.

¹⁸Mathematically, each complete null geodesic should contain a point where $k^a k^b k_{[c} R_{d]ab[e} k_{f]} \neq 0$.

Entanglement Wedge Nesting then becomes a statement about how the quantum extremal surface moves under deformations of the boundary region. In particular, for null deformations of the boundary region, EWN states that $e(A)$ moves in a spacelike (or null) fashion.

To state this more precisely, we can set up a null orthogonal basis about $e(A)$. Let k^μ be the inward-facing, future null orthogonal vector along the quantum extremal surface. Let ℓ^μ be its past facing partner with $\ell \cdot k = 1$. Following the prescription in [126], we denote the locally orthogonal deviation vector of the quantum extremal surface by s^μ . This vector can be expanded in the local null basis as

$$s = \alpha k + \beta \ell \quad (3.24)$$

The statement of entanglement wedge nesting then just becomes the statement that $\beta \geq 0$.

In order to find how β relates to the boundary QNEC, we would like to find its relation to the entropy. We start by examining the expansion of the extremal surface solution in Fefferman-Graham coordinates. Note that the quantum extremal surface obeys an equation of motion including the bulk entropy term as a source

$$K_\mu = -\frac{4G\hbar}{\sqrt{H}} \frac{\delta S_{bulk}}{\delta X^\mu} \quad (3.25)$$

Here, $K^\mu = \theta_k \ell^\mu + \theta_\ell k^\mu$ is the extrinsic curvature of the QES. As discussed in [126], solutions to (3.25) without the bulk source take the form

$$\bar{X}_{HRT}^i(y^a, z) = X^i(y^a) + \frac{1}{2(d-2)} z^2 K^i(y^a) + \dots + \frac{z^d}{d} (V^i(y^a) + W^i(y^a) \log z) + o(z^d) \quad (3.26)$$

We now claim that the terms lower order than z^d are unaffected by the presence of the source. More precisely

$$\bar{X}_{QES}^i(y^a, z) = X^i(y^a) + \frac{1}{2(d-2)} z^2 K^i(y^a) + \dots + \frac{z^d}{d} (V_{QES}^i + W^i(y^a) \log z) + o(z^d) \quad (3.27)$$

This expansion is found by examining the leading order pieces of the extremal surface equation. First, expand (3.25) to derive

$$z^{d-1} \partial_z \left(z^{1-d} f \sqrt{\bar{h}} \bar{h}^{zz} \partial_z \bar{X}^i \right) + \partial_a \left(\sqrt{\bar{h}_{ab}} \bar{h}^{ab} f \partial_b \bar{X}^i \right) = -z^{d-1} 4G\hbar f \frac{\delta S_{bulk}}{\delta \bar{X}^j} g^{ji} \quad (3.28)$$

Here we are parameterizing the near-boundary AdS metric in Fefferman-Graham coordinates by

$$ds^2 = \frac{1}{z^2} (dz^2 + g_{ij} dx^i dx^j) \quad (3.29)$$

$$= \frac{1}{z^2} \left(dz^2 + \left[f(z) \eta_{ij} + \frac{16\pi G_N}{d} z^d t_{ij} \right] dx^i dx^j + o(z^d) \right). \quad (3.30)$$

The function $f(z)$ encodes the possibility of relevant deformations in the field theory which would cause the vacuum state to differ from pure AdS. Here we have set $L_{AdS} = 1$.

One then plugs in (3.27) to (3.28) to see that the terms lower order than z^d remain unaffected by the presence of the bulk entropy source as long as $\delta S_{bulk}/\delta X^i$ remains finite at $z = 0$. We discuss the plausibility of this boundary condition at the end of this section.

For null deformations to locally stationary surfaces on the boundary, one can show using (3.27) that the leading order piece of β in the Fefferman-Graham expansion is order z^{d-2} . Writing the coordinates of the boundary entangling surface as a function of some deformation parameter - $X^i(\lambda)$ - we find that [126],

$$\beta \propto z^{d-2} \left(T_{kk} + \frac{1}{8\pi G_N} k_i \partial_\lambda V_{QES}^i \right). \quad (3.31)$$

We will now show that V_{QES}^i is proportional to the variation in S_{gen} at all orders in $1/N$, as long as one uses the quantum extremal surface and assumes mild conditions on derivatives of the bulk entropy. The key will be to leverage the fact that S_{gen} is extremized on the QES. Thus, its variation will come from pure boundary terms. At leading order in z , we will identify these boundary terms with the vector V_{QES} .

We start by varying the generalized entropy with respect to a boundary deformation

$$\delta S_{gen} = \int_{QES} \frac{\delta S_{gen}}{\delta \bar{X}^i} \delta \bar{X}^i dz d^{d-2}y - \int_{z=\epsilon} \left(\frac{\partial S_{gen}}{\partial (\partial_z \bar{X}^i)} + \dots \right) \delta \bar{X}^i d^{d-2}y \quad (3.32)$$

where the boundary term comes from integrating by parts when deriving the Euler-Lagrange equations for the functional $S_{gen}[\bar{X}]$. The ellipsis denotes terms involving derivatives of S_{gen} with respect to higher derivatives of the embedding functions ($\partial S_{gen}/\partial(\partial^2 X), \dots$). These boundary terms will include two types of terms: one involving derivatives of the surface area and one involving derivatives of the bulk entropy.

The first area term was already calculated in [126]. There it was found that

$$\frac{\partial A}{\partial (\partial_z \bar{X}^i)} = -\frac{1}{z^{d-1}} \int d^{d-2}y \sqrt{\bar{h}} \frac{g_{ij} \partial_z \bar{X}^i}{\sqrt{1 + g_{lm} \partial_z \bar{X}^l \partial_z \bar{X}^m}} \delta \bar{X}^j \Big|_{z=\epsilon} \quad (3.33)$$

One can use (3.27) to expand this equation in powers ϵ , and then contract with the null vector k on the boundary in order to isolate the variation with respect to null deformations. For boundary surfaces which are locally stationary at some point y , one finds that all terms lower order than z^d vanish at y . In fact, it was shown in [126] that the right hand side of (3.33), after contracting with k^i , is just $k^i V_i$ at first non-vanishing order. Finally, we assume that all such derivatives of the bulk entropy in (3.32) vanish as $z \rightarrow 0$. This is similar to the reasonable assumption that entropy variations vanish at infinity, which should be true in a state with finite bulk entropy. It would be interesting to classify the pathologies of states which violate this assumption. Thus, the final result is that

$$k^i V_i^{QES} = -\frac{1}{\sqrt{\bar{h}}} k^i \frac{\delta S_{gen}}{\delta X^i}. \quad (3.34)$$

The quantum extremal surface prescription says that the boundary field theory entropy is equal to the generalized entropy of the QES [67]. Setting $S_{gen} = S_{bdry}$ in (3.34) and combining that with (3.31) shows that the condition $\beta \geq 0$ is equivalent to the QNEC. Since EWN guarantees that $\beta \geq 0$, the proof is complete.

We briefly comment about the assumptions used to derive (3.34). The bulk entropy should - for generic states - not depend on the precise form of the region near the boundary. The intuition is clear in the thermodynamic limit where bulk entropy is extensive. As long as we assume strong enough fall-off conditions on bulk matter, the change in the entropy will have to vanish as $z \rightarrow 0$.

Note here the importance of using the quantum extremal surface. Had we naively continued to use the extremal area prescription, but still assumed $S_A = S_{bulk}(e(A)) + \frac{A}{4G\hbar}$, we would have discovered a correction to the boundary QNEC from the bulk entropy. The variation of the bulk extremal surface area would be given by a pure boundary term, but the QNEC would take the erroneous form

$$T_{kk} \geq \frac{1}{2\pi\sqrt{\hbar}} (S''_A - S''_{bulk}(e(A))). \quad (3.35)$$

In other words, if one wants to preserve the logical connections put forth in Figure 3.1 while accounting for $1/N$ corrections, the use of quantum extremal surfaces is necessary.

We discuss the effects of higher derivative terms in the gravitational action coming from loop corrections at the end of this section.

$C \subseteq E$ implies the QHANEK

We now examine the boundary implication of $\mathcal{C} \subseteq \mathcal{E}$. As before, this proof will hold to all orders in $G\hbar$, again assuming proper fall-off conditions on derivatives of the bulk entropy.

The basic idea will be to realize that general states in AdS/CFT can be treated as perturbations to the vacuum in the limit of small z . Again, we will consider the general case where the boundary field theory includes relevant deformations. Then, near the boundary, the metric can be written

$$ds^2 = \frac{1}{z^2} \left(dz^2 + \left[f(z)\eta_{ij} + \frac{16\pi G_N}{d} z^d t_{ij} \right] dx^i dx^j + o(z^d) \right), \quad (3.36)$$

where $f(z)$ encodes the effects of the relevant deformations. In this proof we take the viewpoint that the order z^d piece of this expansion is a perturbation on top of the vacuum. In other words

$$g_{ab} = g_{ab}^{vac} + \delta g_{ab}. \quad (3.37)$$

Of course, this statement is highly coordinate dependent. In the following calculations, we treat the metric as a field on top of fixed coordinates. We will have to verify the gauge-independence of the final result, and do so below.

For this proof we are interested in regions A of the boundary such that ∂A is a cut of a null plane. In null coordinates, that would look like $\partial A = \{(u = U_0(y), v = 0)\}$. These

regions are special because in the vacuum state $e(A)$ lies on the past causal horizon generated by bulk geodesics coming from $(u = \infty, v = 0)$. This can be shown using Lorentz symmetry as follows:

An arbitrary cut of a null plane can be deformed back to a flat cut by action with an infinite boost (since boosts act by rescalings of u and v). Such a transformation preserves the vacuum, and so the bulk geometry possesses an associated Killing vector. The past causal horizon from $(u = \infty, v = 0)$ is a Killing horizon for this boost, and by symmetry the quantum extremal surface associated to the flat cut will be the bifurcation surface of the Killing horizon. Had $e(A)$ for the arbitrary cut left the horizon, then it would have been taken off to infinity by the boost and not ended up on the bifurcation surface.¹⁹

We can construct an orthogonal null coordinate system around $e(A)$ in the vacuum. We denote the null orthogonal vectors by k and ℓ where $k^z = 0 = \ell^z$ and $k^x = k^t = 1$ so that $k \cdot \ell = 1$. Then the statement of $\mathcal{C} \subseteq \mathcal{E}$ becomes²⁰

$$k \cdot (\eta - \bar{X}_{SD}) \geq 0 \quad (3.38)$$

Here we use η, \bar{X}_{SD} to denote the perturbation of the causal horizon and quantum extremal surface from their vacuum position, respectively. The notation of \bar{X}_{SD} is used to denote the state-dependent piece of the embedding functions for the extremal surface. Over-bars will denote bulk embedding functions of $e(A)$ surface and X^a will denote boundary coordinates. The set up is illustrated in Figure 3.5.

Just as in the previous section, for a locally stationary surface (such as a cut of a null plane), one can write the embedding coordinates of $e(A)$, \bar{X} , as an expansion in z [126]:

$$\bar{X}^i(y^a, z) = X^i(y^a) + \frac{1}{2(d-2)} z^2 K^i(y^a) + \dots + \frac{z^d}{d} (V^i + W^i(y^a) \log z) + o(z^d) \quad (3.39)$$

where V^i is some local “velocity” function that denotes the rate at which the entangling surface diverges from its boundary position and represents the leading term in the state-dependent part of the embedding functions. The state-independent terms of lower order in z are all proportional to k^i . In vacuum, we also have $V^i \propto k^i$, and so for non-vacuum states $k \cdot \bar{X}_{SD} = \frac{1}{d} V \cdot k z^d + o(z^d)$.

¹⁹It is also worth noting that EWN together with $\mathcal{C} \subseteq \mathcal{E}$ can also be used to construct an argument. Suppose we start with a flat cut of a null plane, for which $e(A)$ is also a flat cut of a null plane in the vacuum (the bifurcation surface for the boost Killing horizon). We then deform this cut on the boundary to an arbitrary cut of the null plane in its future. In the bulk, EWN states that $e(A)$ would have to move in a space-like or null fashion, but if it moves in a space-like way, then $\mathcal{C} \subseteq \mathcal{E}$ is violated.

²⁰The issue of gauge invariance for this proof should not be overlooked. On their own, each term in (3.38) is not gauge invariant under a general diffeomorphism. The sum of the two, on the other hand, does not transform under coordinate change:

$$g_{\mu\nu} \rightarrow g_{\mu\nu} + \nabla_{(\mu} \xi_{\nu)}$$

Plugging this into the formula for $k \cdot \eta$ shows that $\delta(k \cdot \eta) = -(k \cdot \xi)$, which is precisely the same as the change in position of the extremal surface $\delta(k \cdot \bar{X}_{SD}) = -(k \cdot \xi)$.

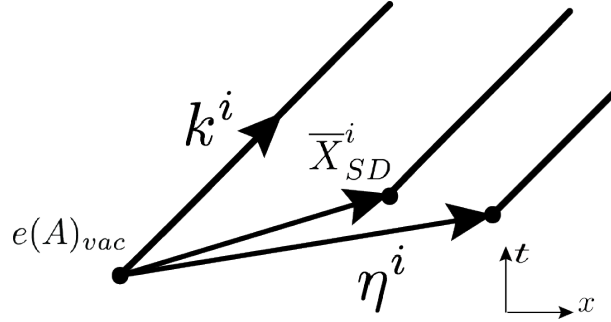


Figure 3.5: This picture shows the various vectors defined in the proof. It depicts a cross-section of the extremal surface at constant z . $e(A)_{vac}$ denotes the extremal surface in the vacuum. For flat cuts of a null plane on the boundary, they agree. For wiggly cuts, they will differ by some multiple of k^i .

Equation (3.34) tells us that \bar{X}_{SD} is proportional to boundary variations of the CFT entropy. Thus, equation (3.39) together with (3.34) tells us the simple result that

$$k \cdot \bar{X}_{SD} = -\frac{4G_N}{d\sqrt{h}} S'_A z^{d-2}. \quad (3.40)$$

Now we explore the η deformation, where η is the vector denoting the shift in the position of the causal horizon. This discussion follows much of the formalism found in [63]. At a specific value of (z, y) , the null generator of the causal surface, k' , is related to the vacuum vector k by

$$k' = k + \delta k = k + k^a \nabla_a \eta \quad (3.41)$$

In the perturbed metric, k' must be null to leading order in $\eta = \mathcal{O}(z^d)$. Imposing this condition we find that

$$k^b \nabla_b (\eta \cdot k) = -\frac{1}{2} \delta g_{ab} k^a k^b \quad (3.42)$$

Here δg_{ab} is simply the difference between the excited state metric and the vacuum metric, which can be treated as a perturbation since we are in the near-boundary limit. This equation can be integrated back along the original null geodesic, with the boundary condition imposed that $\eta(\infty) = 0$. Thus, we find the simple relation

$$(k \cdot \eta)(\lambda) = \frac{1}{2} \int_{\lambda}^{\infty} \delta g_{kk} d\tilde{\lambda}. \quad (3.43)$$

The holographic dictionary tells us how to relate δg_{kk} to boundary quantities. Namely, to leading order in z , the expression above can be recast in terms of the CFT stress tensor

$$k \cdot \eta = \frac{1}{2} \int_{\lambda}^{\infty} \frac{16\pi G_N}{d} z^{d-2} T_{kk} d\tilde{\lambda}. \quad (3.44)$$

Plugging all of this back in to (3.38), we finally arrive at the basic inequality

$$\int_{\lambda}^{\infty} T_{kk} d\tilde{\lambda} + \frac{\hbar}{2\pi\sqrt{\hbar}} S'_A \geq 0. \quad (3.45)$$

Note that all the factors of G_N have dropped out and we have obtained a purely field-theoretic QHANEK.

Loop corrections Here we will briefly comment on how bulk loop corrections affect the argument. Quantum effects do not just require that we add S_{out} to A ; higher derivative terms suppressed by the Planck-scale will be generated in the gravitational action which will modify the gravitational entropy functional. With Planck-scale suppressed higher derivative corrections, derivatives of the boundary entropy of a region have the form

$$S' = \frac{A'}{4G\hbar} + Q' + S'_{out} \quad (3.46)$$

where Q' are the corrections which start at $O((G\hbar)^0)$. The key point is that Q' is always one order behind A' in the $G\hbar$ perturbation theory. As $G\hbar \rightarrow 0$, Q' can only possibly be relevant in situations where $A' = 0$ at $O((G\hbar)^0)$. In this case, $V^i \sim k^i$, and the bulk quantum extremal surface in the vacuum state is a cut of a bulk Killing horizon. But then Q' must be at least $O(G\hbar)$, since $Q' = 0$ on a Killing horizon for any higher derivative theory. Thus we find Eq. (3.34) is unchanged at the leading nontrivial order in $G\hbar$.

Higher derivative terms in the bulk action will also modify the definition of the boundary stress tensor. The appearance of the stress tensor in the QNEC and QHANEK proofs comes from the fact that it appears at $O(z^d)$ in the near-boundary expansion of the bulk metric [126]. Higher derivative terms will modify the coefficient of T_{ij} in this expansion, and therefore in the QNEC and QHANEK. (They will not affect the structure of lower-order terms in the asymptotic metric expansion because there aren't any tensors of appropriate weight besides the flat metric η_{ij} [126]). But the new coefficient will differ from the one in Einstein gravity by the addition of terms containing the higher derivative couplings, which are $1/N$ -suppressed relative to the Einstein gravity term, and will thus only contribute to the sub-leading parts of the QNEC and QHANEK. Thus the validity of the inequalities at small $G\hbar$ is unaffected.

Boundary Causality Condition implies the AANEK

The proof of this statement was first described in [122]. We direct interested readers to that paper for more detail. Here we will sketch the proof and note some similarities to the previous two subsections.

As discussed above, the BCC states that no bulk null curve can connect boundary points that are not connected by a boundary causal curve. In the same way that we took a boundary limit of $\mathcal{C} \subseteq \mathcal{E}$ to prove the QHANEK, the strategy here is to look at nearly null time-like

curves that hug the boundary. These curves will come asymptotically close to beating the boundary null geodesic and so in some sense derive the most stringent condition on the geometry.

Expanding the near boundary metric in powers of z , we use holographic renormalization to identify pieces of the metric as the stress tensor

$$g_{\mu\nu}dx^\mu dx^\nu = \frac{dz^2 + \eta_{ij}dx^i dx^j + z^d \gamma_{ij}(z, x^i)dx^i dx^j}{z^2} \quad (3.47)$$

where $\gamma_{ij}(0, x^i) = \frac{16\pi G_N}{d} \langle T_{ij} \rangle$. Using null coordinates on the boundary, we can parameterize the example bulk curve by $u \mapsto (u, V(u), Z(u), y^i = 0)$. One constructs a nearly null, time-like curve that starts and ends on the boundary and imposes time delay. If $Z(-L) = Z(L) = 0$, then the BCC enforces that $V(L) - V(-L) \geq 0$. For the curve used in [122], the $L \rightarrow \infty$ limit turns this inequality directly into the boundary ANEC.

3.5 Discussion

We have identified two constraints on the bulk geometry, entanglement wedge nesting (EWN) and the $\mathcal{C} \subseteq \mathcal{E}$, coming directly from the consistency of subregion duality and entanglement wedge reconstruction. The former implies the latter, and the latter implies the boundary causality condition (BCC). Additionally, EWN can be understood as a consequence of the quantum focussing conjecture, and $\mathcal{C} \subseteq \mathcal{E}$ follows from the generalized second law. Both statements in turn have implications for the strongly-coupled large- N theory living on the boundary: the QNEC and QHANEC, respectively. In this section, we list possible generalizations and extensions to this work.

Unsuppressed higher derivative corrections There is no guarantee that higher derivative terms with un-suppressed coefficients are consistent with our conclusions. In fact, in [33] it was observed that Gauss-Bonnett gravity in AdS with an intermediate-scale coupling violates the BCC, and this fact was used to place constraints on the theory. We have seen that the geometrical conditions EWN and $\mathcal{C} \subseteq \mathcal{E}$ are fundamental to the proper functioning of the bulk/boundary duality. If it turns out that a higher derivative theory invalidates some of our conclusions, it seems more likely that this would be point to a particular pathology of that theory rather than an inconsistency of our results. It would be interesting if EWN and $\mathcal{C} \subseteq \mathcal{E}$ could be used to place constraints on higher derivative couplings, in the spirit of [33]. We leave this interesting possibility to future work.

A further constraint from subregion duality Entanglement wedge reconstruction implies an additional property that we have not mentioned. Given two boundary regions A and B that are spacelike separated, $\mathcal{E}(A)$ is spacelike separated from $\mathcal{E}(B)$. This property is actually equivalent to EWN for pure states, but is a separate statement for mixed states.

In the latter case, it would be interesting to explore the logical relationships of this property to the constraints in Fig. 3.1.

Beyond AdS In this paper we have only discussed holography in asymptotically AdS spacetimes. While the QFC, QNEC, and GSL make no reference to asymptotically AdS spacetimes, EWN and $\mathcal{C} \subseteq \mathcal{E}$ currently only have meaning in this context. One could imagine however that a holographic correspondence with subregion duality makes sense in more general spacetimes — perhaps formulated in terms of a “theory” living on a holographic screen [18, 22, 24]. In this case, we expect analogues of EWN and $\mathcal{C} \subseteq \mathcal{E}$. For some initial steps in this direction, see [172].

Quantum generalizations of other bulk facts from generalized entropy A key lesson of this paper is that classical results in AdS/CFT relying on the null energy condition (NEC) can often be made semiclassical by appealing to powerful properties of the generalized entropy: the quantum focussing conjecture and the generalized second law. We expect this to be more general than the semiclassical proofs of EWN and $\mathcal{C} \subseteq \mathcal{E}$ presented here. Indeed, Wall has shown that the generalized second law implies semiclassical generalizations of many celebrated results in classical general relativity, including the singularity theorem [191]. It would be illuminating to see how general this pattern is, both in and out of AdS/CFT. As an example, it is known that strong subadditivity of holographic entanglement entropy can be violated in spacetimes which don’t obey the NEC [32]. It seems likely that the QFC can be used to derive strong subadditivity in cases where the NEC is violated due to quantum effects in the bulk.

Gravitational inequalities from field theory inequalities We have seen that the bulk QFC and GSL, which are semi-classical quantum gravity inequalities, imply their non-gravitational limits on the boundary, the QNEC and QHANEC. But we can regard the bulk as an effective field theory of perturbative quantum gravity coupled to matter, and can consider the QNEC and QHANEC for the bulk matter sector. At least when including linearized backreaction of fields quantized on top of a Killing horizon, the QHANEC implies the GSL [188], and the QNEC implies the QFC [26]. In some sense, this “completes” the logical relations of Fig. 3.1.

Support for the quantum extremal surfaces conjecture The logical structure uncovered in this paper relies heavily on the conjecture that the entanglement wedge should be defined in terms of the surface which extremizes the generalized entropy to one side [67] (as opposed to the area). Perhaps similar arguments could be used to prove this conjecture, or at least find an explicit example where extremizing the area is inconsistent with subregion duality, as in [81].

Connections to Recent Proofs of the AANEC Recent proofs of the AANEC have illuminated the origin of this statement within field theory [73, 95]. In one proof, the engine of the inequality came from microcausality and reflection positivity. In the other, the proof relied on monotonicity of relative entropy for half spaces. A natural next question would be how these two proofs are related, if at all. Our paper seems to offer at least a partial answer for holographic CFTs. Both the monotonicity of relative entropy and microcausality - in our case the QHANEC and BCC, respectively - are implied by the same thing in the bulk: $\mathcal{C} \subseteq \mathcal{E}$. In 3.2, we gave a motivation for this geometric constraint from subregion duality. It would be interesting to see how the statement of $\mathcal{C} \subseteq \mathcal{E}$ in a purely field theoretic language is connected to both the QHANEC and causality.

Chapter 4

The Quantum Null Energy Condition, Entanglement Wedge Nesting, and Quantum Focusing

4.1 Introduction and Summary

The Quantum Focusing Conjecture (QFC) is a new principle of semiclassical quantum gravity proposed in [26]. Its formulation is motivated by classical focusing, which states that the expansion θ of a null congruence of geodesics is nonincreasing. Classical focusing is at the heart of several important results of classical gravity [160, 96, 97, 76], and likewise quantum focusing can be used to prove quantum generalizations of many of these results [190, 191, 21, 4].

One of the most important and surprising consequences of the QFC is the Quantum Null Energy Condition (QNEC), which was discovered as a particular nongravitational limit of the QFC [26]. Subsequently the QNEC was proven for free fields [27] and for holographic CFTs on flat backgrounds [126] (and recently extended in [78] in a similar way as we do here). The formulation of the QNEC which naturally comes out of the proofs we provide here is as follows.

Consider a codimension-two Cauchy-splitting surface Σ , which we will refer to as the entangling surface. The Von Neumann entropy $S[\Sigma]$ of the interior (or exterior) of Σ is a functional of Σ , and in particular is a functional of the embedding functions $X^i(y)$ that define Σ . Choose a one-parameter family of deformed surfaces $\Sigma(\lambda)$, with $\Sigma(0) = \Sigma$, such that (i) $\Sigma(\lambda)$ is given by flowing along null geodesics generated by the null vector field k^i normal to Σ for affine time λ , and (ii) $\Sigma(\lambda)$ is either “shrinking” or “growing” as a function of λ , in the sense that the domain of dependence of the interior of Σ is either shrinking or growing. Then for any point on the entangling surface we can define the combination

$$T_{ij}(y)k^i(y)k^j(y) - \frac{1}{2\pi} \frac{d}{d\lambda} \left(\frac{k^i(y)}{\sqrt{h(y)}} \frac{\delta S_{\text{ren}}}{\delta X^i(y)} \right). \quad (4.1)$$

Here $\sqrt{h(y)}$ is the induced metric determinant on Σ . Writing this down in a general curved background requires a renormalization scheme both for the energy-momentum tensor T_{ij} and the renormalized entropy S_{ren} . Assuming that this quantity is scheme-independent (and hence well-defined), the QNEC states that it is positive. Our main task is to determine the necessary and sufficient conditions we need to impose on Σ and the background spacetime at the point y in order that the QNEC hold.

In addition to a proof through the QFC, the holographic proof method of [126] is easily adaptable to answering this question in full generality. The backbone of that proof is Entanglement Wedge Nesting (EWN), which is a consequence of subregion duality in AdS/CFT [4]. A given region on the boundary of AdS is associated with a particular region of the bulk, called the entanglement wedge, which is defined as the bulk region spacelike-related to the extremal surface [171, 111, 67, 51] used to compute the CFT entropy on the side toward the boundary region. This bulk region is dual to the given boundary region, in the sense that there is a correspondence between the algebra of operators in the bulk region and that of the operators in the boundary region which are good semiclassical gravity operators (i.e., they act within the subspace of semiclassical states) [46, 117, 50]. EWN is the statement that nested boundary regions must be dual to nested bulk regions, and clearly follows from the consistency of subregion duality.

While the QNEC can be derived from both the QFC and EWN, there has been no clear connection between these derivations.¹ As it stands, there are apparently two QNECs, the QNEC-from-QFC and the QNEC-from-EWN. We will show in full generality that these two QNECs are in fact the same, at least in $d \leq 5$ dimensions.

Here is a summary of our results:

- The holographic proof of the QNEC from EWN is extended to CFTs on arbitrary curved backgrounds. In $d = 5$ we find that the necessary and sufficient conditions for the ordinary QNEC to hold at a point are that²

$$\theta_{(k)} = \sigma_{ab}^{(k)} = D_a \theta_{(k)} = D_a \sigma_{bc}^{(k)} = R_{ka} = 0 \quad (4.2)$$

at that point. For $d < 5$ only a subset of these conditions are necessary. This is the subject of §4.2.

- We also show holographically that under the weaker set of conditions

$$\sigma_{ab}^{(k)} = D_a \theta_{(k)} + R_{ka} = D_a \sigma_{bc}^{(k)} = 0 \quad (4.3)$$

the Conformal QNEC holds. The Conformal QNEC was introduced in [126] as a conformally-transformed version of the QNEC. This is the strongest inequality that we can get out of EWN. This is the subject of §4.2

¹In [4] it was shown that the QFC in the bulk implies EWN, which in turn implies the QNEC. This is not the same as the connection we are referencing here. The QFC which would imply the boundary QNEC in the sense that we mean is a *boundary* QFC, obtained by coupling the boundary theory to gravity.

²Here $\sigma_{ab}^{(k)}$ and $\theta_{(k)}$ are the shear and expansion in the k^i direction, respectively, and D_a is a surface covariant derivative. Our notation is further explained in Appendix A.2.

- By taking the non-gravitational limit of the QFC we are able to derive the QNEC again under the same set of conditions as we did for EWN. This is the subject of §4.3.
- We argue in §4.3 that the statement of the QNEC is scheme-independent whenever the conditions that allow us to prove it hold. This shows that the two proofs of the QNEC are actually proving the same, unambiguous field-theoretic bound.

We conclude in §4.4 with a discussion and suggest future directions. A number of technical Appendices are included as part of our analysis.

Relation to other work While this work was in preparation, [78] appeared which has overlap with our discussion of EWN and the scheme-independence of the QNEC. The results of [78] relied on a number of assumptions about the background: the null curvature condition and a positive energy condition. From this they derive certain sufficient conditions for the QNEC to hold. We do not assume anything about our backgrounds a priori, and include all relevant higher curvature corrections. This gives our results greater generality, as we are able to find both necessary and sufficient conditions for the QNEC to hold.

4.2 Entanglement Wedge Nesting

Subregion Duality

The statement of AdS/CFT includes a correspondence between operators in the semiclassical bulk gravitational theory and CFT operators on the boundary. Moreover, it has been shown [90, 50] that such a correspondence exists between the operator algebras of subregions in the CFT and certain associated subregions in the bulk as follows: Consider a spatial subregion A in the boundary geometry. The extremal surface anchored to ∂A , which is used to compute the entropy of A [171, 111], bounds the so-called entanglement wedge of A , $\mathcal{E}(A)$, in the bulk. More precisely $\mathcal{E}(A)$ is the codimension-zero bulk region spacelike-related to the extremal surface on the same side of the extremal surface as A . Subregion duality is the statement that the operator algebras of $\mathcal{D}(A)$ and $\mathcal{E}(A)$ are dual, where $\mathcal{D}(A)$ denotes the domain of dependence of A .

Entanglement Wedge Nesting The results of this section follow from EWN, which we now describe. Consider two boundary regions A_1 and A_2 such that $\mathcal{D}(A_1) \subseteq \mathcal{D}(A_2)$. Then consistency of subregion duality implies that $\mathcal{E}(A_1) \subseteq \mathcal{E}(A_2)$ as well, and this is the statement of EWN. In particular, EWN implies that the extremal surfaces associated to A_1 and A_2 cannot be timelike-related.

We will mainly be applying EWN to the case of a one-parameter family of boundary regions, $A(\lambda)$, where $\mathcal{D}(A(\lambda_1)) \subseteq \mathcal{D}(A(\lambda_2))$ whenever $\lambda_1 \leq \lambda_2$. Then the union of the one-parameter family of extremal surfaces associated to $A(\lambda)$ forms a codimension-one surface

Figure 4.1: Here we show the holographic setup which illustrates Entanglement Wedge Nesting. A spatial region A_1 on the boundary is deformed into the spatial region A_2 by the null vector δX^i . The extremal surfaces of A_1 and A_2 are connected by a codimension-one bulk surface \mathcal{M} (shaded blue) that is nowhere timelike by EWN. Then the vectors $\delta\bar{X}^\mu$ and s^μ , which lie in \mathcal{M} , have nonnegative norm.

in the bulk that is nowhere timelike. We denote this codimension-one surface by \mathcal{M} . See Fig. 4.1 for a picture of the setup.

Since \mathcal{M} is nowhere timelike, every one of its tangent vectors must have nonnegative norm. In particular, consider the embedding functions \bar{X}^μ of the extremal surfaces in some coordinate system. Then the vectors $\delta\bar{X}^\mu \equiv \partial_\lambda \bar{X}^\mu$ is tangent to \mathcal{M} , and represents a vector that points from one extremal surface to another. Hence we have $(\delta\bar{X})^2 \geq 0$ from EWN, and this is the inequality that we will discuss for most of the remainder of this section.

Before moving on, we will note that $(\delta\bar{X})^2 \geq 0$ is not necessarily the strongest inequality we get from EWN. At each point on \mathcal{M} , the vectors which are tangent to the extremal surface passing through that point are known to be spacelike. Therefore if $\delta\bar{X}^\mu$ contains any components which are tangent to the extremal surface, they will serve to make the inequality $(\delta\bar{X})^2 \geq 0$ weaker. We define the vector s^μ at any point of \mathcal{M} to be the part of $\delta\bar{X}^\mu$ orthogonal to the extremal surface passing through that point. Then $(\delta\bar{X})^2 \geq s^2 \geq 0$. We will discuss the $s^2 \geq 0$ inequality in §4.2 after handling the $(\delta\bar{X})^2 \geq 0$ case.

Near-Boundary EWN

In this section we explain how to calculate the vector $\delta\bar{X}^\mu$ and s^μ near the boundary explicitly in terms of CFT data. Then the EWN inequalities $(\delta\bar{X})^2 > 0$ and $s^2 > 0$ can be given a CFT meaning. The strategy is to use a Fefferman-Graham expansion of both the metric and extremal surface, leading to equations for $\delta\bar{X}^\mu$ and s^μ as power series in the bulk coordinate z (including possible log terms). In the following sections we will analyze the inequalities that are derived in this section.

Bulk Metric We work with a bulk theory in AdS_{d+1} that consists of Einstein gravity plus curvature-squared corrections. For $d \leq 5$ this is the complete set of higher curvature corrections that have an impact on our analysis. The Lagrangian is³

$$\mathcal{L} = \frac{1}{16\pi G_N} \left(\frac{d(d-1)}{\tilde{L}^2} + \mathcal{R} + \ell^2 \lambda_1 \mathcal{R}^2 + \ell^2 \lambda_2 \mathcal{R}_{\mu\nu}^2 + \ell^2 \lambda_{GB} \mathcal{L}_{GB} \right), \quad (4.4)$$

where $\mathcal{L}_{GB} = \mathcal{R}_{\mu\nu\rho\sigma}^2 - 4\mathcal{R}_{\mu\nu}^2 + \mathcal{R}^2$ is the Gauss-Bonnet Lagrangian, ℓ^2 is the cutoff scale, and \tilde{L}^2 is the scale of the cosmological constant. The bulk metric has the following near

³For simplicity we will not include matter fields explicitly in the bulk, but their presence should not alter any of our conclusions.

boundary expansion in Fefferman-Graham gauge [92]:

$$ds^2 = \frac{L^2}{z^2} (dz^2 + \bar{g}_{ij}(x, z) dx^i dx^j), \quad (4.5)$$

$$\bar{g}_{ij}(x, z) = g_{ij}^{(0)}(x) + z^2 g_{ij}^{(2)}(x) + z^4 g_{ij}^{(4)}(x) + \dots + z^d \log z g_{ij}^{(d, \log)}(x) + z^d g_{ij}^{(d)}(x) + o(z^d). \quad (4.6)$$

Note that the length scale L is different from \tilde{L} , but the relationship between them will not be important for us. Demanding that the above metric solve bulk gravitational equations of motion gives expressions for all of the $g_{ij}^{(n)}$ for $n < d$, including $g_{ij}^{(d, \log)}(x)$, in terms of $g_{ij}^{(0)}(x)$. This means, in particular, that these terms are all state-independent. One finds that $g_{ij}^{(d, \log)}(x)$ vanishes unless d is even. We provide explicit expressions for some of these terms in Appendix A.4.

The only state-dependent term we have displayed, $g_{ij}^{(d)}(x)$, contains information about the expectation value of the energy-momentum tensor T_{ij} of the field theory. In odd dimensions we have the simple formula [72]⁴

$$g_{ij}^{(d=\text{odd})} = \frac{16\pi G_N}{\eta d L^{d-1}} \langle T_{ij} \rangle, \quad (4.7)$$

with

$$\eta = 1 - 2(d(d+1)\lambda_1 + d\lambda_2 + (d-2)(d-3)\lambda_{\text{GB}}) \frac{\ell^2}{L^2} \quad (4.8)$$

In even dimensions the formula is more complicated. For $d = 4$ we discuss the form of the metric in Appendix A.6

Extremal Surface EWN is a statement about the causal relation between entanglement wedges. To study this, we need to calculate the position of the extremal surface. We parametrize our extremal surface by the coordinate (y^a, z) , and the position of the surface is determined by the embedding functions $\bar{X}^\mu(y^a, z)$. The intrinsic metric of the extremal surface is denoted by $\bar{h}_{\alpha\beta}$, where $\alpha = (a, z)$. For convenience we will impose the gauge conditions $\bar{X}^z = z$ and $\bar{h}_{az} = 0$.

The functions $\bar{X}(y^a, z)$ are determined by extremizing the generalized entropy [67, 51] of the entanglement wedge. This generalized entropy consists of geometric terms integrated over the surface as well as bulk entropy terms. We defer a discussion of the bulk entropy terms to §4.4 and write only the geometric terms, which are determined by the bulk action:

$$S_{\text{gen}} = \frac{1}{4G_N} \int \sqrt{\bar{h}} \left[1 + 2\lambda_1 \ell^2 \mathcal{R} + \lambda_2 \ell^2 \left(\mathcal{R}_{\mu\nu} \mathcal{N}^{\mu\nu} - \frac{1}{2} \mathcal{K}_\mu \mathcal{K}^\mu \right) + 2\lambda_{\text{GB}} \ell^2 \bar{r} \right]. \quad (4.9)$$

⁴Even though [72] worked with a flat boundary theory, one can check that this formula remains unchanged when the boundary is curved.

We discuss this entropy functional in more detail in Appendix A.4. The Euler-Lagrange equations for S_{gen} are the equations of motion for \bar{X}^μ . Like the bulk metric, the extremal surface equations can be solved at small- z with a Fefferman–Graham-like expansion:

$$\bar{X}^i(y, z) = X_{(0)}^i(y) + z^2 X_{(2)}^i(y) + z^4 X_{(4)}^i(y) + \dots + z^d \log z X_{(d, \log)}^i(y) + z^d X_{(d)}^i(y) + o(z^d), \quad (4.10)$$

As with the metric, the coefficient functions $X_{(n)}^i$ for $n < d$, including the log term, can be solved for in terms of $X_{(0)}^i$ and $g_{ij}^{(0)}$, and again the log term vanishes unless d is even. The state-dependent term $X_{(d)}^i$ contains information about variations of the CFT entropy, as we explain below.

The z -Expansion of EWN By taking the derivative of (4.10) with respect to λ , we find the z -expansion of $\delta\bar{X}^i$. We will discuss how to take those derivatives momentarily. But given the z -expansion of $\delta\bar{X}^i$, we can combine this with the z -expansion of \bar{g}_{ij} in (4.6) to get the z -expansion of $(\delta\bar{X})^2$:

$$\frac{z^2}{L^2} (\delta\bar{X})^2 = g_{ij}^{(0)} \delta X_{(0)}^i \delta X_{(0)}^j + z^2 \left(2g_{ij}^{(0)} \delta X_{(0)}^i \delta X_{(2)}^j + g_{ij}^{(2)} \delta X_{(0)}^i \delta X_{(0)}^j + X_{(2)}^m \partial_m g_{ij}^{(0)} \delta X_{(0)}^i \delta X_{(0)}^j \right) + \dots \quad (4.11)$$

EWN implies that $(\delta\bar{X})^2 \geq 0$, and we will spend the next few sections examining this inequality using the expansion (4.11). From the general arguments given above, we can get a stronger inequality by considering the vector s^μ and its norm rather than $\delta\bar{X}^\mu$. The construction of s^μ is more involved, but we would similarly construct an equation for s^2 at small z . We defer further discussion of s^μ to §4.2.

Now we return to the question of calculating $\delta\bar{X}^i$. Since all of the $X_{(n)}^i$ for $n < d$ are known explicitly from solving the equation of motion, the λ -derivatives of those terms can be taken and the results expressed in terms of the boundary conditions for the extremal surface. The variation of the state-dependent term, $\delta X_{(d)}^i$, is also determined by the boundary conditions in principle, but in a horribly non-local way. However, we will now show that $X_{(d)}^i$ (and hence $\delta X_{(d)}^i$) can be re-expressed in terms of variations of the CFT entropy.

Variations of the Entropy The CFT entropy S_{CFT} is equal to the generalized entropy S_{gen} of the entanglement wedge in the bulk. To be precise, we need to introduce a cutoff at $z = \epsilon$ and use holographic renormalization to properly define the entropy. Then we can use the calculus of variations to determine variations of the entropy with respect to the boundary conditions at $z = \epsilon$. There will be terms which diverge as $\epsilon \rightarrow 0$, as well as a finite term, which is the only one we are interested in at the moment. In odd dimensions, the finite term is given by a simple integral over the entangling surface in the CFT:

$$\delta S_{\text{CFT}}|_{\text{finite}} = \eta dL^{d-1} \int d^{d-2}y \sqrt{h} g_{ij} X_{(d)}^i \delta X^j. \quad (4.12)$$

This finite part of S_{CFT} is the renormalized entropy, S_{ren} , in holographic renormalization. Eventually we will want to assure ourselves that our results are scheme-independent. This question was studied in [77], and we will discuss it further in §4.3. For now, the important take-away from (4.12) is

$$\frac{1}{\sqrt{h}} \frac{\delta S_{\text{ren}}}{\delta X^i(y)} = -\frac{\eta d L^{d-1}}{4G_N} X^i_{(d,\text{odd})}. \quad (4.13)$$

The case of even d is more complicated, and we will cover the $d = 4$ case in Appendix A.6.

State-Independent Inequalities

The basic EWN inequality is $(\delta\bar{X})^2 \geq 0$. The challenge is to write this in terms of boundary quantities. In this section we will look at the state-independent terms in the expansion of (4.11). The boundary conditions at $z = 0$ are given by the CFT entangling surface and background geometry, which we denote by X^i and g_{ij} without a (0) subscript. The variation vector of the entangling surface is the null vector $k^i = \delta X^i$. We can use the formulas of Appendix A.5 to express the other $X^i_{(n)}$ for $n < d$ in terms of X^i and g_{ij} . This allows us to express the state-independent parts of $(\delta\bar{X})^2 \geq 0$ in terms of CFT data. In this subsection we will look at the leading and subleading state-independent parts. These will be sufficient to fully cover the cases $d \leq 5$.

Leading Inequality From (4.11), we see that the first term is actually $k_i k^i = 0$. The next term is the one we call the leading term, which is

$$L^{-2}(\delta\bar{X})^2|_{z_0} = 2k_i \delta X^i_{(2)} + g_{ij}^{(2)} k^i k^j + X^m_{(2)} \partial_m g_{ij} k^i k^j. \quad (4.14)$$

From (A.49), we easily see that this is equivalent to

$$L^{-2}(\delta\bar{X})^2|_{z_0} = \frac{1}{(d-2)^2} \theta_{(k)}^2 + \frac{1}{d-2} \sigma_{(k)}^2, \quad (4.15)$$

where $\sigma_{ab}^{(k)}$ and $\theta_{(k)}$ are the shear and expansion of the null congruence generated by k^i , and are given by the trace and trace-free parts of $k_i K^i_{ab}$, with K^i_{ab} the extrinsic curvature of the entangling surface. This leading inequality is always nonnegative, as required by EWN. Since we are in the small- z limit, the subleading inequality is only relevant when this leading inequality is saturated. So in our analysis below we will focus on the $\theta_{(k)} = \sigma_{ab}^{(k)} = 0$ case, which can always be achieved by choosing the entangling surface appropriately. Note that in $d = 3$ this is the only state-independent term in $(\delta\bar{X})^2$, and furthermore we always have $\sigma_{ab}^{(k)} = 0$ in $d = 3$.

Subleading Inequality The subleading term in $(\delta\bar{X})^2$ is order z^2 in $d \geq 5$, and order $z^2 \log z$ in $d = 4$. These two cases are similar, but it will be easiest to focus first on $d \geq 5$

and then explain what changes in $d = 4$. The terms we are looking for are

$$\begin{aligned} L^{-2}(\delta\bar{X})^2|_{z^2} &= 2k_i\delta X_{(4)}^i + 2g_{ij}^{(2)}k^i\delta X_{(2)}^j + g_{ij}\delta X_{(2)}^i\delta X_{(2)}^j + g_{ij}^{(4)}k^ik^j + X_{(4)}^m\partial_m g_{ij}k^ik^j \\ &+ 2X_{(2)}^m\partial_m g_{ij}k^ik^j + X_{(2)}^m\partial_m g_{ij}^{(2)}k^ik^j + \frac{1}{2}X_{(2)}^mX_{(2)}^n\partial_m\partial_n g_{ij}k^ik^j. \end{aligned} \quad (4.16)$$

This inequality is significantly more complicated than the previous one. The details of its evaluation are left to Appendix A.5. The result, assuming $\theta_{(k)} = \sigma_{ab}^{(k)} = 0$, is

$$\begin{aligned} L^{-2}(\delta\bar{X})^2|_{z^2} &= \frac{1}{4(d-2)^2}(D_a\theta_{(k)} + 2R_{ka})^2 \\ &+ \frac{1}{(d-2)^2(d-4)}(D_a\theta_{(k)} + R_{ka})^2 + \frac{1}{2(d-2)(d-4)}(D_a\sigma_{bc}^{(k)})^2 \\ &+ \frac{\kappa}{d-4}(C_{kabc}C_k^{abc} - 2C_k^c{}_{ca}C_k^b{}^a). \end{aligned} \quad (4.17)$$

where κ is proportional to $\lambda_{\text{GB}}\ell^2/L^2$ and is defined in Appendix A.5. Aside from the Gauss–Bonnet term we have a sum of squares, which is good because EWN requires this to be positive when $\theta_{(k)}$ and $\sigma_{(k)}$ vanish. Since $\kappa \ll 1$, it cannot possibly interfere with positivity unless the other terms were zero. This would require $D_a\theta_{(k)} = D_a\sigma_{bc}^{(k)} = R_{ka} = 0$ in addition to our other conditions. But, following the arguments of [133], this cannot happen unless the components C_{kabc} of the Weyl tensor also vanish at the point in question. Thus EWN is always satisfied. Also note that the last two terms in middle line of (4.17) are each conformally invariant when $\theta_{(k)} = \sigma_{ab}^{(k)} = 0$, which we have assumed. This will become important later.

Finally, though we have assumed $d \geq 5$ to arrive at this result, we can use it to derive the expression for $L^{-2}(\delta\bar{X})^2|_{z^2 \log z}$ in $d = 4$. The rule, explained in Appendix A.6, is to multiply the RHS by $4 - d$ and then set $d = 4$. This has the effect of killing the conformally non-invariant term, leaving us with

$$L^{-2}(\delta\bar{X})^2|_{z^2 \log z, d=4} = -\frac{1}{4}(D_a\theta_{(k)} + R_{ka})^2 - \frac{1}{4}(D_a\sigma_{bc}^{(k)})^2. \quad (4.18)$$

The Gauss–Bonnet term also disappears because of a special Weyl tensor identity in $d = 4$ [77]. The overall minus sign is required since $\log z < 0$ in the small z limit. In addition, we no longer require that R_{ka} and $D_a\theta_{(k)}$ vanish individually to saturate the inequality: only their sum has to vanish. This still requires that $C_{kabc} = 0$, though.

The Quantum Null Energy Condition

The previous section dealt with the two leading state-independent inequalities that EWN implies. Here we deal with the leading state-*dependent* inequality, which turns out to be the QNEC.

At all orders lower than z^{d-2} , $(\delta\bar{X})^2$ is purely geometric. At order z^{d-2} , however, the CFT energy-momentum tensor enters via the Fefferman–Graham expansion of the metric, and variations of the entropy enter through $X_{(d)}^i$. In odd dimensions the analysis is simple and we will present it here, while in general even dimensions it is quite complicated. Since our state-independent analysis is incomplete for $d > 5$ anyway, we will be content with analyzing only $d = 4$ for the even case. The $d = 4$ calculation is presented in Appendix A.6. Though it is more involved that the odd-dimensional case, the final result is the same.

Consider first the case where d is odd. Then we have

$$L^{-2}(\delta\bar{X})^2|_{z^{d-2}} = g_{ij}^{(d)} k^i k^j + 2k_i \delta X_{(d)}^i + X_{(d)}^m \partial_m g_{ij} k^i k^j = g_{ij}^{(d)} k^i k^j + 2\delta(k_i \delta X_{(d)}^i). \quad (4.19)$$

From (4.7) and (4.13), we find that

$$L^{-2}(\delta\bar{X})^2|_{z^{d-2}} = \frac{16\pi G_N}{\eta d L^{d-1}} \left[\langle T_{kk} \rangle - \delta \left(\frac{k^i}{2\pi\sqrt{h}} \frac{\delta S_{\text{ren}}}{\delta X^i} \right) \right]. \quad (4.20)$$

The nonnegativity of the term in brackets is equivalent to the QNEC. The case where d is even is more complicated, and we will go over the $d = 4$ case in Appendix A.6.

The Conformal QNEC

As mentioned in §4.2, we can get a stronger inequality from EWN by considering the norm of the vector s^μ , which is the part of $\delta\bar{X}^\mu$ orthogonal to the extremal surface. Our gauge choice $\bar{X}^z = z$ means that $s^\mu \neq \delta\bar{X}^\mu$, and so we get a nontrivial improvement by considering $s^2 \geq 0$ instead of $(\delta\bar{X})^2 \geq 0$.

We can actually use the results already derived above to compute s^2 with the following trick. We would have had $\delta\bar{X}^\mu = s^\mu$ if the surfaces of constant z were already orthogonal to the extremal surfaces. But we can change our definition of the constant- z surfaces with a coordinate transformation in the bulk to make this the case, apply the above results to $(\delta\bar{X})^2$ in the new coordinate system, and then transform back to the original coordinates. The coordinate transformation we are interested in performing is a PBH transformation [113], since it leaves the metric in Fefferman–Graham form, and so induces a Weyl transformation on the boundary.

So from the field theory point of view, we will just be calculating the consequences of EWN in a different conformal frame, which is fine because we are working with a CFT. With that in mind it is easy to guess the outcome: the best conformal frame to pick is one in which all of the non-conformally-invariant parts of the state-independent terms in $(\delta\bar{X})^2$ are set to zero, and when we transform the state-dependent term in the new frame back to the original frame we get the so-called Conformal QNEC first defined in [126]. This is indeed what happens, as we will now see.

Orthogonality Conditions First, we will examine in detail the conditions necessary for $\delta\bar{X}^\mu = s^\mu$, and their consequences on the inequalities derived above. We must check that

$$\bar{g}_{ij} \partial_\alpha \bar{X}^i \delta \bar{X}^j = 0. \quad (4.21)$$

for both $\alpha = z$ and $\alpha = a$. As above, we will expand these conditions in z . When $\alpha = z$, at lowest order in z we find the condition

$$0 = k_i X_{(2)}^i, \quad (4.22)$$

which is equivalent to $\theta_{(k)} = 0$. When $\alpha = a$, the lowest-order in z inequality is automatically satisfied because k^i is defined to be orthogonal to the entangling surface on the boundary. But at next-to-lowest order we find the condition

$$0 = k_i \partial_a X_{(2)}^i + e_{ai} \delta X_{(2)}^i + g_{ij}^{(2)} e_a^i k^j + X_{(2)}^m \partial_m g_{ij} e_a^i k^j \quad (4.23)$$

$$= -\frac{1}{2(d-2)} [(D_a - 2w_a)\theta_{(k)} + 2R_{ka}]. \quad (4.24)$$

Combined with the $\theta_{(k)} = 0$ condition, this tells us that that $D_a \theta_{(k)} = -2R_{ka}$ is required. When these conditions are satisfied, the state-dependent terms of $(\delta \bar{X})^2$ analyzed above become⁵

$$L^{-2}(\delta \bar{X})^2 = \frac{1}{d-2} \sigma_{(k)}^2 + \left[\frac{1}{(d-2)^2(d-4)} (R_{ka})^2 + \frac{1}{2(d-2)(d-4)} (D_a \sigma_{bc}^{(k)})^2 \right] z^2 + \dots \quad (4.25)$$

Next we will demonstrate that $\theta_{(k)} = 0$ and $D_a \theta_{(k)} = -2R_{ka}$ can be achieved by a Weyl transformation, and then use that fact to write down the $s^2 \geq 0$ inequality that we are after.

Achieving $\delta \bar{X}^\mu = s^\mu$ with a Weyl Transformation Our goal now is to begin with a generic situation in which $\delta \bar{X}^\mu \neq s^\mu$ and use a Weyl transformation to set $\delta \bar{X}^\mu \rightarrow s^\mu$. This means finding a new conformal frame with $\hat{g}_{ij} = e^{2\phi(x)} g_{ij}$ such that $\hat{\theta}_{(k)} = 0$ and $\hat{D}_a \hat{\theta}_{(k)} = -2\hat{R}_{ka}$, which would then imply that $\delta \hat{X}^\mu = s^\mu$ (we omit the bar on $\delta \hat{X}^\mu$ to avoid cluttering the notation, but logically it would be $\delta \hat{\bar{X}}^\mu$).

Computing the transformation properties of the geometric quantities involved is a standard exercise, but there is one extra twist involved here compared to the usual prescription. Ordinarily a vector such as k^i would be invariant under the Weyl transformation. However, for our setup it is important that k^i generate an affine-parameterized null geodesic. Even though the null geodesic itself is invariant under Weyl transformation, k^i will no longer be the correct generator. Instead, we have to use $\hat{k}^i = e^{-2\phi} k^i$. Another way of saying this is

⁵We have not included some terms at order z^2 which are proportional to $\sigma_{ab}^{(k)}$ because they never play a role in the EWN inequalities.

that $k_i = \hat{k}_i$ is invariant under the Weyl transformation. With this in mind, we have

$$e^{2\phi} \hat{R}_{ka} = R_{ka} - (d-2) [D_a \partial_k \phi - w_a \partial_k \phi - k_j K_{ab}^j \partial^b \phi - \partial_k \phi \partial_a \phi], \quad (4.26)$$

$$e^{2\phi} \hat{\theta}_{(k)} = \theta_{(k)} + (d-2) \partial_k \phi, \quad (4.27)$$

$$e^{2\phi} \hat{D}_a \hat{\theta}_{(k)} = D_a \theta_{(k)} + (d-2) D_a \partial_k \phi - 2 \theta_{(k)} \partial_a \phi - 2(d-2) \partial_k \phi \partial_a \phi, \quad (4.28)$$

$$\hat{\sigma}_{ab}^{(k)} = \sigma_{ab}^{(k)}, \quad (4.29)$$

$$\hat{D}_c \hat{\sigma}_{ab}^{(k)} = D_c \sigma_{ab}^{(k)} - 2 \left[\sigma_{c(b}^{(k)} \partial_a) \phi + \sigma_{ab}^{(k)} \partial_c \phi - g_{c(a} \sigma_{b)d}^{(k)} \nabla^d \phi \right], \quad (4.30)$$

$$\hat{w}_a = w_a - \partial_a \phi. \quad (4.31)$$

So we may arrange $\hat{\theta}_{(k)} = 0$ at a given point on the entangling surface by choosing $\partial_k \phi = -\theta_{(k)}/(d-2)$ at that point. Having chosen that, and assuming $\sigma_{ab}^{(k)} = 0$ at the same point, one can check that

$$e^{2\phi} \left(\hat{D}_a \hat{\theta}_{(k)} + 2 \hat{R}_{ka} \right) = D_a \theta_{(k)} - 2 w_a \theta_{(k)} + 2 R_{ka} - (d-2) D_a \partial_k \phi \quad (4.32)$$

So we can choose $D_a \partial_k \phi$ to make the combination $\hat{D}_a \hat{\theta}_{(k)} + 2 \hat{R}_{ka}$ vanish. Then in the new frame we have $\delta \hat{X}^\mu = s^\mu$.

The $s^2 \geq 0$ Inequality Based on the discussion above, we were able to find a conformal frame that allows us to compute the s^2 . For the state-independent parts we have

$$L^{-2} s^2 = \frac{1}{d-2} \hat{\sigma}_{(k)}^2 + \left[\frac{1}{(d-2)^2(d-4)} (\hat{R}_{ka})^2 + \frac{1}{2(d-2)(d-4)} (\hat{D}_a \hat{\sigma}_{bc}^{(k)})^2 \right] \hat{z}^2 + \dots \quad (4.33)$$

Here we also have a new bulk coordinate $\hat{z} = z e^\phi$ associated with the bulk PBH transformation. All we have to do now is transform back into the original frame to find s^2 . Since $\hat{\theta}_{(k)} = \hat{D}_a \hat{\theta}_{(k)} + 2 \hat{R}_{ka} = 0$, we actually have that

$$\hat{R}_{ka} = \hat{D}_a \hat{\theta}_{(k)} - \hat{w}_a \hat{\theta}_{(k)} - \hat{R}_{ka}, \quad (4.34)$$

which transforms homogeneously under Weyl transformations when $\sigma_{ab}^{(k)} = 0$. Thus, up to an overall scaling factor, we have

$$L^{-2} s^2 = \frac{1}{d-2} \sigma_{(k)}^2 + \left[\frac{1}{(d-2)^2(d-4)} (D_a \theta_{(k)} - w_a \theta_{(k)} - R_{ka})^2 + \frac{1}{2(d-2)(d-4)} (D_a \sigma_{bc}^{(k)})^2 \right] z^2 + \dots, \quad (4.35)$$

where we have dropped terms of order z^2 which vanish when $\sigma_{ab}^{(k)} = 0$. As predicted, these terms are the conformally invariant contributions to $(\delta \bar{X})^2$.

In order to access the state-dependent part of s^2 we need the terms in (4.35) to vanish. Note that in $d = 3$ this always happens. In that case there is no z^2 term, and $\sigma_{ab}^{(k)} = 0$ always. Though our expression is singular in $d = 4$, comparing to (4.25) shows that actually the term in brackets above is essentially the same as the $z^2 \log z$ term in $\delta\bar{X}$. We already noted that this term was conformally invariant, so this is expected. The difference now is that we no longer need $\theta_{(k)} = 0$ in order to get to the QNEC in $d = 4$. In $d = 5$ the geometric conditions for the state-independent parts of s^2 to vanish are identical to those for $d = 4$, whereas in the $(\delta\bar{X})^2$ analysis we found that extra conditions were necessary. These were relics of the choice of conformal frame. Finally, for $d > 5$ there will be additional state-independent terms that we have not analyzed, but the results we have will still hold.

Conformal QNEC Now we analyze the state-dependent part of s^2 at order z^{d-2} . When all of the state-independent parts vanish, the state-dependent part is given by the conformal transformation of the QNEC. This is easily computed as follows:

$$L^{-2} s^2|_{z^{d-2}} = \frac{16\pi G_N}{\eta d L^{d-1}} \left[2\pi \langle \hat{T}_{ij} \rangle k^i k^j - \delta \left(\frac{k^i}{\sqrt{h}} \frac{\delta \hat{S}_{\text{ren}}}{\delta X^i(y)} \right) - \frac{d}{2} \theta_{(k)} \left(\frac{k^i}{\sqrt{h}} \frac{\delta \hat{S}_{\text{ren}}}{\delta X^i(y)} \right) \right]. \quad (4.36)$$

Of course, one would like to replace \hat{T}_{ij} with T_{ij} and \hat{S}_{ren} with S_{ren} . When d is odd this is straightforward, as these quantities are conformally invariant. However, when d is even there are anomalies that will contribute, leading to extra geometric terms in the conformal QNEC [86, 126].

4.3 Connection to Quantum Focusing

The Quantum Focusing Conjecture

We start by reviewing the statement of the QFC [26, 133] before moving on to its connection to EWN and the QNEC. Consider a codimension-two Cauchy-splitting (i.e. entangling) surface Σ and a null vector field k^i normal to Σ . Denote by \mathcal{N} the null surface generated by k^i . The generalized entropy, S_{gen} , associated to Σ is given by

$$S_{\text{gen}} = \langle S_{\text{grav}} \rangle + S_{\text{ren}} \quad (4.37)$$

where S_{grav} is a state-independent local integral on Σ and S_{ren} is the renormalized von Neumann entropy of the interior (or exterior) of Σ . The terms in S_{grav} are determined by the low-energy effective action of the theory in a well-known way [47]. Even though $\langle S_{\text{grav}} \rangle$ and S_{ren} individually depend on the renormalization scheme, that dependence cancels out between them so that S_{gen} is scheme-independent.

The generalized entropy is a functional of the entangling surface Σ , and the QFC is a statement about what happens when we vary the shape of Σ by deforming it within the surface \mathcal{N} . Specifically, consider a one-parameter family $\Sigma(\lambda)$ of cuts of \mathcal{N} generated by

deforming the original surface using the vector field k^i . Here λ is the affine parameter along the geodesic generated by k^i and $\Sigma(0) \equiv \Sigma$. To be more precise, let y^a denote a set of intrinsic coordinates for Σ , let h_{ab} be the induced metric on Σ , and let $X^i(y, \lambda)$ be the embedding functions for $\Sigma(\lambda)$. With this notation, $k^i = \partial_\lambda X^i$. The change in the generalized entropy is given by

$$\left. \frac{dS_{\text{gen}}}{d\lambda} \right|_{\lambda=0} = \int_{\Sigma} d^{d-2}y \frac{\delta S_{\text{gen}}}{\delta X^i(y)} \partial_\lambda X^i(y) \equiv \frac{1}{4G_N} \int_{\Sigma} d^{d-2}y \sqrt{h} \Theta[\Sigma, y] \quad (4.38)$$

This defines the quantum expansion $\Theta[\Sigma, y]$ in terms of the functional derivative of the generalized entropy:

$$\Theta[\Sigma, y] = 4G_N \frac{k^i(y)}{\sqrt{h}} \frac{\delta S_{\text{gen}}}{\delta X^i(y)}. \quad (4.39)$$

Note that we have suppressed the dependence of Θ on k^i in the notation, but the dependence is very simple: if $k^i(y) \rightarrow f(y)k^i(y)$, then $\Theta[\Sigma, y] \rightarrow f(y)\Theta[\Sigma, y]$.

The QFC is simple to state in terms of Θ . It says that Θ is non-increasing along the flow generated by k^i :

$$0 \geq \frac{d\Theta}{d\lambda} = \int_{\Sigma} d^{d-2}y \frac{\delta \Theta[\Sigma, y]}{\delta X^i(y')} k^i(y'). \quad (4.40)$$

Before moving on, let us make two remarks about the QFC.

First, the functional derivative $\delta \Theta[\Sigma, y]/\delta X^i(y')$ will contain local terms (i.e. terms proportional to δ -functions or derivatives of δ -functions with support at $y = y'$) as well as non-local terms that have support even when $y \neq y'$. S_{grav} , being a local integral, will only contribute to the local terms of $\delta \Theta[\Sigma, y]/\delta X^i(y')$. The renormalized entropy S_{ren} will contribute both local and non-local terms. The non-local terms can be shown to be nonpositive using strong subadditivity of the entropy [26], while the local terms coming from S_{ren} are in general extremely difficult to compute.

Second, and more importantly for us here, the QFC as written in (4.40) does not quite make sense. We have to remember that S_{grav} is really an operator, and its expectation value $\langle S_{\text{grav}} \rangle$ is really the thing that contributes to Θ . In order to be well-defined in the low-energy effective theory of gravity, this expectation value must be smeared over a scale large compared to the cutoff scale of the theory. Thus when we write an inequality like (4.40), we are implicitly smearing in y against some profile. The profile we use is arbitrary as long as it is slowly-varying on the cutoff scale. This extra smearing step is necessary to avoid certain violations of (4.40), as we will see below [133].

QNEC from QFC

In this section we will explicitly evaluate the QFC inequality, (4.40), and derive the QNEC in curved space from it as a nongravitational limit. We consider theories with a gravitational

action of the form

$$I_{\text{grav}} = \frac{1}{16\pi G_N} \int \sqrt{g} \left(R + \ell^2 \lambda_1 R^2 + \ell^2 \lambda_2 R_{ij} R^{ij} + \ell^2 \lambda_{\text{GB}} \mathcal{L}_{\text{GB}} \right) \quad (4.41)$$

where $\mathcal{L}_{\text{GB}} = R_{ijmn}^2 - 4R_{ij}^2 + R^2$ is the Gauss-Bonnet Lagrangian. Here ℓ is the cutoff length scale of the effective field theory, and the dimensionless couplings λ_1 , λ_2 , and λ_{GB} are assumed to be renormalized.

The generalized entropy functional for these theories can be computed using standard replica methods [47] and takes the form

$$S_{\text{gen}} = \frac{A[\Sigma]}{4G_N} + \frac{\ell^2}{4G_N} \int_{\Sigma} \sqrt{h} \left[2\lambda_1 R + \lambda_2 \left(R_{ij} N^{ij} - \frac{1}{2} K_i K^i \right) + 2\lambda_{\text{GB}} r \right] + S_{\text{ren}}. \quad (4.42)$$

Here $A[\Sigma]$ is the area of the entangling surface, N^{ij} is the projector onto the normal space of Σ , K^i is the trace of the extrinsic curvature of Σ , and r is the intrinsic Ricci scalar of Σ .

We can easily compute Θ by taking a functional derivative of (4.42), taking care to integrate by parts so that the result is proportional to $k^i(y)$ and not derivatives of $k^i(y)$. One finds

$$\Theta = \theta_{(k)} + \ell^2 \left[2\lambda_1 (\theta_{(k)} R + \nabla_k R) + \lambda_2 \left((D_a - w_a)^2 \theta_{(k)} + K_i K^{iab} K_{ab}^k \right) \right] \quad (4.43)$$

$$\begin{aligned} &+ \theta_{(k)} R_{klkl} + \nabla_k R - 2\nabla_l R_{kk} + \theta_{(k)} R_{kl} - \theta_{(l)} R_{kk} + 2K^{kab} R_{ab} \\ &- 4\lambda_{\text{GB}} \left(r^{ab} K_{ab}^k - \frac{1}{2} r \theta_{(k)} \right) \Big] + 4G_N \frac{k^i}{\sqrt{h}} \frac{\delta S_{\text{ren}}}{\delta X^i} \end{aligned} \quad (4.44)$$

Now we must compute the λ -derivative of Θ . When we do this, the leading term comes from the derivative of $\theta_{(k)}$, which by Raychaudhuri's equation contains the terms $\theta_{(k)}^2$ and $\sigma_{(k)}^2$. Since we are ultimately interested in deriving the QNEC as the non-gravitational limit of the QFC, we need to set $\theta_{(k)} = \sigma_{ab}^{(k)} = 0$ so that the nongravitational limit is not dominated by those terms. So for the rest of this section we will set $\theta_{(k)} = \sigma_{ab}^{(k)} = 0$ at the point of evaluation (but not globally!). Then we find

$$\begin{aligned} \frac{d\Theta}{d\lambda} &= -R_{kk} + 2\lambda_1 \ell^2 (\nabla_k^2 R - R R_{kk}) \\ &+ \lambda_2 \ell^2 \left[2D_a (w^a R_{kk}) + \nabla_k^2 R - D_a D^a R_{kk} - \frac{d}{d-2} (D_a \theta_{(k)})^2 - 2R_{kb} D^b \theta_{(k)} - 2(D_a \sigma_{bc})^2 \right. \\ &- 2\nabla_k \nabla_l R_{kk} - 2R_{kab} R^{ab} - \theta_{(l)} \nabla_k R_{kk} \Big] - 2\lambda_{\text{GB}} \ell^2 \left[\frac{d(d-3)(d-4)}{(d-1)(d-2)^2} R R_{kk} \right. \\ &\left. - 4 \frac{(d-4)(d-3)}{(d-2)^2} R_{kk} R_{kl} - \frac{2(d-4)}{d-2} C_{klkl} R_{kk} - \frac{2(d-4)}{d-2} R^{ab} C_{akbk} + 4C^{kalb} C_{kakb} \right] \\ &+ 4G_N \frac{d}{d\lambda} \left(\frac{k^i}{\sqrt{h}} \frac{\delta S_{\text{ren}}}{\delta X^i} \right) \end{aligned} \quad (4.45)$$

This expression is quite complicated, but it simplifies dramatically if we make use of the equation of motion coming from (4.41) plus the action of the matter sector. Then we have $R_{kk} = 8\pi GT_{kk} - H_{kk}$ where [88]

$$\begin{aligned}
 H_{kk} = & 2\lambda_1 (RR_{kk} - \nabla_k^2 R) + \lambda_2 \left(2R_{kikj}R^{ij} - \nabla_k^2 R + 2\nabla_k \nabla_l R_{kk} - 2R_{klki}R_k^i \right. \\
 & + D_c D^c R_{kk} - 2D_c (w^c R_{kk}) - 2(D_b \theta_{(k)} + R_{bmkj} P^{mj}) R_k^b + \theta_{(l)} \nabla_k R_{kk} \left. \right) \\
 & + 2\lambda_{\text{GB}} \left(\frac{d(d-3)(d-4)}{(d-1)(d-2)^2} RR_{kk} - 4 \frac{(d-4)(d-3)}{(d-2)^2} R_{kk} R_{kl} - 2 \frac{d-4}{d-2} R^{ij} C_{kikj} + C_{kijm} C_k^{ijm} \right)
 \end{aligned} \tag{4.46}$$

For the Gauss-Bonnet term we have used the standard decomposition of the Riemann tensor in terms of the Weyl and Ricci tensors. Using similar methods to those in Appendix A.5, we have also exchanged $k^i k^j \square R_{ij}$ in the R_{ij}^2 equation of motion for surface quantities and ambient curvatures.

After using the equation of motion we have the relatively simple formula

$$\begin{aligned}
 \frac{d\Theta}{d\lambda} = & -\lambda_2 \ell^2 \left(\frac{d}{d-2} (D_a \theta_{(k)})^2 + 4R_k^b D_b \theta_{(k)} + 2R_{bk} R_k^b + 2(D_a \sigma_{bc}^{(k)})^2 \right) \\
 & + 2\lambda_{\text{GB}} \ell^2 (C_{kabc} C_k^{abc} - 2C_{kba}{}^b C_{kc}{}^{ac}) + 4G_N \frac{d}{d\lambda} \left(\frac{k^i}{\sqrt{h}} \frac{\delta S_{\text{ren}}}{\delta X^i} \right) - 8\pi G_N \langle T_{kk} \rangle
 \end{aligned} \tag{4.47}$$

The Gauss-Bonnet term agrees with the expression derived in [77]. However unlike [77] we have not made any perturbative assumptions about the background curvature.

At first glance it seems like (4.47) does not have definite sign, even in the non-gravitational limit, due to the geometric terms proportional to λ_2 and λ_{GB} . The difficulty posed by the Gauss-Bonnet term, in particular, was first pointed out in [78]. However, this is where we have to remember the smearing prescription mentioned in §4.3. We must integrate (4.47) over a region of size larger than ℓ before testing its nonpositivity. The crucial point, used in [133], is that we must also remember to integrate the terms $\theta_{(k)}^2$ and $\sigma_{(k)}^2$ that we dropped earlier over the same region. When we integrate $\theta_{(k)}^2$ over a region of size ℓ centered at a point where $\theta_{(k)} = 0$, the result is $\xi \ell^2 (D_a \theta_{(k)})^2 + o(\ell^2)$, where $\xi \gtrsim 10$ is a parameter associated with the smearing profile. A similar result holds for $\sigma_{ab}^{(k)}$. Thus we arrive at

$$\begin{aligned}
 \frac{d\Theta}{d\lambda} = & -\frac{\xi}{d-2} \ell^2 (D_a \theta_{(k)})^2 - \xi \ell^2 (D_a \sigma_{bc}^{(k)})^2 \\
 & - \lambda_2 \ell^2 \left(\frac{d}{d-2} (D_a \theta_{(k)})^2 + 4R_k^b D_b \theta_{(k)} + 2R_{bk} R_k^b + 2(D_a \sigma_{bc}^{(k)})^2 \right) \\
 & + 2\lambda_{\text{GB}} \ell^2 (C_{kabc} C_k^{abc} - 2C_{kba}{}^b C_{kc}{}^{ac}) \\
 & + 4G_N \frac{d}{d\lambda} \left(\frac{k^i}{\sqrt{h}} \frac{\delta S_{\text{ren}}}{\delta X^i} \right) - 8\pi G_N \langle T_{kk} \rangle + o(\ell^2)
 \end{aligned} \tag{4.48}$$

Since the size of ξ is determined by the validity of the effective field theory, by construction the terms proportional to ξ in (4.48) dominate over the others. Thus in order to take the non-gravitational limit, we must eliminate these smeared terms.

Clearly we need to be able to choose a surface such that $D_a\theta_{(k)} = D_a\sigma_{bc}^{(k)} = 0$. Then smearing $\theta_{(k)}^2$ and $\sigma_{(k)}^2$ would only produce terms of order ℓ^4 (terms of that order would also show up from smearing the operators proportional to λ_2 and λ_{GB}). As explained in [133], this is only possible given certain conditions on the background spacetime at the point of evaluation. We must have

$$C_{kabc} = \frac{1}{d-2}h_{ab}R_{kc} - \frac{1}{d-2}h_{ac}R_{kb}. \quad (4.49)$$

This can be seen by using the Codazzi equation for Σ . Imposing this condition, which allows us to set $D_a\theta_{(k)} = D_a\sigma_{bc}^{(k)} = 0$, we then have.

$$\begin{aligned} \frac{d\Theta}{d\lambda} &= -2\ell^2 \left(\lambda_2 + 2\frac{(d-3)(d-4)}{(d-2)^2}\lambda_{\text{GB}} \right) R_{bk}R_k^b \\ &+ 4G_N \frac{d}{d\lambda} \left(\frac{k^i}{\sqrt{h}} \frac{\delta S_{\text{ren}}}{\delta X^i} \right) - 8\pi G_N \langle T_{kk} \rangle + o(\ell^3). \end{aligned} \quad (4.50)$$

This is the quantity which must be negative according to the QFC. In deriving it, we had to assume that $\theta_{(k)} = \sigma^{(k)} = D_a\theta_{(k)} = D_a\sigma_{bc}^{(k)} = 0$.

We make two observations about (4.50). First, if we assume that $R_{ka} = 0$ as an additional assumption and take $\ell \rightarrow 0$, then we arrive at the QNEC as long as $G_N > o(\ell^3)$. This is the case when ℓ scales with the Planck length and $d \leq 5$. These conditions are similar to the ones we found previously from EWN, and below in §4.3 we will discuss that in more detail.

The second observation has to do with the lingering possibility of a violation of the QFC due to the terms involving the couplings. In order to have a violation, one would need the linear combination

$$\lambda_2 + 2\frac{(d-3)(d-4)}{(d-2)^2}\lambda_{\text{GB}} \quad (4.51)$$

to be negative. Then if one could find a situation where the first line of (4.50) dominated over the second, there would be a violation. It would be interesting to interpret this as a bound on the above linear combination of couplings coming from the QFC, but it is difficult to find a situation where the first line of (4.50) dominates. The only way for R_{ka} to be large compared to the cutoff scale is if T_{ka} is nonzero, in which case we would have $R_{ka} \sim G_N T_{ka}$. Then in order for the first line of (4.50) to dominate we would need

$$G_N \ell^2 T_{ka} T_k^a \gg T_{kk}. \quad (4.52)$$

As an example, for a scalar field Φ this condition would say

$$G_N \ell^2 (\partial_a \Phi)^2 \gg 1. \quad (4.53)$$

This is not achievable within effective field theory, as it would require the field to have super-Planckian gradients. We leave a detailed and complete discussion of this issue to future work.

Scheme-Independence of the QNEC

We take a brief interlude to discuss the issue of the scheme-dependence of the QNEC, which will be important in the following section. It was shown in [77], under some slightly stronger assumptions than the ones we have been using, that the QNEC is scheme-independent under the same conditions where we expect it to hold true. Here we will present our own proof of this fact, which actually follows from the manipulations we performed above involving the QFC.

In this section we will take the point of view of field theory on curved spacetime without dynamical gravity. Then each of the terms in I_{grav} , defined above in (4.41), are completely arbitrary, non-dynamical terms we can add to the Lagrangian at will.⁶ Dialing the values of those various couplings corresponds to a choice of *scheme*, as even though those couplings are non-dynamical they will still contribute to the definitions of quantities like the renormalized energy-momentum tensor and the renormalized entropy (as defined through the replica trick). The QNEC is scheme-independent if it is insensitive to the values of these couplings.

To show the scheme-independence of the QNEC, we will begin with the statement that S_{gen} is scheme-independent. We remarked on this above, when our context was a theory with dynamical gravity. But the scheme-independence of S_{gen} does not require use of the equations of motion, so it is valid even in a non-gravitational theory on a fixed background. In fact, only once in the above discussion did we make use of the gravitational equations of motion, and that was in deriving (4.47). Following the same steps up to that point, but without imposing the gravitational equations of motion, we find instead

$$\begin{aligned} \frac{d\Theta}{d\lambda} = & -\lambda_2 \ell^2 \left(\frac{d}{d-2} (D_a \theta_{(k)})^2 + 4R_k^b D_b \theta_{(k)} + 2R_{bk} R_k^b + 2(D_a \sigma_{bc})^2 \right) \\ & + 2\lambda_{\text{GB}} \ell^2 (C_{kabc} C_k^{abc} - 2C_{kba}{}^b C_{kc}{}^{ac}) + 4G_N \frac{d}{d\lambda} \left(\frac{k^i}{\sqrt{h}} \frac{\delta S_{\text{ren}}}{\delta X^i} \right) - k_i k_j \frac{16\pi G_N}{\sqrt{g}} \frac{\delta I_{\text{grav}}}{\delta g_{ij}}. \end{aligned} \quad (4.54)$$

Since the theory is not gravitational, we would not claim that this quantity has a sign. However, it is still scheme-independent.

To proceed, we will impose all of the additional conditions that are necessary to prove the QNEC. That is, we impose $D_b \theta_{(k)} = R_k^b = D_a \sigma_{bc} = 0$, as well as $\theta_{(k)} = \sigma_{ab}^{(k)} = 0$, which in turn requires $C_{kabc} = 0$. Under these conditions, we learn that the combination

$$\frac{d}{d\lambda} \left(\frac{k^i}{\sqrt{h}} \frac{\delta S_{\text{ren}}}{\delta X^i} \right) - k_i k_j \frac{4\pi}{\sqrt{g}} \frac{\delta I_{\text{grav}}}{\delta g_{ij}} \quad (4.55)$$

is scheme-independent. The second term here is one of the contributions to the renormalized $2\pi \langle T_{kk} \rangle$ in the non-gravitational setup, the other contribution being $k_i k_j \frac{4\pi}{\sqrt{g}} \frac{\delta I_{\text{matter}}}{\delta g_{ij}}$. But I_{matter}

⁶We should really be working at the level of the quantum effective action, or generating functional, for correlation functions of T_{ij} [78]. The geometrical part has the same form as the classical action I_{grav} and so does not alter this discussion.

is already scheme-independent in the sense we are discussing, in that it is independent of the parameters appearing in I_{grav} . So adding that to the terms we have above, we learn that

$$\frac{d}{d\lambda} \left(\frac{k^i}{\sqrt{h}} \frac{\delta S_{\text{ren}}}{\delta X^i} \right) - 2\pi \langle T_{kk} \rangle \quad (4.56)$$

is scheme-independent. This is what we wanted to show.

QFC vs EWN

As we have discussed above, by taking the non-gravitational limit of (4.50) under the assumptions $D_b \theta_{(k)} = R_k^b = D_a \sigma_{bc} = \theta_{(k)} = \sigma_{ab}^{(k)} = 0$ we find the QNEC as a consequence of the QFC (at least for $d \leq 5$). And under the same set of geometric assumptions, we found the QNEC as a consequence of EWN in (4.20). The discussion of the previous section demonstrates that these assumptions also guarantee that the QNEC is scheme-independent. So even though these two QNEC inequalities were derived in different ways, we know that at the end of the day they are the same QNEC. It is natural to ask if there is a further relationship between EWN and the QFC, beyond the fact that they give the same QNEC. We will begin to investigate that question in this section.

The natural thing to ask about is the state-independent terms in the QFC and in $(\delta \bar{X})^2$. We begin by writing down all of the terms of $(\delta \bar{X})^2$ in odd dimensions that we have computed:

$$\begin{aligned} (d-2)L^{-2}(\delta \bar{X}^i)^2 &= \frac{1}{(d-2)} \theta_{(k)}^2 + \sigma_{(k)}^2 \\ &+ z^2 \frac{1}{4(d-2)} (D_a \theta_{(k)} + 2R_{ka})^2 \\ &+ z^2 \frac{1}{(d-2)(d-4)} (D_a \theta_{(k)} + R_{ka})^2 + z^2 \frac{1}{2(d-4)} (D_a \sigma_{bc}^{(k)})^2 \\ &+ z^2 \frac{\kappa}{d-4} (C_{kabc} C_k^{abc} - 2C_k^c{}_{ca} C_k^b{}_{ba}) \\ &+ \dots + z^{d-2} \frac{16\pi(d-2)G_N}{\eta d L^{d-1}} \left[\langle T_{kk} \rangle - \delta \left(\frac{k^i}{2\pi\sqrt{h}} \frac{\delta S_{\text{ren}}}{\delta X^i} \right) \right]. \end{aligned} \quad (4.57)$$

The first line looks like $-\dot{\theta}$, which would be the leading term in $d\Theta/d\lambda$, except it is missing an R_{kk} . Of course, we eventually got rid of the R_{kk} in the QFC by using the equations of motion. Suppose we set $\theta_{(k)} = 0$ and $\sigma_{ab}^{(k)} = 0$ to eliminate those terms, as we did with the QFC. Then we can write $(\delta \bar{X})^2$ suggestively as

$$\begin{aligned} (d-2)L^{-2}(\delta \bar{X}^i)^2 &= z^2 \tilde{\lambda}_2 \left(\frac{d}{(d-2)} (D_a \theta_k)^2 + 4R_k^a D_a \theta + \frac{4(d-3)}{(d-2)} R_{ka} R_k^a + 2(D_a \sigma_{bc}^{(k)})^2 \right) \\ &- 2z^2 \tilde{\lambda}_{\text{GB}} (C_{kabc} C_k^{abc} - 2C_k^c{}_{ca} C_k^b{}_{ba}) \\ &+ \dots + 8\pi \tilde{G}_N \langle T_{kk} \rangle - 4\tilde{G}_N \delta \left(\frac{k^i}{\sqrt{h}} \frac{\delta S_{\text{ren}}}{\delta X^i} \right). \end{aligned} \quad (4.58)$$

where

$$\tilde{G}_N = G_N \frac{2(d-2)z^{d-2}}{\eta d L^{d-1}}, \quad (4.59)$$

$$\tilde{\lambda}_2 = \frac{1}{4(d-4)}, \quad (4.60)$$

$$\tilde{\lambda}_{\text{GB}} = -\frac{\kappa}{2(d-4)}. \quad (4.61)$$

Written this way, it almost seems like $(d-2)L^{-2}(\delta\bar{X}^i)^2 \sim -d\Theta/d\lambda$ in some kind of model gravitational theory. One discrepancy is in the coefficient of the $R_{ka}R^{ka}$ term, unless $d=4$. It is also intriguing that the effective coefficients \tilde{G}_N , $\tilde{\lambda}_2$, and $\tilde{\lambda}_{\text{GB}}$ are close to, but not exactly the same as, the effective braneworld induced gravity coefficients found in [148]. This is clearly something that deserves further study.

4.4 Discussion

We have displayed a strong similarity between the state-independent inequalities in the QFC and the state-independent inequalities from EWN. We now discuss several possible future directions and open questions that follow naturally from these results.

Bulk Entropy Contributions

We ignored the bulk entropy S_{bulk} in this work, but we know that it produces a contribution to CFT entropy [71] and plays a role in the position of the extremal surface [67, 51]. The bulk entropy contributions to the entropy are subleading in N^2 and do not interfere with the gravitational terms in the entropy. We could include the bulk entropy as a source term in the equations determining \bar{X} , which could lead to extra contributions to the $X_{(n)}$ coefficients. However, it does not seem possible for the bulk entropy to have an effect on the state-independent parts of the extremal surface, namely on $X_{(n)}$ for $n < d$, which means the bulk entropy would not affect the conditions we derived for when the QNEC should hold.

Another logical possibility is that the bulk entropy term could affect the statement of the QNEC itself, meaning that the schematic form $T_{kk} - S''$ would be altered. This would be problematic, especially given that the QFC always produces a QNEC of that same form. It was argued in [4] that this does not happen, and that argument holds here as well.

Smearing of EWN

We were careful to include a smearing prescription for defining the QFC, and it was an important ingredient in the analysis of §4.3. But what about smearing of EWN? Of course, the answer is that we *should* smear EWN appropriately, but as we will see now it would not make a difference to our analysis.

The issue is that the bulk theory is a low-energy effective theory of gravity with a cutoff scale ℓ , and the quantities that we use to probe EWN, like $(\delta\bar{X})^2$, are operators in that theory. As such, these operators need to be smeared over a region of proper size ℓ on the extremal surface. Of course, due to the warp factor, such a region has coordinate size $z\ell/L$. We can ask what effect such a smearing would have on the inequality $(\delta\bar{X})^2$.

When we performed our QNEC derivation, we assumed that $\theta_{(k)} = 0$ at the point of evaluation, so that the $\theta_{(k)}^2$ term in $(\delta\bar{X})^2|_{z_0}$ would not contribute. However, after smearing this term would contribute a term of the form $\ell^2(D_a\theta_{(k)})^2/L^2$ to $(\delta\bar{X})^2|_{z_2}$. But we already had such a term at this order, so all this does is shift the coefficient. Furthermore, the coefficient is shifted only by an amount of order ℓ^2/L^2 . If the cutoff ℓ is of order the Planck scale, then this is suppressed in powers of N^2 . In other words, this effect is negligible for the analysis. A similar statement applies for $\sigma_{ab}^{(k)}$. So in summary, EWN should be smeared, but the analysis we performed was insensitive to it.

Future Work

There are a number of topics that merit investigation in future work. We will touch on a few of them to finish our discussion.

Relevant Deformations Perhaps the first natural extension of our work is to include relevant deformations in the EWN calculation. There are a few reasons why this is interesting. First, one would like to test the continued correspondence between the QFC and EWN when it comes to the QNEC. The QFC arguments do not care whether relevant deformations are turned on, so one would expect that the same is true in EWN. This is indeed the case when the boundary theory is formulated on flat space [126], and one would expect similar results to hold when the boundary is curved.

Another reason to add in relevant deformations is to test the status of the Conformal QNEC when the theory is not a CFT. To be more precise, the $(\delta\bar{X})^2$ and s^2 calculations we performed differed by a Weyl transformation on the boundary, and since our boundary theory was a CFT this was a natural thing to do. When the boundary theory is not a CFT, what is the relationship between $(\delta\bar{X})^2$ and s^2 ? One possibility, perhaps the most likely one, is that they simply reduce to the same inequality, and the Conformal QNEC no longer holds.

Finally, and more speculatively, having a relevant deformation turned on when the background is curved allows for interesting state-independent inequalities from EWN. We saw that for a CFT the state-independent terms in both $(\delta\bar{X})^2$ and s^2 were trivially positive. Perhaps when a relevant deformation is turned on more nontrivial results uncover themselves, such as the possibility of a c -theorem hiding inside of EWN. We are encouraged by the similarity of inequalities used in recent proofs of the c -theorems to inequalities obtained from EWN [43].

Higher Dimensions Another pressing issue is extending our results to $d = 6$ and beyond. This is an algebraically daunting task using the methods we have used for $d \leq 5$. Considering the ultimate simplicity of our final expressions, especially compared to the intermediate steps in the calculations, it is likely that there are better ways of formulating and performing the analyses we performed here. It is hard to imagine performing the full $d = 6$ analysis without such a simplification.

Further Connections Between EWN and QFC Despite the issues outlined in §4.3, we are still intrigued by the similarities between EWN and the QFC. It is extremely natural to couple the boundary theory in AdS/CFT to gravity using a braneworld setup [164, 184, 87, 148]. Upon doing this, one can formulate the QFC on the braneworld. However, at the same time near-boundary EWN becomes lost, or at least changes form: extremal surfaces anchored to a brane will in general not be orthogonal to the brane, and in that case a null deformation on the brane will induce a timelike deformation of the extremal surface in the vicinity of the brane. Of course, one has to be careful to take into account the uncertainty in the position of the brane since we are dealing with expectation values of operators, which complicates things. We hope that such an analysis could serve to unify the QFC with EWN, or at least illustrate their relationship with each other.

Conformal QNEC from QFC While we emphasized the apparent similarity between the EWN-derived inequality $(\delta\bar{X})^2 \geq 0$ and the QFC, the stronger EWN inequality $s^2 \geq 0$ is nowhere to be found in the QFC discussion. It would be interesting to see if there is a direct QFC calculation that yields the Conformal QNEC (rather than first deriving the ordinary QNEC and then performing a Weyl transformation). In particular, the Conformal QNEC applies even in cases where $\theta_{(k)}$ is nonzero, while in those cases the QFC is dominated by classical effects. Perhaps there is a useful change of variables that one can do in the semiclassical gravity when the matter sector is a CFT which makes the Conformal QNEC manifest from the QFC point of view. This is worth exploring.

Chapter 5

The Boundary of the Future

5.1 Theorem

In this paper, we prove the following theorem establishing necessary and sufficient conditions for a point to be on the boundary of the future of a surface in spacetime. (An analogous theorem holds for the past of K .)

Theorem 1 *Let (M, g) be a smooth,¹ globally hyperbolic spacetime and let K be a smooth codimension-two submanifold of M that is compact and acausal. Then a point $b \in M$ is on the boundary of the future of K if and only if all of the following statements hold:*

- (i) *b lies on a future-directed null geodesic γ that intersects K orthogonally.*
- (ii) *γ has no points conjugate to K strictly before b .*
- (iii) *γ does not intersect any other null geodesic orthogonal to K strictly between K and b .*

Theorem 1 enumerates the conditions under which a light ray, launched normally from a surface, can exit the boundary of the future of that surface and enter its chronological future. In essence, this happens only when the light ray either hits another null geodesic launched orthogonally from the surface or when the light ray encounters a caustic, in a sense that will be made precise in terms of special conditions on the deviation vectors for a family of infinitesimally-separated geodesics. These two possibilities for the fate of the light ray are illustrated in Fig. 5.1.

The theorem is useful for characterizing the causal structure induced by spatial surfaces. In particular, if K splits a Cauchy surface into two parts, then Theorem 1 implies that the four orthogonal null congruences fully characterize the associated split of the spacetime into four portions: the future and past of K and the domains of dependence of each of the two spatial sides (see Fig. 5.2). This is of particular interest when K is a holographic screen [19].

¹Nowhere in the proof will more than two derivatives be needed, so the assumption of smoothness for M and K can be relaxed everywhere in this paper to C^2 .

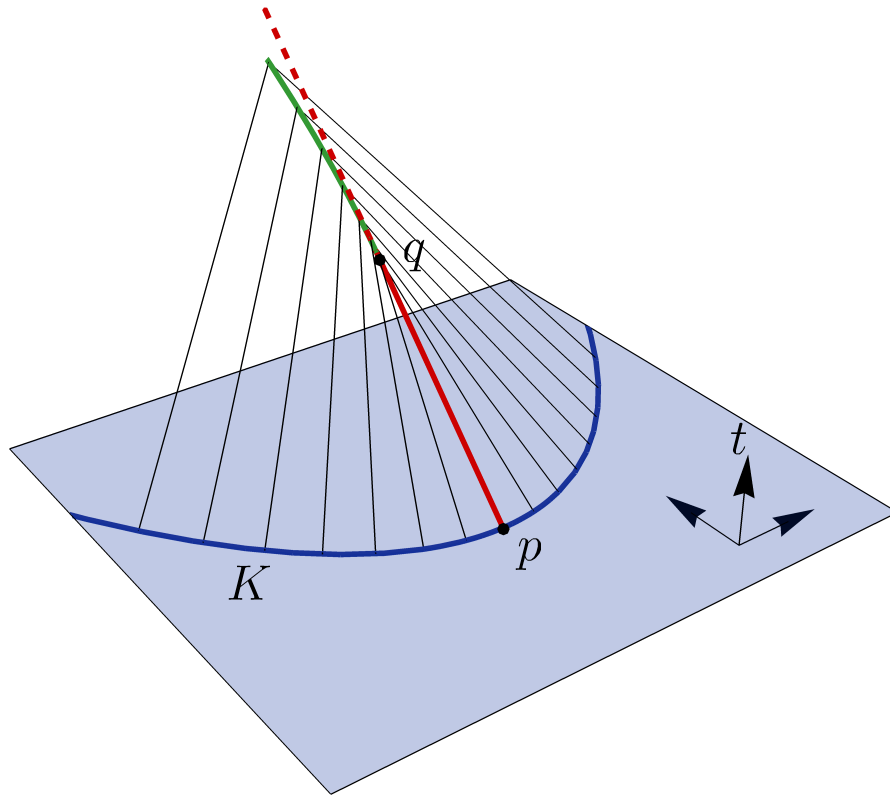


Figure 5.1: Possibilities for how a null geodesic orthogonal to a surface can exit the boundary of its future. In this example, a parabolic surface K (blue line) lies in a particular spatial slice. A future-directed null geodesic (red line) is launched orthogonally from p . At q , it encounters a caustic, entering the interior of the future of K (red dashed line). The point q is conjugate to K . Other null geodesics orthogonal to K (black lines) encounter nonlocal intersections with other such geodesics along the green line, where they exit the boundary of the future of K .

Then some of the orthogonal congruences form *light sheets* [17] such that the entropy of matter on a light sheet is bounded by the area of K . This relation makes precise the notion that the universe is like a “hologram” [108, 180, 75] and should be described as such in a quantum gravity theory. Such holographic theories have indeed been identified for a special class of spacetimes [140].

Specifically, Theorem 1 plays a role in the recent proof of a novel area theorem for holographic screens [23, 25], where it was assumed without proof. It also enters the analogous derivation of a related Generalized Second Law in cosmology [21] from the Quantum Focusing

Conjecture [28].

Although our motivation lies in applications to General Relativity and quantum gravity, we stress that the theorem itself is purely a statement about Lorentzian geometry. It does not assume Einstein's equations and so in particular does not assume any conditions on the stress tensor of matter.

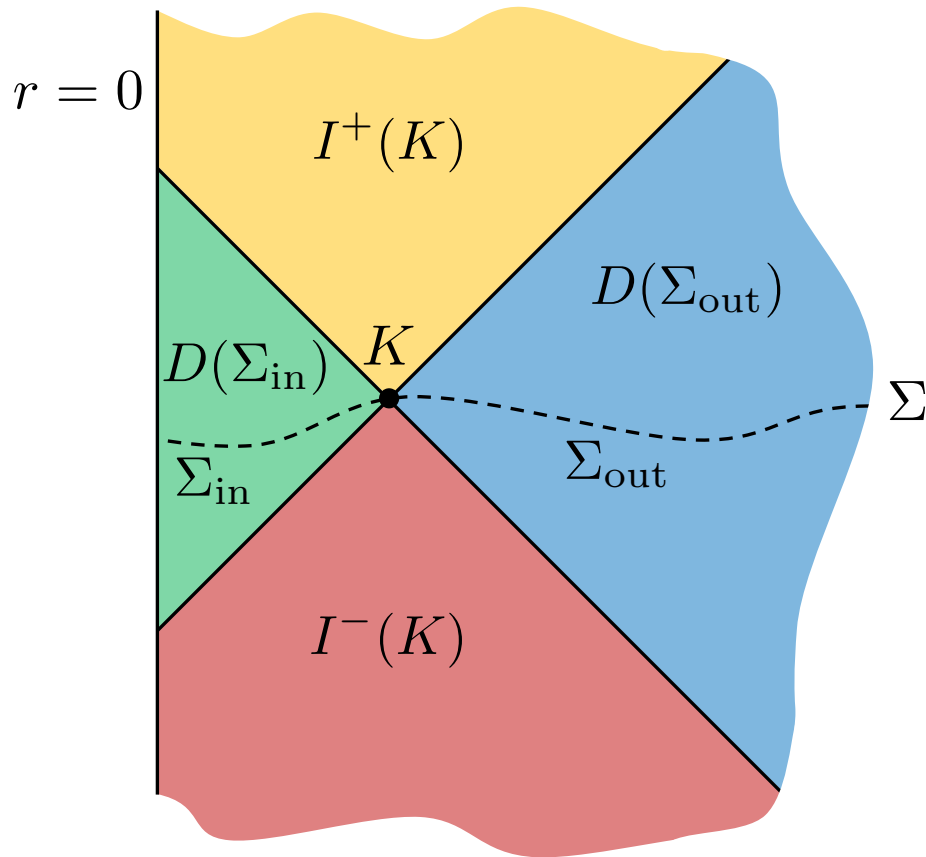


Figure 5.2: In this generic Penrose diagram, the codimension-two surface K (black dot) splits a Cauchy surface Σ (dashed line) into two parts $\Sigma_{in}, \Sigma_{out}$. This induces a splitting of the spacetime M into four parts: the past and future of K (red, yellow) and the domains of dependence of Σ_{in} and Σ_{out} (green, blue) [25]. Theorem 1 guarantees that this splitting is fully characterized by the four orthogonal null congruences originating on K (black diagonal lines).

Related Work. Parts of the “only if” direction of the theorem are a standard textbook result [186], except for (iii), which we easily establish. The “if” direction is nontrivial and takes up the bulk of our proof.

Ref. [13] considers the cut locus, i.e., the set of all cut points associated with geodesics starting at some point $p \in M$. Given a geodesic γ originating at p , a future null cut point, in particular, can be defined in terms of the Lorentzian distance function or equivalently as the final point on γ that is in the boundary of the future of p . As shown in Theorem 5.3 of Ref. [13], if q is the future null cut point on γ of p , then either q corresponds to the first future conjugate point of p along γ , or another null geodesic from p intersects γ at q , or both. Our theorem can be viewed as an analogous result for geodesics orthogonal to codimension-two surfaces and a generalization of our theorem implies the result of Ref. [13] as a special case. The codimension-two surfaces treated by our theorem are of significant physical interest due to the important role of holographic screens in the study of quantum gravity (see, e.g., Ref. [65] for very recent results on the coarse-grained black hole entropy). We encountered nontrivial differences in proving the theorem for surfaces. Moreover our condition (ii) places stronger constraints on the associated deviation vector, as we discuss in Sec. 5.2.²

The previously known parts of the “only if” direction of Theorem 1 were originally established in the context of proving singularity theorems [161, 98]. It would be interesting to see whether Theorem 1 can be used to derive new or stronger results on the formation or the cosmic censorship of spacetime singularities.

Generalizations. As we are only concerned with the causal structure, the metric can be freely conformally rescaled. Thus, a version of Theorem 1 still holds for noncompact K , as long as it is compact in the conformal completion of the spacetime, i.e., in a Penrose diagram. A situation in which this may be of interest is for surfaces anchored to the boundary of anti-de Sitter space.

Furthermore, the theorem can be generalized to surfaces of codimension other than two, but in that case we can say less about the type of conjugate point that orthogonal null geodesics may encounter. We will discuss this further in Sec. 5.3.

Notation. Throughout, we use standard notation for causal structure. A causal curve is one for which the tangent vector is always timelike or null. The causal (respectively, chronological) future of a set S in our spacetime M , denoted by $J^+(S)$ (respectively, $I^+(S)$) is the set of all $q \in M$ such that there exists $p \in S$ for which there is a future-directed causal (respectively, timelike) curve in M from p to q . For the past ($I^-(S)$, $J^-(S)$, etc.), similar definitions apply. We will denote the boundary of a set S by \dot{S} . Standard results [186] include that $I^\pm(S)$ is open and that $J^\pm(S) = \dot{I}^\pm(S)$. We will call a set S *acausal* if there do not exist distinct $p, q \in S$ for which there is a causal path in M from p to q . A spacetime is said to be *globally hyperbolic* if it contains no closed causal curves and if $J^+(p) \cap J^-(q)$ is

²After this paper first appeared, we were made aware of Refs. [130, 123], which also generalize the results of Ref. [13] to codimension-two surfaces. Our work goes further in that we more strongly constrain the type of conjugacy to be that of Def. 17. This is crucial for making contact with the notion of points “conjugate to a surface” used in the physics literature, e.g., in Ref. [186].

compact for all $p, q \in M$. Equivalently [83], M has the topology of $\Sigma \times \mathbb{R}$ for some *Cauchy surface* Σ ; that is, Σ is a surface for which, for all $p \in M$, every inextendible timelike curve through p intersects Σ exactly once.

Outline. In Sec. 5.2, we review the notion of a conjugate point and establish some useful lemmas. In Sec. 5.3, we prove Theorem 1.

5.2 Conjugate Points to a Surface

Exponential Map

Let (M, g) be a smooth, globally hyperbolic spacetime of dimension $n > 2$. Thus, M is a manifold with metric g of signature $(-, +, \dots, +)$. (As already noted, we will be concerned only with the causal structure of M , so g need only be known up to conformal transformations.)

For $p \in M$, let $T_p M$ be the tangent vector space at p and let $TM \equiv \bigcup_{p \in M} \{p\} \times T_p M$ be the tangent bundle of M . TM has a natural topology that makes it a manifold of dimension $2n$. In the open subsets associated with charts of M , TM is diffeomorphic to open subsets of \mathbb{R}^{2n} , corresponding to n coordinates for the location of $p \in M$ and n components of a tangent vector $v \in T_p M$. The tangent space of TM at (p, v) is

$$T_{p,v}TM = T_p M \times T_v T_p M. \quad (5.1)$$

For every $(p, v) \in TM$, there is a unique inextendible geodesic,

$$c_{p,v} : (a, b) \rightarrow M, \quad s \mapsto c_{p,v}(s), \quad (5.2)$$

where $a, b \in \mathbb{R} \cup \{-\infty, \infty\}$, with affine parameter s and tangent vector $v \in T_p M$ given by the pushforward of d/ds by $c_{p,v}$ at the point $p = c_{p,v}(0) \in M$. It is convenient to include the degenerate curves obtained with $v = 0$.

Definition 2 *The exponential map is defined by:*³

$$\exp : TM \rightarrow M, \quad (p, v) \mapsto c_{p,v}(1). \quad (5.3)$$

Restrictions of \exp to submanifolds of TM are frequently of interest. To study the congruence of geodesics emanating from a given point, one may restrict to $\exp_p : T_p M \rightarrow M$, $v \mapsto c_{p,v}(1)$. Moreover, one can define the differential of \exp_p , $\exp_{p*} : T_v T_p M \rightarrow T_{c_{p,v}(1)} M$, which describes how $\exp_p v$ varies due to small changes in v . See Fig. 5.3 for an illustration of the exponential map and its differential. In this paper, we will consider a different restriction suited to the study of the geodesics orthogonal to a given spatial surface; we will define the differential in more detail for this restriction below.

³If the spacetime is not geodesically complete, the exponential map can only be defined on the subset of TM consisting of the (p, v) such that $c_{p,v}$ can be extended to $\lambda = 1$. This restriction will be left implicit in this paper.

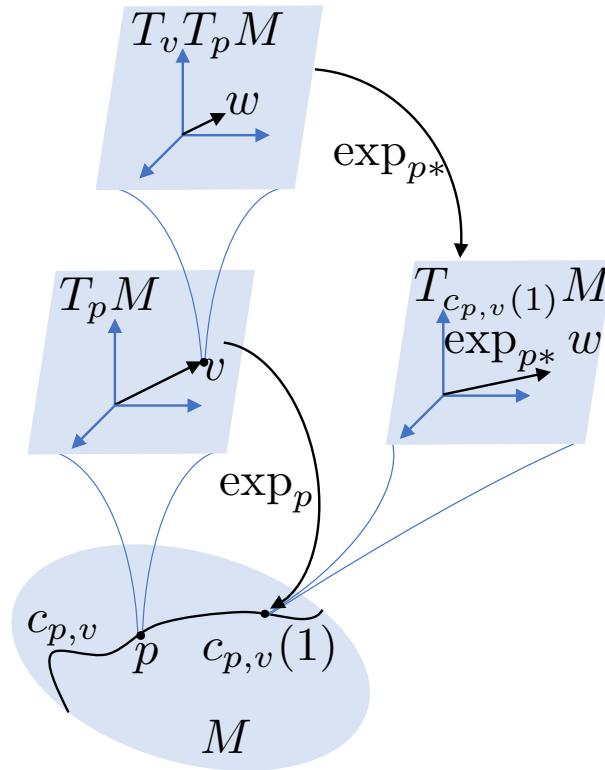


Figure 5.3: An illustration of the exponential map \exp , which takes a vector in TM to a point in M , and the Jacobian of the exponential map, which takes a vector in the tangent space TTM of TM to a vector in TM .

Let $K \subset M$ be a smooth submanifold. We consider the normal bundle

$$NK \equiv \bigcup_{p \in K} \{p\} \times T_p K^\perp,$$

where $T_p K^\perp$ is the two-dimensional tangent vector space perpendicular to K at p . The normal bundle has the structure of an n -dimensional manifold. Its tangent space at $(p, v) \in NK$ is

$$T_{p,v} NK = T_p K \times T_v T_p K^\perp. \tag{5.4}$$

Here, $T_p K$ is the tangent space of p in the manifold K ; that is, $T_p K$ is the subspace of $T_p M$ normal to $T_p K^\perp$. Note that $T_p K$ is of the same dimension as K .

Definition 3 *The surface-orthogonal exponential map*

$$\exp_K : NK \rightarrow M, (p, v) \mapsto c_{p,v}(1) \tag{5.5}$$

is the restriction of \exp to NK .

Definition 4 *The Jacobian or differential of the exponential map is given by*

$$\exp_{K^*} : T_{p,v}NK \rightarrow TM, \quad w \mapsto \exp_{K^*} w. \quad (5.6)$$

It is a linear map between vectors that captures the response of \exp_K to small variations in its argument. It is defined by requiring that $(\exp_{K^} w)(f) = w(f \circ \exp_K)$ for any function $f : M \rightarrow \mathbb{R}$. Note $\exp_{K^*} w$ is the pushforward of w by \exp_K . If x^α are coordinates in an open neighborhood of $(p, v) \in NK$ and y^β are coordinates in an open neighborhood of $\exp_K(p, v) \in M$ and we write the vectors in coordinate form, $w = \sum w^\alpha (\partial/\partial x^\alpha)$ and $\exp_{K^*} w = \sum \hat{w}^\beta (\partial/\partial y^\beta)$, then the components are related by the Jacobian matrix,*

$$\hat{w}^\beta = \sum_\alpha \frac{\partial y^\beta}{\partial x^\alpha} w^\alpha. \quad (5.7)$$

See Fig. 5.4 for an illustration of \exp_K , \exp_{K^*} , and the various tangent spaces used in this paper.

Definition 5 *A Jacobian is an isomorphism if it is invertible, i.e., if it has no eigenvectors with eigenvalue zero.*

Since (M, g) and K are smooth, \exp_K is smooth. The inverse function theorem [169] thus implies the following.

Lemma 6 *If the Jacobian \exp_{K^*} at $(p, v) \in NK$ is an isomorphism, then \exp_K is a diffeomorphism of an open neighborhood of (p, v) onto an open neighborhood of $\exp_K(p, v) \in M$.*

Definition 7 *The exponential map \exp_K is called singular at $(p, v) \in NK$ if \exp_{K^*} is not an isomorphism. Then (p, v) is called a conjugate point in NK .*

Jacobi Fields

It is instructive to relate the above definition of *conjugate point* to an equivalent definition in terms of Jacobi fields.

Definition 8 *Let Q be an open set in \mathbb{R}^2 and let $f : Q \rightarrow M$, $(r, s) \mapsto f(r, s)$ be a smooth map. If the curves of constant r and varying s , $\gamma_r : Q \rightarrow M$, $s \mapsto f(r, s)$, are geodesics in M , then f is called a one-parameter family (or congruence) of geodesics.*

Definition 9 *Let ∂_s denote the partial derivative with respect to s . It follows from the above definition that the pushforward $S \equiv f_*(\partial_s) \in TM$ is tangent to any geodesic γ_r . Similarly, $R \equiv f_*(\partial_r) \in TM$ is tangent to any curve $\mu_s : Q \rightarrow M$, $r \mapsto f(r, s)$ at fixed s . For general families of curves, R represents the deviation vector field of the congruence. In the special case of a geodesic congruence, R restricted to any γ_r is called a Jacobi field on γ_r .*

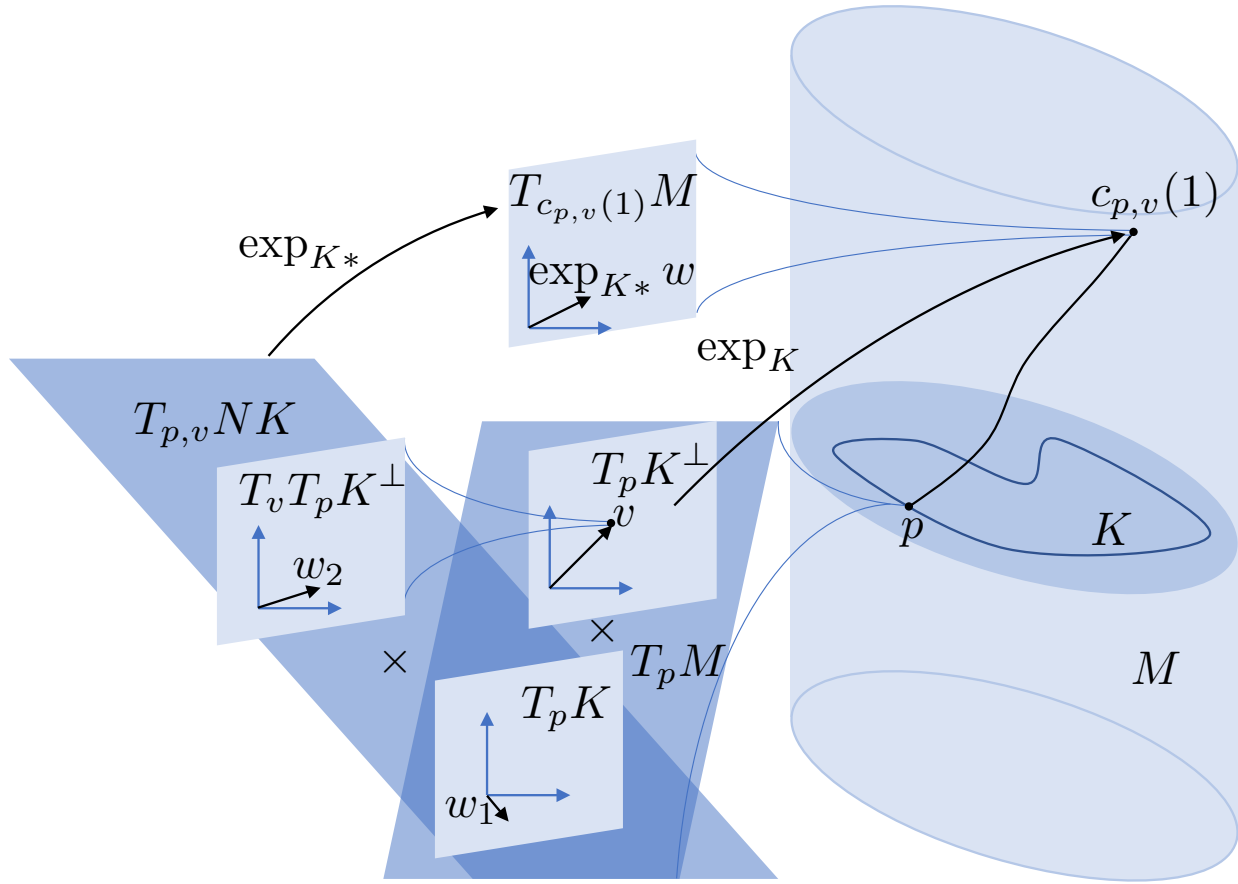


Figure 5.4: An illustration of the surface-orthogonal exponential map \exp_K evaluated at $p \in K$, which takes a vector in $T_p K^\perp$ to a point $c_{p,v}(1)$ in M . Here, as in text, the tangent space at p , $T_p M$, is broken up as a product $T_p K^\perp \times T_p K$. Also shown is the Jacobian \exp_{K*} at $v \in T_p K^\perp$, which takes a vector $w = (w_1, w_2) \in T_{p,v} NK = T_p K \times T_p K^\perp$ to a vector in $T_{c_{p,v}(1)} M$.

Remark 10 *The Jacobi field R satisfies the geodesic deviation equation on Q ,*

$$D_S^2 R = \mathcal{R}(S, R)S, \tag{5.8}$$

where $\mathcal{R}(A, B) \equiv [D_A, D_B] - D_{[A, B]}$ is the curvature tensor [107, 186] and $D_V = V^\mu \nabla_\mu$ is the covariant derivative, defined with respect to the Levi-Civita connection, along a vector V .

The exponential map can be used to generate a one-parameter family of geodesics and its derivative \exp_* generates the associated Jacobi fields. We first recall the more familiar case of geodesics through a point p , generated by \exp_p , as follows.

Remark 11 Let $\hat{R}, \hat{S} \in T_p M$ and let \tilde{R} and \tilde{S} be the naturally associated constant vector fields in $TT_p M$.⁴ Then $f(r, s) = \exp_p[s(\hat{S} + r\hat{R})]$ is smooth and defines a one-parameter family of geodesics. Its tangent vector field is $S = \exp_{p*}|_{s(\hat{S}+r\hat{R})}(\tilde{S} + r\tilde{R})$ and its deviation or Jacobi field is $R = \exp_{p*}|_{s(\hat{S}+r\hat{R})}s\tilde{R}$.⁵ It is clear from this construction that \exp_p is singular (i.e., \exp_{p*} fails to be an isomorphism) at $s(\hat{S} + r\hat{R})$ if and only if there exists a nontrivial Jacobi field of the geodesic γ_r that vanishes at $f(r, s)$ and $f(r, 0)$. This establishes the equivalence of two common definitions of conjugacy to a point p .

Remark 12 A conjugate point in a geodesic congruence with tangent vector k^μ corresponds to a caustic, which is a point at which the expansion $\theta = \nabla_\mu k^\mu$ goes to $-\infty$.

We turn to the case relevant to this paper: a one-parameter family of geodesics orthogonal to a smooth, compact, acausal, codimension-two submanifold K . (For example, K could be a topological sphere at an instant of time.) Subject to this restriction, the map f and vector fields R and S are defined as before, with $T_p M$ replaced by $T_p K^\perp$. One can choose the parameters (r, s) such that $f(r, 0) \in K$ and $f(0, 0) = p$. The map $\nu : r \mapsto (f(r, 0), S|_{(r,0)})$ is a smooth curve in NK with tangent vector $\bar{R} \in TNK$. From this curve, the one-parameter family can be recovered as

$$f(r, s) = \exp_{f(r,0)} sS|_{(r,0)} = \exp_K(f(r, 0), sS|_{(r,0)}). \quad (5.9)$$

Remark 13 We will be interested in the Jacobi field $R \equiv f_*\partial_r$ only along one geodesic, say γ at $r = 0$. By Eq. (5.8) this depends only on the initial data S and \bar{R} at p . Thus $R|_{(0,s)}$ will be the same for any curve ν with tangent vector \bar{R} at $(p, S|_{(0,0)}) \in NK$. Conversely, one can extend any given \bar{R} at $(p, S|_{(0,0)}) \in NK$ to a (non-unique) one-parameter family of geodesics by picking such a curve ν . We now take advantage of this freedom in order to find an explicit expression for the Jacobi field in terms of \exp_{K*} .

By Eq. (5.4), one can uniquely decompose $\bar{R} = (\check{R}, \tilde{R})$, with $\check{R} \in T_p K$ and $\tilde{R} \in T_S T_p K^\perp$. Let π be the defining projection of the fiber bundle, $\pi : NK \rightarrow K$. Then $\mu \equiv \pi(\nu)$ is a curve on K with tangent vector \check{R} at p . Let $f(r, 0) = \mu(r)$.

Further, let $S|_{(r,0)} \in T_{f(r,0)} K^\perp$ be defined by K -normal parallel transport⁶ of the vector $S|_{(0,0)} + r\hat{R} \in T_p K^\perp$ along μ from p to $\mu(r)$. Here $\hat{R} \in T_p K^\perp$ is the vector naturally associated with $\tilde{R} \in T_S T_p K^\perp$. Similarly, we define $\tilde{S} \in T_S T_p K^\perp$ to be the vector naturally associated with $S|_{(0,0)}$.

⁴Concretely, one can first choose a neighborhood U of p diffeomorphic to \mathbb{R}^n , which exists since M is a manifold, and then choose a map $\phi : U \rightarrow T_p M$ such that the pushforward ϕ_* is the identity map from $T_p M$ to $T_v T_p M$ for some v ; then \tilde{R} and \tilde{S} can be defined as $\tilde{R} = \phi_* \hat{R}$ and $\tilde{S} = \phi_* \hat{S}$ for $v = \hat{R}$ or \hat{S} , respectively.

⁵The subscript is the point where the Jacobian map is evaluated. The vector the Jacobian acts on appears to its right.

⁶Given a vector $v \in T_p K^\perp$, normal parallel transport defines a vector field $v(r)$ along μ normal to K such that the normal component of its covariant derivative along μ vanishes, $D_r^\perp v(r) = 0$. Given $\mu(r)$ and the initial vector in $T_p K^\perp$, $v(r)$ is unique by Lemma 4.40 of Ref. [156].

Lemma 14 *With the above choices and definitions, Eq. (5.9) yields a suitable one-parameter family of geodesics. The corresponding Jacobi field and tangent vector along γ can be written as:*

$$R|_{(0,s)} \equiv f_* \partial_r |_{(0,s)} = \exp_{K^*} |_{(p,sS|_{(0,0)})} (\check{R}, s\check{R}) \quad (5.10)$$

and

$$S|_{(0,s)} \equiv f_* \partial_s |_{(0,s)} = \exp_{K^*} |_{(p,sS|_{(0,0)})} (0, \check{S}), \quad (5.11)$$

respectively.

See App. A.7 for a proof of Lemma 14 via a direct calculation.

We note that \check{R} and \check{R} encode the initial value and derivative, respectively, of R , in accordance with the initial value problem set up in Remark 13. From Eq. (5.10), we obtain a criterion for conjugacy equivalent to that of Def. 7:

Remark 15 *In the above notation, the map \exp_K is singular at $(p, sS|_{(0,0)}) \in NK$ if and only if the geodesic γ possesses a nontrivial Jacobi field that vanishes at $\exp_K(p, sS|_{(0,0)})$ and is tangent to K at p .*

Specifically, our interest lies in null geodesics orthogonal to K . We now show that their conjugate points satisfy an additional criterion on the associated eigenvector of \exp_{K^*} .

Lemma 16 *Let γ be a geodesic orthogonal to K at p , with conjugate point $(p, sS|_{(0,0)}) \in NK$. By Def. 7 there exists a nonzero vector $\bar{R} \in T_{p,sS|_{(0,0)}} NK$ such that $\exp_{K^*} |_{(p,sS|_{(0,0)})} \bar{R} = 0$. If γ is null, i.e., if $\|S|_{(0,0)}\| = 0$, then the projection of \bar{R} onto $T_p K$ is nonvanishing: $\check{R} \neq 0$.*

By Eqs. (5.10) and (5.11), the Jacobi field $R|_{(0,s)}$ is orthogonal to γ at two points: at p (by construction) and (trivially) at the assumed conjugate point. By Lemma 8.7 of Ref. [156], this implies that $R|_{(0,s)} \perp S|_{(0,s)}$ for all s . Again using Eqs. (5.10) and (5.11), along with linearity of \exp_{K^*} , this implies that $\check{R} \perp \check{S}$ and thus $\exp_{K^*} |_{(p,sS|_{(0,0)})} (0, s\check{R}) \perp S$.

Prior to the conjugate point, the map \exp_{K^*} is a linear isomorphism; hence it maps the (1+1)-dimensional subspace $T_S T_p K^\perp \ni \check{R}$ of $T_{p,S} NK$ into a (1+1)-dimensional subspace $\exp_{K^*} T_S T_p K^\perp$ of $T_{f(0,1)} M$. This subspace contains both the null tangent vector $S|_{(0,s)}$ and the component $\exp_{K^*} |_{(p,sS|_{(0,0)})} (0, s\check{R})$ of the Jacobi field R , which is itself a Jacobi field since our choice of initial data \bar{R} was arbitrary. In a (1+1)-dimensional space, the only vectors orthogonal to a null vector S are proportional to S . The general solution to Eq. (5.8) for a Jacobi field proportional to the tangent vector S is $(\alpha + \beta s)S|_{(0,s)}$. Therefore $\exp_{K^*} |_{(p,sS|_{(0,0)})} (0, s\check{R})$ must have this form for some real constants α, β . At $s = 0$, $\exp_{K^*} |_{(p,sS|_{(0,0)})} (0, s\check{R})$ vanishes trivially, so $\alpha = 0$.

Now, suppose $\check{R} = 0$, so $R|_{(0,s)}$ is just $\beta s S|_{(0,s)}$. Since our Jacobi field is nontrivial and S does not vanish, we must have $\beta \neq 0$. Thus, $R|_{(s,0)}$ vanishes only at p and hence cannot vanish at $\exp_K(p, sS|_{(0,0)})$. This contradiction implies that $\check{R} \neq 0$.

We now define a refinement of the notion of a conjugate point.

Definition 17 Let $\gamma(s)$ be a geodesic orthogonal to K at p , with $\gamma(0) = p$ and with conjugate point (p, v) . Then there exists a nontrivial Jacobi field $R(s) \in TM$ that vanishes at $q = \exp_K(p, v)$ and is tangent to K at p . We say that q is conjugate to (the surface) K if R is nonvanishing at p .

Remark 18 By Lemma 16, $\check{R} \neq 0$, so the Jacobi field associated with \bar{R} as defined in Eq. (5.10) does not vanish at p and hence, if $(p, sS|_{(0,0)}) \in NK$ is a conjugate point, then the point $\exp_K(p, sS|_{(0,0)})$ is conjugate to K for γ null.

Moreover, we can similarly define the notion of a point conjugate to another point.

Definition 19 Given a nontrivial Jacobi field R for a segment γ of a geodesic such that R vanishes at p and q , we say that q is conjugate to (the point) p .

See Fig. 5.5 for an illustration of the two types of conjugate points defined in Defs. 17 and 19.

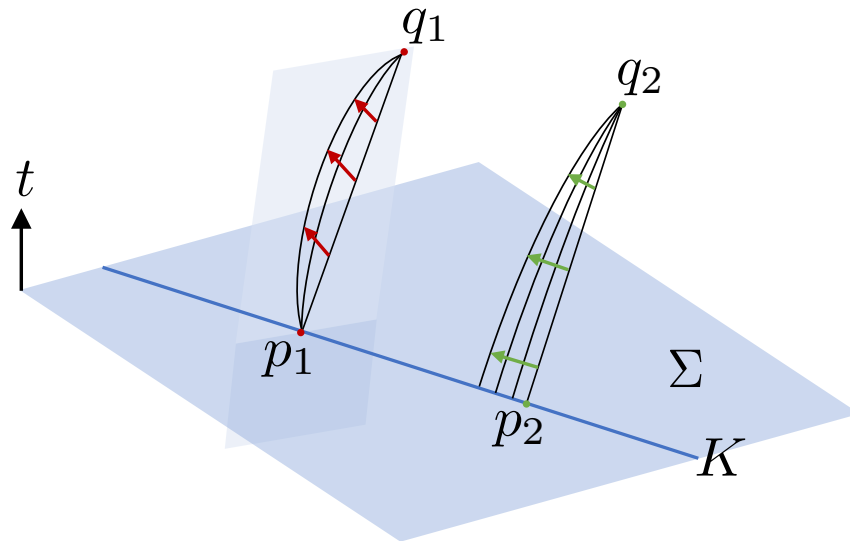


Figure 5.5: The two types of conjugate points defined in Defs. 17 and 19. The point q_1 is conjugate to the *point* p_1 , with the Jacobi field illustrated by the red arrows. The point q_2 is conjugate to the *surface* K (blue line), at the point p_2 , with the Jacobi field illustrated by the green arrows. Geodesics orthogonal to K are shown in black. If a general conjugate point lies along an orthogonal null geodesic, then by Lemma 16 there exists a Jacobi field such that the conjugate point is of the *surface* type. Hence, this type of conjugacy appears in Theorem 1.

5.3 Proof of the Theorem

We now prove Theorem 1. For the “only if” direction, we may assume that $b \in \dot{I}^+(K)$. Then conclusions (i), (ii) are already established explicitly elsewhere in the literature (e.g., Theorem 9.3.11 of Ref. [186] and Theorem 7.27 of Ref. [159]; see also Lemma VII of Ref. [161], as well as Ref. [98]).

Conclusion (iii) follows by contradiction: let γ' be a distinct null geodesic orthogonal to K that intersects γ at some point q strictly between b and K . By acausality of K , $\gamma' \cap K$ is a single point, p' , which is distinct from q . Hence, K can be connected to b by a causal curve that is not an unbroken null geodesic, namely, by following γ' from p' to q and γ from q to b . By Proposition 4.5.10 in Ref. [99], this implies that some $r \in K$ can be joined to b by a timelike curve, in contradiction with $b \in \dot{I}^+(K)$. Hence, no such γ' can exist.

The “if” direction of the theorem states that if (i), (ii), (iii) hold, then $b \in \dot{I}^+(K)$. We will prove the following equivalent statement: If $b \notin \dot{I}^+(K)$ satisfies (i), then b will fail to satisfy (ii) or (iii).

Let the geodesic $\gamma(s)$ guaranteed by (i) be parametrized so that $\gamma(0) = p \equiv \gamma \cap K$ and $\gamma(1) = b$. By (i), $b \in J^+(K)$, the causal future of K . By assumption, $b \notin \dot{I}^+(K) = \dot{J}^+(K)$, so it follows that $b \in I^+(K)$, the chronological future of K . Since $p \in \dot{I}^+(K)$, there exists an s_* between 0 and 1 where γ leaves the boundary of the future:

$$s_* \equiv \sup \gamma^{-1}(\gamma([0, 1]) \cap \dot{I}^+(K)). \quad (5.12)$$

The point where γ leaves $\dot{I}^+(K)$, $q \equiv \gamma(s_*)$, lies in $\dot{I}^+(K)$.⁷ Thus $s_* < 1$. Moreover, $s_* > 0$ by the obvious generalization of Proposition 4.5.1 in Ref. [99] and achronality of K . We conclude that

$$p \in \dot{I}^-(q) \cap K, \quad q \neq b, \quad \text{and} \quad q \neq p. \quad (5.13)$$

Recall that $q = \gamma(s_*)$ is the future-most point on γ that is not in $I^+(K)$. Let s_n be a strictly decreasing sequence of real numbers that converges to s_* . That is, $s_n > s_*$ and, for n sufficiently large, the points $q_n \equiv \gamma(s_n)$ exist and lie in $I^+(K)$. Now, since K is acausal and M is globally hyperbolic, there exists a Cauchy surface $\Sigma \supset K$. Given $p_1, p_2 \in M$, define $C(p_1, p_2)$ to be the set of all causal curves from p_1 to p_2 . Since by Corollary 6.6 of Ref. [159] $C(\Sigma, q_n)$ is compact, it is closed and bounded. Thus, $C(K, q_n) \subset C(\Sigma, q_n)$ is bounded. Consider a sequence of curves μ_m from K to q_n . By Lemma 6.2.1 of Ref. [99], the limit curve μ of $\{\mu_m\}$ is causal; since K is compact and thus contains its limit points, μ runs from K to q_n , so $\mu \in C(K, q_n)$. Hence, $C(K, q_n)$ is closed and therefore compact. Since the proper time is an upper semicontinuous function on $C(\Sigma, q_n)$, it attains its maximum over a compact domain, so we conclude in analogy with Theorem 9.4.5 of Ref. [186] that there exists a timelike geodesic γ_n that maximizes the proper time from K to q_n . By Theorem 9.4.3 of Ref. [186], γ_n is orthogonal to K .

⁷This follows because $\dot{I}^+(K)$ is closed and hence its intersection with a closed segment of γ is closed. Therefore, the argument of the supremum is a closed interval and the supremum is its upper endpoint.

By construction, the point q is a convergence point (and hence a limit point) of the sequence $\{\gamma_n\}$. By the time-reverse of Lemma 6.2.1 of Ref. [99], there exists, through q , a causal limit curve γ' of the sequence $\{\gamma_n\}$. This curve must intersect K because all γ_n intersect K and K is compact. Since γ' passes through $q \in \dot{I}^+(K)$, it must not be smoothly deformable to a timelike curve since $I^+(K)$ is open. Thus, by Theorem 9.3.10 of Ref. [186], γ' must be a null geodesic orthogonal to K , so if $\gamma' \neq \gamma$, condition (iii) fails to hold. See Fig. 5.6 for an illustration.

The only alternative is that γ is the only limit curve of the sequence $\{\gamma_n\}$. In this case, $\{\gamma_n\}$ contains a subsequence whose convergence curve is γ . From now on, let $\{\gamma_n\}$ denote this subsequence. Orthogonality to K of the γ_n implies that we can write

$$q_n = \exp_K(p_n, v_n), \quad (5.14)$$

where $p_n = \gamma_n \cap K$, for some vector $v_n \in T_{p_n}K^\perp$ tangent to γ_n . But since $q_n \in \gamma$, we can also write

$$q_n = \exp_K(p, k_n), \quad (5.15)$$

where k_n is tangent to γ . Thus, every q_n has a non-unique pre-image.

By the above construction, the sequences $\{(p, k_n)\}$ and $\{(p_n, v_n)\}$ in NK each have (p, v) as their limit point, where $q = \exp_K(p, v)$. Hence there exists no open neighborhood O of (p, v) such that \exp_K is a diffeomorphism of O onto an open neighborhood of q . By Lemma 6, it follows that \exp_K is singular at (p, v) , i.e., (p, v) is a conjugate point. By Lemma 16 and Remark 18, q is conjugate to K . Thus, condition (ii) fails to hold; again, see Fig. 5.6.

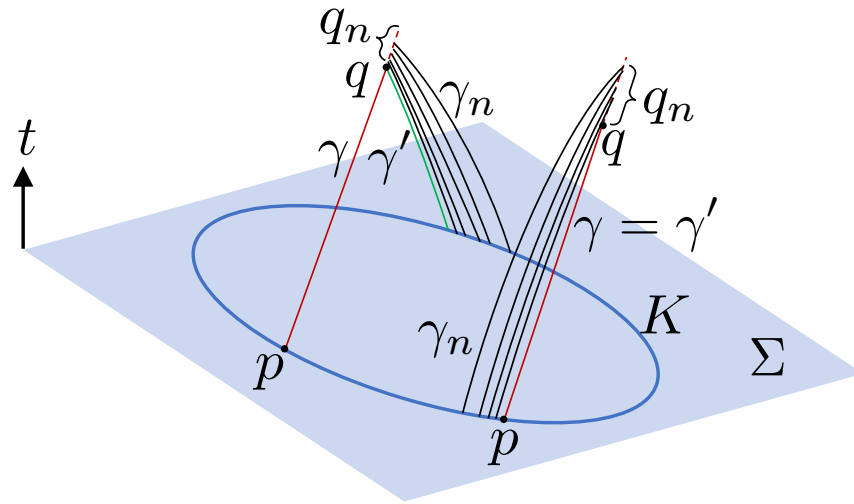


Figure 5.6: Possibilities in the proof. The sequence of timelike geodesics γ_n (black) connects K with a sequence of points $q_n \in I^+(K)$ on the orthogonal null geodesic γ (red) that joins $p \in K$ with q , after which γ leaves $I^+(K)$ (red dashed). In the case on the left, γ' (green) is distinct from γ , so condition (iii) fails. In the case on the right, $\gamma' = \gamma$, which we prove corresponds to a failure of condition (ii).

Remark 20 *The fact that K had codimension two was only important in the last step in the proof of Theorem 1, i.e., going from knowing that (p, v) is a conjugate point to showing that q is conjugate to the surface K . For K a compact, acausal submanifold that is not of codimension two, the steps in the proof of Theorem 1 still establish that (p, v) is a conjugate point in the sense of Def. 7. Moreover, that the corresponding Jacobi field is orthogonal to S remains true without the codimension-two assumption (see the proof of Lemma 16) and the one-parameter family of geodesics is orthogonal to K (because it was defined via normal parallel transport). As a result, the Jacobi field defines a deviation of γ in terms of only orthogonal null geodesics (as proven in, e.g., Corollary 10.40 of Ref. [156]), but in general that will not mean that q is conjugate to the surface K in the sense of Def. 17. Specifically, the Jacobi field is not necessarily nonvanishing at K if K has codimension greater than two.*

Chapter 6

Holographic Renyi Entropy from Quantum Error Correction

6.1 Introduction

While the quantum error-correction interpretation of AdS/CFT was discovered by trying to resolve certain paradoxes [9], it has exceeded its original purpose. Among other things, it has led to proofs of entanglement wedge reconstruction [50, 45] and a better understanding of the black hole interior [100, 8].

One remarkable result was an appreciation of the Ryu-Takayanagi (RT) formula [171, 170, 111] as a property of the code [90]. The RT formula computes the von Neumann entropy $S(\rho_A) \equiv -\text{tr} \rho_A \log \rho_A$ of a subregion A of a holographic CFT via the area \mathcal{A} of an extremal surface in the AdS dual:

$$S(\rho) = \frac{\mathcal{A}}{4G_N} + S_{\text{bulk}} \quad (6.1)$$

where S_{bulk} is the entropy of the matter in the bulk subregion dual to A [71]. While the area term is in general $\mathcal{O}(1/G_N)$, S_{bulk} is in general $\mathcal{O}(1)$ and is the quantum (or “FLM”) correction to RT [71].

The RT formula naturally appears when one computes the von Neumann entropy of an encoded state in a quantum error-correcting code. We demonstrate this now in the context of the type of code we will be using throughout: an operator-algebra quantum error-correcting (OQEC) code with complementary recovery. These appear to be the best codes to model AdS/CFT [90], and we will explain their details in Section 6.2. For now, it suffices to say that we consider a finite-dimensional Hilbert space $\mathcal{H} = \mathcal{H}_A \otimes \mathcal{H}_{\bar{A}}$, and a Hilbert space $\mathcal{H}_{\text{code}} \subseteq \mathcal{H}$. Furthermore, these Hilbert spaces have the following decompositions

$$\mathcal{H}_A = \oplus_{\alpha} (\mathcal{H}_{A_1^{\alpha}} \otimes \mathcal{H}_{A_2^{\alpha}}) \oplus \mathcal{H}_{A_3} , \quad (6.2)$$

$$\mathcal{H}_{\text{code}} = \oplus_{\alpha} (\mathcal{H}_{a_{\alpha}} \otimes \mathcal{H}_{\bar{a}_{\alpha}}) , \quad (6.3)$$

with $\dim \mathcal{H}_{A_1^\alpha} = \dim \mathcal{H}_{a_\alpha}$. In these codes, a “logical” density matrix ρ acting on $\mathcal{H}_{\text{code}}$ is encoded in a “physical” density matrix acting on \mathcal{H} . Moreover, we say that A encodes a if there exists a unitary operation U_A on \mathcal{H}_A such that

$$\tilde{\rho}_A = U_A (\oplus_\alpha (p_\alpha \rho_\alpha \otimes \chi_\alpha)) U_A^\dagger, \quad (6.4)$$

and the density matrices ρ_α act on $\mathcal{H}_{A_1^\alpha}$ and correspond to the state ρ_{a_α} that we wished to encode in $\tilde{\rho}_A$. I.e. ρ_α acts on $\mathcal{H}_{A_1^\alpha}$ in the same way that ρ_{a_α} does on \mathcal{H}_{a_α} . The density matrices χ_α act on $\mathcal{H}_{A_2^\alpha}$ and correspond to the extra degrees of freedom that help encode. The von Neumann entropy is

$$S(\tilde{\rho}_A) = \text{tr}(\tilde{\rho}_A \mathcal{L}_A) - \sum_\alpha p_\alpha \log p_\alpha + \sum_\alpha p_\alpha S(\rho_\alpha) \quad (6.5)$$

where the “area operator” is defined as

$$\mathcal{L}_A \equiv \oplus_\alpha S(\chi_\alpha) \mathbb{1}_{a_\alpha \bar{a}_\alpha}. \quad (6.6)$$

Compare this to Eq. (6.1). The first term on the RHS of both are the expectation value of linear operators evaluated in the state of interest. The other terms are naturally the algebraic von Neumann entropy of the logical state [90]. This is the basic connection between RT and quantum error-correcting codes.

In AdS/CFT, there is a natural generalization of the RT formula that we now describe. The von Neumann entropy $S(\rho)$ has a well-known generalization called the Renyi entropies, $S_n(\rho) \equiv \frac{1}{1-n} \log \text{tr} \rho^n$. While the Renyi entropy equals the von Neumann entropy for $n = 1$, it is widely believed that the Renyi entropy does not satisfy anything qualitatively similar to the RT formula for $n \neq 1$ [48, 10]. However, a related quantity called the refined Renyi entropy

$$\tilde{S}_n(\rho) \equiv n^2 \partial_n \left(\frac{n-1}{n} S_n(\rho) \right) \quad (6.7)$$

also reduces to the von Neumann entropy for $n = 1$ but in fact does satisfy a generalized version of the RT formula [48]. One computes $\tilde{S}_n(\rho_A)$ holographically via the so-called “cosmic brane prescription,” which works roughly as follows. Into the state ρ_A , insert an extremal codimension-2 cosmic brane in AdS homologous to the boundary region A , and let this brane have tension $T_n = \frac{n-1}{4nG_N}$. The refined Renyi entropy is related to the area of this brane:

$$\tilde{S}_n(\rho_A) = \frac{\mathcal{A}_{\text{brane}}}{4G_N} + \tilde{S}_{n,\text{bulk}}, \quad (6.8)$$

where $\tilde{S}_{n,\text{bulk}}$ is the refined Renyi entropy of bulk matter fields in a particular state ρ_n which is defined naturally by an n -sheeted path integral on the boundary (for details see [52]).¹

¹It is important to note that ρ_n is different in general than the original bulk state dual to ρ_A . It is the state of the matter fields prepared by a path integral on a bulk geometry with an n -sheeted boundary and that satisfies the gravitational equations of motion everywhere. This matches our results below, in which $\tilde{S}_{n,\text{bulk}}$ comes predominantly from the state of the bulk fields on the saddle geometry dual to the n -sheeted boundary state.

We describe this prescription in detail in Section 6.4. As one might expect, the cosmic brane prescription limits to the RT formula as $n \rightarrow 1$, because in that limit the tension vanishes and the cosmic brane reduces to an extremal surface.

Because the cosmic brane prescription generalizes RT, it behooves us to investigate whether the connection between RT and quantum error-correcting codes can be generalized to the cosmic brane prescription. Let us formulate this question more precisely. Does the refined Renyi entropy of $\tilde{\rho}_A$ from Eq. (6.4) satisfy some formula like

$$\tilde{S}_n(\tilde{\rho}_A) \stackrel{?}{=} \text{tr}(\tilde{\rho}_{\text{brane},A} \mathcal{L}_A) + \tilde{S}_{n,\text{logical}} , \quad (6.9)$$

for some state $\tilde{\rho}_{\text{brane},A}$, where $\tilde{S}_{n,\text{logical}}$ represents the refined Renyi entropy of the logical state? If $\tilde{\rho}_A$ indeed satisfies such a formula, what determines the state $\tilde{\rho}_{\text{brane},A}$, and why does this state manifest in AdS/CFT as inserting a brane with a particular tension into $\tilde{\rho}_A$?

Our main result is to answer these questions. In short, yes: one can derive the cosmic brane prescription within the formalism of OQEC, and we do this in Section 6.4. Notably, this derivation requires that the AdS/CFT code has certain special properties, which we now explain by discussing refined Renyi entropy in general OQEC codes.

For a general OQEC code, the refined Renyi entropy of $\tilde{\rho}_A$ from Eq. (6.4) is

$$\tilde{S}_n(\tilde{\rho}_A) = \sum_{\alpha} p_{\alpha}^{(n)} \tilde{S}_n(\chi_{\alpha}) + \tilde{S}_{n,\text{logical}} , \quad (6.10)$$

where

$$p_{\alpha}^{(n)} = \text{tr} \left(P_{\alpha} \frac{\tilde{\rho}_A^n}{\text{tr}(\tilde{\rho}_A^n)} \right) \quad (6.11)$$

and $P_{\alpha} = \sum_i |\alpha, i\rangle \langle \alpha, i|$ is a projector onto a particular value of α . While this equation bears some resemblance to Eq. (6.9), they do not match in general.

Indeed, there are two aspects of the code that need to be true for Eq. (6.9) to hold. First, it must be the case that

$$\sum_{\alpha} p_{\alpha}^{(n)} \tilde{S}_n(\chi_{\alpha}) = \text{tr} \left(\tilde{\rho}_A^{(n)} \mathcal{L}_A \right) \quad (6.12)$$

for some state $\tilde{\rho}_A^{(n)}$ in the code subspace. We show that this is true if and only if χ_{α} is maximally mixed. Second, when interpreted in the context of the AdS/CFT code, $\tilde{\rho}_A^{(n)}$ needs to manifest as the state $\tilde{\rho}_A$ with an inserted cosmic brane of exactly the right tension. One of our primary focuses is to demonstrate that CFT states with geometric duals indeed admit such an interpretation, as long as χ_{α} is maximally mixed. Formulating this argument requires that we carefully interpret Eq. (6.4) in gravity. For example, we must understand that each α -block corresponds to a particular geometry so that we can interpret some α -blocks as geometries with cosmic branes. We must also understand that CFT states with geometric duals have non-vanishing support p_{α} on α -blocks corresponding to many different

classical geometries. This way, $\tilde{\rho}_A^{(n)}$ can have its support predominantly on a different classical geometry than $\tilde{\rho}_A$ does. We provide these interpretations in Section 6.3, and we explicitly show how they manifest as a cosmic brane prescription within quantum error-correction in Section 6.4.

Also in Section 6.4, we emphasize the fact that a maximally-mixed χ_α for each α implies both properties needed for a code to match the cosmic brane prescription. This leads us to conclude that χ_α is maximally-mixed in AdS/CFT. This has a number of interesting implications, such as an improved definition of the area operator

$$\mathcal{L}_A = \oplus_\alpha \log \dim(\chi_\alpha) \mathbb{1}_{a_\alpha \bar{a}_\alpha} . \quad (6.13)$$

In Section 6.5, we discuss the implications of these results for tensor network models of AdS/CFT. While tensor networks tend to nicely satisfy the RT formula [182, 158, 101], historically they have struggled to have a non-flat spectrum of Renyi entropies. Our results suggest that there is a natural way to construct a holographic tensor network that not only has the correct Renyi entropy spectrum, but also computes the Renyi entropies via a method qualitatively similar to the cosmic brane prescription.

Finally, in Section 6.6 we conclude with a discussion of implications, future directions and related work. Note that this paper was released jointly with [49] where similar ideas are discussed.

6.2 Operator-algebra Quantum Error Correction

We start by reviewing the framework of operator-algebra quantum error correction (OQEC) as discussed in [90]. Consider a finite dimensional “physical” Hilbert space $\mathcal{H} = \mathcal{H}_A \otimes \mathcal{H}_{\bar{A}}$ and a “logical” code subspace $\mathcal{H}_{\text{code}} \subseteq \mathcal{H}$.² In the context of holography, one can think of \mathcal{H} as the boundary Hilbert space and $\mathcal{H}_{\text{code}}$ as the Hilbert space of the bulk effective field theory (EFT).

Let $\mathcal{L}(\mathcal{H}_{\text{code}})$ be the algebra of all operators acting on $\mathcal{H}_{\text{code}}$ and $M \subseteq \mathcal{L}(\mathcal{H}_{\text{code}})$ be a subalgebra. In particular, we require that M be a von Neumann algebra, i.e. it is closed under addition, multiplication, hermitian conjugation and contains all scalar multiples of the identity operator.

Any von Neumann algebra has an associated decomposition of the Hilbert space given by

$$\mathcal{H}_{\text{code}} = \oplus_\alpha (\mathcal{H}_{a_\alpha} \otimes \mathcal{H}_{\bar{a}_\alpha}) , \quad (6.14)$$

such that the operators in the von Neumann algebra are the set of α block diagonal operators that only act non-trivially on the \mathcal{H}_{a_α} factor within each block. Namely, they are of the form

$$\tilde{O}_M = \oplus_\alpha \left(\tilde{O}_{a_\alpha} \otimes \mathbb{1}_{\bar{a}_\alpha} \right) , \quad (6.15)$$

²More generally the physical Hilbert space need not factorize, e.g. if the boundary theory has gauge constraints. We expect the qualitative features of our result to be unchanged in that case.

where from now onward, we use the “tilde” to denote objects that naturally act on the code subspace.³ The commutant of M , denoted M' , is defined by the set of operators that commute with all the operators in M . The operators in M' are then similarly of the form

$$\tilde{O}_{M'} = \oplus_{\alpha} \left(\mathbb{1}_{a_{\alpha}} \otimes \tilde{O}_{\bar{a}_{\alpha}} \right) . \quad (6.16)$$

The center Z_M consists of operators that belong to both M and M' take the form

$$\tilde{O}_{M'} = \oplus_{\alpha} (\lambda_{\alpha} \mathbb{1}_{a_{\alpha}} \otimes \mathbb{1}_{\bar{a}_{\alpha}}) , \quad (6.17)$$

where λ_{α} could in general be different for each α block.

The OQEC code is then defined by requiring that for any state in the code subspace, the operators in the von Neumann algebra M are robust against erasure of the subfactor $\mathcal{H}_{\bar{A}}$ of the physical Hilbert space. Equivalently, we require that all the operators in M can be represented as physical operators acting non-trivially only on \mathcal{H}_A . In addition, by taking inspiration from AdS/CFT, we restrict to OQEC codes with complementary recovery, i.e. where operators in M' are robust against erasure of A . Thus, we require that for all $|\tilde{\psi}\rangle \in \mathcal{H}_{\text{code}}$, $\tilde{O}_M \in M$ and $\tilde{O}_{M'} \in M'$, there exists $O_A \in \mathcal{L}(\mathcal{H}_A)$ and $O_{\bar{A}} \in \mathcal{L}(\mathcal{H}_{\bar{A}})$ such that

$$\tilde{O}_M |\tilde{\psi}\rangle = O_A |\tilde{\psi}\rangle \quad (6.18)$$

$$\tilde{O}_M^{\dagger} |\tilde{\psi}\rangle = O_A^{\dagger} |\tilde{\psi}\rangle \quad (6.19)$$

$$\tilde{O}_{M'} |\tilde{\psi}\rangle = O_{\bar{A}} |\tilde{\psi}\rangle \quad (6.20)$$

$$\tilde{O}_{M'}^{\dagger} |\tilde{\psi}\rangle = O_{\bar{A}}^{\dagger} |\tilde{\psi}\rangle \quad (6.21)$$

Let us pause for a moment to make connections with holography. Suppose A is a boundary subregion and $\gamma(A)$ is the bulk codimension 2 extremal surface of minimal area anchored to ∂A , i.e. the RT surface of A . [111, 189]. The entanglement wedge $\text{EW}(A)$ is defined as the bulk domain of dependence of any bulk spacelike surface Σ such that $\partial\Sigma = A \cup \gamma(A)$ [46, 104, 115]. Given a pure boundary state, $\gamma(A) = \gamma(\bar{A})$ and thus, $\text{EW}(A) \cup \text{EW}(\bar{A})$ includes a complete Cauchy slice in the bulk.⁴ Interpreting M and M' as the algebra of operators in $\text{EW}(A)$ and $\text{EW}(\bar{A})$ respectively, it is clear that Eq. (6.18) is the statement of entanglement wedge reconstruction [50, 70]. In holography, the surface $\gamma(A)$ is fixed irrespective of the state of bulk quantum fields at leading order in G_N . In fact even at first subleading order in G_N , one could calculate $S(A)$ by keeping $\gamma(A)$ fixed and including bulk entropy corrections at $\mathcal{O}(1)$ [71]. At higher orders in G_N , one has to take into account the quantum extremal surface prescription for $\gamma(A)$ wherein the surface can move depending on the bulk state [67, 52]. In general there would be a “no man’s land” region in the bulk that cannot be reconstructed state-independently by either A or \bar{A} . Thus, the OQEC code with complementary recovery

³The only exception to this is the notation for the refined Renyi entropy \tilde{S}_n .

⁴If the boundary state is mixed, e.g. a thermal state, one could purify it, e.g. to a thermofield double [141].

only works as a toy model of holography when computing entanglement entropy to $\mathcal{O}(1)$ and hence, all our results hold only to this order.

As shown in [90], one can equivalently find unitaries U_A and $U_{\bar{A}}$ such that

$$|\widetilde{\alpha}, i j\rangle = U_A U_{\bar{A}} \left(|\alpha, i\rangle_{A_1^\alpha} |\alpha, j\rangle_{\bar{A}_1^\alpha} |\chi_\alpha\rangle_{A_2^\alpha \bar{A}_2^\alpha} \right), \quad (6.22)$$

where $|\widetilde{\alpha}, i j\rangle \equiv |\widetilde{\alpha}, i\rangle \otimes |\widetilde{\alpha}, j\rangle$ is a complete orthonormal basis for the code subspace. Here, the Hilbert space \mathcal{H}_A has been decomposed as $\mathcal{H}_A = \oplus_\alpha (\mathcal{H}_{A_1^\alpha} \otimes \mathcal{H}_{A_2^\alpha}) \oplus \mathcal{H}_{A_3^\alpha}$ where $\dim(\mathcal{H}_{A_1^\alpha}) = \dim(\mathcal{H}_{a_\alpha})$. A similar decomposition has been applied to $\mathcal{H}_{\bar{A}}$.

This allows us to write a general density matrix $\tilde{\rho}$ in the code subspace as

$$\tilde{\rho} = U_A U_{\bar{A}} \left(\oplus_\alpha p_\alpha \rho_{A_1^\alpha \bar{A}_1^\alpha} \otimes |\chi_\alpha\rangle \langle \chi_\alpha|_{A_2^\alpha \bar{A}_2^\alpha} \right) U_{\bar{A}}^\dagger U_A^\dagger, \quad (6.23)$$

where we choose the normalizations such that $\text{tr}_{A\bar{A}}(\tilde{\rho}) = \text{tr}_{A_1^\alpha \bar{A}_1^\alpha}(\rho_{A_1^\alpha \bar{A}_1^\alpha}) = \sum_\alpha p_\alpha = 1$. Restricting to subregion A , we obtain

$$\tilde{\rho}_A = U_A \left(\oplus_\alpha p_\alpha \rho_\alpha \otimes \chi_\alpha \right) U_A^\dagger, \quad (6.24)$$

where we have relaxed the notation by using $\rho_\alpha = \text{tr}_{\bar{A}_1^\alpha}(\rho_{A_1^\alpha \bar{A}_1^\alpha})$ and $\chi_\alpha = \text{tr}_{\bar{A}_2^\alpha}(|\chi_\alpha\rangle \langle \chi_\alpha|_{A_2^\alpha \bar{A}_2^\alpha})$.

Using this it is straightforward to compute the von Neumann entropy of $\tilde{\rho}_A$ and show that it satisfies a Ryu-Takayanagi formula, i.e.

$$S(\tilde{\rho}_A) = \text{tr}(\tilde{\rho} \mathcal{L}_A) + S(\tilde{\rho}, M), \quad (6.25)$$

where \mathcal{L}_A is the area operator,⁵ an operator in the center of M defined by

$$\mathcal{L}_A \equiv \oplus_\alpha S(\chi_\alpha) \mathbb{1}_{a_\alpha \bar{a}_\alpha}. \quad (6.26)$$

In a gravitational theory with the Einstein-Hilbert action, the area operator is given by

$$\mathcal{L}_A = \frac{\mathcal{A}(\gamma(A))}{4G_N}. \quad (6.27)$$

The second term in Eq. (6.25) is the algebraic entropy defined by

$$S(\tilde{\rho}, M) \equiv - \sum_\alpha p_\alpha \log p_\alpha + \sum_\alpha p_\alpha S(\tilde{\rho}_{a_\alpha}). \quad (6.28)$$

⁵Note that the important feature of \mathcal{L}_A is that it is localized to the RT surface $\gamma(A)$. For theories of higher derivative gravity, it would naturally correspond to the Dong entropy [47]

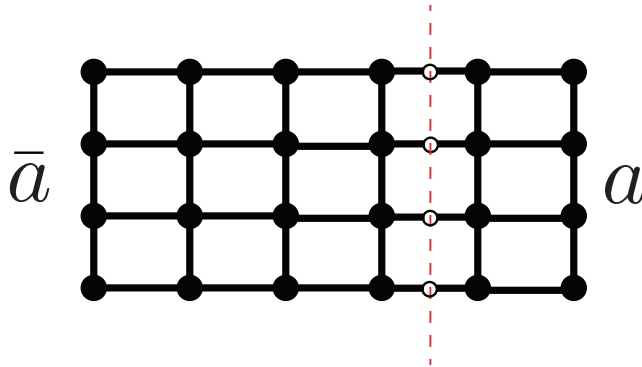


Figure 6.1: Decomposing a lattice gauge theory into subregions a and \bar{a} requires the introduction of extra degrees of freedom (denoted as white dots) at the entangling surface (denoted by a dashed red line).

6.3 Interpretation of OQEC

In order to understand our result in Section 6.4, it will be crucial to interpret each piece of the state in Eq. (6.24) in holography. The unitary U_A is simply a unitary operation that “encodes” the logical state ρ_α by mixing it with the redundant degrees of freedom χ_α . We ignore this piece and focus directly on the bulk reduced density matrix

$$\rho_a = \bigoplus_\alpha p_\alpha \rho_\alpha \otimes \chi_\alpha , \tag{6.29}$$

where one should think of the bulk subregion a as $\text{EW}(A)$. We interpret these pieces by first reviewing lattice gauge theory, which has a similar block decomposition and was argued in [57] to have a similar interpretation. We then proceed by analogy for the case of gravity.

Lattice Gauge Theory

Understanding the structure of the reduced density matrix in a gauge theory requires dealing with the novel feature that the Hilbert space doesn’t factorize across a spatial partition due to gauge constraints [55, 40, 56, 57]. This can be easily visualized in lattice gauge theory, where the gauge field lives on the links of the graph, whereas other fields that transform under the gauge symmetry live on the nodes. These links are necessarily cut when partitioning the vertices to extract the reduced density matrix for a bulk subregion a . A prescription to compute ρ_a was given in [55, 61] and has several consistency checks backing it [59, 60]. In order to find the reduced density matrix ρ_a , the prescription is to define an extended Hilbert space by first adding extra degrees of freedom at the entangling surface which are not required to satisfy a gauge constraint (see Figure 6.1). These extra degrees of freedom allow the extended Hilbert space to factorize. The physical states that satisfy the gauge constraint form a subspace of this extended Hilbert space.

As shown in [55, 56], the requirement that physical states commute with the action of gauge transformations implies that the reduced density matrix must take the form

$$\rho_a = \oplus_R p(R) \rho(R) \otimes \frac{\mathbb{1}_R}{\dim R}, \quad (6.30)$$

where the direct sum is over all the different irreducible representations of the entangling surface symmetry group. Comparing this to Eq. (6.29), the state has a similar form with the restriction that $\chi_\alpha = \frac{\mathbb{1}}{\dim \chi_\alpha}$. This χ_α can be interpreted as the maximally mixed state of the extra degrees of freedom that were added inside the entangling region.

The block-diagonal structure of Eq. (6.30) comes from the following. The representations R determine all the local gauge invariant observables, e.g. the Casimir operator, and are thus distinguishable within the region a . Hence, the reduced density matrix is in a classical mixture of these superselection sectors with probability distribution $p(R)$.

It is worth commenting here on one aspect of the connection to gravity. When the bulk is treated semiclassically, one might interpret Eq. (6.29) as the gravitational equivalent of Eq. (6.30) [57, 137]. Diffeomorphisms then play the role of the gauge symmetry, and χ_α represents degrees of freedom added across the boundary to enable factorization [57].

Gravity

Armed with the previous discussion, we now interpret each piece of Eq. (6.29) in gravity, occasionally drawing an analogy to Eq. (6.30).

α -blocks

Recall that the α -blocks were defined by first choosing a von Neumann algebra M and then finding the natural associated block decomposition of the Hilbert space. The algebra M has a non-trivial center Z_M since the gauge constraints from diffeomorphism invariance inhibit the low energy bulk Hilbert space from factorizing. Then, the simplest physical interpretation of the α -blocks is as eigenspaces of the operators in the center Z_M . In holography, these include various gauge invariant observables localized to the RT surface, and in particular the area operator \mathcal{L}_A from Eq. (6.26) is one such operator [57].⁶ Hence the states in a given α -block can be thought of as area eigenstates with the same value of the area operator.

Of course, we do not require infinite precision when comparing eigenvalues. Since we compute entropies accurately up to $\mathcal{O}(1)$, we could rightfully consider two states to be in the same α -block if they have the same eigenvalue of \mathcal{L}_A at $\mathcal{O}(1)$. However, in the rest of this paper we are interested in fixing the area eigenvalue only at leading order, and therefore

⁶In the presence of other gauge constraints, e.g. $U(1)$ gauge fields in the bulk, there would in general be more center observables, e.g. the electric flux. The α -blocks would then be labelled by the values of all such observables. We expect the observables related to non-gravitational constraints to leave the α -block structure unchanged at leading order in G_N , though this is not important for our analysis.

when we refer to α -blocks, we will always mean the coarser α -blocks in which every state has the same area eigenvalue at leading order.

Note that our code subspace is relatively large: we include an α -block for every allowed value of $\mathcal{A}/4G_N$.⁷ Indeed, we identify the code subspace as the entire Hilbert space of bulk EFT. This is important for our results in Section 6.4, and so we emphasize that we are explicitly assuming this. We think it is likely to be well-grounded based on an extension of [10]; the analysis in that paper motivates the inclusion of different classical background geometries in the code subspace when working at $\mathcal{O}(1/G_N)$. Once that is established, it is easier to define a code subspace on top of each classical background. Perhaps an argument along these lines justifies including many classically different geometries in the same code subspace, even when working to $\mathcal{O}(1)$.

We are primarily interested in bulk states that are smooth geometries. In the $G_N \rightarrow 0$ limit, smooth geometries become area eigenstates, and hence have support exclusively on α -blocks with one particular value of $\mathcal{A}/4G_N$ at leading order. When G_N is finite, overlap with other blocks is best computed using the Euclidean path integral [116]. This formalism makes it clear that two classically different geometries have $e^{-\mathcal{O}(1/G_N)}$ overlap. We will go into more depth when we discuss p_α below.

We assume that non-perturbative corrections do not ruin the exactly block-diagonal structure of Eq. (6.29). As we will see in Section 6.4, this suffices to derive a prescription resembling the AdS/CFT calculation. It is unclear whether this is well-justified, but one argument for it is the following. We work exclusively in the context of semi-classical gravity, and semi-classical gravity states are non-perturbatively gauge invariant [116]. Gauge invariance demands the direct sum structure exactly. I.e., non-perturbatively small off block-diagonal terms might break non-perturbative gauge invariance. Again, this argument is intended heuristically, not as a proof. For our purposes, we simply assume that the off-diagonal terms are exactly zero.

State ρ_α

This physical understanding of α -blocks lends itself to an easy interpretation of ρ_α . The state ρ_α is the state of the bulk matter fields when restricted to the subspace of the bulk Hilbert space with a definite value of $\mathcal{A}/4G_N$ to $\mathcal{O}(1/G_N)$. From Eq. (6.26), we see that the definite value of $\mathcal{A}/4G_N$ is $S(\chi_\alpha)$.

State χ_α

Since the bulk EFT degrees of freedom are captured by the ρ_α state, the χ_α state must correspond to the high energy, quantum gravity degrees of freedom that were integrated out to define the semiclassical gravity EFT.

This is nicely consistent with the fact that the area operator \mathcal{L}_A measures the entropy of these degrees of freedom. In semiclassical gravity, the generalized entropy of a subregion is

⁷Again with precision only to $\mathcal{O}(1)$.

defined as

$$S_{\text{gen}} = \frac{\mathcal{A}}{4G_N} + S_{\text{matter}} , \quad (6.31)$$

where S_{matter} is the von Neumann entropy of the bulk matter fields. While S_{gen} is defined purely in semiclassical gravity, it is widely believed that it corresponds to the von Neumann entropy of all the degrees of freedom in the “full” quantum gravity theory. The entropy of the quantum gravity degrees of freedom that were integrated out shows up as the area term in S_{gen} . Comparing with Eq. (6.25), we see that the entropy $S(\tilde{\rho}_A)$ is interpreted in exactly this way: the part $S(\rho_\alpha)$ is the bulk matter entropy, and $S(\chi_\alpha)$ can be interpreted as the area.

One can gain further insight into the degrees of freedom described by χ_α by drawing an analogy to lattice gauge theory. By comparing Eq. (6.29) and Eq. (6.30), one sees that the χ_α degrees of freedom seem analogous to the surface symmetry degrees of freedom, which are in the state $\frac{\mathbb{1}_R}{\text{dim } R}$. This was pointed out in [57, 137], in which they argue that because semi-classical gravity is a gauge theory, this should be understood as more than an analogy. One should expect that the χ_α can be interpreted as playing the role of surface symmetry degrees of freedom for the diffeomorphism group.

This interpretation would come with an interesting implication. Because gauge invariance imposes that surface symmetry degrees of freedom are in the singlet state, it would have to be the case that $\chi_\alpha = \frac{\mathbb{1}_\alpha}{\text{dim } \chi_\alpha}$. Confirming that χ_α is indeed in this state in the AdS/CFT code will be one of our main results in Section 6.4.

Distribution p_α

How would we compute p_α within the CFT? We could first prepare the state $\tilde{\rho}_A$ with the Euclidean path integral. Then, based on Eq. (6.24), project onto block α – which has area eigenvalue $S(\chi_\alpha)$ – and take the trace to isolate p_α .

The analogous procedure in the bulk first prepares a bulk density matrix with the Euclidean path integral. We define the bulk density matrix as follows. Let (g_-, ϕ_-) and (g_+, ϕ_+) correspond to two classical metric and matter field configurations at Euclidean time $\tau = 0$. The density matrix $\rho[g_-, \phi_-; g_+, \phi_+]$ is a functional of these two configurations defined by the path integral:

$$\rho[g_-, \phi_-; g_+, \phi_+] = \frac{1}{Z} \int_{\substack{g', \phi' |_{\infty} = \mathcal{J} \\ (g_-, \phi_-; g_+, \phi_+)}} Dg' D\phi' e^{-I_{\text{bulk}}[g', \phi']} , \quad (6.32)$$

where the notation $(g_-, \phi_-; g_+, \phi_+)$ is taken to enforce the following two boundary conditions, one on the integration over Euclidean time from $(-\infty, 0)$, and the other over $(0, \infty)$:

$$\tau \in (-\infty, 0) : \quad g(\tau = 0) = g_- , \quad \phi(\tau = 0) = \phi_- , \quad (6.33)$$

$$\tau \in (0, +\infty) : \quad g(\tau = 0) = g_+ , \quad \phi(\tau = 0) = \phi_+ . \quad (6.34)$$

The other boundary conditions on the path integral come from the AdS asymptotics: $g', \phi'|_\infty$, must be consistent with boundary conditions at infinity set by the boundary sources \mathcal{J} . With this bulk density matrix, one then defines the reduced density matrix ρ_a by tracing out the complement of a , which is $\bar{a} \equiv \text{EW}(\bar{A})$. This tracing is done by first identifying $g_- = g_+$ and $\phi_- = \phi_+$ in the region being traced out, then integrating over all metric and matter configurations in that region.

To obtain p_α , we wish to project onto states in that α -block and then take the trace. This is performed by tracing out a from ρ_a while including an extra boundary condition in the path integral that the RT area operator takes on definite value $S(\chi_\alpha)$.

All of these bulk path integral computations can be lumped into one step: we compute p_α by performing the entire Euclidean path integral subject to the boundary condition that the $\mathcal{A}/4G_N$ of $\gamma(A)$ takes on definite value $S(\chi_\alpha)$ at $\mathcal{O}(1/G_N)$:⁸

$$p_\alpha = \frac{1}{Z} \int_{\substack{\mathcal{L}_A=S(\chi_\alpha) \\ g', \phi'|_\infty=\mathcal{J}}} Dg' D\phi' e^{-I_{\text{bulk}}[g', \phi']} . \quad (6.35)$$

The leading order contribution to p_α can be computed with the saddle-point approximation:

$$p_\alpha \approx \frac{e^{-I_{\text{bulk}}[g_\alpha, \phi_\alpha]}}{Z} \Big|_{g_\alpha, \phi_\alpha|_\infty=\mathcal{J}} . \quad (6.36)$$

We have denoted the saddle-point metric and field configuration for each α as g_α, ϕ_α . We later schematically shorten this to $p_\alpha = e^{-I_{\text{bulk}}[\alpha]}/Z|_{\text{b.c.}}$, for boundary conditions ‘‘b.c.’’ Higher order corrections can be computed from a perturbative expansion of the path integral. We will pay special attention to the leading order piece in Section 6.4, because it will play the most important role in connecting to the cosmic brane prescription [48] for computing the refined Renyi entropy. Indeed, given a set of boundary conditions at infinity, we will interpret some α -blocks as geometries with cosmic branes⁹, and we will see that computing the refined Renyi entropy is exactly like computing the von Neumann entropy of a state with support predominantly in one of these cosmic brane α -blocks.

What we have said here is so important to our main point that we emphasize it again now. A general CFT state $\tilde{\rho}$ has non-vanishing support on many α , not just the blocks that correspond to its dominant geometric dual. This support is computable, and is schematically $p_\alpha = e^{-I_{\text{bulk}}[\alpha]}/Z$. Therefore, the boundary reduced density matrix $\tilde{\rho}_A$ will in general be a mixture of states on different α -blocks. We will use these facts when arguing that the cosmic brane prescription for computing refined Renyi entropy [48] is derivable from within OQEC.

⁸The path integration must also respect the boundary conditions at infinity.

⁹Equivalently, we interpret them as geometries with conical deficits.

6.4 Cosmic Brane Prescription in OQEC

Having established the framework, we now use the formalism of OQEC to compute the refined Renyi entropy defined as

$$\tilde{S}_n(\tilde{\rho}_A) \equiv n^2 \partial_n \left(\frac{n-1}{n} S_n(\tilde{\rho}_A) \right), \quad (6.37)$$

where $S_n(\tilde{\rho}_A) \equiv \frac{1}{1-n} \log \text{tr} \tilde{\rho}_A^n$ is the Renyi entropy of subregion A . In [48, 52] it was shown that in AdS/CFT, the refined Renyi entropy of a boundary subregion A is given by

$$\tilde{S}_n(A) = \frac{\mathcal{A}}{4G_N} + \tilde{S}_{n,\text{bulk}}, \quad (6.38)$$

where \mathcal{A} is the area of a brane with tension $T_n = \frac{n-1}{4nG_N}$ and extremal area. Here, the quantity $\tilde{S}_{n,\text{bulk}}$ is the refined Renyi entropy of bulk matter fields prepared by a path integral on the bulk geometry dual to the n -sheeted boundary state. Our main result in this section will be to derive this prescription from the formalism of quantum error correction. By doing so we uncover an improved understanding of the high energy degrees of freedom in quantum gravity, as well as a more refined definition of the area operator.

Quantum Error Correction calculation

The refined Renyi entropy of a general density matrix ρ can be shown to satisfy

$$\tilde{S}_n(\rho) = S(\rho^{(n)}) = -\text{tr}(\rho^{(n)} \log \rho^{(n)}), \quad (6.39)$$

$$\rho^{(n)} \equiv \frac{\rho^n}{\text{tr}(\rho^n)}. \quad (6.40)$$

We now use this to compute the refined Renyi entropy of a reduced density matrix in OQEC. Consider an arbitrary state $\tilde{\rho}$. From Eq. (6.24), we read off the reduced density matrix of subregion A as

$$\tilde{\rho}_A = U_A (\oplus_{\alpha} p_{\alpha} \rho_{\alpha} \otimes \chi_{\alpha}) U_A^{\dagger}. \quad (6.41)$$

Plugging this into Eq. (6.40) defines the state

$$\tilde{\rho}_A^{(n)} = U_A \left(\oplus_{\alpha} p_{\alpha}^{(n)} \frac{\rho_{\alpha}^n}{\text{tr}(\rho_{\alpha}^n)} \otimes \frac{\chi_{\alpha}^n}{\text{tr}(\chi_{\alpha}^n)} \right) U_A^{\dagger}. \quad (6.42)$$

where

$$p_{\alpha}^{(n)} \equiv \frac{p_{\alpha}^n \text{tr}(\chi_{\alpha}^n) \text{tr}(\rho_{\alpha}^n)}{\sum_{\alpha'} p_{\alpha'}^n \text{tr}(\chi_{\alpha'}^n) \text{tr}(\rho_{\alpha'}^n)} = \frac{p_{\alpha}^n e^{-(n-1)S_n(\chi_{\alpha}) - (n-1)S_n(\rho_{\alpha})}}{Z^{(n)}} \quad (6.43)$$

represents a normalized probability distribution that depends on n . Using this in Eq. (6.39) leads us to a crucial ingredient of our main result:

$$\tilde{S}_n(\tilde{\rho}_A) = \sum_{\alpha} p_{\alpha}^{(n)} \tilde{S}_n(\chi_{\alpha}) - \sum_{\alpha} p_{\alpha}^{(n)} \log p_{\alpha}^{(n)} + \sum_{\alpha} p_{\alpha}^{(n)} \tilde{S}_n(\rho_{\alpha}) . \quad (6.44)$$

It is illuminating to note the following connection to the Ryu-Takayanagi formula. In the special case where χ_{α} is maximally mixed¹⁰, one can write

$$\tilde{S}_n(\tilde{\rho}_A) = \text{tr} \tilde{\rho}_A^{(n)} \mathcal{L}_A - \sum_{\alpha} p_{\alpha}^{(n)} \log p_{\alpha}^{(n)} + \sum_{\alpha} p_{\alpha}^{(n)} S(\rho_{\alpha}^{(n)}) . \quad (6.45)$$

Written this way, $\tilde{S}_n(\tilde{\rho}_A)$ equals the expectation value of the area operator \mathcal{L}_A plus the algebraic von Neumann entropy of the logical degrees of freedom, all evaluated in a state $\tilde{\rho}_A^{(n)}$ that belongs to the code subspace.

Notably, to write Eq. (6.44) in the form Eq. (6.45) for arbitrary states $\tilde{\rho}_A$ in the code subspace, the identification

$$\sum_{\alpha} p_{\alpha}^{(n)} \tilde{S}_n(\chi_{\alpha}) = \text{tr} \tilde{\rho}_A^{(n)} \mathcal{L}_A \quad (6.46)$$

must hold term by term, because one could choose states with support on a single α -block. This is equivalent to having $\tilde{S}_n(\chi_{\alpha}) = S(\chi_{\alpha})$ for all α -blocks, and we show in Appendix A.8 that, for this, it is both necessary and sufficient that χ_{α} be maximally mixed. Moreover, a maximally mixed χ_{α} has another important implication. In the next subsection we shall argue that it is a necessary and sufficient condition for the gravitational interpretation of $\tilde{\rho}_A^{(n)}$ to be a geometry containing a brane with the precise n -dependent tension required to match the cosmic brane prescription in [48].

Connection to gravity

Review of holographic refined Renyi entropy: We start by carefully reviewing the cosmic brane prescription of [48]. One considers a CFT state $\tilde{\rho}$ that can be prepared by the Euclidean path integral. The bulk dual of the reduced density matrix ρ_A is given by the Hartle-Hawking wavefunction [94], which has the saddle-point approximation

$$\rho_A[g_-, \phi_-; g_+, \phi_+] = \frac{e^{-I_{\text{bulk}}[g, \phi]}}{\mathcal{Z}} \Bigg|_{\substack{g, \phi|_{\infty} = \mathcal{J} \\ (g_-, \phi_-; g_+, \phi_+)}} , \quad (6.47)$$

where g, ϕ are the saddle point field configurations given the boundary conditions at Euclidean time $\tau = 0$, $(g_-, \phi_-; g_+, \phi_+)$. Moreover, the AdS asymptotics $g, \phi|_{\infty}$ must be consistent with boundary conditions \mathcal{J} at infinity that define the state $\tilde{\rho}$.

¹⁰More generally it is given by a normalized projector, which can be thought of as being maximally mixed over the subspace on which it has support.

The cosmic brane prescription computes the refined Renyi entropy $\tilde{S}_n(\tilde{\rho}_A)$ in two steps. First, consider the bulk reduced density matrix

$$\rho_{\text{brane},A}[g_-, \phi_-; g_+, \phi_+] = \frac{e^{-nI_{\text{bulk}}[g,\phi] - (n-1)\frac{\mathcal{A}[g]}{4G_N}}}{Z} \Bigg|_{\substack{g,\phi|_{\infty}=\mathcal{J} \\ (g_-, \phi_-; g_+, \phi_+)}}. \quad (6.48)$$

The action is n times the sum of the bulk action I_{bulk} and the area \mathcal{A} of a brane with tension $T_n = \frac{n-1}{4nG_N}$ anchored to the boundary of region A . We refer to this as a “brane state,” because of its bulk interpretation as ρ with an inserted cosmic brane.

Second, in this brane state compute the expectation value of the area operator $\hat{\mathcal{A}}/4G_N$:

$$\tilde{S}_n(\tilde{\rho}_A) = \frac{\text{tr}(\rho_{\text{brane},A}\hat{\mathcal{A}})}{4G_N}. \quad (6.49)$$

This computes the refined Renyi entropy to $\mathcal{O}(1/G_N)$. The $\mathcal{O}(1)$ part can be computed by including the $\mathcal{O}(1)$ contribution of the area operator and adding the bulk contribution [48, 52]. However, we remind the reader that the interpretation of the bulk term in OQEC is subtle, and we restrict our analysis to leading order in G_N .

Let us forestall a possible confusion. It is often said that the refined Renyi entropy equals the area of the extremal cosmic brane, and rightly so. Yet, the prescription above was to evaluate the area operator in the brane state. The area operator corresponds to the area of the tensionless extremal surface, so it’s not obvious a priori why it should also correspond to the area of the brane with tension. In fact, in these brane states, the tensionless extremal surface coincides with the brane. Indeed, the branes satisfy the very strong condition that their extrinsic curvature tensor vanishes everywhere.¹¹ (Note, in the limit $n \rightarrow 1$ only the trace of the extrinsic curvature remains vanishing.)

This concludes the cosmic brane prescription for computing the refined Renyi entropy.

Branes in quantum error-correction: We now argue that this prescription is simply Eq. (6.45) combined with three special features of gravity. This is our main result.

The first special feature is the geometric interpretation of α -blocks. As we discussed at length in Section 6.3, each α in $\tilde{\rho}_A$ corresponds to states of definite area eigenvalue. We are interested in CFT states with smooth geometric bulk duals. Such states have support on many α -blocks, and different distributions p_α correspond to different smooth geometries. Of course, one does not expect all possible distributions to correspond to some smooth geometry – after all, an equal mixture of two different classical geometries is likely not itself a smooth geometry. The point is that certain mixtures, such as those prepared by the Euclidean path integral, correspond to smooth geometries. This is crucial for deriving the cosmic brane prescription in OQEC, because immediately below, we will interpret a particular distribution $p_\alpha^{(n)}$ as defining a “brane geometry”.

¹¹We thank Aitor Lewkowycz for helping us understand this.

The second special feature is the type of support p_α has on many α -blocks for smooth geometries. As we described in Section 6.3, p_α can be computed by performing the Euclidean path integral subject to the constraint that the area takes on the appropriate value. The leading order in G_N part of p_α is given by the saddle-point approximation, and should be understood as a weight assigned to the classical geometry with that value of the area. Hence we can write the p_α of the state $\tilde{\rho}_A$ as

$$p_\alpha = \frac{e^{-I_{\text{bulk}}[\alpha]}}{Z} \Big|_{b.c.} . \quad (6.50)$$

Here, the AdS asymptotics are required to match the boundary conditions (b.c.) that define the state $\tilde{\rho}$. With this p_α in hand, plug Eq. (6.50) into Eq. (6.43) to obtain the distribution over α -blocks of the state $\tilde{\rho}_A^{(n)}$:

$$p_\alpha^{(n)} = \frac{e^{-nI_{\text{bulk}}[\alpha] - (n-1)S_n(\chi_\alpha) - (n-1)S_n(\rho_\alpha)}}{Z^{(n)}} \Big|_{b.c.} . \quad (6.51)$$

Note the boundary conditions are the same as those for p_α . This is remarkably similar to Eq. (6.48), and includes the known quantum correction to the action from the matter Renyi entropy [52]. Indeed, if it were the case that $S_n(\chi_\alpha) = S(\chi_\alpha)$ for all α , then $p_\alpha^{(n)}$ would look exactly like p_α but with the action shifted by the area operator:¹²

$$I_{\text{bulk}}[\alpha] \rightarrow nI_{\text{bulk}}[\alpha] + (n-1) \text{tr}(P_\alpha \tilde{\rho}_A P_\alpha \mathcal{L}_A) . \quad (6.52)$$

where $P_\alpha = \sum_i |\alpha, i\rangle \langle \alpha, i|$ is a projector onto the particular α -block we are looking at. Compare this to the AdS/CFT calculation of refined Renyi entropy. The action defining the brane state Eq. (6.48) is shifted in exactly this way relative to the state whose refined Renyi entropy we're computing, Eq. (6.47). This strongly suggests that indeed $S_n(\chi_\alpha) = S(\chi_\alpha)$ for all α and n in the AdS/CFT code.

We already saw separate evidence for this. In order to write Eq. (6.44) in the form Eq. (6.45), it is necessary that χ_α is maximally mixed. So, the same condition that allows us to relate the refined Renyi entropy to the expectation value of the area operator in a state $\tilde{\rho}_A^{(n)}$ also guarantees that $\tilde{\rho}_A^{(n)}$ has an interpretation as the ‘‘brane state’’ Eq. (6.48)!

This is strong evidence that in the AdS/CFT code, χ_α is indeed maximally mixed. We label this the third special feature of gravity. With this conclusion, we have completed the argument that Eq. (6.45) is the cosmic brane prescription.

It is worth pausing to emphasize where the brane came from, from the point of view of the code. I.e., we now emphasize how one can look at the state $\tilde{\rho}_A^{(n)}$ and determine that it equals $\tilde{\rho}_A$ with a brane inserted into the action. The original sum over α in Eq. (6.41) included states of every possible geometry, including geometries with conical deficits. Morally, the reweighting $p_\alpha \rightarrow p_\alpha^{(n)}$ enhanced the contribution from the conical deficit geometries relative

¹²We have dropped $S_n(\rho_\alpha)$ for simplicity, but its presence only increases the resemblance.

to the others, exactly like inserting a brane. It does this via the factor $e^{-(n-1)\text{tr}(P_\alpha \tilde{\rho}_A P_\alpha \mathcal{L}_A)}$ in Eq. (6.43) – where we have used our conclusion that $S_n(\chi_\alpha) = S(\chi_\alpha)$ to write this in terms of the area operator like in Eq. (6.52). That factor suppresses geometries with large eigenvalues of the area operator in exactly the same way that inserting $e^{-(n-1)\mathcal{A}/4G_N}$ does when inserted into the bulk action.

Notably, the fact that χ_α is maximally mixed has a number of interesting implications. For instance, it gives us an improved form of the area operator. Instead of Eq. (6.26), the AdS/CFT code’s area operator is

$$\mathcal{L}_A = \oplus_\alpha \log \dim(\chi_\alpha) \mathbb{1}_{a_\alpha \bar{a}_\alpha} , \quad (6.53)$$

where $\dim(\chi_\alpha)$ is the dimension of the subspace on which χ_α has support. This strengthens the argument that χ_α corresponds to the surface symmetry degrees of freedom in lattice gauge theory. We discuss this more in Section 6.6.

Another implication is that states restricted to a single α -block have flat Renyi spectra at leading order in G_N . In order for a holographic CFT state to have a non-flat spectrum, it must have support on many α -blocks. In other words, the well-known n -dependence of S_n and \tilde{S}_n for CFTs evidently comes entirely from the n -dependent support on α -blocks, given by Eq. (6.43). This suggests an interesting fix to the notorious inability of tensor networks to have the correct Renyi spectrum [158, 101, 163, 61]. We explore this in detail in Section 6.5.

6.5 Tensor Networks

Holographic tensor networks have modeled certain aspects of AdS/CFT remarkably well [158, 101, 163, 61]. Yet, a common mismatch between these models and AdS/CFT has been the flatness of the tensor networks’ Renyi spectrum. This flatness is in part a result of the maximal entanglement of the bonds. Hence some proposals for correcting the spectrum involve modifying the entanglement of the bonds to be less than maximal, often thermal, to match the expected Rindler entanglement across a spatial divide in quantum field theory [101].

It was proposed in [10] that since the code subspace can be enlarged to include very different background geometries, one might consider a direct sum of tensor networks with different graph structures as a natural toy model for holography. We now discuss how our results in Section 6.4 suggest that this approach of defining a “super tensor network” (STN) with a Hilbert space that is a direct sum of the Hilbert space of many dissimilar constituent tensor networks resolves the Renyi spectrum mismatch.

The key ingredient is the following. Instead of considering a tensor network to be a smooth geometry, tensor networks should be thought of as a single α -block! I.e., one should think of states on a single tensor network as states with support on a single α -block in the code subspace described in Section 6.2. Indeed, tensor networks are natural area eigenstates, because the “area” equals the product of the number of bonds cut and the bond dimension, which is independent of the state.

Moreover, considering tensor networks to be α -blocks makes the maximal bond entanglement in tensor networks a feature for matching AdS/CFT's Renyi spectrum, instead of a bug. If a tensor network's bonds are maximally entangled, the degrees of freedom defining the area operator are maximally mixed (i.e. the state on the bonds cut by the minimal surface is maximally mixed). In Section 6.4, we called these degrees of freedom χ_α , and indeed we found that for a given α , χ_α is maximally mixed. Thus, there are strong reasons to treat tensor networks as area eigenstates (i.e. α -blocks) and to model smooth geometries as coherent superpositions of tensor networks with different graph structures. The particular sorts of superpositions that correspond to smooth geometries are discussed in Section 6.3.

In fact, tensor networks are even more constraining than a single α -block since they are eigenstates of the area operator for arbitrary subregions of the boundary. In AdS/CFT, it is not precisely clear how one would simultaneously project onto eigenstates of the area operators for different subregions. RT surfaces anchored to different subregions could cross, and in fact in the time-dependent generalization of RT [111], generically it wouldn't be possible to constrain all extremal surfaces to lie on the same Cauchy slice. Since tensor networks represent a coarse grained picture of the bulk with each tensor roughly corresponding to a single AdS volume, it might be possible to impose all the constraints simultaneously. Since tensor networks manage to perform this simultaneous projection, understanding them better may lead to an improved understanding of holography. It is also interesting to note that time evolution of tensor networks is not well understood. This potentially stems from the fact that they model eigenstates of the area operator at a given time and thus, very quickly evolve into states that are not geometric. It would be interesting to explore this further.

To summarise, a single tensor network with maximal bond entanglement is a good toy model for gravitational states with definite value of the area operator. The code subspace of AdS/CFT is nicely represented by a direct sum over these different tensor networks.

In fact, the tensor network in [61] takes precisely this form. By including additional "link" degrees of freedom resembling lattice gauge theory, this tensor network allows for a non-trivial area operator and a direct sum structure for the code subspace. Thus, it serves as a concrete example of an OQEC, and reproduces all the results obtained here.

The tensor network in [163] also approximately takes this form since there is very small overlap between different networks and thus, any given state is roughly consistent with the direct sum structure. Our results imply that not only will the STN have a non-flat spectrum, but computing Renyi entropies will be qualitatively similar to the AdS/CFT prescription involving an extremal brane. One should also compare our results to those of [89]. They obtained the correct Renyi entropies in the case of AdS₃ by using the specific form of the gravitational action. We have taken inspiration from the result of [48] and instead considered the refined Renyi entropies, which seem to be a more natural quantity in holography.

6.6 Discussion

Inspired by the AdS/CFT result that \tilde{S}_n equals the area of an extremal cosmic brane, we showed that a similar, more general prescription holds for any operator-algebra quantum error correcting code. This helps better our understanding of the emergent bulk in terms of error correction.

Under plausible assumptions about the AdS/CFT error-correcting code made in Section 6.3, this result helps us constrain the entanglement structure of the OQEC. Namely, for the code to satisfy the cosmic brane prescription, the redundant, quantum gravity degrees of freedom split by the entangling surface must be maximally entangled. Somehow this fact is encoded in the gravitational path integral, because that was the only input into deriving the brane prescription in AdS/CFT. It would be interesting to see a direct way of proving this within gravity.

We now proceed to discuss some interesting implications of our work and some potential future directions that would be interesting to pursue.

Edge Modes and Lattice Gauge Theory

As we reviewed in Section 6.3, the reduced density matrix in a lattice gauge theory must take the form

$$\rho_A = \oplus_R p(R) \rho(R) \otimes \frac{\mathbb{1}_R}{\dim R}, \quad (6.54)$$

where the direct sum is over all the different representations of the entangling surface symmetry group. This strongly resembles states in the OQEC formalism, namely Eq. (6.24), given our conclusion from Section 6.4 that $\chi_\alpha = \frac{\mathbb{1}}{\dim \chi_\alpha}$.

There have been various arguments in favour of understanding the bulk as an emergent gauge theory [91]. The above picture then suggests that the area term in the Ryu Takayanagi formula could be analogous to the $\log \dim R$ term that arises in lattice gauge theory [137]. In order for this story to hold true, an important restriction as we saw above was that the state χ_α be maximally mixed. However, we arrived at this from the independent consideration of requiring that the OQEC code satisfy the Dong prescription. Thus, this puts the emergent gravity proposal on a stronger footing.

In order to understand how the Ryu Takayanagi formula arises more precisely, one would have to study the representations of the surface symmetry group in the context of gravity. The results of [57, 178] motivate that the entropy from the χ_α degrees of freedom must scale with the area. The real test would be to obtain the correct prefactor. The results in [66, 64, 154] might help provide a statistical interpretation to understand the edge mode counting in the case of a restricted class of codimension 2 surfaces.

Holography in General Spacetimes

Holography beyond AdS/CFT has been quite elusive as yet. In fact, the AdS/CFT dictionary at length scales shorter than l_{AdS} hasn't been completely understood and has been conjectured to involve the N^2 matrix degrees of freedom of the boundary theory in an important way. Various attempts at understanding holography more generally include [155, 151, 153, 152, 6, 54, 146, 147]. In each of these cases, there have been attempts to find some form of a Ryu Takayanagi (RT) formula [173, 54, 145]. To be precise, extremal surfaces anchored to subregions of the proposed boundary theory exist, and satisfy the expected holographic inequalities. However, it is not clear whether the area of such extremal surfaces really computes the entanglement entropy of some boundary theory.

As [50, 90] showed, if the RT formula is indeed computing the entropy of a boundary subregion, it automatically implies the existence of an error correcting code with subregion duality. Since our results have demonstrated that any such holographic duality must satisfy Dong's prescription for the Renyi entropy, it should be an additional feature of any of the above proposals in order for them to be consistent.

Another interesting direction to understand sub-AdS locality, while staying within the realm of AdS/CFT, is the $T\bar{T}$ deformation [142]. The $T\bar{T}$ deformation is an irrelevant deformation to the boundary CFT that has been conjectured to be dual to AdS with a Dirichlet boundary at finite radius. Interestingly, in [58], both the Ryu Takayanagi formula and the Dong prescription were shown to work precisely for a very symmetric setup of the $T\bar{T}$ deformation. This strongly motivates that one might in fact have a similar error correcting code with subregion duality even without referring to a conformal boundary.

Properties of refined Renyi entropy

Entanglement entropies are known to satisfy various inequalities such as subadditivity and strong subadditivity. Despite the fact that their linear algebra proofs are quite involved, the holographic proofs are remarkably simple [103, 189]. The geometric dual and the minimization involved in the RT formula easily allow one to prove these inequalities. In fact, a large set of non-trivial inequalities satisfied by holographic states can be proven [12, 11].

Both Renyi and refined Renyi entropies are not in general subadditive, even though certain interesting classes of states [34] have been shown to satisfy such inequalities. In the holographic context, since the refined Renyi entropies are also obtained by following a minimization procedure on a dual geometry, one might be led to believe that similar proofs could be used to prove inequalities for the refined Renyi entropies. These could then be used to constrain the class of holographic states, i.e. a holographic refined Renyi entropy cone.¹³

However, there are subtleties in proving such inequalities due to the back-reaction from the cosmic brane. When considering refined Renyi entropies of two disjoint regions A and B , one would in general have to consider different geometries for computing $\tilde{S}_n(A)$, $\tilde{S}_n(B)$

¹³We thank Ning Bao for discussions about this.

and $\tilde{S}_n(A \cup B)$. It's possible that the QEC formalism provides a useful, alternative way to prove such inequalities.

More generally, understanding properties of the refined Renyi entropy is interesting future work. The refined Renyi entropies seem to be a more natural generalization of von Neumann entropy in holography than the Renyi entropies. They can be computed by a quantity localized to a codimension 2 surface, while the Renyi entropies in general involve a non-local integral, even at leading order in G_N . It would be interesting to find quantum information theoretic uses for the refined Renyi entropy, perhaps stemming from Eq. (6.39). For example, if the von Neumann entropy of ρ is too difficult to compute experimentally, one could instead compute the n -th refined Renyi entropy of σ , provided $\rho = \sigma^n / \text{tr}(\sigma^n)$.

Error Correction and Holography

Our analysis involved computing a quantity within the quantum error correction framework and comparing it with results from AdS/CFT. This helped us learn about novel aspects of both error correcting codes and AdS/CFT. Thus, it seems like a fruitful direction to analyze other known holographic results within the framework of error correction in order to refine our understanding of the emergent bulk. As we have seen, many results in AdS/CFT, such as the RT formula and the Dong prescription, are simple “kinematic” results from QEC. We have also seen that AdS/CFT puts constraints on the type of QEC that relates the boundary to the bulk. It seems plausible that there is much mileage to be gained from simply exploiting the QEC framework without needing to reference the dynamics of the boundary theory.

A small caveat to keep in mind is that all our results were obtained by working with a finite dimensional Hilbert space. Interesting effects might arise from considering infinite dimensional Hilbert spaces. For example, [10] found that the Renyi entropies are discontinuous around $n = 1$ when taking the large N limit. This is also true for the refined Renyi entropies that we have analyzed. Some features of infinite dimensional Hilbert spaces could be modeled by using the framework of approximate error correction [100].¹⁴ Understanding the nuances of the large N limit is an interesting direction that we leave for future work.

¹⁴We thank Patrick Hayden for a discussion about this.

Appendix A

Appendix

A.1 F_Λ counterterm

In this Appendix we carry out an independent calculation of F_Λ in order to verify (2.27). As argued in [29], F_Λ is directly related to the divergences of the massless correlator $\langle [\vec{\phi}^2](x)[\vec{\phi}^2](y) \rangle$, where [...] denotes a renormalized composite operator. Such divergences are removed by adding a counter term proportional to a delta function,

$$\frac{1}{4} \langle [\vec{\phi}^2](x)[\vec{\phi}^2](y) \rangle + \mu^{-\epsilon} N A(u, \epsilon) \delta^d(x, y) = \frac{1}{4} \left(\frac{t_0}{t} \right)^2 \langle \vec{\phi}^2(x) \vec{\phi}^2(y) \rangle + \mu^{-\epsilon} N A(u, \epsilon) \delta^d(x, y) = \text{finite}, \quad (\text{A.1})$$

where $A(u, \epsilon)$ has poles in ϵ , and [29]¹

$$F_\Lambda(u, \epsilon) = -\frac{1}{2} \left(\frac{t}{t_0} \right)^2 A(u, \epsilon). \quad (\text{A.2})$$

To leading order in large- N , there are two diagrams that contribute to $A(u, \epsilon)$, see Fig. A.1. To evaluate these diagrams we have to calculate the propagator of the auxiliary field s . To this end, we expand the generating functional (2.14) around the saddle point $s = \bar{s} + s'$ and use cyclicity of Tr , e.g.,

$$\text{Tr} \ln \hat{O}_s = \text{Tr} \ln \left(\hat{O}_{\bar{s}} (1 + \hat{O}_{\bar{s}}^{-1} s') \right) = \text{Tr} \ln \hat{O}_{\bar{s}} + \text{Tr} (\hat{O}_{\bar{s}}^{-1} s') - \frac{1}{2} \text{Tr} (\hat{O}_{\bar{s}}^{-1} s' \hat{O}_{\bar{s}}^{-1} s') + \dots \quad (\text{A.3})$$

Constant terms in the expansion of the action are part of the normalization and can therefore be suppressed. Linear terms vanish since we are expanding around the saddle point. As a result, the expansion of the action to second order is given by,

$$S_{\text{eff}}(s') = -\frac{N}{4} \int d^d x \sqrt{g(x)} \int d^d y \sqrt{g(y)} s'(x) \left(D^2(x, y) + \frac{\delta^d(x, y)}{u_0} \right) s'(y) + \dots, \quad (\text{A.4})$$

¹Since we are using Euclidean signature there is a difference in the relative sign between F_Λ and A in comparison to [29].

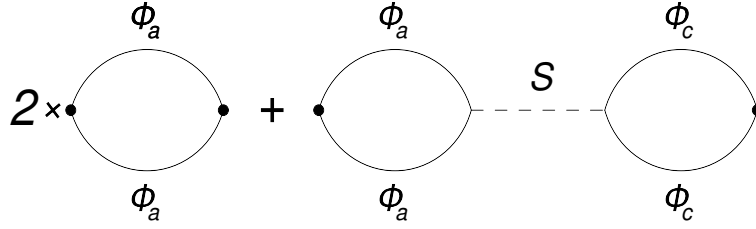


Figure A.1: Two diagrams of order N which contribute to the Green's function $\langle \vec{\phi}^2(x) \vec{\phi}^2(y) \rangle$. Solid and dashed lines represent propagators of the scalar, $\vec{\phi}$, and auxiliary field, s , respectively. The dots represent insertions of $\vec{\phi}^2$.

where $D(x, y) \equiv \langle x | \hat{O}_s^{-1} | y \rangle$ denotes the full propagator of the scalar field, $\vec{\phi}$, to leading order in the large- N expansion.

The propagator of the auxiliary field s' can be easily obtained by inverting the above quadratic form. On a sphere, such an inversion can be done in closed form by noting that this quadratic form is diagonal in the basis of spherical harmonics. We will not carry out the full calculation since we only need the δ -functions in the propagator of s' , for which a short distance expansion and flat space approximation are sufficient. In particular,

$$D^2(x - y) = \frac{\mu^{-\epsilon}}{8\pi^2\epsilon} \delta^d(x - y) + \mathcal{O}(\epsilon^0), \quad (\text{A.5})$$

where we suppressed (finite) terms without δ -functions. Substituting into (A.4), and using (2.22), yields

$$\langle s'(x) s'(y) \rangle = -\frac{2u\mu^\epsilon}{N} \delta^d(x - y) + \dots \quad (\text{A.6})$$

As expected, (2.22) renders the effective action finite to leading order in large- N . Using now (A.5) and (A.6), the diagrams in Fig. A.1 can be readily evaluated. The final result reads

$$A = -\frac{1}{(4\pi)^2\epsilon} \left(\frac{t_0}{t} \right)^2 \left(1 - \frac{u}{8\pi^2\epsilon} \right) \Rightarrow F_\Lambda(u, \epsilon) = \frac{1}{2(4\pi)^2\epsilon} \left(1 - \frac{u}{8\pi^2\epsilon} \right), \quad (\text{A.7})$$

in full agreement with (2.27) and [74].

A.2 Notation and Definitions

Basic Notation

Notation for basic bulk and boundary quantities

- Bulk indices are μ, ν, \dots

- Boundary indices are i, j, \dots . Then $\mu = (z, i)$.
- We assume a Fefferman–Graham form for the metric: $ds^2 = \frac{L^2}{z^2} (dz^2 + \bar{g}_{ij} dx^i dx^j)$.
- The expansion for $\bar{g}_{ij}(x, z)$ at fixed x is

$$\bar{g}_{ij} = g_{ij}^{(0)} + z^2 g_{ij}^{(2)} + z^4 g_{ij}^{(4)} + \dots + z^d \log z g_{ij}^{(d, \log)} + z^d g_{ij}^{(d)} + \dots \quad (\text{A.8})$$

The coefficients $g_{ij}^{(n)}$ for $n < d$ and $g_{ij}^{(d, \log)}$ are determined in terms of $g_{ij}^{(0)}$, while $g_{ij}^{(d)}$ is state-dependent and contains the energy-momentum tensor of the CFT. If d is even, then $g_{ij}^{(d, \log)} = 0$. To avoid clutter we will often write $g_{ij}^{(0)}$ simply as g_{ij} . Unless otherwise indicated, i, j indices are raised and lowered by $g_{ij}^{(0)}$.

- We use \mathcal{R} , $\mathcal{R}_{\mu\nu}$, $\mathcal{R}_{\mu\nu\rho\sigma}$ to denote bulk curvature tensors, and R , R_{ij} , R_{ijmn} to denote boundary curvature tensors.

Notation for extremal surface and entangling surface quantities

- Extremal surface indices are α, β, \dots
- Boundary indices are a, b, \dots . Then $\alpha = (z, a)$.
- The extremal surface is parameterized by functions $\bar{X}^\mu(z, y^a)$. We choose a gauge such that $X^z = z$, and expand the remaining coordinates as

$$\bar{X}^i = X_{(0)}^i + z^2 X_{(2)}^i + z^4 X_{(4)}^i + \dots + z^d \log z X_{(d, \log)}^i + z^d X_{(d)}^i + \dots \quad (\text{A.9})$$

The coefficients $X_{(n)}^i$ for $n < d$ and $X_{(d, \log)}^i$ are determined in terms of $X_{(0)}^i$ and $g_{ij}^{(0)}$, while $X_{(d)}^i$ is state-dependent and is related to the renormalized entropy of the CFT region.

- The extremal surface induced metric will be denoted $\bar{h}_{\alpha\beta}$ and gauge-fixed so that $\bar{h}_{za} = 0$.
- The entangling surface induced metric will be denoted h_{ab} .
- Note that we will often want to expand bulk quantities in z at fixed y instead of fixed x . For instance, the bulk metric at fixed y is

$$\begin{aligned} \bar{g}_{ij}(y, z) &= \bar{g}_{ij}(\bar{X}(z, y), z) = \bar{g}_{ij}(X_{(0)}(y) + z^2 X_{(2)}(y) + \dots, z) \\ &= g_{ij}^{(0)} + z^2 \left(g_{ij}^{(2)} + X_{(2)}^m \partial_m g_{ij}^{(0)} \right) + \dots \end{aligned} \quad (\text{A.10})$$

Similar remarks apply for things like Christoffel symbols. The prescription is to always compute the given quantity as a function of x first, the plug in $\bar{X}(y, z)$ and expand in a Taylor series.

Intrinsic and Extrinsic Geometry

Now will introduce several geometric quantities, and their notations, which we will need. First, we define a basis of surface tangent vectors by

$$e_a^i = \partial_a X^i. \quad (\text{A.11})$$

We will also make use of the convention that ambient tensors which are not inherently defined on the surface but are written with surface indices (a, b , etc.) are defined by contracting with e_a^i . For instance:

$$g_{aj}^{(2)} = e_a^i g_{ij}^{(2)}. \quad (\text{A.12})$$

We can form the surface projector by contracting the surface indices on two copies of e_a^i :

$$P^{ij} = h^{ab} e_a^i e_b^j = e_a^i e^{ja}. \quad (\text{A.13})$$

We introduces a surface covariant derivative D_a that acts as the covariant derivative on both surface and ambient indices. So it is compatible with both metrics:

$$D_a h_{bc} = 0 = D_a g_{ij}. \quad (\text{A.14})$$

Note also that when acting on objects with only ambient indices, we have the relationship

$$D_a V_{pq\dots}^{ij\dots} = e_a^m \nabla_m V_{pq\dots}^{ij\dots}, \quad (\text{A.15})$$

where ∇_i is the ambient covariant derivative compatible with g_{ij} .

The extrinsic curvature is computed by taking the D_a derivative of a surface basis vector:

$$K_{ab}^i = -D_a e_b^i = -\partial_a e_b^i + \gamma_{ab}^c e_b^i - \Gamma_{ab}^i. \quad (\text{A.16})$$

Note the overall sign we have chosen. Here γ_{ab}^c is the Christoffel symbol of the metric h_{ab} , and the lower indices on the Γ symbol were contracted with two basis tangent vectors to turn them into surface indices. Note that K_{ab}^i is symmetric in its lower indices. It is an exercise to check that it is normal to the surface in its upper index:

$$e_{ic} K_{ab}^i = 0. \quad (\text{A.17})$$

The trace of the extrinsic curvature is denoted by K^i :

$$K^i = h^{ab} K_{ab}^i. \quad (\text{A.18})$$

Below we will introduce the null basis of normal vectors k^i and l^i . Then we can define expansion $\theta_{(k)}$ ($\theta_{(l)}$) and shear $\sigma_{ab}^{(k)}$ ($\sigma_{ab}^{(l)}$) as the trace and traceless parts of $k_i K_{ab}^i$ ($l_i K_{ab}^i$), respectively.

There are a couple of important formulas involving the extrinsic curvature. First is the Codazzi Equation, which can be computed from the commutator of covariant derivatives:

$$\begin{aligned} D_c K_{ab}^i - D_b K_{ac}^i &= (D_b D_c - D_c D_b) e_a^i \\ &= R_{abc}^i - r_{abc}^d e_d^i. \end{aligned} \quad (\text{A.19})$$

Here R_{abc}^i is the ambient curvature (appropriately contracted with surface basis vectors), while r_{abc}^d is the surface curvature. We can take traces of this equation to get others. Another useful thing to do is contract this equation with e_d^i and differentiate by parts, which yields the Gauss–Codazzi equation:

$$K_{cdi} K_{ab}^i - K_{bdi} K_{ac}^i = R_{dabc} - r_{dabc}. \quad (\text{A.20})$$

Various traces of this equation are also useful.

Null Normals k and l

A primary object in our analysis is the null vector k^i , which is orthogonal to the entangling surface and gives the direction of the surface deformation. It will be convenient to also introduce the null normal l^i , which is defined so that $l_i k^i = +1$. This choice of sign is different from the one that is usually made in these sorts of analysis, but it is necessary to avoid a proliferation of minus signs. With this convention, the projector onto the normal space of the surface is

$$N^{ij} \equiv g^{ij} - P^{ij} = k^i l^j + k^j l^i = 2k^{(i} l^{j)}. \quad (\text{A.21})$$

As we did with the tangent vectors e_a^i , we will introduce a shorthand notation to denote contraction with k^i or l^i : any tensor with k or l index means it has been contracted with k^i or l^i . As such we will avoid using the letters k and l as dummy indices. For instance,

$$R_{kl} \equiv k^i l^j R_{ij}. \quad (\text{A.22})$$

Another quantity associated with k^i and l^i is the normal connection w^a , defined through

$$w_a \equiv l_i D_a k^i. \quad (\text{A.23})$$

With this definition, the tangent derivative of k^i can be shown to be

$$D_a k^i = w_a k^i + K_{ab}^k e^{bi}, \quad (\text{A.24})$$

which is a formula that is used repeatedly in our analysis.

At certain intermediate stages of our calculations it will be convenient to define extensions of k^i and l^i off of the entangling surface, so here we will define such an extension. Surface deformations in both the QNEC and QFC follow geodesics generated by k^i , so it makes sense to define k^i to satisfy the geodesic equation:

$$\nabla_k k^i = 0. \quad (\text{A.25})$$

However, we will *not* define l^i by parallel transport along k^i . It is conceptually cleaner to maintain the orthogonality of l^i to the surface even as the surface is deformed along the geodesics generated by k^i . This means that l^i satisfies the equation

$$\nabla_k l^i = -w^a e_a^i. \quad (\text{A.26})$$

These equations are enough to specify l^i and k^i on the null surface formed by the geodesics generated by k^i . To extend k^i and l^i off of this surface, we specify that they are both parallel-transported along l^i . In other words, the null surface generated by k^i forms the initial condition surface for the vector fields k^i and l^i which satisfy the differential equations

$$\nabla_l k^i = 0, \quad \nabla_l l^i = 0. \quad (\text{A.27})$$

This suffices to specify k^i and l^i completely in a neighborhood of the original entangling surface. Now that we have done that, we record the commutator of the two fields for future use:

$$[k, l]^i = \nabla_k l^i - \nabla_l k^i = -w^c e_c^i. \quad (\text{A.28})$$

A.3 Surface Variations

Most of the technical parts of our analysis have to do with variations of surface quantities under the deformation $X^i \rightarrow X^i + \delta X^i$ of the surface embedding coordinates. Here δX^i should be interpreted a vector field defined on the surface. In principle it can include both normal and tangential components, but since tangential components do not actually correspond to physical deformations of the surface we will assume that δX^i is normal. The operator δ denotes the change in a quantity under the variation. In the case where $\delta X^i = \partial_\lambda X^i$, which is the case we are primarily interested in, δ can be identified with ∂_λ . With this in mind, we will always impose the geodesic equation on k^i whenever convenient. In terms of the notation we are introducing here, this is

$$\delta k^i = -\Gamma_{kk}^i. \quad (\text{A.29})$$

To make contact with the main text, we will use the notation $k^i \equiv \delta X^i$, and assume that k^i is null since that is ultimately the case we care about. Some of the formulas we discuss below will not depend on the fact that k^i is null, but we will not make an attempt to distinguish them.

Ambient Quantities For ambient quantities, like curvature tensors, the variation δ can be interpreted straightforwardly as $k^i \partial_i$ with no other qualification. Thus we can freely use, for instance, the ambient covariant derivative ∇_k to simplify the calculations of these quantities. Note that δ itself is not the covariant derivative. As defined, δ is a coordinate dependent operator. This may be less-than-optimal from a geometric point of view, but it has the most

conceptually straightforward interpretation in terms of the calculus of variations. In all of the variational formulas below, then, we will see explicit Christoffel symbols appear. Of course, ultimately these non-covariant terms must cancel out of physical quantities. That they do serves as a nice check on our algebra.

Tangent Vectors The most fundamental formula is that of the variation of the tangent vectors $e_a^i \equiv \partial_a X^i$. Directly from the definition, we have

$$\delta e_a^i = \partial_a k^i = D_a k^i - \Gamma_{ak}^i = w_a k^i + K_{ab}^k e^{bi} - \Gamma_{ak}^i. \quad (\text{A.30})$$

This formula, together with the discussion of how ambient quantities transform, can be used together to compute the variations of many other quantities.

Intrinsic Geometry and Normal Vectors The intrinsic metric variation is easily computed from the above formula as

$$\delta h_{ab} = 2K_{ab}^k. \quad (\text{A.31})$$

From here we can find the variation of the tangent projector, for instance:

$$\begin{aligned} \delta P^{ij} &= \delta h^{ab} e_a^i e_b^j + 2h^{ab} e_a^{(i} \partial_b k^{j)} \\ &= -2K_k^{ab} e_a^i e_b^j + 2h^{ab} e_a^{(i} D_b k^{j)} - 2h^{ab} e_a^{(i} \Gamma_{bk}^{j)} \\ &= 2w^a e_a^{(i} k^{j)} - 2h^{ab} e_a^{(i} \Gamma_{bk}^{j)}. \end{aligned} \quad (\text{A.32})$$

Notice that the second line features a derivative of $k^i = \delta X^i$. In a context where we are taking functional derivatives, such as when computing equations of motion, this term would require integration by parts. We can write the last line covariantly as

$$\nabla_k P^{ij} = 2w^a e_a^{(i} k^{j)}. \quad (\text{A.33})$$

Earlier we saw that l^i satisfied the equation $\nabla_k l^i = -w^a e_a^i$ as a result of keeping l^i orthogonal to the surface even as the surface is deformed. In the language of this section, this is seen by the following manipulation:

$$e_a^i \delta l_i = -l_i \partial_a k^i = -w_a - \Gamma_{ak}^l. \quad (\text{A.34})$$

Again, note the derivative of k^i . It is easy to confirm that represents the only nonzero component of $\nabla_k l^i$.

The normal connection $w_a = l^i D_a k_i$ makes frequent appearances in our calculations, and we will need to know its variation. We can calculate that as follows:

$$\begin{aligned} \delta w_a &= \delta l^i D_a k_i + l^i \partial_a \delta k_i - l^i \delta \Gamma_{ji}^n e_a^j k_n - l^i \Gamma_{ji}^n \partial_a k^j k_n - l^i \Gamma_{ji}^n e_a^j \delta k_n \\ &= \nabla_k l^i D_a k_i + R_{klak} \\ &= -w^c K_{ac} + R_{klak}. \end{aligned} \quad (\text{A.35})$$

Extrinsic Curvatures The simplest extrinsic curvature variation is that of the trace of the extrinsic curvature

$$\delta K^i = -K^m \Gamma_{mk}^i - D_a D^a k^i - R_{mkj}^i P^{mj} + (2D^a(K_{ad}^k) - D_d(K^k)) e^{di} - 2K_k^{ab} K_{ab}^i \quad (\text{A.36})$$

Note that the combination $\delta K^i + K^k \Gamma_{km}^i k^m$ is covariant, so it makes sense to write

$$\nabla_k K^i = -D_a D^a k^i - R_{mkj}^i P^{mj} + (2D^a(K_{ad}^k) - D_d(K^k)) e^{di} - 2K_k^{ab} K_{ab}^i \quad (\text{A.37})$$

This formula is noteworthy because of the first term, which features derivatives of $k^i = \delta X^i$. This is important because when K^i occurs inside of an integral and we want to compute the functional derivative then we have to first integrate by parts to move those derivatives off of k^i . This issue arises when computing Θ as in the QFC, for instance.

We can contract the previous formulas with l^i and k^i to produce other useful formulas. For instance, contracting with k^i leads to

$$\delta K^k = -K^{kab} K_{ab}^k - R_{kk}, \quad (\text{A.38})$$

which is nothing but the Raychaudhuri equation.

The variation of the full extrinsic curvature K_{ab}^i is quite complicated, but we will not needed. However, its contraction with k^i will be useful and so we record it here:

$$k_i \delta K_{ab}^i = -K_{ab}^j \Gamma_{jn}^m k_m k^n - k_i D_a D_b k^i - R_{kakk}. \quad (\text{A.39})$$

A.4 z -Expansions

Bulk Metric

We are focusing on bulk theories with gravitational Lagrangians

$$\mathcal{L} = \frac{1}{16\pi G_N} \left(\frac{d(d-1)}{\tilde{L}^2} + \mathcal{R} + \ell^2 \lambda_1 \mathcal{R}^2 + \ell^2 \lambda_2 \mathcal{R}_{\mu\nu}^2 + \ell^2 \lambda_{GB} \mathcal{L}_{GB} \right). \quad (\text{A.40})$$

where $\mathcal{L}_{GB} = \mathcal{R}_{\mu\nu\rho\sigma}^2 - 4\mathcal{R}_{\mu\nu}^2 + \mathcal{R}^2$ is the Gauss-Bonnet Lagrangian, ℓ is the cutoff length scale of the bulk effective field theory, and the couplings λ_1 , λ_2 , and λ_{GB} are defined to be dimensionless. We have decided to include \mathcal{L}_{GB} as part of our basis of interactions rather than $\mathcal{R}_{\mu\nu\rho\sigma}^2$ because of certain nice properties that the Gauss-Bonnet term has, but this is not important.

We recall that the Fefferman–Graham form of the metric is defined by

$$ds^2 = \frac{1}{z^2} (dz^2 + \bar{g}_{ij} dx^i dx^j), \quad (\text{A.41})$$

where $\bar{g}_{ij}(x, z)$ is expanded as a series in z :

$$\bar{g}_{ij} = g_{ij}^{(0)} + z^2 g_{ij}^{(2)} + z^4 g_{ij}^{(4)} + \cdots + z^d \log z g_{ij}^{(d, \log)} + z^d g_{ij}^{(d)} + \cdots. \quad (\text{A.42})$$

In principle, one would evaluate the equation of motion from the above Lagrangian using the Fefferman–Graham metric form as an ansatz to compute these coefficients. The results of this calculation are largely in the literature, and we quote them here. To save notational clutter, in this section we will set $g_{ij} = g_{ij}^{(0)}$.

The first nontrivial term in the metric expansion is independent of the higher-derivative couplings, and in fact is completely determined by symmetry [113]:

$$g_{ij}^{(2)} = -\frac{1}{d-2} \left(R_{ij} - \frac{1}{2(d-1)} R g_{ij} \right). \quad (\text{A.43})$$

The next term is also largely determined by symmetry, except for a pair of coefficients [113]. We are only interested in the kk -component of $g_{ij}^{(4)}$, and where one of the coefficients drops out. The result is

$$g_{kk}^{(4)} = \frac{1}{d-4} \left[\kappa C_{kijm} C_k^{ijm} + \frac{1}{8(d-1)} \nabla_k^2 R - \frac{1}{4(d-2)} k^i k^j \square R_{ij} - \frac{1}{2(d-2)} R^{ij} R_{kikj} + \frac{d-4}{2(d-2)^2} R_{ki} R_k^i + \frac{1}{(d-1)(d-2)^2} R R_{kk} \right], \quad (\text{A.44})$$

where C_{ijmn} is the Weyl tensor and

$$\kappa = -\lambda_{GB} \frac{\ell^2}{L^2} \left(1 + O\left(\frac{\ell^2}{L^2}\right) \right). \quad (\text{A.45})$$

In $d = 4$ we will need an expression for $g_{kk}^{(4,log)}$ as well. One can check that this is obtainable from $g_{kk}^{(4)}$ by first multiplying by $4-d$ and then setting $d \rightarrow 4$. We record the answer for future reference:

$$g_{kk}^{(4,log)} = - \left[\kappa C_{kijm} C_k^{ijm} + \frac{1}{24} \nabla_k^2 R - \frac{1}{8} k^i k^j \square R_{ij} - \frac{1}{4} R^{ij} R_{kikj} + \frac{1}{12} R R_{kk} \right]. \quad (\text{A.46})$$

Extremal Surface Coordinates

The extremal surface position is determined by extremizing the generalized entropy functional [67, 51]:

$$S_{gen} = \frac{1}{4G_N} \int \sqrt{\bar{h}} \left[1 + 2\lambda_1 \ell^2 \mathcal{R} + \lambda_2 \ell^2 \left(\mathcal{R}_{\mu\nu} \mathcal{N}^{\mu\nu} - \frac{1}{2} \mathcal{K}_\mu \mathcal{K}^\mu \right) + 2\lambda_{GB} \ell^2 \bar{r} \right] + S_{bulk}. \quad (\text{A.47})$$

Here we are using \mathcal{K}^i to denote the extrinsic curvature and \bar{r} the intrinsic Ricci scalar of the surface.

The equation of motion comes from varying S_{gen} and is (ignoring the S_{bulk} term for simplicity)

$$\begin{aligned}
0 = & \mathcal{K}^\mu \left[1 + 2\lambda_1 \ell^2 \mathcal{R} + \lambda_2 \ell^2 \left(\mathcal{R}_{\rho\nu} \mathcal{N}^{\rho\nu} - \frac{1}{2} \mathcal{K}_\rho \mathcal{K}^\rho \right) + 2\lambda_{GB} \ell^2 \bar{r} \right] + 2\lambda_1 \ell^2 \nabla^\mu \mathcal{R} \\
& + \lambda_2 \ell^2 \left(\mathcal{N}^{\rho\nu} \nabla^\mu \mathcal{R}_{\rho\nu} + 2\mathcal{P}^{\rho\nu} \nabla_\rho \mathcal{R}_\nu^\mu - 2\mathcal{R}_\rho^\mu \mathcal{K}^\rho + 2\mathcal{K}^{\mu\alpha\beta} \mathcal{R}_{\alpha\beta} + D_\alpha D^\alpha \mathcal{K}^\mu \right. \\
& \left. + \mathcal{K}^\rho \mathcal{R}_{\mu\sigma\rho\nu} \mathcal{P}^{\nu\sigma} + 2\mathcal{K}^{\mu\alpha\beta} \mathcal{K}_\nu \mathcal{K}_{\alpha\beta}^\nu \right) - 4\lambda_{GB} \ell^2 \bar{r}^{\alpha\beta} \mathcal{K}_{\alpha\beta}^\mu.
\end{aligned} \tag{A.48}$$

This equation is very complicated, but since we are working in $d \leq 5$ dimensions we only need to solve perturbatively in z for $X_{(2)}^i$ and $X_{(4)}^i$ ². Furthermore, $X_{(2)}^i$ is fully determined by symmetry to be [174]

$$X_{(2)}^i = \frac{1}{2(d-2)} D^a \partial_a X_{(0)}^i = -\frac{1}{2(d-2)} K^i, \tag{A.49}$$

where K^i denotes the extrinsic curvature of the $X_{(0)}^i$ surface, but we are leaving off the (0) in our notation to save space.

The computation of $X_{(4)}^i$ is straightforward but tedious. We will only need to know $k_i X_{(4)}^i$ (where indices are being raised and lowered with $g_{ij}^{(0)}$), and the answer turns out to be

$$\begin{aligned}
4(d-4)X_{(4)}^k = & 2X_{(2)}^k \left(P^{jm} g_{jm}^{(2)} - 4(X_{(2)})^2 \right) \\
& + K_{ab}^k g_{(2)}^{ab} + 4g_{km}^{(2)} X_{(2)}^m + 2X_j^{(2)} K_{ab}^j K^{kab} + k_i D_a D^a X_{(2)}^i \\
& + k^j \left(\nabla_n g_{jm}^{(2)} - \frac{1}{2} \nabla_j g_{mn}^{(2)} \right) P^{mn} + X_{(2)}^n R_{kmnj} P^{jm} \\
& + 8\kappa \sigma_{(k}^{ab} C_{kalb} - 2(d-4) \Gamma_{jm}^k X_{(2)}^j X_{(2)}^m.
\end{aligned} \tag{A.50}$$

Here κ depends on λ_{GB} as in (A.45). Notice that the last term in this expression is the only source of noncovariant-ness. One can confirm that this noncovariant piece is required from the definition of $X_{(4)}^i$ —despite its index, $X_{(4)}^i$ does not transform like a vector under boundary diffeomorphisms.

We also note that the terms in $X_{(4)}^k$ with covariant derivatives of $g_{ij}^{(2)}$ can be simplified using the extended k^i and l^i fields described §A.2 and the Bianchi identity:

$$k^j \left(\nabla_n g_{jm}^{(2)} - \frac{1}{2} \nabla_j g_{mn}^{(2)} \right) P^{mn} = -\frac{1}{4(d-1)} \nabla_k R + \frac{1}{d-2} \nabla_l R_{kk}. \tag{A.51}$$

²It goes without saying that these formulas are only valid for $d > 2$ and $d > 4$, respectively.

Finally, we record here the formula for $X_{(4,log)}^k$ which is obtained from $X_{(4)}^k$ by multiplying by $4 - d$ and sending $d \rightarrow 4$:

$$\begin{aligned}
-4X_{(4,log)}^k &= 2X_{(2)}^k \left(P^{jm} g_{jm}^{(2)} - 4(X_{(2)})^2 \right) \\
&+ K_{ab}^k g_{(2)}^{ab} + 4g_{km}^{(2)} X_{(2)}^m + 2X_j^{(2)} K_{ab}^j K^{kab} + k_i D_a D^a X_{(2)}^i \\
&+ k^j (\nabla_n g_{jm}^{(2)} - \frac{1}{2} \nabla_j g_{mn}^{(2)}) P^{mn} + X_{(2)}^n R_{kmnj} P^{jm} \\
&+ 8\kappa \sigma_{(k}^{ab} C_{kalb}.
\end{aligned} \tag{A.52}$$

We will not bother unpacking all of the definitions, but the main things to notice is that the noncovariant part disappears.

A.5 Details of the EWN Calculations

In this section we provide some insight into the algebra necessary to complete the calculations of the main text, primarily regarding the calculation of the subleading part of $(\delta\bar{X})^2$ in §4.2. The task is to simplify (4.16),

$$\begin{aligned}
L^{-2}(\delta\bar{X})^2|_{z^2} &= 2k_i \delta X_{(4)}^i + 2g_{ij}^{(2)} k^i \delta X_{(2)}^j + g_{ij} \delta X_{(2)}^i \delta X_{(2)}^j + g_{ij}^{(4)} k^i k^j + X_{(4)}^m \partial_m g_{ij} k^i k^j \\
&+ 2X_{(2)}^m \partial_m g_{ij} k^i \delta X_{(2)}^j + X_{(2)}^m \partial_m g_{ij}^{(2)} k^i k^j + \frac{1}{2} X_{(2)}^m X_{(2)}^n \partial_m \partial_n g_{ij} k^i k^j.
\end{aligned} \tag{A.53}$$

After some algebra, we can write this as

$$L^{-2}(\delta\bar{X})^2|_{z^2} = g_{kk}^{(4)} + 2\delta(X_{(4,cov)}^k) + 2g_{ik}^{(2)} \nabla_k X_{(2)}^i + \nabla_k X_j^{(2)} \nabla_k X_{(2)}^j - \frac{1}{d-2} (X_{(2)}^l) \nabla_k R_{kk}. \tag{A.54}$$

Here we have defined

$$X_{(4,cov)}^i = X_{(4)}^i + \frac{1}{2} \Gamma_{lm}^i X_{(2)}^l X_{(2)}^m, \tag{A.55}$$

which transforms like a vector (unlike $X_{(4)}^i$). From here, the algebra leading to (4.17) is mostly straightforward, though tedious. The two main tasks which require further explanation are the simplification of one of the terms in $g_{kk}^{(4)}$ and one of the terms in $\delta X_{(4,cov)}^k$. We will explain those now.

$g_{kk}^{(4)}$ **Simplification** We recall the formula for $g_{kk}^{(4)}$ from (A.44):

$$\begin{aligned}
g_{kk}^{(4)} &= \frac{1}{d-4} \left[\kappa C_{kijm} C_k^{ijm} + \frac{1}{8(d-1)} \nabla_k^2 R - \frac{1}{4(d-2)} k^i k^j \square R_{ij} \right. \\
&\left. - \frac{1}{2(d-2)} R^{ij} R_{kikj} + \frac{d-4}{2(d-2)^2} R_{ki} R_k^i + \frac{1}{(d-1)(d-2)^2} R R_{kk} \right].
\end{aligned} \tag{A.56}$$

The main difficulty is with the term $k^i k^j \square R_{ij}$. We will rewrite this term by making use of the geometric quantities introduced in the other appendices, and in particular we make use of the extended k and l field from §A.2. We first separate it into two terms:

$$k^i k^j \square R_{ij} = k^i k^j N^{rs} \nabla_r \nabla_s R_{ij} + k^i k^j P^{rs} \nabla_r \nabla_s R_{ij}. \quad (\text{A.57})$$

Now we compute each of these terms individually:

$$\begin{aligned} k^i k^j N^{rs} \nabla_r \nabla_s R_{ij} &= 2k^i k^j l^s \nabla_k \nabla_s R_{ij} + 2R_{km lk} R_k^m \\ &= 2\nabla_k \nabla_l R_{kk} + 2w^c k^i k^j D_c R_{ij} + 2R_{km lk} R_k^m \\ &= 2\nabla_k \nabla_l R_{kk} + 2w^c D_c R_{kk} - 4w^c w_c R_{kk} - 4w^c K_{ck}^a R_{ka} + 2R_{km lk} R_k^m \\ &= 2\nabla_k \nabla_l R_{kk} + 2w^c D_c R_{kk} - 4w^c w_c R_{kk} + 2R_{km lk} R_k^m. \end{aligned} \quad (\text{A.58})$$

In the last line we assumed that $\sigma_{(k)} = 0$ and $\theta_{(k)} = 0$, which is the only case we will need to worry about. The other term is slightly messier, becoming

$$\begin{aligned} k^i k^j P^{rs} \nabla_r \nabla_s R_{ij} &= k^i k^j e^{sc} D_c \nabla_s R_{ij} \\ &= D_c (k^i k^j D^c R_{ij}) - D_c (k^i k^j e^{sc}) \nabla_s R_{ij} \\ &= D_c (k^i k^j D^c R_{ij}) - 2w_c D^c R_{kk} + 4w_c w^c R_{kk} + 6w_c K_k^{ca} R_{ak} \\ &\quad - 2K_k^{ca} D_c R_{ka} + 2K_k^{ca} K_{ca}^i R_{ik} + 2K_k^{ca} K_c^{bk} R_{ab} + K^s \nabla_s R_{kk} \\ &= D_c D^c R_{kk} - 2D_c (w^c R_{kk}) - 2D_c (K^{cak} R_{ka}) - 2w_c D^c R_{kk} + 4w_c w^c R_{kk} + 6w_c K_k^{ca} R_{ak} \\ &\quad - 2K_k^{ca} D_c R_{ka} + 2K_k^{ca} K_{ca}^i R_{ik} + 2K_k^{ca} K_c^{bk} R_{ab} + K^s \nabla_s R_{kk} \\ &= D_c D^c R_{kk} - 2D_c (w^c R_{kk}) - 2D_c (K^{cak}) R_{ka} - 2w_c D^c R_{kk} + 4w_c w^c R_{kk} + K^s \nabla_s R_{kk}. \end{aligned} \quad (\text{A.59})$$

In the last line we again assumed that $\sigma_{(k)} = 0$ and $\theta_{(k)} = 0$. Putting the two terms together leads to some cancellations:

$$\begin{aligned} k^i k^j \square R_{ij} &= 2\nabla_k \nabla_l R_{kk} + 2R_{km lk} R_k^m + D_c D^c R_{kk} - 2D_c (w^c R_{kk}) \\ &\quad - 2(D_a \theta_{(k)} + R_{kcac}) R_k^a + K^s \nabla_s R_{kk}. \end{aligned} \quad (\text{A.60})$$

$\delta X_{(4,cov)}^k$ **Simplification** The most difficult term in (A.50), which also gives the most interesting results, is

$$k_i D_a D^a X_{(2)}^i = -\frac{1}{2(d-2)} (D_a - w_a)^2 \theta_{(k)} + \frac{1}{2(d-2)} K_{ab} K^{abi} K_i. \quad (\text{A.61})$$

The interesting part here is the first term, so we will take the rest of this section to discuss its variation. The underlying formula is (A.35),

$$\delta w_a = -w^c K_{ac} + R_{klak}. \quad (\text{A.62})$$

From this we can compute the following related variations, assuming that $\theta_{(k)} = 0$ and $\sigma_{(k)} = 0$:

$$\delta(D^a w_a) = D^a R_{klak} + w^a \partial_a \theta_{(k)} - 3D_a(K_k^{ab} w_b) \quad (\text{A.63})$$

$$\delta(w^a D_a \theta_{(k)}) = -3K_k^{ab} w_a D_b \theta_{(k)} + R_{klak} D^a \theta_{(k)} + w^a D_a \dot{\theta}_{(k)} \quad (\text{A.64})$$

$$\delta(D^a D_a \theta_{(k)}) = D^a D_a \dot{\theta} - \partial_a \theta_{(k)} \partial^a \theta_{(k)} - 2P^{jm} R_{kjbm} D^b \theta_{(k)}. \quad (\text{A.65})$$

Here $\dot{\theta}_{(k)} \equiv \delta\theta_{(k)}$ is given by the Raychaudhuri equation. We can combine these equations to get

$$\begin{aligned} \delta((D_a - w_a)^2 \theta_{(k)}) &= \delta(D^a D_a \theta_{(k)}) - 2\delta(w^a D_a \theta_{(k)}) - \delta((D_a w^a) \theta_{(k)}) + \delta(w_a w^a \theta_{(k)}) \\ &= -D^a D_a R_{kk} + 2w^a D_a R_{kk} + (D_a w^a) R_{kk} - w_a w^a R_{kk} \\ &\quad - \frac{d}{d-2} (D_a \theta_{(k)})^2 - 2R_{kb} D^b \theta_{(k)} - 2(D\sigma)^2. \end{aligned} \quad (\text{A.66})$$

A.6 The $d = 4$ Case

As mentioned in the main text, many of our calculations are more complicated in even dimensions, though most of the end results are the same. The only nontrivial even dimension we study is $d = 4$, so in this section we record the formulas and special derivations necessary for understanding the $d = 4$ case. Some of these have been mentioned elsewhere already, but we repeat them here so that they are all in the same place.

Log Terms In $d = 4$ we get log terms in the extremal surface, the metric, and the EWN inequality. By looking at the structure of the extremal surface equation, it's easy to see that the log term in the extremal surface is related to $X_{(4)}^i$ in $d \neq 4$ by first multiplying by $4 - d$ and then setting $d \rightarrow 4$. The result was recorded in (A.52), and we repeat it here:

$$\begin{aligned} -4X_{(4,log)}^k &= 2X_{(2)}^k \left(P^{jm} g_{jm}^{(2)} - 4(X_{(2)})^2 \right) \\ &\quad + K_{ab}^k g_{(2)}^{ab} + 4g_{km}^{(2)} X_{(2)}^m + 2X_j^{(2)} K_{ab}^j K^{kab} + k_i D_a D^a X_{(2)}^i \\ &\quad + k^j (\nabla_n g_{jm}^{(2)} - \frac{1}{2} \nabla_j g_{mn}^{(2)}) P^{mn} + X_{(2)}^n R_{kmnj} P^{jm} \\ &\quad + 8\kappa \sigma_{(k)}^{ab} C_{kalb}. \end{aligned} \quad (\text{A.67})$$

There is a similar story for $g_{kk}^{(4,log)}$, which was recorded earlier in (A.46):

$$g_{kk}^{(4,log)} = - \left[\kappa C_{kijm} C_k^{ijm} + \frac{1}{24} \nabla_k^2 R - \frac{1}{8} k^i k^j \square R_{ij} - \frac{1}{4} R^{ij} R_{kikj} + \frac{1}{12} R R_{kk} \right]. \quad (\text{A.68})$$

From these two equations, it is easy to see that the log term in $(\delta\bar{X})^2$ has precisely the same form as the subleading EWN inequality (4.17) in $d \geq 5$, except we first multiply by $4 - d$

and then set $d \rightarrow 4$. This results in

$$L^{-2}(\delta\bar{X})^2\Big|_{z^2 \log z, d=4} = -\frac{1}{4}(D_a\theta^{(k)} + R_{ka})^2 - \frac{1}{4}(D_a\sigma_{bc}^{(k)})^2. \quad (\text{A.69})$$

Note that the Gauss-Bonnet term drops out completely due to special identities of the Weyl tensor valid in $d = 4$ [77]. The overall minus sign is important because $\log z$ should be regarded as negative.

QNEC in Einstein Gravity For simplicity we will only discuss the case of Einstein gravity for the QNEC in $d = 4$, so that the entropy functional is just given by the extremal surface area divided by $4G_N$. At order z^2 , the norm of $\delta\bar{X}^\mu$ is formally the same as the expression in other dimensions:

$$L^{-2}(\delta\bar{X})^2\Big|_{z^2} = g_{kk}^{(4)} + 2g_{ik}^{(2)}\nabla_k X_{(2)}^i + \nabla_k X_j^{(2)}\nabla_k X_{(2)}^j - \frac{1}{2}X_{(2)}^l\nabla_k R_{kk} + 2\delta(k_i X_{(4)cov}^i). \quad (\text{A.70})$$

Now, though, $X_{(4)}^k$ and $g_{kk}^{(4)}$ are state-dependent and must be related to the entropy and energy-momentum, respectively.

We begin with the entropy. From the calculus of variations, we know that the variation of the extremal surface area is given by

$$\delta A = -\lim_{\epsilon \rightarrow 0} \frac{L^3}{\epsilon^3} \int \sqrt{h} \frac{1}{\sqrt{1 + g_{nm}\partial_z \bar{X}^n \partial_z \bar{X}^m}} g_{ij} \partial_z \bar{X}^i \delta X^j. \quad (\text{A.71})$$

A few words about this formula are required. The \bar{X}^μ factors appearing here must be expanded in ϵ , but the terms without any (n) in their notation do *not* refer to (0), unlike elsewhere in this paper. The reason is that we have to do holographic renormalization carefully at this stage, and that means the boundary conditions are set at $z = \epsilon$. So when we expand out \bar{X}^μ we will find its coefficients determined by the usual formulas in terms of $X_{(0)}^i$. We need to then solve for $X_{(0)}^i$ in term of $X^i \equiv \bar{X}^i(z = \epsilon)$ re-express the result in terms of X^i alone. Since we are not in a high dimension this task is relatively easy. An intermediate result is

$$\frac{k^i}{L^3\sqrt{h}} \frac{\delta A}{\delta X^i} \Big|_{\epsilon^0} = -2 X_{(2)}^k \Big|_{\epsilon^2} - 4 (X_{(4)}^k - (X_{(2)})^2 X_{(2)}^k) - X_{(4,log)}^k. \quad (\text{A.72})$$

The notation on the first term refers to the order ϵ^2 part of $X_{(2)}^i$ that is generated when $X_{(2)}^i$ is written in terms of $\bar{X}^i(z = \epsilon)$. The result of that calculation is

$$\begin{aligned} -4 X_{(2)}^k \Big|_{\epsilon^2} &= 2X_j^{(2)} K^{jab} K_{ab}^i k_i + k_i D^b D_b X_{(2)}^i + K^m \Gamma_{ml}^i X_{(2)}^l k_i \\ &+ g_{(2)}^{ab} K_{ab}^i k_i + P^{kj} R_{jmk}^i X_{(2)}^m k_i + k^m \left(\nabla_j g_{mk}^{(2)} - \frac{1}{2} \nabla_m g_{jk}^{(2)} \right) P^{jk} \\ &= -4X_{(4,log)}^k - 2X_{(2)}^k \left(P^{jm} g_{jm}^{(2)} - 4(X_{(2)})^2 \right) - 4g_{km}^{(2)} X_{(2)}^m + K^m \Gamma_{ml}^i X_{(2)}^l k_i. \end{aligned} \quad (\text{A.73})$$

We have dropped terms of higher order in ϵ . Thus we can write

$$\frac{k^i}{L^3\sqrt{h}} \frac{\delta A}{\delta X^i} \Big|_{\epsilon^0} = -3X_{(log)}^k - X_{(2)}^k P^{jm} g_{jm}^{(2)} + 8X_{(2)}^k (X_{(2)})^2 - 2g_{km}^{(2)} X_{(2)}^m - 4X_{(4)cov}^k. \quad (\text{A.74})$$

We will want to take one more variation of this formula so that we can extract $\delta X_{(4)cov}^k$. We can get some help by demanding that the $z^2 \log z$ part of EWN be saturated, which states

$$g_{kk}^{(log)} + 2\delta X_{log}^k = 0. \quad (\text{A.75})$$

Then we have

$$\delta \left(\frac{k^i}{L^3\sqrt{h}} \frac{\delta A}{\delta X^i} \Big|_{\epsilon^0} \right) = \frac{3}{2} g_{kk}^{(log)} - \delta(X_{(2)}^k P^{jm} g_{jm}^{(2)}) + 8\delta(X_{(2)}^k (X_{(2)})^2) - 2\delta(g_{km}^{(2)} X_{(2)}^m) - 4\delta X_{(4)cov}^k. \quad (\text{A.76})$$

Assuming that $\theta_{(k)} = \sigma_{(k)} = 0$, we can simplify this to

$$\delta \left(\frac{k^i}{L^3\sqrt{h}} \frac{\delta A}{\delta X^i} \Big|_{\epsilon^0} \right) = \frac{3}{2} g_{kk}^{(log)} - \frac{1}{4} R_{kk} P^{jm} g_{jm}^{(2)} - \frac{1}{4} \nabla_k (\theta_{(l)} R_{kk}) - \frac{1}{2} g_{kl}^{(2)} R_{kk} - 4\delta X_{(4)cov}^k. \quad (\text{A.77})$$

We can combine this with the holographic renormalization formula [93]

$$\begin{aligned} g_{kk}^{(4)} &= 4\pi G_N L^{-3} T_{kk} + \frac{1}{2} (g_{(2)}^2)_{kk} - \frac{1}{4} g_{kk}^{(2)} g^{ij} g_{ij}^{(2)} - \frac{3}{4} g_{kk}^{(log)} \\ &= 4\pi G_N L^{-3} T_{kk} + \frac{1}{8} R_k^i R_{ik} - \frac{1}{16} R_{kk} R - \frac{3}{4} g_{kk}^{(log)} \end{aligned} \quad (\text{A.78})$$

to get

$$L^{-2} (\delta \bar{X}^i)^2 \Big|_{z^2} = 4\pi G_N L^{-3} T_{kk} - \frac{1}{2} \delta \left(\frac{k^i}{L^3\sqrt{h}} \frac{\delta A}{\delta X^i} \Big|_{\epsilon^0} \right). \quad (\text{A.79})$$

After dividing by $4G_N$, we recognize the QNEC.

A.7 Proof of Lemma 14

We now prove Lemma 14 by direct calculation.

We wish to show that

$$R|_{(0,s)} \equiv f_* \partial_r |_{(0,s)} = \exp_{K^*} |_{(p,sS|_{(0,0)})} (\check{R}, s\check{R}) \quad (\text{A.80})$$

and

$$S|_{(0,s)} \equiv f_* \partial_s |_{(0,s)} = \exp_{K^*} |_{(p,sS|_{(0,0)})} (0, \check{S}), \quad (\text{A.81})$$

where

$$\begin{aligned} f(r, s) &= \exp_{f(r,0)} sS|_{(r,0)} \\ &= \exp_K(f(r, 0), sS|_{(r,0)}), \end{aligned} \quad (\text{A.82})$$

as defined in Sec. 5.2.

Using the definition of the pushforward, we can write $f_*\partial_r|_{(0,s)}$ as the differential \exp_{K^*} , associated with f in Eq. (A.82), evaluated along the tangent direction $sS|_{(0,0)}$,

$$\begin{aligned} R|_{(0,s)} &\equiv f_*\partial_r|_{(0,s)} \\ &= \exp_{K^*}|_{(p,sS|_{(0,0)})} (\check{R}, s\phi_*(\partial_r S|_{(r,0)})|_{r=0}). \end{aligned} \quad (\text{A.83})$$

In the second line, we used the definition of \check{R} as the tangent to $\mu(r)$ at p , along with linearity of \exp_{K^*} . We have again used the notation ϕ_* for the identity map between vectors in T_pM and their naturally associated counterparts in $T_S T_p M$.

Next, we must evaluate the derivative of S , $\phi_*(\partial_r S|_{(r,0)})|_{r=0} \in T_S T_p K^\perp$. Let us write $S|_{(r,0)}$ as an explicit function of both the parameter r along the path $\mu(r) \equiv f(r, 0) \in K$ and the vector $S|_{(0,0)} + r\hat{R} \in T_p K^\perp$ that is normal parallel transported along μ from $\mu(0) = p$ to $\mu(r)$:

$$\begin{aligned} S|_{(r,0)} &= S(r, S|_{(0,0)} + r\hat{R})|_{r_1=r_2=r} \\ &\equiv S(r_1, r_2)|_{r_1=r_2=r}, \end{aligned} \quad (\text{A.84})$$

so that the derivative in question can be written as $\phi_*\partial_r S(r, S|_{(0,0)} + r\hat{R})|_{r=0}$. Since $S(r_1, r_2)$ is defined by normal parallel transporting a particular vector $(S|_{(0,0)} + r\hat{R})$ in $T_p K^\perp$ to $\mu(r_1)$, its variation with respect to r_1 gives the normal part of the covariant derivative of S along μ , which vanishes, i.e., $\partial_{r_1} S(r_1, r_2) = 0$. Hence,

$$\begin{aligned} &\frac{\partial}{\partial r} \left[S(r_1, S|_{(0,0)} + r_2\hat{R})|_{r_1=r_2=r} \right] \\ &= \left[\frac{\partial}{\partial r_2} S(r, r_2) \right]_{r_2=r} \\ &= \hat{R}. \end{aligned} \quad (\text{A.85})$$

Inputting this result into Eq. (A.83), we have

$$\begin{aligned} R|_{(0,s)} &= \exp_{K^*}|_{(p,sS|_{(0,0)})} (\check{R}, s\phi_*\hat{R}) \\ &= \exp_{K^*}|_{(p,sS|_{(0,0)})} (\check{R}, s\tilde{R}). \end{aligned} \quad (\text{A.86})$$

We have thus derived the claimed formula for the Jacobi field stated in Eq. (A.80). The proof of Eq. (A.81) follows similarly. Neither $f(r, 0)$ or $S|_{(r,0)}$ depend on s . Therefore

$$\begin{aligned} S|_{(0,s)} &\equiv f_*\partial_s|_{(0,s)} \\ &= \partial_s \exp_K(f(0, 0), sS|_{(0,0)}) \\ &= \exp_{K^*}|_{(p,sS|_{(0,0)})} (0, \phi_*S|_{(0,0)}) \\ &= \exp_{K^*}|_{(p,sS|_{(0,0)})} (0, \tilde{S}). \end{aligned} \quad (\text{A.87})$$

This derivation of the Jacobi field and tangent vector completes the proof of Lemma 14.

A.8 Flat Renyi Spectrum

Here we prove that if a density matrix ρ satisfies the condition $\tilde{S}_n(\rho) = S(\rho)$ for all n , it must be a normalized projector. We show this by first showing that this condition of having a flat refined Renyi entropy spectrum is equivalent to having a flat Renyi entropy spectrum.

From the definition of the refined Renyi entropy and the above condition, we have

$$\tilde{S}_n(\rho) = n^2 \partial_n \left(\frac{n-1}{n} S_n(\rho) \right) \quad (\text{A.88})$$

$$= S(\rho) . \quad (\text{A.89})$$

We can integrate with respect to n to obtain

$$\int_1^{n'} \frac{S(\rho)}{n^2} = \left[\frac{n-1}{n} S_n(\rho) \right]_1^{n'} \quad (\text{A.90})$$

$$\implies S(\rho) = S_{n'}(\rho) , \quad (\text{A.91})$$

where this condition is true for arbitrary n' . Now we can use the fact that ρ and ρ^n can be simultaneously diagonalized to arrive at the identity

$$\partial_n S_n(\rho) = -\frac{1}{(1-n)^2} \sum_{i=1}^{\dim(\rho)} q_i \log \left(\frac{q_i}{p_i} \right) , \quad (\text{A.92})$$

where p_i are the eigenvalues of ρ and $q_i = p_i^n / (\sum_{i=1}^{\dim(\rho)} p_i^n)$. If indeed Eq. (A.91) is true, then the LHS equals zero for all n . For the RHS to equal zero implies the relative entropy (Kullback-Leibler divergence) between probability distributions q_i and p_i vanishes. Using a standard result, we can conclude that the distributions are indeed identical. This gives us our desired result that

$$p_i = \left(\sum_{i=1}^{\text{rank}(\rho)} p_i^n \right)^{1/(n-1)} \quad (\text{A.93})$$

$$= \frac{1}{\text{rank}(\rho)} , \quad (\text{A.94})$$

where we have restricted to the non-zero elements only and used the normalization condition. Thus, in its diagonal basis ρ takes the form

$$\rho = \frac{1}{\text{rank}(\rho)} \sum_{i=1}^{\text{rank}(\rho)} |i\rangle \langle i| , \quad (\text{A.95})$$

namely, it is a normalized projector.

Bibliography

- [1] Chris Akers and Pratik Rath. “Holographic Renyi Entropy from Quantum Error Correction”. In: *JHEP* 05 (2019), p. 052. DOI: 10.1007/JHEP05(2019)052. arXiv: 1811.05171 [hep-th].
- [2] Chris Akers et al. “Boundary of the future of a surface”. In: *Phys. Rev. D* 97.2 (2018), p. 024018. DOI: 10.1103/PhysRevD.97.024018. arXiv: 1711.06689 [hep-th].
- [3] Chris Akers et al. “Entanglement and RG in the $O(N)$ vector model”. In: (2015). arXiv: 1512.00791 [hep-th].
- [4] Chris Akers et al. “Geometric Constraints from Subregion Duality Beyond the Classical Regime”. In: (Oct. 2016). eprint: 1610.08968. URL: <https://arxiv.org/abs/1610.08968>.
- [5] Chris Akers et al. “The Quantum Null Energy Condition, Entanglement Wedge Nesting, and Quantum Focusing”. In: (2017). arXiv: 1706.04183 [hep-th].
- [6] Mohsen Alishahiha et al. “The dS/dS correspondence”. In: *AIP Conf. Proc.* 743 (2005). [,393(2004)], pp. 393–409. DOI: 10.1063/1.1848341. arXiv: hep-th/0407125 [hep-th].
- [7] Andrea Allais and Márk Mezei. “Some results on the shape dependence of entanglement and Rényi entropies”. In: (2014). arXiv: 1407.7249 [hep-th].
- [8] Ahmed Almheiri. “Holographic Quantum Error Correction and the Projected Black Hole Interior”. In: (2018). arXiv: 1810.02055 [hep-th].
- [9] Ahmed Almheiri, Xi Dong, and Daniel Harlow. “Bulk Locality and Quantum Error Correction in AdS/CFT”. In: *JHEP* 04 (2015), p. 163. DOI: 10.1007/JHEP04(2015)163. arXiv: 1411.7041 [hep-th].
- [10] Ahmed Almheiri, Xi Dong, and Brian Swingle. “Linearity of Holographic Entanglement Entropy”. In: *JHEP* 02 (2017), p. 074. DOI: 10.1007/JHEP02(2017)074. arXiv: 1606.04537 [hep-th].
- [11] Ning Bao et al. “Holographic entropy inequalities and gapped phases of matter”. In: *JHEP* 09 (2015), p. 203. DOI: 10.1007/JHEP09(2015)203. arXiv: 1507.05650 [hep-th].

- [12] Ning Bao et al. “The Holographic Entropy Cone”. In: *JHEP* 09 (2015), p. 130. DOI: 10.1007/JHEP09(2015)130. arXiv: 1505.07839 [hep-th].
- [13] J. K. Beem and P. E. Ehrlich. “The Space-Time Cut Locus”. In: *General Relativity and Gravitation* 11 (1979), p. 89. DOI: 10.1007/BF00756581.
- [14] Omer Ben-Ami, Dean Carmi, and Michael Smolkin. “Renormalization group flow of entanglement entropy on spheres”. In: *JHEP* 08 (2015), p. 048. DOI: 10.1007/JHEP08(2015)048. arXiv: 1504.00913 [hep-th].
- [15] Omer Ben-Ami, Dean Carmi, and Jacob Sonnenschein. “Holographic Entanglement Entropy of Multiple Strips”. In: *JHEP* 1411 (2014), p. 144. DOI: 10.1007/JHEP11(2014)144. arXiv: 1409.6305 [hep-th].
- [16] Lorenzo Bianchi et al. “Rényi entropy and conformal defects”. In: *JHEP* 07 (2016), p. 076. DOI: 10.1007/JHEP07(2016)076. arXiv: 1511.06713 [hep-th].
- [17] Raphael Bousso. “A covariant entropy conjecture”. In: *JHEP* 07 (1999), p. 004. eprint: hep-th/9905177.
- [18] Raphael Bousso. “Holography in general space-times”. In: *JHEP* 06 (1999), p. 028. DOI: 10.1088/1126-6708/1999/06/028. arXiv: hep-th/9906022 [hep-th].
- [19] Raphael Bousso. “Holography in general space-times”. In: *JHEP* 06 (1999), p. 028. eprint: hep-th/9906022.
- [20] Raphael Bousso. “The Holographic principle”. In: *Rev. Mod. Phys.* 74 (2002), pp. 825–874. DOI: 10.1103/RevModPhys.74.825. arXiv: hep-th/0203101 [hep-th].
- [21] Raphael Bousso and Netta Engelhardt. “Generalized Second Law for Cosmology”. In: *Phys. Rev. D* 93.2 (2016), p. 024025. DOI: 10.1103/PhysRevD.93.024025. arXiv: 1510.02099 [hep-th].
- [22] Raphael Bousso and Netta Engelhardt. “New Area Law in General Relativity”. In: *Phys. Rev. Lett.* 115.8 (2015), p. 081301. DOI: 10.1103/PhysRevLett.115.081301. arXiv: 1504.07627 [hep-th].
- [23] Raphael Bousso and Netta Engelhardt. “New Area Law in General Relativity”. In: *Phys. Rev. Lett.* 115 (2015), p. 081301. DOI: 10.1103/PhysRevLett.115.081301. arXiv: 1504.07627 [hep-th].
- [24] Raphael Bousso and Netta Engelhardt. “Proof of a New Area Law in General Relativity”. In: *Phys. Rev. D* 92.4 (2015), p. 044031. DOI: 10.1103/PhysRevD.92.044031. arXiv: 1504.07660 [gr-qc].
- [25] Raphael Bousso and Netta Engelhardt. “Proof of a New Area Law in General Relativity”. In: *Phys. Rev. D* 92 (2015), p. 044031. DOI: 10.1103/PhysRevD.92.044031. arXiv: 1504.07660 [gr-qc].
- [26] Raphael Bousso et al. “A Quantum Focussing Conjecture”. In: (2015). arXiv: 1506.02669 [hep-th].

- [27] Raphael Bousso et al. “Proof of the Quantum Null Energy Condition”. In: (2015). arXiv: 1509.02542 [hep-th].
- [28] Raphael Bousso et al. “Quantum focusing conjecture”. In: *Phys. Rev. D* 93 (2016), p. 064044. DOI: 10.1103/PhysRevD.93.064044. arXiv: 1506.02669 [hep-th].
- [29] Lowell S. Brown and John C. Collins. “Dimensional Renormalization of Scalar Field Theory in Curved Space-time”. In: *Annals Phys.* 130 (1980), p. 215. DOI: 10.1016/0003-4916(80)90232-8.
- [30] William Bunting, Zicao Fu, and Donald Marolf. “A coarse-grained generalized second law for holographic conformal field theories”. In: *Class. Quant. Grav.* 33.5 (2016), p. 055008. DOI: 10.1088/0264-9381/33/5/055008. arXiv: 1509.00074 [hep-th].
- [31] Jr. Callan Curtis G. and Frank Wilczek. “On geometric entropy”. In: *Phys.Lett.* B333 (1994), pp. 55–61. DOI: 10.1016/0370-2693(94)91007-3. arXiv: hep-th/9401072 [hep-th].
- [32] Robert Callan, Jian-Yang He, and Matthew Headrick. “Strong subadditivity and the covariant holographic entanglement entropy formula”. In: *JHEP* 06 (2012), p. 081. DOI: 10.1007/JHEP06(2012)081. arXiv: 1204.2309 [hep-th].
- [33] Xian O. Camanho et al. “Causality Constraints on Corrections to the Graviton Three-Point Coupling”. In: *JHEP* 02 (2016), p. 020. DOI: 10.1007/JHEP02(2016)020. arXiv: 1407.5597 [hep-th].
- [34] Giancarlo Camilo, Gabriel T. Landi, and Sebas Eliëns. “On the Strong Subadditivity of the Rényi entropies for bosonic and fermionic Gaussian states”. In: (2018). arXiv: 1810.07070 [cond-mat.stat-mech].
- [35] John L. Cardy. “Is There a c Theorem in Four-Dimensions?” In: *Phys.Lett.* B215 (1988), pp. 749–752. DOI: 10.1016/0370-2693(88)90054-8.
- [36] Dean Carmi. “On the Shape Dependence of Entanglement Entropy”. In: (2015). arXiv: 1506.07528 [hep-th].
- [37] H. Casini and M. Huerta. “A Finite Entanglement Entropy and the C-Theorem”. In: *Phys. Lett.* B600 (2004), pp. 142–150. DOI: 10.1016/j.physletb.2004.08.072. arXiv: hep-th/0405111 [hep-th].
- [38] H. Casini and Marina Huerta. “On the RG Running of the Entanglement Entropy of a Circle”. In: *Phys. Rev. D* 85 (2012), p. 125016. DOI: 10.1103/PhysRevD.85.125016. arXiv: 1202.5650 [hep-th].
- [39] Horacio Casini, Marina Huerta, and Robert C. Myers. “Towards a Derivation of Holographic Entanglement Entropy”. In: *JHEP* 05 (2011), p. 036. DOI: 10.1007/JHEP05(2011)036. arXiv: 1102.0440 [hep-th].
- [40] Horacio Casini, Marina Huerta, and Jose Alejandro Rosabal. “Remarks on entanglement entropy for gauge fields”. In: *Phys. Rev. D* 89.8 (2014), p. 085012. DOI: 10.1103/PhysRevD.89.085012. arXiv: 1312.1183 [hep-th].

- [41] Horacio Casini, F. D. Mazzitelli, and Eduardo TestE. “Area terms in entanglement entropy”. In: *Phys. Rev. D* 91.10 (2015), p. 104035. DOI: 10.1103/PhysRevD.91.104035. arXiv: 1412.6522 [hep-th].
- [42] Horacio Casini, Eduardo Teste, and Gonzalo Torroba. “Holographic RG flows, entanglement entropy and the sum rule”. In: *JHEP* 03 (2016), p. 033. DOI: 10.1007/JHEP03(2016)033. arXiv: 1510.02103 [hep-th].
- [43] Horacio Casini, Eduardo Teste, and Gonzalo Torroba. “The a-theorem and the Markov property of the CFT vacuum”. In: (2017). arXiv: 1704.01870 [hep-th].
- [44] Horacio Casini et al. “Mutual information and the F-theorem”. In: *JHEP* 10 (2015), p. 003. DOI: 10.1007/JHEP10(2015)003. arXiv: 1506.06195 [hep-th].
- [45] Jordan Cotler et al. “Entanglement Wedge Reconstruction via Universal Recovery Channels”. In: (2017). arXiv: 1704.05839 [hep-th].
- [46] Bartłomiej Czech et al. “The Gravity Dual of a Density Matrix”. In: *Class. Quant. Grav.* 29 (2012), p. 155009. DOI: 10.1088/0264-9381/29/15/155009. arXiv: 1204.1330 [hep-th].
- [47] Xi Dong. “Holographic Entanglement Entropy for General Higher Derivative Gravity”. In: *JHEP* 01 (2014), p. 044. DOI: 10.1007/JHEP01(2014)044. arXiv: 1310.5713 [hep-th].
- [48] Xi Dong. “The Gravity Dual of Renyi Entropy”. In: *Nature Commun.* 7 (2016), p. 12472. DOI: 10.1038/ncomms12472. arXiv: 1601.06788 [hep-th].
- [49] Xi Dong, Daniel Harlow, and Donald Marolf. “Flat entanglement spectra in fixed-area states of quantum gravity”. In: (2018). arXiv: 1811.05382 [hep-th].
- [50] Xi Dong, Daniel Harlow, and Aron C. Wall. “Reconstruction of Bulk Operators Within the Entanglement Wedge in Gauge-Gravity Duality”. In: *Phys. Rev. Lett.* 117.2 (2016), p. 021601. DOI: 10.1103/PhysRevLett.117.021601. arXiv: 1601.05416 [hep-th].
- [51] Xi Dong and Aitor Lewkowycz. “Entropy, Extremality, Euclidean Variations, and the Equations of Motion”. In: (May 2017). eprint: 1705.08453. URL: <https://arxiv.org/abs/1705.08453>.
- [52] Xi Dong and Aitor Lewkowycz. “Entropy, Extremality, Euclidean Variations, and the Equations of Motion”. In: *JHEP* 01 (2018), p. 081. DOI: 10.1007/JHEP01(2018)081. arXiv: 1705.08453 [hep-th].
- [53] Xi Dong, Aitor Lewkowycz, and Mukund Rangamani. “Deriving covariant holographic entanglement”. In: *JHEP* 11 (2016), p. 028. DOI: 10.1007/JHEP11(2016)028. arXiv: 1607.07506 [hep-th].
- [54] Xi Dong, Eva Silverstein, and Gonzalo Torroba. “De Sitter Holography and Entanglement Entropy”. In: *JHEP* 07 (2018), p. 050. DOI: 10.1007/JHEP07(2018)050. arXiv: 1804.08623 [hep-th].

- [55] William Donnelly. “Decomposition of entanglement entropy in lattice gauge theory”. In: *Phys. Rev. D* 85 (2012), p. 085004. DOI: 10.1103/PhysRevD.85.085004. arXiv: 1109.0036 [hep-th].
- [56] William Donnelly. “Entanglement entropy and nonabelian gauge symmetry”. In: *Class. Quant. Grav.* 31.21 (2014), p. 214003. DOI: 10.1088/0264-9381/31/21/214003. arXiv: 1406.7304 [hep-th].
- [57] William Donnelly and Laurent Freidel. “Local subsystems in gauge theory and gravity”. In: *JHEP* 09 (2016), p. 102. DOI: 10.1007/JHEP09(2016)102. arXiv: 1601.04744 [hep-th].
- [58] William Donnelly and Vasudev Shyam. “Entanglement entropy and $T\bar{T}$ deformation”. In: *Phys. Rev. Lett.* 121 (2018), p. 131602. DOI: 10.1103/PhysRevLett.121.131602. arXiv: 1806.07444 [hep-th].
- [59] William Donnelly and Aron C. Wall. “Entanglement entropy of electromagnetic edge modes”. In: *Phys. Rev. Lett.* 114.11 (2015), p. 111603. DOI: 10.1103/PhysRevLett.114.111603. arXiv: 1412.1895 [hep-th].
- [60] William Donnelly and Aron C. Wall. “Geometric entropy and edge modes of the electromagnetic field”. In: *Phys. Rev. D* 94.10 (2016), p. 104053. DOI: 10.1103/PhysRevD.94.104053. arXiv: 1506.05792 [hep-th].
- [61] William Donnelly et al. “Living on the Edge: A Toy Model for Holographic Reconstruction of Algebras with Centers”. In: *JHEP* 04 (2017), p. 093. DOI: 10.1007/JHEP04(2017)093. arXiv: 1611.05841 [hep-th].
- [62] J.S. Dowker. “Expansion of Rényi entropy for free scalar fields”. In: (2014). arXiv: 1408.4055 [hep-th].
- [63] Netta Engelhardt and Sebastian Fischetti. “The Gravity Dual of Boundary Causality”. In: *Class. Quant. Grav.* 33.17 (2016), p. 175004. DOI: 10.1088/0264-9381/33/17/175004. arXiv: 1604.03944 [hep-th].
- [64] Netta Engelhardt and Aron C. Wall. “Coarse Graining Holographic Black Holes”. In: (2018). arXiv: 1806.01281 [hep-th].
- [65] Netta Engelhardt and Aron C. Wall. “Decoding the Apparent Horizon: A Coarse-Grained Holographic Entropy”. In: (2017). arXiv: 1706.02038 [hep-th].
- [66] Netta Engelhardt and Aron C. Wall. “Decoding the Apparent Horizon: A Coarse-Grained Holographic Entropy”. In: (2017). arXiv: 1706.02038 [hep-th].
- [67] Netta Engelhardt and Aron C. Wall. “Quantum Extremal Surfaces: Holographic Entanglement Entropy Beyond the Classical Regime”. In: *JHEP* 01 (2015), p. 073. DOI: 10.1007/JHEP01(2015)073. arXiv: 1408.3203 [hep-th].
- [68] Thomas Faulkner. “Bulk Emergence and the RG Flow of Entanglement Entropy”. In: (2014). arXiv: 1412.5648 [hep-th].

- [69] Thomas Faulkner, Robert G. Leigh, and Onkar Parrikar. “Shape Dependence of Entanglement Entropy in Conformal Field Theories”. In: (2015). arXiv: 1511.05179 [hep-th].
- [70] Thomas Faulkner and Aitor Lewkowycz. “Bulk locality from modular flow”. In: *JHEP* 07 (2017), p. 151. DOI: 10.1007/JHEP07(2017)151. arXiv: 1704.05464 [hep-th].
- [71] Thomas Faulkner, Aitor Lewkowycz, and Juan Maldacena. “Quantum Corrections to Holographic Entanglement Entropy”. In: *JHEP* 11 (2013), p. 074. DOI: 10.1007/JHEP11(2013)074. arXiv: 1307.2892 [hep-th].
- [72] Thomas Faulkner et al. “Gravitation from Entanglement in Holographic CFTs”. In: *JHEP* 03 (2014), p. 051. DOI: 10.1007/JHEP03(2014)051. arXiv: 1312.7856 [hep-th].
- [73] Thomas Faulkner et al. “Modular Hamiltonians for Deformed Half-Spaces and the Averaged Null Energy Condition”. In: (2016). arXiv: 1605.08072 [hep-th].
- [74] Lin Fei et al. “Generalized F -Theorem and the ϵ Expansion”. In: *JHEP* 12 (2015), p. 155. DOI: 10.1007/JHEP12(2015)155. arXiv: 1507.01960 [hep-th].
- [75] W. Fischler and L. Susskind. “Holography and cosmology”. In: (1998). eprint: hep-th/9806039.
- [76] John L. Friedman, Kristin Schleich, and Donald M. Witt. “Topological Censorship”. In: *Phys. Rev. Lett.* 71 (1993). [Erratum: *Phys. Rev. Lett.* 75,1872(1995)], pp. 1486–1489. DOI: 10.1103/PhysRevLett.71.1486. arXiv: gr-qc/9305017 [gr-qc].
- [77] Zicao Fu, Jason Koeller, and Donald Marolf. “The Quantum Null Energy Condition in Curved Space”. In: (June 2017). eprint: 1706.01572. URL: <https://arxiv.org/abs/1706.01572>.
- [78] Zicao Fu, Jason Koeller, and Donald Marolf. “Violating the Quantum Focusing Conjecture and Quantum Covariant Entropy Bound in $d \geq 5$ dimensions”. In: (May 2017). eprint: 1705.03161. URL: <https://arxiv.org/abs/1705.03161>.
- [79] Zicao Fu and Donald Marolf. “Does horizon entropy satisfy a Quantum Null Energy Conjecture?” In: (2016). arXiv: 1606.04713 [hep-th].
- [80] Dmitri V. Fursaev and Sergey N. Solodukhin. “On the description of the Riemannian geometry in the presence of conical defects”. In: *Phys.Rev.* D52 (1995), pp. 2133–2143. DOI: 10.1103/PhysRevD.52.2133. arXiv: hep-th/9501127 [hep-th].
- [81] Ping Gao, Daniel Louis Jafferis, and Aron Wall. “Traversable Wormholes via a Double Trace Deformation”. In: (2016). arXiv: 1608.05687 [hep-th].
- [82] Sijie Gao and Robert M. Wald. “Theorems on Gravitational Time Delay and Related Issues”. In: *Class. Quant. Grav.* 17 (2000), pp. 4999–5008. DOI: 10.1088/0264-9381/17/24/305. arXiv: gr-qc/0007021 [gr-qc].
- [83] Robert P. Geroch. “Domain of Dependence”. In: *J. Math. Phys.* 11 (1970), p. 437. DOI: 10.1063/1.1665157.

- [84] Simone Giombi and Igor R. Klebanov. “Interpolating between a and F ”. In: (2014). arXiv: 1409.1937 [hep-th].
- [85] Mikhail Goykhman. “On entanglement entropy in ’t Hooft model”. In: (2015). arXiv: 1501.07590 [hep-th].
- [86] C. Robin Graham and Edward Witten. “Conformal Anomaly of Submanifold Observables in AdS / CFT Correspondence”. In: *Nucl. Phys.* B546 (1999), pp. 52–64. DOI: 10.1016/S0550-3213(99)00055-3. arXiv: hep-th/9901021 [hep-th].
- [87] Steven S. Gubser. “AdS / CFT and gravity”. In: *Phys. Rev.* D63 (2001), p. 084017. DOI: 10.1103/PhysRevD.63.084017. arXiv: hep-th/9912001 [hep-th].
- [88] Metin Gurses, Tahsin Cagri Sisman, and Bayram Tekin. “New Exact Solutions of Quadratic Curvature Gravity”. In: *Phys. Rev.* D86 (2012), p. 024009. DOI: 10.1103/PhysRevD.86.024009. arXiv: 1204.2215 [hep-th].
- [89] Muxin Han and Shilin Huang. “Discrete gravity on random tensor network and holographic Rényi entropy”. In: *JHEP* 11 (2017), p. 148. DOI: 10.1007/JHEP11(2017)148. arXiv: 1705.01964 [hep-th].
- [90] Daniel Harlow. “The Ryu-Takayanagi Formula from Quantum Error Correction”. In: (2016). arXiv: 1607.03901 [hep-th].
- [91] Daniel Harlow. “Wormholes, Emergent Gauge Fields, and the Weak Gravity Conjecture”. In: *JHEP* 01 (2016), p. 122. DOI: 10.1007/JHEP01(2016)122. arXiv: 1510.07911 [hep-th].
- [92] Sebastian de Haro, Sergey N. Solodukhin, and Kostas Skenderis. “Holographic Reconstruction of Space-Time and Renormalization in the AdS / CFT Correspondence”. In: *Commun. Math. Phys.* 217 (2001), pp. 595–622. DOI: 10.1007/s002200100381. arXiv: hep-th/0002230 [hep-th].
- [93] Sebastian de Haro, Sergey N. Solodukhin, and Kostas Skenderis. “Holographic reconstruction of space-time and renormalization in the AdS / CFT correspondence”. In: *Commun. Math. Phys.* 217 (2001), pp. 595–622. DOI: 10.1007/s002200100381. arXiv: hep-th/0002230 [hep-th].
- [94] J. B. Hartle and S. W. Hawking. “Wave Function of the Universe”. In: *Phys. Rev.* D28 (1983). [Adv. Ser. Astrophys. Cosmol.3,174(1987)], pp. 2960–2975. DOI: 10.1103/PhysRevD.28.2960.
- [95] Thomas Hartman, Sandipan Kundu, and Amirhossein Tajdini. “Averaged Null Energy Condition from Causality”. In: (2016). arXiv: 1610.05308 [hep-th].
- [96] S. W. Hawking. “Gravitational Radiation from Colliding Black Holes”. In: *Phys. Rev. Lett.* 26 (1971), pp. 1344–1346. DOI: 10.1103/PhysRevLett.26.1344.
- [97] S. W. Hawking. “The Chronology Protection Conjecture”. In: *Phys. Rev.* D46 (1992), pp. 603–611. DOI: 10.1103/PhysRevD.46.603.

- [98] S. W. Hawking. “The occurrence of singularities in cosmology. III. Causality and singularities”. In: *Proc. Roy. Soc. Lond.* A300 (1967), p. 187. DOI: 10.1098/rspa.1967.0164.
- [99] S. W. Hawking and G. F. R. Ellis. *The large scale structure of space-time*. Cambridge, England: Cambridge University Press, 1973.
- [100] Patrick Hayden and Geoffrey Penington. “Learning the Alpha-bits of Black Holes”. In: (2018). arXiv: 1807.06041 [hep-th].
- [101] Patrick Hayden et al. “Holographic duality from random tensor networks”. In: *JHEP* 11 (2016), p. 009. DOI: 10.1007/JHEP11(2016)009. arXiv: 1601.01694 [hep-th].
- [102] Matthew Headrick. “General properties of holographic entanglement entropy”. In: *JHEP* 03 (2014), p. 085. DOI: 10.1007/JHEP03(2014)085. arXiv: 1312.6717 [hep-th].
- [103] Matthew Headrick and Tadashi Takayanagi. “A Holographic proof of the strong subadditivity of entanglement entropy”. In: *Phys. Rev. D* 76 (2007), p. 106013. DOI: 10.1103/PhysRevD.76.106013. arXiv: 0704.3719 [hep-th].
- [104] Matthew Headrick et al. “Causality & Holographic Entanglement Entropy”. In: *JHEP* 12 (2014), p. 162. DOI: 10.1007/JHEP12(2014)162. arXiv: 1408.6300 [hep-th].
- [105] Mark P. Hertzberg and Frank Wilczek. “Some Calculable Contributions to Entanglement Entropy”. In: *Phys.Rev.Lett.* 106 (2011), p. 050404. DOI: 10.1103/PhysRevLett.106.050404. arXiv: 1007.0993 [hep-th].
- [106] Christopher P. Herzog. “Universal Thermal Corrections to Entanglement Entropy for Conformal Field Theories on Spheres”. In: *JHEP* 10 (2014), p. 28. DOI: 10.1007/JHEP10(2014)028. arXiv: 1407.1358 [hep-th].
- [107] Noel J. Hicks. *Notes on Differential Geometry*. Van Nostrand Reinhold Company, 1965.
- [108] G. 't Hooft. “Dimensional reduction in quantum gravity”. In: (1993). eprint: gr-qc/9310026.
- [109] M. Hotta, T. Kato, and K. Nagata. “A Comment on geometric entropy and conical space”. In: *Class.Quant.Grav.* 14 (1997), pp. 1917–1925. DOI: 10.1088/0264-9381/14/7/024. arXiv: gr-qc/9611058 [gr-qc].
- [110] Veronika E. Hubeny and Mukund Rangamani. “Causal Holographic Information”. In: *JHEP* 06 (2012), p. 114. DOI: 10.1007/JHEP06(2012)114. arXiv: 1204.1698 [hep-th].
- [111] Veronika E. Hubeny, Mukund Rangamani, and Tadashi Takayanagi. “A Covariant holographic entanglement entropy proposal”. In: *JHEP* 07 (2007), p. 062. DOI: 10.1088/1126-6708/2007/07/062. arXiv: 0705.0016 [hep-th].

- [112] Marina Huerta. “Numerical Determination of the Entanglement Entropy for Free Fields in the Cylinder”. In: *Phys.Lett.* B710 (2012), pp. 691–696. DOI: 10.1016/j.physletb.2012.03.044. arXiv: 1112.1277 [hep-th].
- [113] C. Imbimbo et al. “Diffeomorphisms and Holographic Anomalies”. In: *Class. Quant. Grav.* 17 (2000), pp. 1129–1138. DOI: 10.1088/0264-9381/17/5/322. arXiv: hep-th/9910267 [hep-th].
- [114] Ted Jacobson and Renaud Parentani. “Horizon entropy”. In: *Found. Phys.* 33 (2003), pp. 323–348. DOI: 10.1023/A:1023785123428. arXiv: gr-qc/0302099 [gr-qc].
- [115] Daniel L. Jafferis and S. Josephine Suh. “The Gravity Duals of Modular Hamiltonians”. In: (2014). arXiv: 1412.8465 [hep-th].
- [116] Daniel Louis Jafferis. “Bulk reconstruction and the Hartle-Hawking wavefunction”. In: (2017). arXiv: 1703.01519 [hep-th].
- [117] Daniel L. Jafferis et al. “Relative entropy equals bulk relative entropy”. In: *JHEP* 06 (2016), p. 004. DOI: 10.1007/JHEP06(2016)004. arXiv: 1512.06431 [hep-th].
- [118] Daniel L. Jafferis et al. “Towards the F-Theorem: N=2 Field Theories on the Three-Sphere”. In: *JHEP* 1106 (2011), p. 102. DOI: 10.1007/JHEP06(2011)102. arXiv: 1103.1181 [hep-th].
- [119] Peter A. R. Jones and Marika Taylor. “Entanglement entropy and differential entropy for massive flavors”. In: *JHEP* 08 (2015), p. 014. DOI: 10.1007/JHEP08(2015)014. arXiv: 1505.07697 [hep-th].
- [120] Daniel N. Kabat. “Black hole entropy and entropy of entanglement”. In: *Nucl.Phys.* B453 (1995), pp. 281–299. DOI: 10.1016/0550-3213(95)00443-V. arXiv: hep-th/9503016 [hep-th].
- [121] Daniel N. Kabat and M.J. Strassler. “A Comment on entropy and area”. In: *Phys.Lett.* B329 (1994), pp. 46–52. DOI: 10.1016/0370-2693(94)90515-0. arXiv: hep-th/9401125 [hep-th].
- [122] William R. Kelly and Aron C. Wall. “Holographic Proof of the Averaged Null Energy Condition”. In: *Phys. Rev.* D90.10 (2014). [Erratum: *Phys. Rev.* D91, no.6, 069902(2015)], p. 106003. DOI: 10.1103/PhysRevD.90.106003, 10.1103/PhysRevD.91.069902. arXiv: 1408.3566 [gr-qc].
- [123] Paul Martin Kemp. “Focal and Focal-Cut Points”. PhD thesis. University of California, San Diego, 1984.
- [124] Igor R. Klebanov et al. “Is Renormalized Entanglement Entropy Stationary at RG Fixed Points?” In: *JHEP* 1210 (2012), p. 058. DOI: 10.1007/JHEP10(2012)058. arXiv: 1207.3360 [hep-th].
- [125] G. Klinkhammer. “Averaged energy conditions for free scalar fields in flat spacetimes”. In: *Phys. Rev.* D43 (1991), pp. 2542–2548. DOI: 10.1103/PhysRevD.43.2542.

- [126] Jason Koeller and Stefan Leichenauer. “Holographic Proof of the Quantum Null Energy Condition”. In: (2015). arXiv: 1512.06109 [hep-th].
- [127] Jason Koeller et al. “In Progress”. In: ().
- [128] Zohar Komargodski. “The Constraints of Conformal Symmetry on RG Flows”. In: *JHEP* 1207 (2012), p. 069. DOI: 10.1007/JHEP07(2012)069. arXiv: 1112.4538 [hep-th].
- [129] Zohar Komargodski and Adam Schwimmer. “On Renormalization Group Flows in Four Dimensions”. In: *JHEP* 12 (2011), p. 099. DOI: 10.1007/JHEP12(2011)099. arXiv: 1107.3987 [hep-th].
- [130] Demir N. Kupeli. “Null cut loci of spacelike surfaces”. In: *General Relativity and Gravitation* 20 (1988), p. 415. DOI: 10.1007/BF00758117.
- [131] Finn Larsen and Frank Wilczek. “Renormalization of black hole entropy and of the gravitational coupling constant”. In: *Nucl.Phys.* B458 (1996), pp. 249–266. DOI: 10.1016/0550-3213(95)00548-X. arXiv: hep-th/9506066 [hep-th].
- [132] Jeongseog Lee et al. “Renyi entropy, stationarity, and entanglement of the conformal scalar”. In: (2014). arXiv: 1407.7816 [hep-th].
- [133] Stefan Leichenauer. “The Quantum Focusing Conjecture Has Not Been Violated”. In: (2017). arXiv: 1705.05469 [hep-th].
- [134] Aitor Lewkowycz and Juan Maldacena. “Generalized gravitational entropy”. In: *JHEP* 08 (2013), p. 090. DOI: 10.1007/JHEP08(2013)090. arXiv: 1304.4926 [hep-th].
- [135] Aitor Lewkowycz, Robert C. Myers, and Michael Smolkin. “Observations on entanglement entropy in massive QFT’s”. In: *JHEP* 1304 (2013), p. 017. DOI: 10.1007/JHEP04(2013)017. arXiv: 1210.6858 [hep-th].
- [136] Aitor Lewkowycz and Eric Perlmutter. “Universality in the geometric dependence of Renyi entropy”. In: (2014). arXiv: 1407.8171 [hep-th].
- [137] Jennifer Lin. “Ryu-Takayanagi Area as an Entanglement Edge Term”. In: (2017). arXiv: 1704.07763 [hep-th].
- [138] Hong Liu and Mark Mezei. “A Refinement of entanglement entropy and the number of degrees of freedom”. In: *JHEP* 1304 (2013), p. 162. DOI: 10.1007/JHEP04(2013)162. arXiv: 1202.2070 [hep-th].
- [139] R. Lohmayer et al. “Numerical determination of entanglement entropy for a sphere”. In: *Phys. Lett.* B685 (2010), pp. 222–227. DOI: 10.1016/j.physletb.2010.01.053. arXiv: 0911.4283 [hep-lat].
- [140] Juan Maldacena. “The Large- N Limit of Superconformal Field Theories and Supergravity”. In: *Adv. Theor. Math. Phys.* 2 (1998), p. 231. eprint: hep-th/9711200.
- [141] Juan Martin Maldacena. “Eternal black holes in anti-de Sitter”. In: *JHEP* 04 (2003), p. 021. DOI: 10.1088/1126-6708/2003/04/021. arXiv: hep-th/0106112 [hep-th].

- [142] Lauren McGough, Márk Mezei, and Herman Verlinde. “Moving the CFT into the bulk with $T\bar{T}$ ”. In: *JHEP* 04 (2018), p. 010. DOI: 10.1007/JHEP04(2018)010. arXiv: 1611.03470 [hep-th].
- [143] Max A. Metlitski, Carlos A. Fuertes, and Subir Sachdev. “Entanglement entropy in the $O(N)$ model”. In: *Phys. Rev. B* 80 (11 Sept. 2009), p. 115122. DOI: 10.1103/PhysRevB.80.115122. arXiv: cond-mat/0904.4477 [cond-mat].
- [144] Mxfffdxfffdxffdrk Mezei. “Entanglement entropy across a deformed sphere”. In: (2014). arXiv: 1411.7011 [hep-th].
- [145] Masamichi Miyaji and Tadashi Takayanagi. “Surface/State Correspondence as a Generalized Holography”. In: *PTEP* 2015.7 (2015), 073B03. DOI: 10.1093/ptep/ptv089. arXiv: 1503.03542 [hep-th].
- [146] Masamichi Miyaji, Tadashi Takayanagi, and Kento Watanabe. “From path integrals to tensor networks for the AdS/CFT correspondence”. In: *Phys. Rev. D* 95.6 (2017), p. 066004. DOI: 10.1103/PhysRevD.95.066004. arXiv: 1609.04645 [hep-th].
- [147] Masamichi Miyaji et al. “Continuous Multiscale Entanglement Renormalization Ansatz as Holographic Surface-State Correspondence”. In: *Phys. Rev. Lett.* 115.17 (2015), p. 171602. DOI: 10.1103/PhysRevLett.115.171602. arXiv: 1506.01353 [hep-th].
- [148] Robert C. Myers, Razieh Pourhasan, and Michael Smolkin. “On Spacetime Entanglement”. In: *JHEP* 06 (2013), p. 013. DOI: 10.1007/JHEP06(2013)013. arXiv: 1304.2030 [hep-th].
- [149] Robert C. Myers and Aninda Sinha. “Seeing a C-Theorem with Holography”. In: *Phys. Rev. D* 82 (2010), p. 046006. DOI: 10.1103/PhysRevD.82.046006. arXiv: 1006.1263 [hep-th].
- [150] Tatsuma Nishioka. “Relevant Perturbation of Entanglement Entropy and Stationarity”. In: *Phys. Rev. D* 90 (2014), p. 045006. DOI: 10.1103/PhysRevD.90.045006. arXiv: 1405.3650 [hep-th].
- [151] Yasunori Nomura, Pratik Rath, and Nico Salzetta. “Classical Spacetimes as Amplified Information in Holographic Quantum Theories”. In: *Phys. Rev. D* 97.10 (2018), p. 106025. DOI: 10.1103/PhysRevD.97.106025. arXiv: 1705.06283 [hep-th].
- [152] Yasunori Nomura, Pratik Rath, and Nico Salzetta. “Pulling the Boundary into the Bulk”. In: *Phys. Rev. D* 98.2 (2018), p. 026010. DOI: 10.1103/PhysRevD.98.026010. arXiv: 1805.00523 [hep-th].
- [153] Yasunori Nomura, Pratik Rath, and Nico Salzetta. “Spacetime from Unentanglement”. In: *Phys. Rev. D* 97.10 (2018), p. 106010. DOI: 10.1103/PhysRevD.97.106010. arXiv: 1711.05263 [hep-th].
- [154] Yasunori Nomura and Grant N. Remmen. “Area Law Unification and the Holographic Event Horizon”. In: *JHEP* 08 (2018), p. 063. DOI: 10.1007/JHEP08(2018)063. arXiv: 1805.09339 [hep-th].

- [155] Yasunori Nomura et al. “Toward a Holographic Theory for General Spacetimes”. In: *Phys. Rev. D* 95.8 (2017), p. 086002. DOI: 10.1103/PhysRevD.95.086002. arXiv: 1611.02702 [hep-th].
- [156] Barrett O’Neill. *Semi-Riemannian Geometry: with Applications to Relativity*. Academic Press, 1983.
- [157] Chanyong Park. “Logarithmic Corrections to the Entanglement Entropy”. In: *Phys. Rev. D* 92.12 (2015), p. 126013. DOI: 10.1103/PhysRevD.92.126013. arXiv: 1505.03951 [hep-th].
- [158] Fernando Pastawski et al. “Holographic quantum error-correcting codes: Toy models for the bulk/boundary correspondence”. In: *JHEP* 06 (2015), p. 149. DOI: 10.1007/JHEP06(2015)149. arXiv: 1503.06237 [hep-th].
- [159] R. Penrose. *Techniques of Differential Topology in Relativity*. Society for Industrial and Applied Mathematics, 1972.
- [160] Roger Penrose. “Gravitational Collapse and Space-Time Singularities”. In: *Phys. Rev. Lett.* 14 (1965), pp. 57–59. DOI: 10.1103/PhysRevLett.14.57.
- [161] Roger Penrose. “Structure of Space-Time”. In: *Battelle Rencontres: 1967 Lectures in Mathematics and Physics*. Ed. by C. M. DeWitt and J. A. Wheeler. W. A. Benjamin, 1968.
- [162] Eric Perlmutter, Mukund Rangamani, and Massimiliano Rota. “Central Charges and the Sign of Entanglement in 4D Conformal Field Theories”. In: *Phys. Rev. Lett.* 115.17 (2015), p. 171601. DOI: 10.1103/PhysRevLett.115.171601. arXiv: 1506.01679 [hep-th].
- [163] Xiao-Liang Qi, Zhao Yang, and Yi-Zhuang You. “Holographic coherent states from random tensor networks”. In: *JHEP* 08 (2017), p. 060. DOI: 10.1007/JHEP08(2017)060. arXiv: 1703.06533 [hep-th].
- [164] Lisa Randall and Raman Sundrum. “An Alternative to compactification”. In: *Phys. Rev. Lett.* 83 (1999), pp. 4690–4693. DOI: 10.1103/PhysRevLett.83.4690. arXiv: hep-th/9906064 [hep-th].
- [165] Vladimir Rosenhaus and Michael Smolkin. “Entanglement Entropy: a Perturbative Calculation”. In: *JHEP* 12 (2014), p. 179. DOI: 10.1007/JHEP12(2014)179. arXiv: 1403.3733 [hep-th].
- [166] Vladimir Rosenhaus and Michael Smolkin. “Entanglement Entropy Flow and the Ward Identity”. In: *Phys. Rev. Lett.* 113.26 (2014), p. 261602. DOI: 10.1103/PhysRevLett.113.261602. arXiv: 1406.2716 [hep-th].
- [167] Vladimir Rosenhaus and Michael Smolkin. “Entanglement Entropy for Relevant and Geometric Perturbations”. In: *JHEP* 02 (2015), p. 015. DOI: 10.1007/JHEP02(2015)015. arXiv: 1410.6530 [hep-th].

- [168] Vladimir Rosenhaus and Michael Smolkin. “Entanglement entropy, planar surfaces, and spectral functions”. In: *JHEP* 1409 (2014), p. 119. DOI: 10.1007/JHEP09(2014)119. arXiv: 1407.2891 [hep-th].
- [169] W. Rudin. *Principles of Mathematical Analysis*. McGraw-Hill, 1976. ISBN: 9780070856134.
- [170] Shinsei Ryu and Tadashi Takayanagi. “Aspects of Holographic Entanglement Entropy”. In: *JHEP* 08 (2006), p. 045. DOI: 10.1088/1126-6708/2006/08/045. arXiv: hep-th/0605073 [hep-th].
- [171] Shinsei Ryu and Tadashi Takayanagi. “Holographic derivation of entanglement entropy from AdS/CFT”. In: *Phys. Rev. Lett.* 96 (2006), p. 181602. DOI: 10.1103/PhysRevLett.96.181602. arXiv: hep-th/0603001 [hep-th].
- [172] Fabio Sanches and Sean J. Weinberg. “A Holographic Entanglement Entropy Conjecture for General Spacetimes”. In: (Mar. 2016). eprint: 1603.05250. URL: <https://arxiv.org/abs/1603.05250>.
- [173] Fabio Sanches and Sean J. Weinberg. “Holographic entanglement entropy conjecture for general spacetimes”. In: *Phys. Rev. D* 94.8 (2016), p. 084034. DOI: 10.1103/PhysRevD.94.084034. arXiv: 1603.05250 [hep-th].
- [174] A. Schwimmer and S. Theisen. “Entanglement Entropy, Trace Anomalies and Holography”. In: *Nucl. Phys.* B801 (2008), pp. 1–24. DOI: 10.1016/j.nuclphysb.2008.04.015. arXiv: 0802.1017 [hep-th].
- [175] Sergei N. Solodukhin. “Nonminimal coupling and quantum entropy of black hole”. In: *Phys.Rev.* D56 (1997), pp. 4968–4974. DOI: 10.1103/PhysRevD.56.4968. arXiv: hep-th/9612061 [hep-th].
- [176] Sergey N. Solodukhin. “Entanglement entropy, conformal invariance and extrinsic geometry”. In: *Phys.Lett.* B665 (2008), pp. 305–309. DOI: 10.1016/j.physletb.2008.05.071. arXiv: 0802.3117 [hep-th].
- [177] Sergey N. Solodukhin. “Entanglement entropy of black holes”. In: *Living Rev. Rel.* 14 (2011), p. 8. DOI: 10.12942/lrr-2011-8. arXiv: 1104.3712 [hep-th].
- [178] Antony J. Speranza. “Local phase space and edge modes for diffeomorphism-invariant theories”. In: *JHEP* 02 (2018), p. 021. DOI: 10.1007/JHEP02(2018)021. arXiv: 1706.05061 [hep-th].
- [179] Mark Srednicki. “Entropy and area”. In: *Phys.Rev.Lett.* 71 (1993), pp. 666–669. DOI: 10.1103/PhysRevLett.71.666. arXiv: hep-th/9303048 [hep-th].
- [180] Leonard Susskind. “The world as a hologram”. In: *J. Math. Phys.* 36 (1995), p. 6377. eprint: hep-th/9409089.
- [181] Leonard Susskind and John Uglum. “Black hole entropy in canonical quantum gravity and superstring theory”. In: *Phys. Rev. D* 50 (1994), pp. 2700–2711. eprint: hep-th/9401070.

- [182] Brian Swingle. “Entanglement Renormalization and Holography”. In: *Phys. Rev. D* 86 (2012), p. 065007. DOI: 10.1103/PhysRevD.86.065007. arXiv: 0905.1317 [cond-mat.str-el].
- [183] D.V. Vassilevich. “Heat kernel expansion: User’s manual”. In: *Phys.Rept.* 388 (2003), pp. 279–360. DOI: 10.1016/j.physrep.2003.09.002. arXiv: hep-th/0306138 [hep-th].
- [184] Herman L. Verlinde. “Holography and compactification”. In: *Nucl. Phys.* B580 (2000), pp. 264–274. DOI: 10.1016/S0550-3213(00)00224-8. arXiv: hep-th/9906182 [hep-th].
- [185] Matt Visser. “Gravitational vacuum polarization. 2: Energy conditions in the Boulware vacuum”. In: *Phys. Rev. D* 54 (1996), pp. 5116–5122. DOI: 10.1103/PhysRevD.54.5116. arXiv: gr-qc/9604008 [gr-qc].
- [186] Robert M. Wald. *General Relativity*. The University of Chicago Press, 1984. DOI: 10.7208/chicago/9780226870373.001.0001.
- [187] Robert M. Wald and U. Yurtsever. “General proof of the averaged null energy condition for a massless scalar field in two-dimensional curved space-time”. In: *Phys. Rev. D* 44 (1991), pp. 403–416. DOI: 10.1103/PhysRevD.44.403.
- [188] Aron C. Wall. “A proof of the generalized second law for rapidly changing fields and arbitrary horizon slices”. In: *Phys. Rev. D* 85 (2012), p. 104049. DOI: 10.1103/PhysRevD.85.104049. arXiv: 1105.3445 [gr-qc].
- [189] Aron C. Wall. “Maximin Surfaces, and the Strong Subadditivity of the Covariant Holographic Entanglement Entropy”. In: *Class. Quant. Grav.* 31.22 (2014), p. 225007. DOI: 10.1088/0264-9381/31/22/225007. arXiv: 1211.3494 [hep-th].
- [190] Aron C. Wall. “Proving the Achronal Averaged Null Energy Condition from the Generalized Second Law”. In: *Phys. Rev. D* 81 (2010), p. 024038. DOI: 10.1103/PhysRevD.81.024038. arXiv: 0910.5751 [gr-qc].
- [191] Aron C. Wall. “The Generalized Second Law Implies a Quantum Singularity Theorem”. In: *Class. Quant. Grav.* 30 (2013). [Erratum: *Class. Quant. Grav.* 30,199501(2013)], p. 165003. DOI: 10.1088/0264-9381/30/19/199501, 10.1088/0264-9381/30/16/165003. arXiv: 1010.5513 [gr-qc].
- [192] A.B. Zamolodchikov. “Irreversibility of the Flux of the Renormalization Group in a 2D Field Theory”. In: *JETP Lett.* 43 (1986), pp. 730–732.